Development of Polymer Gel Systems to Improve Volumetric Sweep and Reduce Producing Water/Oil Ratios

Final Report

for the reporting period
7/01/2002 – 12/31/2005

by

G. Paul Willhite, Stan McCool, Don W. Green
Min Cheng, Feiyan Chen

March 2006

Contract Number DE-FC26-02NT15363
Contract Dates 7/01/2002 - 12/31/2005

The University of Kansas Center for Research, Inc.
Tertiary Oil Recovery Project
Lawrence, KS 66045

Disclaimer

Abstract

Gelled polymer treatments are applied to oil reservoirs to increase oil production and to reduce water production by altering the fluid movement within the reservoir. This report describes the results of a 42-month research program that focused on the understanding of gelation chemistry and the fundamental mechanisms that alter the flows of oil and water in reservoir rocks after a gel treatment. Work was conducted on a widely applied system in the field, the partially hydrolyzed polyacrylamide-chromium acetate gel. Gelation occurs by network formation through the crosslinking of polyacrylamide molecules as a result of reaction with chromium acetate. Pre-gel aggregates form and grow as reactions between chromium acetate and polyacrylamide proceed. A rate equation that describes the reaction between chromium acetate and polymer molecules was regressed from experimental data. A mathematical model that describes the crosslinking reaction between two polymer molecules as a function of time was derived. The model was based on probability concepts and provides molecular-weight averages and molecular-weight distributions of the pre-gel aggregates as a function of time and initial system conditions. Average molecular weights of pre-gel aggregates were measured as a function of time and were comparable to model simulations. Experimental methods to determine molecular weight distributions of pre-gel aggregates were unsuccessful. Dissolution of carbonate minerals during the injection of gelants causes the pH of the gelant to increase. Chromium precipitates from solution at the higher pH values robbing the gelant of crosslinker. Experimental data on the transport of chromium acetate solutions through dolomite cores were obtained. A mathematical model that describes the transport of brine and chromium acetate solutions through rocks containing carbonate minerals was used to simulate the experimental results and data from literature. Gel treatments usually reduce the permeability to water to a greater extent than the permeability to oil is reduced. This phenomenon is referred to as disproportionate permeability reduction (DPR). Flow experiments were conducted in sandpacks to determine the effect of polymer and chromium concentrations on DPR. All gels studied reduced the permeability to water by a greater factor than the factor by which the oil permeability was reduced. Greater DPR was observed as the concentrations of polymer and chromium were increased. A conceptual model of the mechanisms responsible for DPR is presented. Primary features of the model are (1) the development of flow channels through the gel by dehydration and displacement of the gel and by re-connection of pre-treatment, residual oil volume and (2) high flow resistance in the channels during water flow is caused by significant saturations of oil remaining in the channels. A similar study of DPR was conducted in Berea sandstone cores. Both oil and water permeabilities were reduced by much smaller factors in Berea sandstone cores than in similar treatments in sandpacks. Poor maturation of the gelant in the Berea rock was thought to be caused by fluid-rock interactions that interfered with the gelation process.

Table of Contents

List of Figures

List of Tables

Chapter 1

Introduction

The research goals were to improve the effectiveness of polymer gels to increase volumetric sweep efficiency of fluid displacement processes and to reduce water production in production wells. Improvements in these areas have the potential to slow the rate of decline in oil production from existing wells and increase the ultimate oil recovery from existing reservoirs. The program was organized into two major tasks: (1) In-depth Treatment of Matrix Rock from Injection Wells, and (2) Treatment of Production Wells to Control Water Production.

Both tasks focused on a gel system containing partially hydrolyzed polyacrylamide and chromium acetate, a common system applied in field treatments. Gels are formed by building a network by crosslinking the polymer molecules. A crosslink is formed when two HPAM molecules react with one Cr(III) complex ion. These reactions are described by:

$$Cr + P1 \rightarrow Cr\text{-}P1 \qquad \text{(uptake)} \qquad \text{Eq. 1.1}$$

$$Cr\text{-}P1 + P2 \rightarrow P2\text{-}Cr\text{-}P1 \qquad \text{(crosslink)} \qquad \text{Eq. 1.2}$$

P1 and P2 represent different polymer molecules. The first reaction of polymer P1 with the chromium complex ion is commonly called the uptake reaction. The reaction with the second polymer P2 creates a crosslink between the polymers and is termed the crosslink reaction. As additional crosslinks occur, pre-gel aggregates form and grow in size until a 3D network or gel is formed.

Kinetic studies of the uptake and crosslink reactions were a major portion of Task 1. A kinetic study of the uptake reaction between chromium acetate and polyacrylamide (Eq. 1.1) is presented in Chapter 2. The reaction was followed by determining the concentration of unreacted chromium in the solvent as a function of time. The experimental data were regressed to derive a reaction rate equation for the chromium species as a function of chromium concentration, polymer concentration and pH value.

The crosslinking reaction (Eq. 1.2) was the subject of Chapters 3, 4 and 5. A mathematical model describing the crosslinking reaction was derived and is presented in Chapter 3. The model is based on probability concepts using the Theory of Branching Process (TBP) which provides molecular weight quantities of the pre-gel aggregates as a function of conversion of reaction sites. The model is extended by use of the kinetic study of the uptake reaction (Chapter 2) to provide molecular weight quantities as a function of time. Experimental data of weight-average molecular weights of pre-gel aggregates as a function of time were measured and were comparable to model results.

The model also simulated the molecular weight distribution of the pre-gel aggregates during the gelation process. Efforts were conducted to measure the size distribution of gel aggregates by fractionating the samples prior to measurement of molecular weight. Two experimental methods to fractionate gel aggregates were evaluated and the results are presented in Chapters 4 and 5.

Polymer samples were fractionated successfully but problems occurred with gelant samples in both fractionating methods.

Dissolution of carbonate minerals during the injection of gelants causes the gelant pH to increase. Chromium precipitates from solution at the higher pH values robbing the gelant of crosslinker. A mathematical model was developed that describes the transport of brine and chromium acetate solutions through rocks containing carbonate minerals. Phenomena considered in the model were convection, dispersion, kinetic reactions of carbonate dissolution and chromium precipitation, and chemical equilibria of aqueous components. Experimental data on the transport of chromium acetate solutions through dolomite cores were also obtained. The model was compared to the data and to data taken from the literature. Chromium propagation was simulated well by the model for steady-state and equilibrium results. A description of the model, simulations by the model, and the experimental data are reported in Chapter 6.

Filtration of pre-gel aggregates occurs during placement of gelant in reservoir rocks. The retained aggregates increase flow resistance significantly reducing the distance gelant can be placed in the reservoir. A study of the filtration of pre-gel aggregates during gelant flow is presented in Chapter 9.

Fundamental studies on disproportionate permeability reduction (DPR) were conducted to address the application of gel treatments in production wells. Favorable DPR is a phenomenon where a gel treatment of a porous medium reduces the permeability to water by a factor that is greater than the permeability to oil is reduced. Two studies of DPR, one in sandpacks and one in Berea sandstone cores, were conducted under Task 2.

Permeability reduction in sandpacks by a partially hydrolyzed polyacrylamide-chromium acetate gels was studied as functions of gel composition and the pressure gradients imposed on the gels. For the range of parameters studied, increased gel composition increased the factors by which the permeabilities to water and oil were reduced. Increased gel composition also increased selectivity, a measure of the water permeability reduction with respect to oil permeability reduction. Applied pressure gradients during steady-state flows had little effect on oil permeability and a moderate effect on water permeability. Material balances on phases and components in the sandpacks provided insights into mechanisms responsible for the development of flow channels through gelled sandpacks and mechanisms contributing to favorable disproportionate permeability reduction. Increased pressure gradient during channel development decreased the selectivity of the treatment. The study of DPR in sandpacks is presented in Chapter 7. A similar study in Berea cores was conducted and is presented in Chapter 8. Permeabilities to oil and water were reduced in the Berea cores by factors much less than those in sandpacks and was caused by fluid-rock interactions that interfered with the maturation of the gel.

Task 3 covers technology transfer. Presentations and technical papers that present results from this work and work conducted in a previous DOE contract are documented in Chapter 10.

Chapter 2

Reaction Kinetics of the Uptake of Chromium(III) Acetate by Polyacrylamide

Graduate Research Assistant: Rajeev Jain

Introduction

The application of crosslinked-polymers gels for permeability modification of petroleum reservoirs has been effective to improve displacement efficiency, increase crude oil production and to reduce water production. The treatment of an injection well consists of injecting an aqueous solution containing polymer and a crosslinker into the high permeability zones or fractures of the reservoir where the polymer and crosslinker react to form a three dimensional gel network, reducing the effective permeability of these zones. Displacing fluids injected after the treatment are diverted into the previously unswept, low permeability zones resulting in additional oil recovery and less water production. Gel treatments applied in production wells can also reduce water production and increase oil production although the mechanisms are not as well defined.

One widely used gel system is an aqueous solution of partially hydrolyzed polyacrylamide and a chromium(III) salt. Chromium(III) forms a complex ion in solution and reacts by a ligand-exchange reaction with the carboxylate, or hydrolyzed, groups on the polymer molecules to form crosslinks resulting in a network or gel. These reactions are described by

$$Cr(L)_n + P1\text{-}CO_2^- \rightarrow Cr(L)_{n-1}(P1\text{-}CO_2^-) + L \qquad \text{Eq. 2.1}$$

and

$$Cr(L)_{n-1}(P1\text{-}CO_2^-) + P2\text{-}CO_2^- \rightarrow (P2\text{-}CO_2^-)Cr(L)_{n-2}(P1\text{-}CO_2^-) + L, \qquad \text{Eq. 2.2}$$

where L represents a ligand in the chromium complex and $-CO_2$ represents a carboxylate group on a polymer molecule (P1 or P2). The first reaction of polymer P1 with the chromium complex is called the uptake reaction. The reaction of a second polymer, P2, with the chromium complex creates a crosslink between the polymers and is termed the crosslink reaction.

Partially hydrolyzed polyacrylamide (HPAM) is a linear polymer with amide and carboxylate side groups. The reactivity of HPAM is dependent on the fraction of carboxylate side groups that is described as the degree of hydrolysis, usually stated as a percentage value. The degree of hydrolysis for HPAMs used to form gels ranges between 2 and 20%. Gel times are shorter (faster reaction rates) with increased carboxylate content of the HPAM.

The reactivity of the chromium(III) complex ion at a given temperature is dependent on its structure and the types and concentrations of ligands [Lochart and Albonico, 1994]. Generally, inorganic salts are present as chromium monomers and have relatively short gel times. Chromium acetate is a preferred crosslinker for lower temperature reservoirs due to its relative inertness to reservoir conditions and relatively long gel times that are due to the stronger affinity of acetate as a ligand as compared to inorganic ligands. The structure of chromium acetate complex ion is affected by pH and age. Tackett [1989] found that at pH values below 4.5 and

after sufficient time a green cyclic chromium trimer was the dominant species in solution. As pH of the solution is increased, hydroxyl groups replace the bridging acetate group. The cyclic structure is retained up to pH 5.5. Further increase in pH converts the cyclic trimer to a linear trimer. Hydroxyl ligands are substituted with increased pH and precipitation of the complex occurs at higher pH values. The trimer species were the dominant structures. Other structures were indicated including chromium oxylate in the commercial product from McGean-Rohco, the source of chromium acetate used in this work.

Hydrogen ion is involved in the gelation reactions and its role is complex and is not explicitly described in Eqs. 2.1 and 2.2. Gel times for gelants prepared with inorganic chromium salts decrease sharply with increase in pH between 4 and 5.5 of the gelant [Albonico et al., 1992]. Inorganic chromium salts precipitate and are not available for crosslinking at pH values above 5.5. Gel times are longer and the influence of pH is less for chromium(III) acetate gelants as compared to systems prepared with inorganic chromium salts. Acetate systems also tolerate higher pH values before detrimental precipitation occurs. Longer gel times for longer injection times and tolerance of higher pH values are favorable characteristics of the acetate system for field applications.

Several studies [Hamm et al., 1958; Banerjea and Chaudhari, 1968; Khan and Ud-din, 1981; Hartley, 1970; Hunt, 1987; Montanari et al., 1994; Dona, 1993] of the kinetics of the Cr(III)-carboxyl reaction have been conducted using different sources of carboxyl groups and two inorganic chromium salts. The data were fitted to empirical rate equations that gave the reaction orders for the concentrations of Cr(III), carboxyl group and hydrogen ion. Experimental conditions and the reaction orders for theses studies are given in Table 2.1. The reaction orders for each reactant are in general agreement.

The objective of this study was to determine the rate of the reaction between Cr(III) and polyacrylamide when the chromium is supplied as the acetate salt. This reaction, referred to as the uptake reaction, is known to be a function of reactant concentrations, salinity, temperature, and solution pH. An experimental approach was based on the use of a centrifugal filter device to separate solvent from the gelant. The solvent was analyzed for unreacted chromium. A reaction rate model for chromium uptake was developed. This chapter is based on a MS thesis by Jain [2004].

The rate of the reactions between chromium and the polymer control the development of the network structure which, in turn, controls the injection time or distance that a gelant/gel can be place from a wellbore. Kinetic models of the reactions involved provide a basis for treatment design and placement strategies.

Experimental Materials and Procedures

Experiments were conducted to determine the effect of chromium concentration, polymer concentration and pH on the reaction of chromium acetate and HPAM (uptake reaction) in aqueous 1.0% KCl solvent at a temperature of 25°C. The reaction was followed by determining the concentration of unreacted chromium in the solvent as a function of time. Solvent was separated from an aliquot of the reacting gelant using a centrifugal filtration device. A reaction

Table 2.1 – Experimental conditions and reaction orders for previous studies on the Cr(III)-carboxyl reaction.

Reference	Cr(III) source	Carboxyl source	Brine salt	pH	Temp. (°C)	Cr(III) reaction order	Carboxyl reaction order	H^+ reaction order
Hamm et al.	$Cr(NO_3)_3$	glycolic acid ($HOCH_2CO_2H$)	$KClO_4$ or KNO_3	3.5–6.0	25	+1	0	-1
Banerjea and Chaudhuri	$Cr(ClO_4)_3$	Glycine ($H_2NCH_2CO_2H$)	$NaClO_4$	3.0–3.8	40	+1	+1	-1
Khan and Kabir-Ud-Din	$Cr(NO_3)_3$	Glycine	KNO_3	3.4–4.5	45	Cr(III) held constant	+1	-1
Hartley	$CrCl_3$	Carboxyl group on wool protein	KNO_3	1.7–2.5	93	+1	+1	not determined
Hunt	$Cr(NO_3)_3$	PAAm (2.3 mole% carboxyl)	KNO_3	4.0–5.5	25	+1.32	+0.8	-1
Montanari et al.	$Cr(NO_3)_3$	PAAm (7.5 mole% carboxyl)	$NaClO_4$	4.2–4.9	20	+1	+0.8	-0.8
Dona	$Cr(NO_3)_3$	PAAm (2.3 mole% carboxyl)	$NaClO_4$	4.0	25	+1	+1	-1

rate model of HPAM-Cr(III) uptake reaction was developed through regression of the experimental data.

Gelants were prepared by mixing water and stock solutions of HPAM, chromium acetate and sodium azide. Sodium azide was used as a bactericide at a concentration of 10 mg/kg in the gelant. The pH was measured and sometimes adjusted with drops of solutions of HCl or KOH. Gelants were kept at 25°C by a temperature-controlled water bath. Samples were removed periodically for viscosity and pH measurements and for analyses of unreacted chromium. For chromium analysis, solvent was removed from the sample with a Centricon® Plus-20 Centrifugal Filter Device (Millipore Corp.) rated at a 5,000 nominal molecular weight cutoff (MWCO). The centrifugal filters were cleaned (spun with water) before use to remove trace amounts of glycerine that is used as a humectant. The samples were spun in a centrifuge at a radius of 9 cm and at a speed of 2700 rpm for 15 minutes. The volume of filtrate decreased with longer reaction times. The mass of filtrate and retentate were measured. Chromium concentrations were determined for the filtrate, retentate and for the original gelant charged to the filter device. Chromium material balances showed that the amount of chromium removed after the centrifugation was usually within 2% of the chromium initially charged. Total organic carbon measurements were conducted on the filtrate to determine the amount of polymer that passed through the centrifugal filter devices.

Chromium concentrations were determined by oxidizing Cr(III) to Cr(VI) and measuring the absorbance with a UV-VIS spectrometer at a wavelength of 373 nm and applying a calibration curve. Oxidation of the chromium was accomplished by combining equal portions of the sample, 3% hydrogen peroxide and 1M KOH solutions and heating the mixture for an hour at 87°C. The oxidized samples were diluted to chromium concentrations between 5 and 10 ppm for absorption measurement. Relative standard deviations of less than 0.1% were typical for eleven absorbance measurements on a given sample.

Polymer concentrations were determined in the polymer stock solutions and in the filtrate from the centrifugal devices by determining the concentration of the total organic carbon (TOC). A Shimadzu-5000(A) TOC analyzer was used and calibrated with potassium hydrogen phthalate standards of known carbon concentrations and then calibrated with polymer standards that were prepared from the solid polymer. No provision was made for the active amount of polymer in the weighed solid samples. The determination of polymer concentrations in samples containing chromium (e.g. filtrates from the centrifugal filter devices) was complicated by the presence of additional carbon from acetate that was introduced with the chromium. In those cases, it was assumed that the molar concentration of acetate was 3.0 times the molar concentration of chromium (measured values) and the TOC measurements were adjusted to account for the acetate for the determination of polymer concentrations. The molar ratio of acetate to chromium was verified by TOC measurements on chromium acetate solutions.

A Brookfield digital viscometer (Model DV- I +) was used to monitor the viscosity and determine the gel time of the gelants. The gel time was defined as the time when the viscosity of the gel solution increases abruptly to a value greater than 1,000 cP at a shear rate of 2.25 s^{-1}. The temperature of the viscometer was controlled at 25°C.

Polymer stock solutions were usually prepared at concentrations of 10,000 mg/kg polyacrylamide (Alcoflood 935, Lot # A2247 BOV) and 2.00 wt.% KCl in water. Polymer stocks with alternate KCl concentrations were prepared for gelants with polymer concentrations other than 5,000 mg/kg. Solid polymer beads were added gradually to the vortex shoulder of the stirred, cold 2.0 % KCl solvent. The container was sealed and the mixture stirred for 3 days for complete dissolution of the polymer. The polymer solution was slightly cloudy after dissolution. The polymer solution was then pressure filtered through a glass fiber filter (1 micron pore size) at 10 psi. The filtered polymer solution was clear. The solution was then dialyzed exhaustively in 12,000-14,000 MWCO pore size regenerated cellulose membrane tubing against KCl solvent of the same KCl concentration. The dialysis removed the low molecular-weight polymers in order to minimize the amount of polymer that would pass through the centrifugal filter device. The solvent-to-polymer solution ratio for the dialysis was approximately 30:1 by volume. The solvent was stirred continuously at low speed and was changed each day for three days. Carbon concentration was measured in each solvent batch. No carbon was detected in the solvent (dialysate) removed from the second and third batch. The polymer concentration in the dialyzed solution was determined as described above.

Chromium stock solutions at concentrations of 500 mg/kg or 1000 mg/kg were prepared by diluting an aqueous solution of 50% chromium(III) acetate (McGean Rohco, Inc.; Lot # 40086816) with water. Aqueous stock solutions of sodium azide were prepared at a

concentration of 1,000 mg/kg. Water purified by reversed osmosis, filtration, and deionization (> 18 MΩ-cm) was used in all solutions.

Solution preparation was conducted on a weight basis. Concentration units of mg/kg, or ppm, represent the mass of a component per mass of the solution. Density of a gelant containing 5,000 mg/kg HPAM, 200 mg/kg chromium (acetate salt) and 1.0 wt.% KCl was 1.0054 g/mL at 25°C.

The Kinetic Model and Data Processing

The uptake reaction of chromium by HPAM was followed by determining and mathematically modeling the concentration of unreacted chromium in the gelant. The uptake reaction was assumed to be a reaction between a chromium trimer complex (cyclic or linear form) with the carboxylate group on the HPAM. Stoichiometry of the reaction was represented by

$$Cr_3 \; + \; P\text{-}CO_2^- \; \rightarrow \; P\text{-}\,CO_2^-\text{-}Cr_3\,, \qquad \text{Eq. 2.3}$$

where Cr_3 represents chromium trimer ion, P-CO_2 represents a carboxylate group on a polymer molecule and P- CO_2^--Cr_3 is the reaction product. Based on Eq. 2.3, an empirical rate expression for the disappearance of the unreacted Cr(III) trimer in the gelant is given by

$$r_{Cr3} = -\frac{\mathrm{d}C_{Cr3}}{\mathrm{d}t} = k\,C_{Cr3}^{a}[(C_{carb})_0 - ((C_{Cr3})_0 - C_{Cr3})]^b\,C_H^c\,, \qquad \text{Eq. 2.4}$$

which includes the dependence of the hydrogen ion concentration. Participation of hydrogen ion in the reaction (Eq. 2.3) is not known but its effect is well documented [Hamm et al., 1958; Banerjea and Chaudhari, 1968; Khan and Ud-din, 1981; Hunt, 1987; Montanari et al., 1994; Dona, 1993].

Data from the series of experimental runs were processed and applied in Eq. 2.4 to regress values of the reaction rate constant, k, and the reaction orders, a, b and c. Data were processed by the following procedures and assumptions.

The pH of the gelant was measured and the chromium concentration in the filtrate from the centrifugal device was determined at selected reaction times during a gelation experiment. Polymer concentration in the filtrate was also determined since it was found that small amounts of polymer passed through the filter. Chromium concentrations measured in the filtrate were corrected for the amount of chromium that was attached, or reacted with, the polymer. Measured chromium concentrations were converted to unreacted chromium trimer concentration by

$$C_{Cr3} = \frac{C_{CrS}}{1000\,M_{Cr3}}\left[1 - \frac{1-(C_{CrF}/C_{CrS})}{1-(C_{PF}/C_{PS})}\right]. \qquad \text{Eq. 2.5}$$

Eq. 2.5 was derived from a material balance on chromium and polymer in the centrifugal filter device due to the chromium that passed through the filter by being attached and/or reacted with the polymer that passed through the filter. Assumptions used in the material balance were (1) the concentrations of unreacted chromium in the filtrate and gelant were equal, and (2) the mass ratio of reacted chromium to polymer was equal in the filtrate and gelant. Derivation of the material balance is given in the Appendix.

The derivative term in Eq. 2.4, $\mathrm{d}C_{cr3}/\mathrm{d}t$, was determined by curve-fitting the C_{Cr3} *–time* data (Levenberg-Marquardt method in Polymath software) to

$$C_{Cr3} = A e^{Bt} \qquad \text{Eq. 2.6}$$

and then using the regressed coefficients, A and B, to calculate the derivative term by

$$\frac{dC_{Cr3}}{dt} = B A e^{Bt} . \qquad \text{Eq. 2.7}$$

Hydrogen ion concentrations, C_H, were calculated from the measured pH values according to

$$C_H = 10^{-pH} . \qquad \text{Eq. 2.8}$$

Eq. 2.4 gives the carboxylate concentration, C_{carb}, as $[(C_{carb})_0 - ((C_{Cr3})_0 - C_{Cr3})]$, where C_{carb} decreases with reaction with the chromium trimer on a mole-to-mole basis. No provision was provided for the decrease in C_{carb} due to the crosslinking reaction. The initial carboxylate concentration, $(C_{carb})_0$, was determined from the initial polymer concentration (measured by the TOC method described above), a degree of hydrolysis of 10% (measured in-house by a titration method) and assuming sodium was the cation associated with the carboxylate group of the polymer.

Processed data at each measurement time for all of the runs were regressed to determine the rate constant and the three reaction orders of Eq. 2.4. The regression was performed with Polymath© software (http://www.polymath-software.com) using the Levenberg-Marquardt method which minimizes the sum of squares of a function that depends on a common set of parameters.

The kinetic model, Eq. 2.4 with the regressed parameters, was integrated numerically to give unreacted chromium trimer concentrations as a function of time for each run. The model values were plotted with the data to assess the model fit. To accomplish the numerical integration, the pH data of each run were curve fitted to various functions of time to provide hydrogen ion concentrations at each time step of the integration. The RK-56 method in Polymath© was used for the integration. RK-56 is a fifth-order Runge-Kutta method using coefficients given by Verner [1978].

Results and Discussion

Three series of runs were conducted to determine the effects of initial concentration of chromium (acetate salt), initial concentration of HPAM and initial pH on the rate of reaction between chromium acetate and HPAM. Gelant compositions and the gel time determined by viscosity measurements are show in Table 2.2. Concentrations in the table are given by the commonly used weight/weight units. Wide ranges of chromium and HPAM concentrations were studied in Series I and II. The pH range in Series III was limited to an upper value of 5.5 due to difficulty in maintaining a stable pH at higher values.

Gel times for the runs decreased with increased chromium concentration, polymer concentration and initial pH values. Small changes in pH values occurred during gelation as shown by the initial and final values given in Table 2.2. The values of chromium uptake and pH at the gel time in Table 2.2 were determined from lines regressed through the data. Chromium uptake and pH measurements were conducted up to the vicinity of the gel time.

Unreacted chromium trimer concentrations, C_{Cr3} in units of moles/kg, for Series I runs that were conducted with different initial chromium concentrations are shown in Figure 2.1 as a function

Table 2.2 – Gelant composition, gel time and amount of chromium reacted at gel time.

Series	Gelant Compostion*			Gel Time (h)	Cr Uptake at gel time (mg/kg)	pH at gel time
	Cr (mg/kg)	Polymer (mg/kg)	Initial pH			
I Cr Conc.	252	5410	4.82	18	41	4.75
	201	5010	4.93	19	36	4.86
	150	4900	4.91	25	30	4.84
	100	5040	4.87	31	22	4.85
	101	4860	4.87	31	22	4.84
	102	4980	4.89	33	23	4.87
	75.5	5520	4.88	41	20	4.84
	50.6	5040	4.94	61	18	4.93
	20.7	5000	4.91	140	10.2	4.96
II Polymer Conc.	201	7530	4.92	12	30	4.86
	202	6330	4.92	16	30	4.88
	202	3550	4.90	42	40	4.81
	201	2010	4.94	No gel in 17 days.		4.81
III pH	201	4800	5.51	16	34	5.39
	200	4940	5.22	16	35.5	5.13
	202	4870	4.62	25	34	4.62
	200	4890	4.32	28	31	4.34
	202	4800	4.02	34	33	4.08

All gelants contained 1.00 wt % KCl.

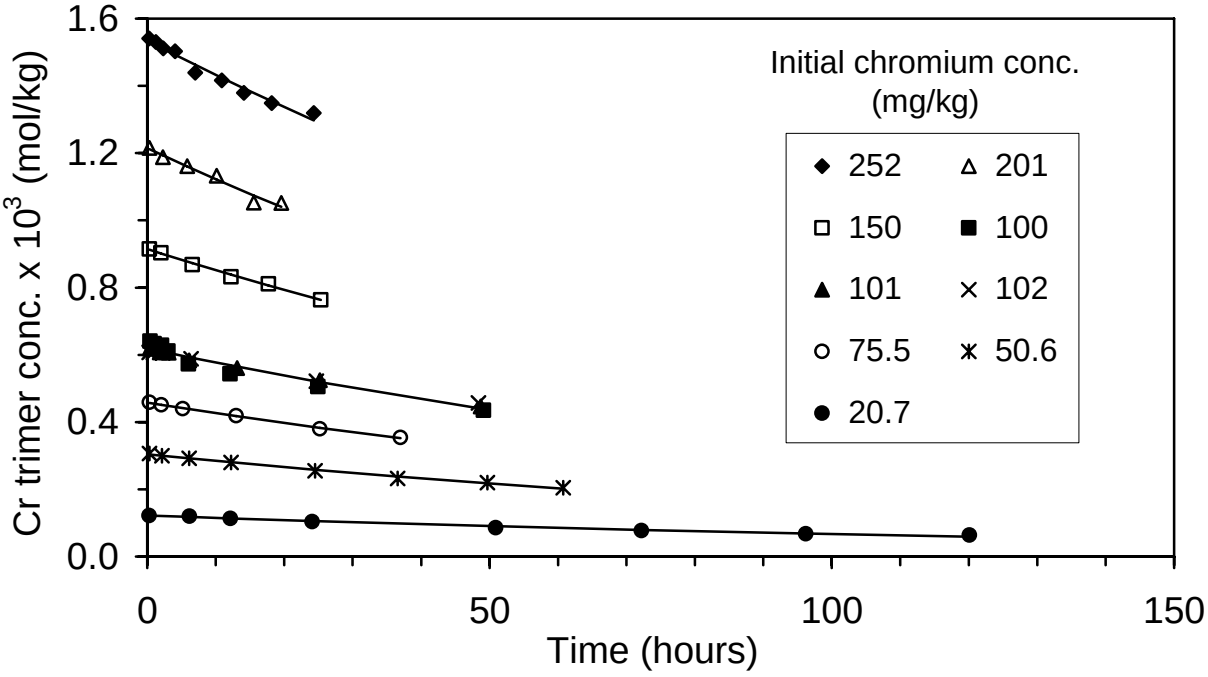

Figure 2.1 – Data and curve fit to unreacted chromium trimer concentration as a function of time for different initial chromium concentrations; ~5000 mg/kg polymer conc. and a pH of ~4.9.

of time. Regressed lines (Eq. 2.6) for each initial chromium concentration are also shown in the figure. Three runs were conducted at an initial chromium concentration of 100 ppm. (C_{Cr3} = 0.641×10^{3} g-moles/kg) and one line was regressed using the combined data. The regressed lines were extrapolated to zero time and the values of the chromium concentration were always about 5% lower than the measured initial chromium concentration in the gelant. Tests were conducted that showed neglible losses of chromium to the centrifugal filter device. The 5% lower extrapolated chromium concentrations at zero time were also observed in an earlier investigation [Hunt et al., 1989] that used different experimental techniques to study the kinetics of the reaction between polyacrylamide and chromium nitrate. The agreement between that study and this work indicate a real phenomenon that possibly is a fast initial reaction between chromium and polymer.

Unreacted chromium trimer concentrations, C_{Cr3}, for Series II and III Runs that were conducted with different initial polymer concentrations and initial pH values are shown as functions of time in Figures 2.2 and 2.3 along with the regressed lines. The extrapolated values of chromium concentration at zero time for Series II and III were also about 5% lower than the measured chromium concentration in the gelant.

The rate constant and reaction orders for the equation of the reaction rate were regressed from the data for all the runs in Series I, II and III. The results are given by

$$r_{Cr3} = -\frac{\mathrm{d}C_{Cr3}}{\mathrm{d}t} = k\, C_{Cr3}^{1.01}\,[(C_{carb})_0 - ((C_{Cr3})_0 - C_{Cr3})]^{0.84}\, C_H^{-0.39}, \qquad \text{Eq. 2.9}$$

where k = 6.2 x 10^{-3} h^{-1} $(mol/kg)^{-0.46}$ The regression yielded an R^2 of 0.979. Reaction orders for chromium trimer (acetate salt) and polymer (carboxyl group) were approximately one, similar to the reaction orders determined for the reaction of inorganic chromium salts with carboxylates (Table 2.1). The reaction order for the hydrogen ion was -0.39. This value was significantly different than the values for systems with inorganic chromium salts (about -1) and corresponded to the weaker effect that pH has on the gelation of systems prepared with chromium acetate (organic salts). This is consistent with the observations made by Lockhart [1991].

Eq. 2.9 was integrated numerically for all the runs using the initial conditions except the initial chromium concentrations were reduced by 5% to reflect the observation that the extrapolation of the data to zero time yielded an initial concentration that was about 95% of the measured value. Comparisons of the integration of Eq. 2.9 and the data are shown in Figures 2.4 through 2.6.

A master curve was constructed where unreacted chromium(III) concentration was plotted versus time for all runs in Series I experiments that were conducted at different initial chromium concentrations. The rate equation (Eq. 2.9) was simplified by assuming a constant polymer concentration of 5000 mg/kg (6.81 x 10^{-3} mol carboxylate/kg) and a constant pH value of 4.9 ($[H^+]$ = 1.26 x 10^{-5} mol/kg) during the course of the reaction and the order of the reaction with respect to chromium(III) to be one to give

$$(r_{Cr3}) = -\frac{\mathrm{d}C_{Cr}}{\mathrm{d}t} = 0.0076 C_{Cr3}\ . \qquad \text{Eq. 2.10}$$

Integration of Eq. 2.9 gives

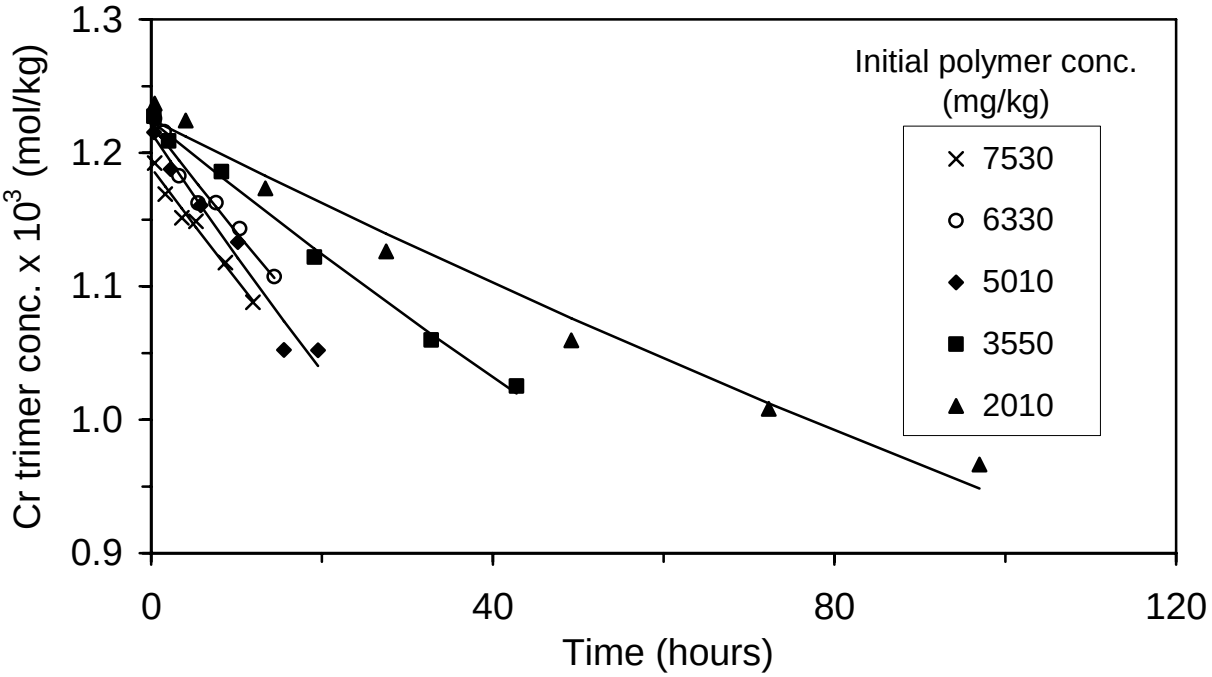

Figure 2.2 – Data and curve fit of unreacted chromium trimer concentration as a function of time for different initial polymer concentrations; ~200 mg/kg chromium conc. and a pH of 4.9.

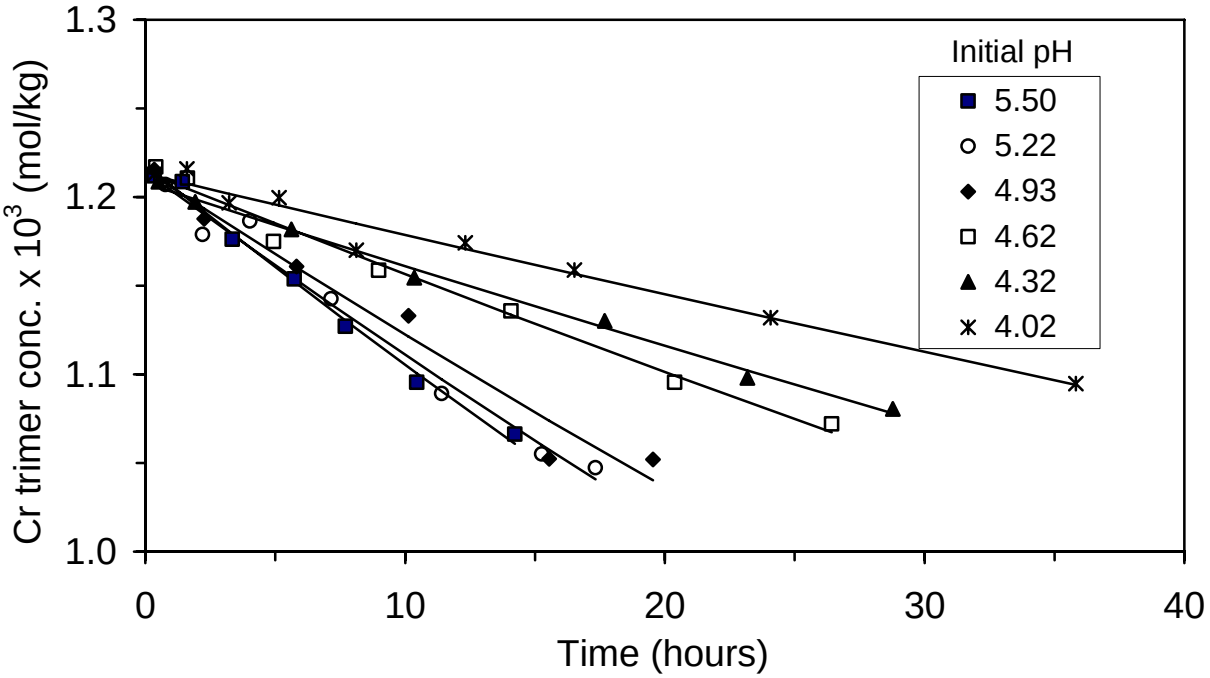

Figure 2.3 - Data and curve fit of unreacted chromium trimer concentration as a function of time for different initial pH values; ~200 mg/kg chromium conc. and a pH of 4.9.

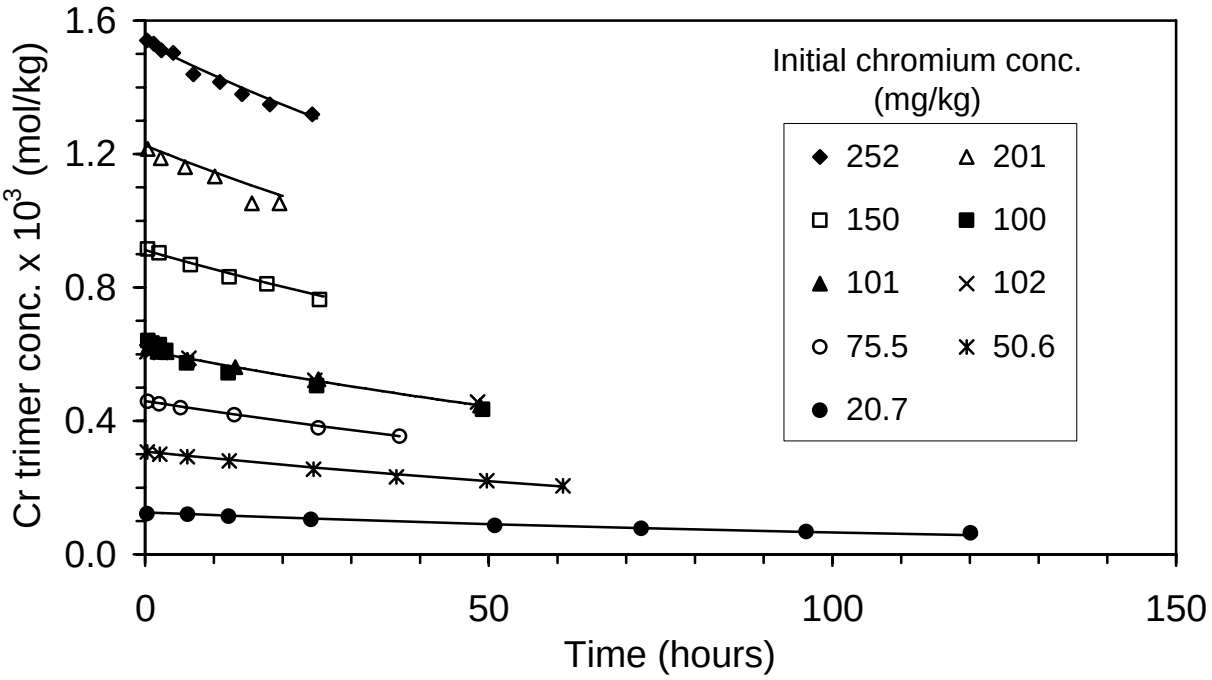

Figure 2.4 – Comparison of the results of the integration of the rate equation with data of the unreacted chromium trimer concentration as a function of time at different initial chromium concentrations; ~5000 mg/kg polymer conc. and a pH of ~4.9.

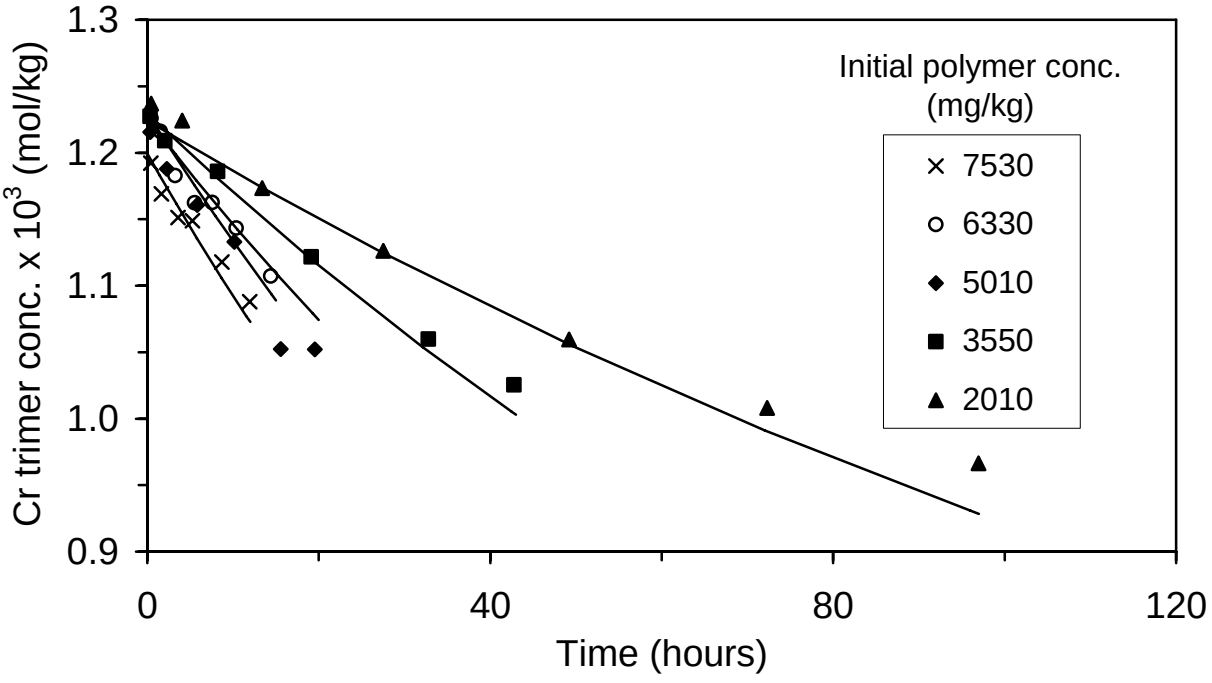

Figure 2.5 – Comparison of the results of the integration of the rate equation with data of the unreacted chromium trimer concentration as a function of time at different initial polymer concentrations; ~200 mg/kg chromium conc. and a pH of 4.9.

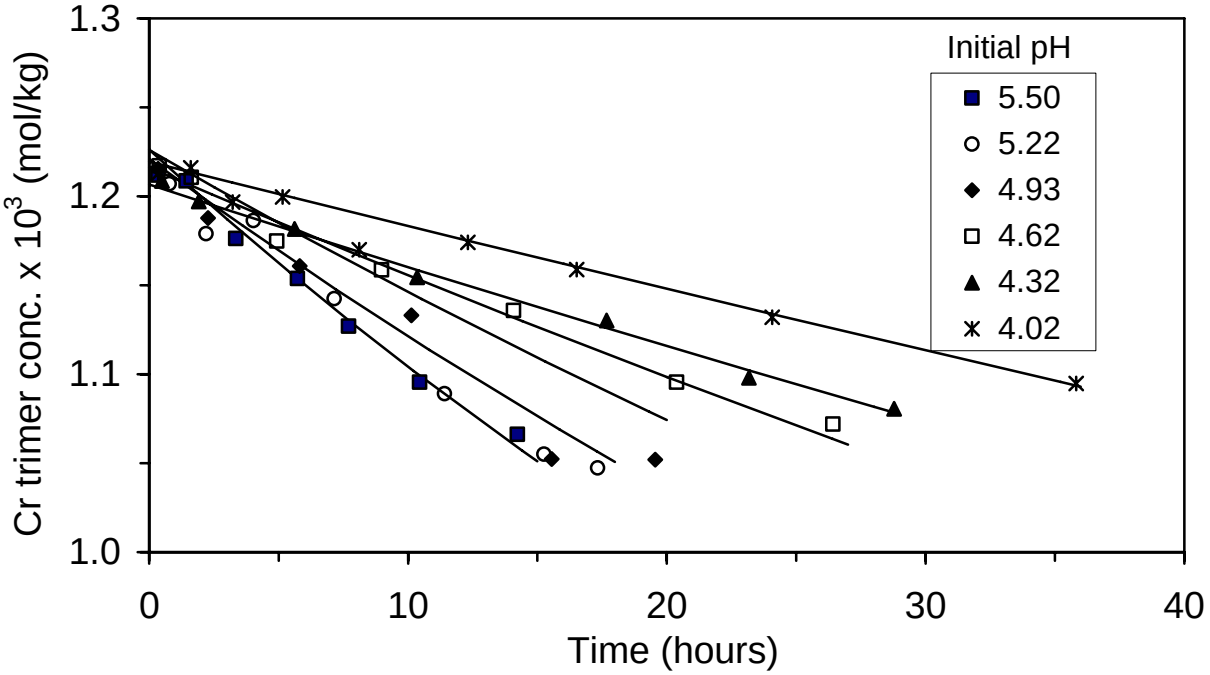

Figure 2.6 – Comparison of the results of the integration of the rate equation with data of the unreacted chromium trimer concentration as a function of time at different initial pH values; ~200 mg/kg chromium conc. and a pH of 4.9.

$$C_{Cr3} = C_{Cr3\,0}\, e^{-0.0076\,t} \quad . \qquad \text{Eq. 2.11}$$

Eq. 2.11 is plotted in Figure 2.7 along with data from Series I experiments. Data from the experiment with the highest initial chromium(III) concentration (252 mg/kg) were plotted against time. Data from experiments with lower initial chromium(III) concentrations were plotted on a shifted time axis. The time shift for each data set was the time taken for the unreacted chromium(III) concentration in the reacting mixture to reach the first concentration value measured in that particular set and was calculated gy Eq. 2.11. The fit of the master curve to the data indicates that the order of reaction for chromium and the reaction rate constant obtained are consistent for all data sets.

The amount of chromium reacted at the gel time for each run is listed in Table 2.2 and is plotted in Figure 2.8 for Series I runs as a function of the initial chromium concentration. Less chromium was reacted at the gel time for lower initial chromium concentrations. Only 10 mg/kg of chromium reacted with the polymer at the gel time for the run with the lowest initial chromium concentration of 20 mg/kg showing that less than 10 mg/kg of chromium is required to gel a typical 5,000 mg/kg polymer solution. Data from Series I runs were also correlated in Figure 2.9 where the reciprocal of the gel time is plotted as a function the amount of chromium reacted at the gel time. Extrapolation of the data to an infinite gel time (1/[gel time] = 0) gave a value of chromium reacted of about 5.5 mg/kg, a value indicative of the minimum amount required for gelation.

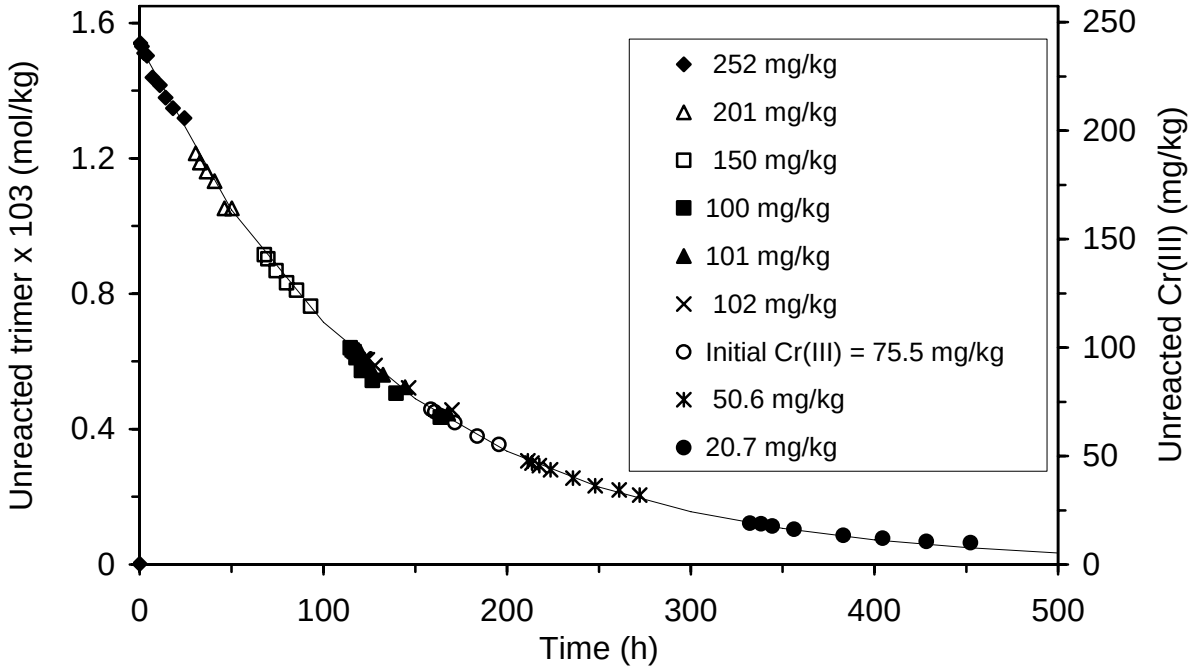

Figure 2.7 – Master curve for Series I experiments.

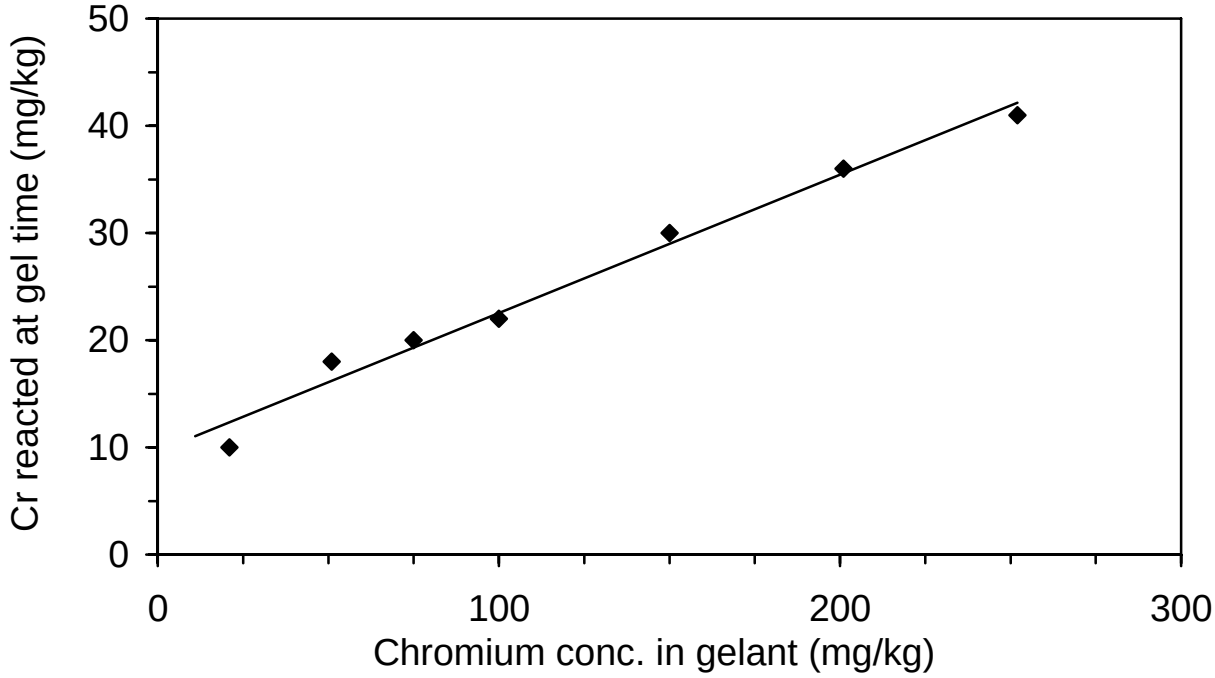

Figure 2.8 – Concentration of reacted chromium at the gel time as a function of the chromium concentration in the gelant; ~5000 mg/kg polymer conc. and a pH of ~4.9.

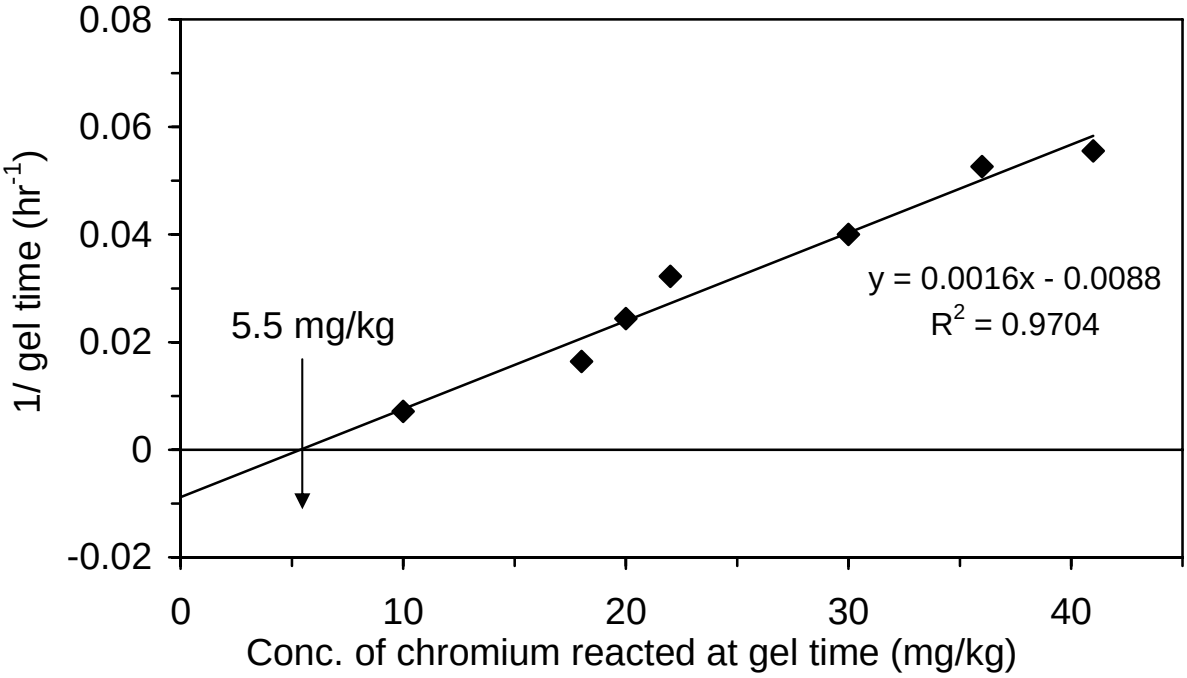

Figure 2.9 – Correlation of the reciprocal of the gel time with concentration of reacted chromium at the gel time; ~5000 mg/kg polymer conc. and a pH of ~4.9.

Conclusions

The following conclusions from this study of the uptake of chromium by HPAM are applicable over the range of conditions that were investigated.

1. The rate of the reaction between chromium acetate and hydrolyzed polyacrylamide was described well by

$$r_{Cr3} = -\frac{dC_{Cr3}}{dt} = k\, C_{Cr3}^{1.01}\,[(C_{carb})_0 - ((C_{Cr3})_0 - C_{Cr3})]^{0.84} C_H^{-0.39}, \qquad \text{Eq. 12}$$

   where the value of the reaction rate constant, k, was 6.2 x 10^{-3} h^{-1} $(mol/kg)^{-0.46}$. The above rate expression was regressed for chromium trimer concentrations between 20 mg/kg (1.3 x 10^{-4} mol/kg) and 250 mg/kg (1.6 x 10^{-3} mol/kg), HPAM concentrations from 2000 mg/kg to 7500 mg/kg and pH values from 4.0 to 5.5. Conditions used in the development of the rate expression were a temperature of 25°C, 10% degree of hydrolysis of the HPAM, aqueous solvent containing 1% KCl and an acetate-to-Cr(III) mole ratio of 3.0.
2. The orders of the reactions with respect to the concentrations of Cr(III) and carboxylate groups on polymer were comparable to those found in studies of the reaction using inorganic salts of Cr(III). The absolute value of the order of reaction with respect to hydrogen ion concentration was less than that for inorganic chromium salts which indicated the weaker effect of pH on the reaction rate.
3. The minimum concentration of chromium required to gel a solution containing 5,000 mg/kg HPAM was between 5 and 10 mg/kg.

Nomenclature

A, B = regressed parameters in Eq. 2.6 to fit data,
a,b,c = order of reactions with respect to chromium trimer, carboxylate groups and hydrogen ion.
C_{carb} = concentration of unreacted carboxylate groups, mol/kg.
C_{CrF} = concentration of chromium in filtrate, mg/kg.
C_{CrS} = concentration of chromium in sample, mg/kg.
C_{Cr3} = concentration of unreacted chromium trimer, mol/kg,
C_H = concentration of hydrogen ion, mol/kg.
C_{PS} = concentration of polymer in sample, mg/kg.
C_{PF} = concentration of polymer in filtrate, mg/kg.
f_s = *fraction of chromium(III) reacted in sample.*
k = reaction rate constant, $h^{-1}(mol/kg)^{-0.46}$.
M_{Cr3} = molar mass of chromium trimer (56 g/mol).
M_S = mass of sample, kg.
M_F = mass of filtrate, kg.
r_{Cr3} = rate of chromium uptake, mol/(kg h).
t = reaction time, h.
0 = subscript denoting initial concentration.

References

Albonico, P., Burrafato, G. and Lockhart, T.P.: "Polyacrylamide Gels Formed with Cr^{+3} Ion and $Cr(Acetate)_3$: Thermodynamically and Kinetically Controlled Crosslinking Reactions," *Journal Of Polymer Science: Part A: Polymer Chemistry,* **30**, No. 6 (1992) 1071.

Banerjea, D. and Chaudhari, S.D.: "Kinetics Studies on the Formation of Metal Chelates-II: Reaction of Hexa-aquo-chromium(III) Ion with Glycine and the Nature of the Product Formed in Weakly Acidic Aqueous Solution," *J. Inorganic Nuclear Chemisty,* **30** (1968) 871.

Dona, C.L.: "An Experimental Study of the Uptake and Gelation Reactions of CR(III) Oligomers with Polyacrylamide," PhD dissertation, The University of Kansas, Lawrence, KS (1993).

Hamm, R.E., Johnson, R.L. Perkins, R.H. and Davis, R.E.: "Complex Ions of Chromium. VIII. Mechanism of Reaction of Organic Acid Anions with Chromium(III)," *J. American Chemical Society*, **80** (1958) 4469.

Hartley, F.R.: "Studies in Chrome Mordanting: V. Kinetics and Mechanism of the Interaction of Chromium(III) Salts with Wool", *Australian J. Chem.*, **23** (1970) 275.

Hunt, J.A.: "An Experimental Study of the Kinetics of the Crosslinking Reaction Between Chromium(III) and Polyacrylamide," PhD dissertation, The University of Kansas, Lawrence, KS (1987).

Hunt, J.A., Young, T.S., Green, D.W. and Willhite, G.P.: "A Study of Cr(III)-Polyacrylamide Reaction Kinetics by Equilibrium Dialysis," *AIChE Journal,* **35**, No.2 (Feb. 1989) 250.

Jain, R.: "An Experimental Study of the Kinetics of the Chromium(III) Acetate–Hydrolyzed Polyacrylamide Uptake Reaction," MS thesis, The University of Kansas, Lawrence, KS (2004).

Khan, A.K. and Ud-din, K.: "Anation of Hexaaquochromium(III) by Glycine", *J. Inorganic Nuclear Chemistry,* **43** (1981) 1082.

Lockhart, T.P.: "Chemical and Structural Studies on Cr+3/Polyacrylamide Gels," paper SPE 20998 presented at the SPE Intl. Symp. on Oilfield Chemistry, Anaheim, CA (February 20-22, 1991).

Lockhart, T.P., Albonico, P.: "New Chemistry for the Placement of Chromium(III)/Polymer Gels in High-Temperature Reservoirs," *SPE Production and Facilities* **9**, No. 4 (November 1994) 273.

Montanari, L., Scotti, R. and Lockhart, T.P.: " Kinetics and Mechanism of the Reaction of Hydrated Chromium(III) with Partially Hydrolyzed Polyacrylamide," *Macromolecules*, **27** (1994) 3341.

Tackett, J.E.: "Characterization of Chromium(III) Acetate in Aqueous Solution," *Applied Spectroscopy,* **43** (1989) 490-499.

Verner, J.H.: "Explicit Runge-Kutta Methods with Estimates of the Local Truncation Error," *SIAM Journal of Numerical Analysis,* **15**, No. 4 (Aug. 1978) 772.

Appendix

Determination of Un-Reacted Chromium Concentration using the Centrifugal Filter Device

Small concentrations of polymer passed through the centrifugal filter device. Chromium concentrations measured in the filtrate were corrected for the amount of chromium that was attached or reacted with the polymer in order to determine the concentration of un-reacted chromium in the solvent. Material balances around the centrifugal filter device were developed using the following assumptions: (1) un-reacted chromium concentrations were the same in the sample and filtrate (and retentate), and (2) the mass ratio of reacted chromium to polymer is the same in the sample and filtrate (and retentate).

A sample of gelant was placed in the top compartment of the filter device and centrifuged, resulting in a retentate that remained in the top compartment and a filtrate that passed through the filter. The following definitions were used to describe the mass quantities shown in Figure 2.A1.

M = mass of solution, kg
C_{Cr} = concentration of chromium, mg/kg
C_P = concentration of polymer, mg/kg
f_S = fraction of Cr(III) reacted in sample.

subscripts

Cr = chromium
P = polymer

S = sample
R = retentate
F = filtrate

Mass balances on sample
The mass of chromium reacted in the sample (mg) equals

$M_S C_{Cr\,S} f_S$.

The concentration of un-reacted chromium in the sample (mg/kg) equals

$\frac{M_S C_{Cr\,S} - M_S C_{Cr\,S} f_S}{M_S} = C_{CrS}(1 - f_S)$.

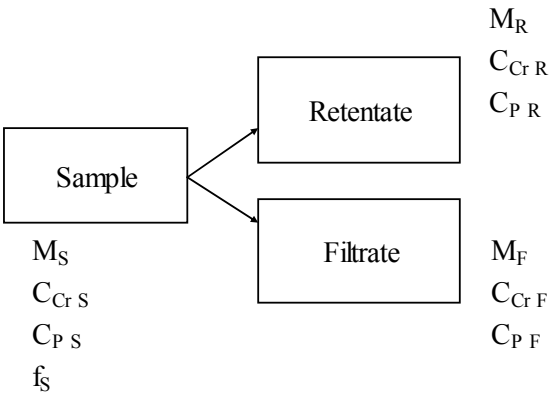

Figure 2.A1 – Variables used in mass balances on the centrifugal filter device.

The mass of chromium reacted per mass of polymer equals

$\frac{M_S C_{Cr\,S} f_S}{M_S C_{P\,S}} = \frac{C_{CrS}}{C_{PS}} f_S$.

Mass balances on Filtrate
It was assumed that the un-reacted chromium concentration in the filtrate was the same as in the sample. This assumption makes the concentraion of un-reacted chromium in filtrate (mg/kg) equal to

$C_{CrS}(1 - f_S)$,

and the mass of un-reacted chromium in the filtrate (mg) equal to

$M_F C_{CrS}(1 - f_S)$.

A second assumption equated the mass ratio of reacted chromium to polymer in the sample to that in the filtrate. This gives the mass of reacted chromium in filtrate (mg) as

$M_F C_{PF} \frac{C_{CrS}}{C_{PS}} f_S$.

The total mass of chromium in the filtrate is equal to the sum of the masses of reacted and un-reacted chromium in the filtrate which is described by

$$M_F C_{CrF} = M_F C_{CrS}(1 - f_S) + M_F C_{PF} \frac{C_{CrS}}{C_{PS}} f_S \,. \qquad \text{Eq. 2.A1}$$

Division of Eq. 2.A1 by M_F and solving for f_S gives

$$f_S = \frac{1 - (C_{CrF} / C_{CrS})}{1 - (C_{PF} / C_{PS})} \,. \qquad \text{Eq. 2.A2}$$

The fraction of chromium reacted, f_S, was calculated by Eq. 2.A2 by measuring the concentrations of chromium and polymer in the Filtrate and knowing or measuring the concentrations of chromium and polymer in the original sample (gelant). The concentration of un-reacted chromium trimer in moles per kg, C_{Cr3}, was then determined by

$$C_{Cr3} = \frac{C_{Crs}}{1000 M_{Cr3}} (1 - f_S) \,, \qquad \text{Eq. 2.A3}$$

where M_{Cr3} is the molecular weight of chromium trimer (156).

Chapter 3

Modeling the Gelation Process of a Polyacrylamide-Chromium(III) Gel System Using the Theory of Branching Processes

Graduate Research Assistant: Min Cheng

Introduction

Aqueous gel systems produced by the crosslinking of partially hydrolyzed polyacrylamide (HPAM) with chromium(III) ions are used to improve volumetric sweep efficiency and reduce water production in oil reservoirs. Gelation is characterized by the growth of pre-gel aggregates. A pre-gel aggregate is defined as any soluble molecule containing one or more of the polymer molecules. Pre-gel aggregates continue to crosslink until they form a 3-dimensional network. Pre-gel aggregates formed during the in situ gelation are filtered and retained in the reservoir rocks, causing high flow resistance and impeding further penetration [McCool, et al., 1991; Bryant, et al., 1997]. Filtration is dependent on the size or molecular weight of pre-gel aggregates. A fundamental understanding of the pre-gel aggregate growth will improve the design of gel treatments.

A mathematical model to simulate the growth of pre-gel aggregates during the gelation of a polymer gel system was developed during the course of the project. In the annual report covering the second year of work[Willhite, et. al, 2004], the theory of branching processes (TBP) [Dusek, 1985, 1986, 1998, 2002; Huybrechts and Dusek, 1998] was applied to track the reaction process as a function of the conversion of the reactive sites on the polymer and/or chromium crosslinker. TBP Models I and II were developed to calculate the molecular weight quantities as a function of the conversion of the reactive sites up to a critical conversion that represents the gel point. The gel point is defined as the point where a sufficient number of reactions have occurred, such that one branched molecule with infinite molecular weight appears the first time. The gel point roughly corresponds to experimentally measured gel times. Derivations of the equations for TBP Models I and II are given in the appendices of Willhite, et al. [2004].

Models are usually more applicable when time, rather than conversion, is the independent variable. The TBP models were extended by the incorporation of a relationship between the conversion of functional groups (reactive sites on the molecules) and the reaction time based on a kinetic study of the chromium-polymer uptake reaction for a polyacrylamide-chromium(III) acetate gel system [Chapter 2 of this report and Jain, et al., 2004]. The TBP models and their kinetic extensions are described in the following section. The models compute the gel time of a particular system and the molecular weight averages and distributions of pre-gel aggregates as functions of reaction times (or conversions) and initial conditions (concentrations of polymer and crosslinker, molecular weight and degree of hydrolysis of the polymer, *etc*).

Several experimental methods were pursued to measure molecular weight quantities as a function of reaction time to verify the mathematical models. The methods result in two types of data, weight-average molecular weights and molecular weight distributions. Experimental procedures and results of a method to determine weight-average molecular weights are presented

and compared to the models in this chapter. Procedures and results of two methods to determine molecular weight distributions are presented in Chapters 4 and 5.

Models Simulating the Gelation of a HPAM – Chromium(III) Gel System

TBP Models I and II. TBP Model I provides mathematical expressions for the molecular weight averages and Model II provides expressions for the molecular weight distributions of pre-gel aggregates, both as a function of the *conversion* of the reactive sites on the molecules. Reactive sites on molecules are termed *functional groups* and the number of functional groups on a molecule is its functionality. Two general assumptions were applied in both models: (1) The functional groups have the same and independent reactivity. (2) There is no intra-molecular crosslinking (cyclization).

TBP Models I and II were developed based on different descriptions of the gel system. In Model I described by Willhite et al. [2004], the starting chemical system is composed of two components: partially hydrolyzed polyacrylamide (HPAM) molecules (Unit A; primary polymer) and chromium(III) acetate trimer (Unit B). The HPAM molecules are considered to be polydispersed, and the functional groups (carboxylate groups) along the polymer backbone are randomly distributed. Polydispersity of the primary polymer is described by known values of the number-average and weight-average molecular weights (or degree of polymerization). HPAM chains are crosslinked by the reactions between carboxylate groups and chromium acetate trimer that has f_B functional groups. A value of f_B equal to two was usually used to give the chromium trimer two sites to react with the carboxylate groups on the polymer. Alternating reactions are assumed, which means only HPAM can react with chromium trimer. No polymer-polymer or trimer-trimer reactions are allowed.

The gelation process is described by two ligand exchange reactions in Equations 3.1 and 3.2.

$$Cr_3(L)_n + P1\text{-}CO_2^- \rightarrow Cr_3(L)_{n-1}(P1\text{-}CO_2^-) + L \qquad \text{Eq. 3.1}$$

$$Cr_3(L)_{n-1}(P1\text{-}CO_2^-) + P2\text{-}CO_2^- \rightarrow (P2\text{-}CO_2^-)Cr_3(L)_{n-2}(P1\text{-}CO_2^-) + L \qquad \text{Eq. 3.2}$$

L represents any ligand like an acetate ion or water; P1 and P2 represent different polymer molecules and the $-CO_2^-$ represents one functional group on each of the polymers in these equations. The first reaction of a polymer (P1) with the chromium complex is commonly called the *uptake* reaction. The reaction of a second polymer (P2) with the chromium complex creates a crosslink between the polymers and is termed the *crosslink* reaction.

Examples of some of the important expressions of Model I are reviewed. The conversion at the gel point where the first appearance of a molecule with infinite molecular weight occurs is called the critical conversion. The critical conversions of carboxylate groups and the chromium functional groups are, respectively:

$$\alpha_{crit,A} = \left[\frac{1}{x_A(P_{w0}-1)(f_B-1)r_A}\right]^{1/2} \qquad \text{Eq. 3.3}$$

$$\alpha_{crit,B} = \left[\frac{r_A}{x_A(P_{w0}-1)(f_B-1)}\right]^{1/2} \qquad \text{Eq. 3.4}$$

where, $r_A = \frac{n_A x_A P_{n0}}{n_B f_B}$ Eq. 3.5

$r_A$is the initial molar ratio of carboxylate groups to chromium functional groups; $\alpha_{crit,A}$ and $\alpha_{crit,B}$ are the critical conversions of carboxylate groups and chromium functional groups at the gel point, respectively; f_B is the functionalities of chromium trimer, $f_B = 2$; n_A and n_B are the initial number fractions of polymer and chromium trimer, respectively; x_A is the degree of hydrolysis of primary polymer; P_{n0} and P_{w0} are the number- and weight- average degree of polymerization of the primary polymer, repectively.

The conversions of carboxylate groups and the chromium functional groups are related according to the following equation.

$$\alpha_B = r_A \alpha_A \quad \text{Eq. 3.6}$$

The number-average molecular weight of pre-gel aggregates as a function of α_B is:

$$M_{n-agg} = \frac{n_A M_{n0} + n_B M_B [1-(1-\alpha_B)^{f_B}]}{1 - n_B f_B \alpha_B - n_B (1-\alpha_B)^{f_B}} \quad \text{Eq. 3.7}$$

The weight-average molecular weight of the pre-gel aggregates is:

$$M_{w-agg} = \frac{M_w - w_B M_B (1-\alpha_B)^{f_B}}{1 - w_B (1-\alpha_B)^{f_B}} \quad \text{Eq. 3.8}$$

where

$$M_w = w_A M_{w0} + w_B M_B + \frac{1}{D}\begin{Bmatrix} w_A \left[M_{w0} x_A P_{w0} (f_B - 1) \alpha_A \alpha_B + M_B x_A P_{w0} \alpha_A \right] \\ + w_B \left[M_B x_A (P_{w0} - 1) f_B \alpha_A \alpha_B + M_{w0} f_B \alpha_B \right] \end{Bmatrix}, \quad \text{Eq. 3.9}$$

$$D = 1 - x_A (P_{w0} - 1)(f_B - 1) \cdot \alpha_A \alpha_B \quad \text{Eq. 3.10}$$

and w_A, w_B are the initial weight fractions of polymer and chromium trimer, respectively; M_{n0} and M_{w0} are the number- and weight-average molecular weight of the primary polymer, respectively. M_w can be also represented as a function of either α_A or α_B through the substitution of Equation 3.6.

The expressions given above for Model I simulate the various averages of molecular weight and the value of conversion at the gel point, or critical conversion. The critical conversion is dependent only on initial parameters of the gel system and the various molecular-weight averages are dependent on the initial parameters and conversion (independent variable).

In Model II described by Willhite et al. [2004], the gel system was simplified in that the starting reactant is polydispersed HPAM only, without the chromium crosslinker. Polymer chains are crosslinked hypothetically by the formation of bonds between two carboxylate groups on two different polymer molecules. The primary (initial) polymer chains follow a Schulz-Zimm distribution and the carboxylate groups are randomly distributed along the polymer molecules. Differential molecular weight distributions (or distributions of degree of polymerization) of pre-

gel aggregates are calculated as a function of the conversion of carboxylate groups, α, by Model II. The Schulz-Zimm distribution is given by

$$w(0,x) = \left[\frac{\sigma^{\sigma}}{P_{n0}{}^{\sigma+1}\Gamma(\sigma)}\right] x^{\sigma} \exp\left(-\frac{\sigma}{P_{n0}}x\right) \qquad \text{Eq. 3.11}$$

where x is the degree of polymerization of an x-mer; $w(0,x)$ is the initial weight fraction distribution of the primary polymer, or the differential weight fraction of an x-mer at conversion zero; Γ is the standard mathematical gamma function; and σ is a parameter related to polydispersity index of the polymer, PI, according to

$$PI = M_{w0}/M_{n0} = P_{w0}/P_{n0} = (\sigma+1)/\sigma \quad . \qquad \text{Eq. 3.12}$$

The critical conversion of functional (carboxylate) groups at the gel point, α_{crit}, is [Dusek, 1998]:

$$\alpha_{crit} = \frac{1}{x_A(P_{w0}-1)} \qquad \text{Eq. 3.13}$$

The differential weight fraction of an x-mer at conversion α, $w(\alpha,x)$, is given by Equation 3.14 [Vojta and Dusek, 1980],

$$w(\alpha,x) \approx x^{-1}\ln(2)\sum_{i=1}^{N} V_i W(\alpha,Z) = x^{-1}\ln(2)\sum_{i=1}^{N} V_i W(\alpha,\exp(-ix^{-1}\ln(2)) \qquad \text{Eq. 3.14}$$

where $Z = \exp(-p) = \exp(-ix^{-1}\ln(2))$,

$p = -ln(Z) = ix^{-1}\,ln(2)$,

$i = 1, 2, \ldots N$.

$$V_i = (-1)^{i+N/2} \sum_{k=[(i+1)/2]}^{\min(i,N/2)} \frac{k^{N/2}(2k)!}{(N/2-k)!k!(k-1)!(i-k)!(2k-i)!} \qquad \text{Eq. 3.15}$$

V_i are constants that only depend on i and an even number N. The symbol [ ] in Equation 3.15 designates the integer part of the number.

To solve Equation 3.14, values for $W(\alpha,Z)$ are required. $W(\alpha,Z)$ is calculated by Equation 3.16.

$$W(\alpha,Z) = \left[\frac{\sigma}{P_{n0}(\sigma/P_{n0} + p - \ln\beta)}\right]^{\sigma+1} \qquad \text{Eq. 3.16}$$

where $\beta = 1 - x_A + x_A(1-\alpha+\alpha u)$ and

$$u = \frac{1}{\beta}\left[\frac{\sigma}{P_{n0}(\sigma/P_{n0} + p - \ln\beta)}\right]^{\sigma+1} . \qquad \text{Eq. 3.17}$$

At any conversion α between 0 and α_{crit}, Equation 3.17 was solved numerically, followed by evaluation of $W(\alpha,Z)$ by Equation 3.16. Then $w(\alpha,x)$ was obtained by Equation 3.14 for N = 16.

The molecular weight distribution calculated by Model II can be translated to the conditions of the reaction system of Model I, which is a better representation of a gel polymer system, through Equation 3.18 when the number of crosslinks in both models is the same.

$$\alpha = \alpha_B^2 / r_A = r_A \alpha_A^2 \qquad \text{Eq. 3.18}$$

The utility of Equation 3.18 is the ability to determine the differential molecular weight distributions of pre-gel aggregates at any value of the conversions selected in Model I.

Kinetic Extension for Model I. A relationship between the conversion of functional groups and reaction time is required to transform the TBP models as functions of time. An empirical rate expression for the time dependence of the conversion of chromium functional group, α_B, was written based on the stoichiometry of the reaction where only one carboxylate group can react with only one chromium functional group.

$$\frac{\mathrm{d}\alpha_B}{\mathrm{d}t} = kC_{Af}{}^a C_{Bf}{}^b = k[C_{Af\,0} - C_{Bf\,0} \cdot \alpha_B]^a [C_{Bf\,0}(1-\alpha_B)]^b \qquad \text{Eq. 3.19}$$

where *a* and *b* are the reaction orders with respect to carboxylate group and chromium functional group, repectively; *k* is the reaction rate constant at 25 ^{o}C; *t* is reaction time in hours; C_{Af} and C_{Bf} are the concentrations of unreacted carboxylate groups and chromium functional groups in mol/kg, respectively; C_{Af0} and C_{Bf0} are the initial concentrations of carboxylate groups and chromium functional groups in mol/kg.

The kinetic extension of Model I relies on the regression of experimental data [Jain, et al., 2004] to determine the fitting parameters in Equation 3.19. Two relationships were required to apply Model I and Equation 3.19 to the experimental data. First, a relationship between the type of experimental data and Model I parameters was derived. This relationship includes a correction factor that addresses intra-molecular crosslinking that was measured in the experiments and not included in the model. Second, a relationship between α_B and time was required so that the left-hand side of Equation 3.19 could be evaluated.

The previous kinetic study of the chromium-polymer uptake reaction [Jain, et al., 2004] measured the concentration of *unreacted* chromium trimers as a function of time. This concentration in the Model I is given by Equation 3.20.

$$C_{B0} - C_{B0}(b_1 + b_2) = C_{B0} - C_{B0}[2(1-\alpha_B)\alpha_B + \alpha_B^2] = C_{B0}[1-(2\alpha_B - \alpha_B^2)] \qquad \text{Eq. 3.20}$$

where b_1 and b_2 are the number or weight fractions of chromium trimers which have one and two reacted functional groups, respectively, $b_1 = 2(1-\alpha_B)\alpha_B$, $b_2 = \alpha_B^2$; C_{B0} is the initial chromium trimer concentration in mol/kg.

The TBP models assume no intra-molecular crosslinking while the experimental data represents both inter- and intra-molecular crosslinking. To address this difference, a correction factor, λ, was introduced in Equation 3.20 to give

$$C_{B0} - \lambda C_{B0}(b_1 + b_2) = C_{B0}[1-\lambda(2\alpha_B - \alpha_B^2)] \qquad \text{Eq. 3.21}$$

where λ represents the ratio of the number of reacted chromium trimers in the experimental data to the number of reacted chromium trimers in Model I. The value of λ was determined by comparing the reacted chromium concentration at the gel point in Model I to experimental data of the reacted chromium concentration at the experimental gel time.

The experimental chromium uptake data of Series I and II experiments [Jain, et al., 2004] were used and the data ranges are shown in Table 3.1. Assuming the gel point corresponds to the experimental gel time determined by viscosity measurement, the experimental and calculated chromium uptake (*reacted* chromium trimer; $C_{B0}(b_1+b_2)$) concentrations at the gel time/point in Series I are plotted in Figure 3.1. The experimental values are about 3.86 times the values calculated in Model I. In the Model I, only the uptake and inter-molecular crosslinking reactions are considered, however, in the experimental data additional amounts of chromium trimer (or carboxylate groups) participate in intra-molecular crosslinking reactions (cyclization), *i.e.*, two carboxylate groups on the same polymer molecule are crosslinked through a chromium trimer. Therefore, this coefficient 3.86, designated λ, represents the intra-molecular crosslinking effect and should be at least a function of the polymer concentration and the degree of hydrolysis. For a specific polymer lot, the degree of hydrolysis is a constant, so λ was made a function of the polymer concentration and is assumed to be constant through the reaction process.

Table 3.1 – Compositions of gel systems [Jain et al., 2004] in 1% KCl, 25 °C.

Series	Cr_3 (mg/kg)	Polymer (mg/kg)	pH
I	250 – 20	~ 5000	~ 4.9
II	200	7530 – 3550	~ 4.9

Figure 3.2 shows the comparisons of experimental and modeled *unreacted* chromium concentrations for several gel systems in Series I. In Figure 3.2, the squares are experimental data points: concentration *versus* reaction time. The lines represent Model I according to Equation 3.21. The upper limits for two x-axes in Figure 3.2 are the gel time for the time axis and $\alpha_{crit,B}$, for the conversion axis, representing a linear relationship between α_B and time. Results of Equation 3.21 match the data well according to this linear relationship. Conversion is often linear with time for many reactions at small values of conversion. This linear relationship was represented by the following equation.

$$\alpha_B / \alpha_{crit,B} = t / t_{gel\ time} \qquad \text{Eq. 3.22}$$

where t is the reaction time and $t_{gel\ time}$ is the measured gel time. Equation 3.22 is used to obtain $d\alpha_B/dt$ in Equation 3.19. Differentiation of Equation 3.22 gives the required value:

$$d\alpha_B / dt = \alpha_{crit,B} / t_{gel\ time} \qquad \text{Eq. 3.23}$$

Applying Equation 3.23 for each gel system in Series I and II experiments of Jain et al.[2004], the rate constant, k, and the reaction orders, a and b, in Equation 3.19 were regressed by processing data at each measurement time for all runs giving the relationship

$$\frac{d\alpha_B}{dt} = k[C_{Af\,0} - C_{Bf\,0} \cdot \alpha_B]^{2.07}[C_{Bf\,0}(1-\alpha_B)]^{0.23} \qquad \text{Eq. 3.24}$$

where k = 98.46 h^{-1} $(mol/kg)^{-2.30}$.

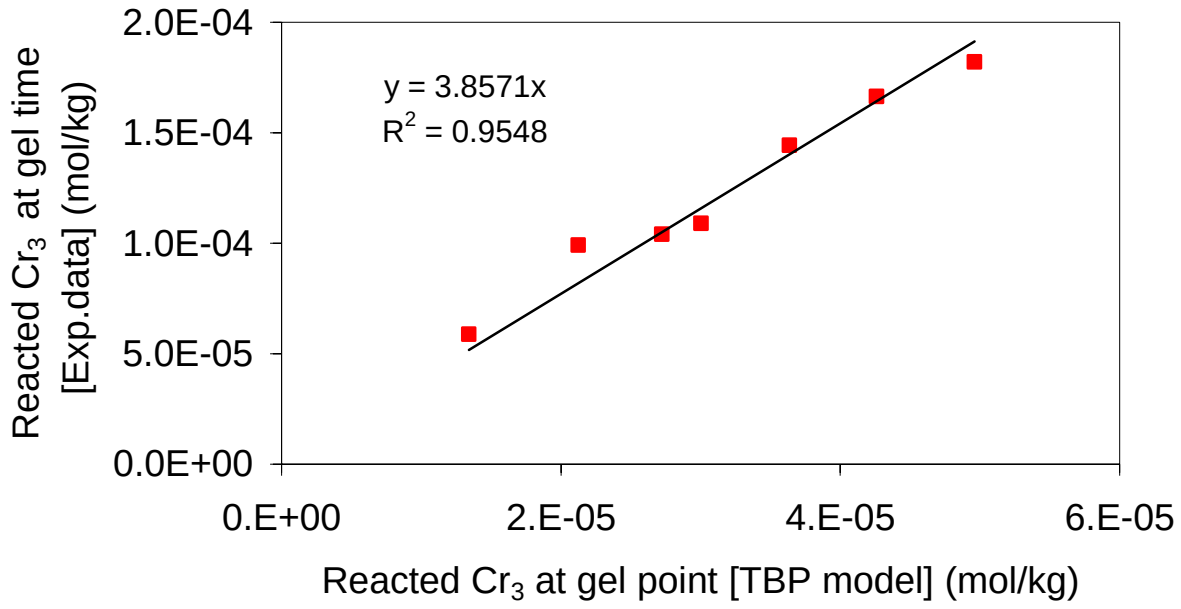

Figure 3.1 - Comparison of experimental data [Jain, et al., 2004] and calculated values (Model I) of chromium uptake at the gel time/point. ~ 5000 mg/kg polymer.

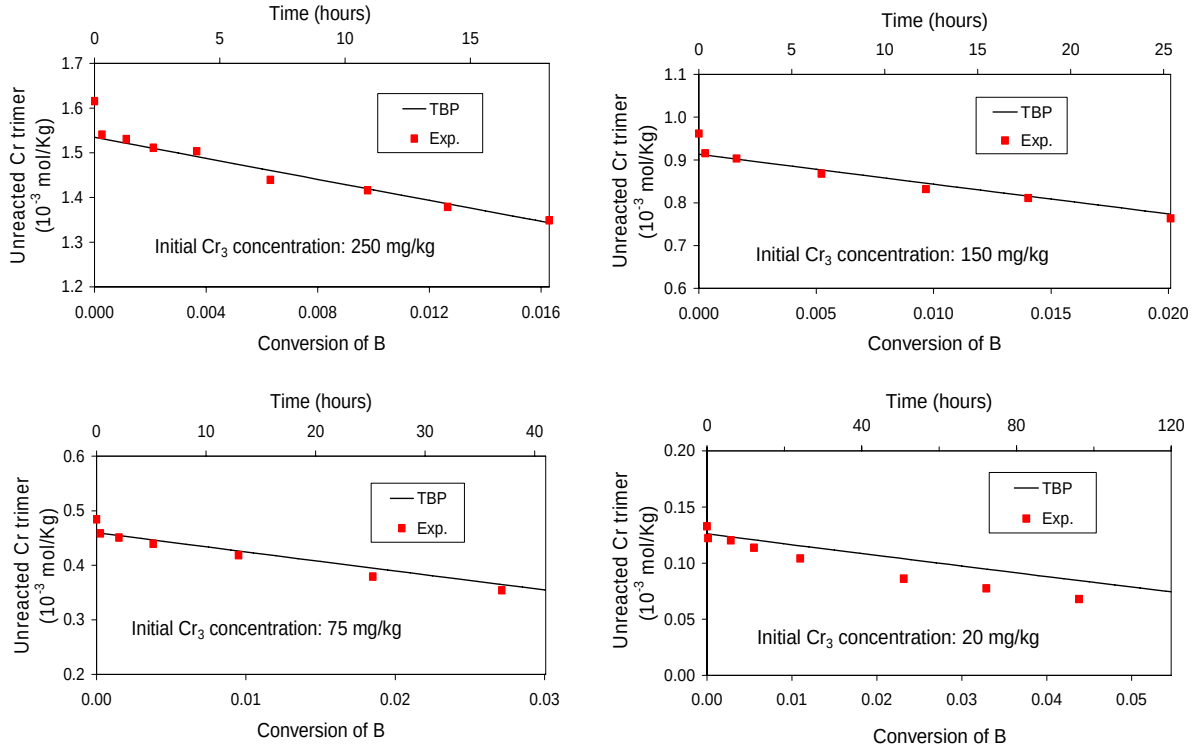

Figure 3.2 - Comparison of experimental data [Jain, et al., 2004] and calculated values (Model I) of the unreacted chromium trimer concentrations. ~ 5000 mg/kg polymer and different initial chromium concentrations.

The regression yielded a multiple - R of 0.976 and an R^2 of 0.953. Integration of Equation 3.24 from 0 to any selected time gives a value for α_B ($<\alpha_{B,crit}$). Knowing α_B, the unreacted chromium concentrations can be calculated by Equation 3.21 and molecular weight averages can be calculated by Equations 3.7 - 3.10. The gel time for a given system is determined by integrating Equation 3.24 up to the time when α_B corresponds to the critical conversion $\alpha_{crit,B}$ (as calculated by Equation 3.4).

Figures 3.3 and 3.4 present a comparison of calculated and experimental uptake data where the unreacted chromium concentration is plotted as a function of reaction time. For gel systems with 5000 mg/kg polymer, $\lambda = 3.86$; for gel systems with different polymer concentrations, λ was assumed to be inversely proportional to the polymer concentration. It can be seen the model fits the experimental data reasonably well.

Kinetic Extension for Model II. The procedure to determine the time that corresponds to the conversion, α, in Model II was: (1) select a time value, (2) integrate Equation 3.24 from 0 to the selected time to determine α_B, and (3) determine α by Equation 3.18. Then the differential distribution of molecular weight of the system at a given α can be calculated through Equations 3.14 - 3.17.

Experimental Materials, Equipment, and Procedures

Experiments were conducted to measure the weight-average molecular weights of pre-gel aggregates as a function of reaction time. A multi-angle laser light scattering (MALLS) instrument was used in this work.

The gel system used in this study consisted of 5000 mg/kg HPAM and 100 mg/kg chromium(III) at a temperature of 25 ^oC. The solvent used to prepare polymer and chromium stock solution was 1% KCl, 0.01% sodium azide (w/w) aqueous solution filtrated through a 0.02 μm membrane. It was also used as the carrier solvent in the measurement of the molecular weight.

Polyacrylamide (Alcoflood 935 Lots A2247 BOV) was dried in an oven under 17.5-inch vacuum mercury pressure and 100 °C. A 6667 mg/kg polymer stock solution was prepared and then filtrated through a 5-micron screen filter twice. A 400 mg/kg chromium stock solution was diluted from an aqueous solution of 50% chromium(III) acetate (McGean-Rohco, Inc., Lot No.40086816). The chromium stock solution was prepared and filtrated through a 0.02-micron filter immediately before mixing with the polymer stock. Then the polymer and chromium stock solutions were mixed at the ratio of 3:1 on a weight basis to form a gelant with 5000 mg/kg polymer and 100 mg/kg chromium(III) concentrations. The acetate-to-chromium(III) mole ratio was 3.0. Then the gelant was kept at 25 ^oC by a temperature-controlled water bath.

The gelation time of the gel system was determined by viscosity measurement at the temperature of 25 ^oC. A Brookfield digital viscometer (Model DV-I +) was used. Viscosity was measured every few hours till the gel time, which was defined in this work as the time when the viscosity of the gelant reached 1028 cp at the shear rate of 2.25 sec^{-1}, which was the maximum limit of the viscometer.

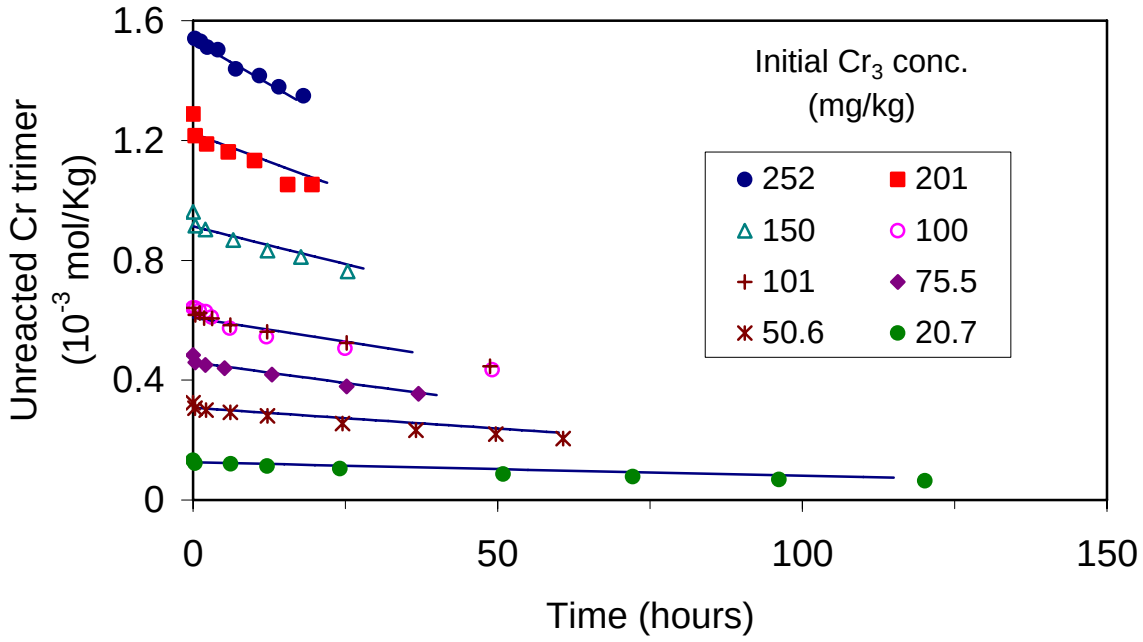

Figure 3.3 – Model I fit to the unreacted chromium trimer concentration[Jain, et al., 2004] as a function of time for different initial chromium concentrations; ~ 5000 mg/kg polymer concentration.

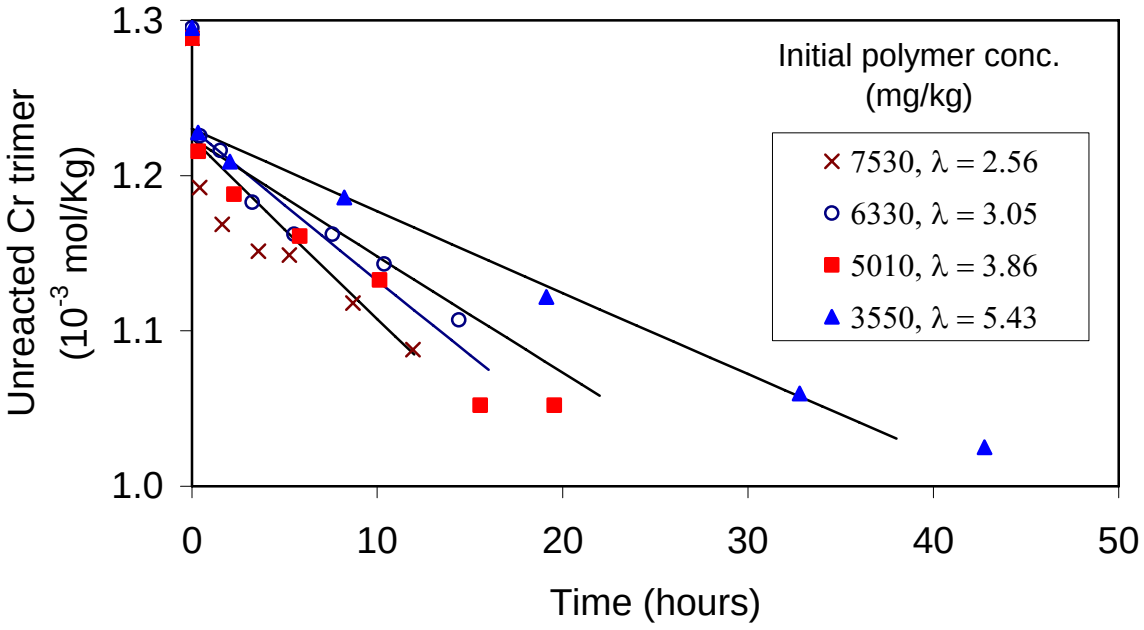

Figure 3.4 – Model I fit to the unreacted chromium trimer concentration[Jain, et al., 2004] as a function of time for different initial polymer concentrations; ~ 200 mg/kg chromium concentration.

An OPTILAB DSP (Wyatt Technology Corporation, Santa Barbara, CA) interferometer was used to determine the refractive index increment (dn/dc) of the polymer, which was required to determine the molecular weight of polymer and pre-gel aggregates. The dn/dc value of HPAM in 1% KCl at the temperature of 25 ^{o}C and the wavelength of 690 nm was measured as 0.182 mL/g. This value was also used for the pre-gel aggregates.

A DAWN EOS^{TM} (Wyatt Technology Corporation, Santa Barbara, CA) detector was used to measure the absolute molecular weight of the polymer and the pre-gel aggregates. This instrument employs a MALLS technique and the light scattering theory can be found elsewhere[13,14]. There are two operation modes: *batch mode* for measuring the weight-average molecular weight of polydispersed and unfractionated samples; *inline mode* for measuring the molecular weight distributions of fractionated samples.

The procedure to measure the weight-average molecular weight of pre-gel aggregates in batch mode was set up in our laboratory.[15] The experimental schematic is shown in Figure 1. Carrier solvent containing 1% KCl and 0.01% sodium azide was degassed and pumped at a flow rate of 0.5 mL/min from the solution reservoir through a 0.02 micron online filter and then through the injection valve to the MALLS detector (wavelength 690 nm, ambient temperature). Samples over a range of low concentrations spanning about an order of magnitude were prepared. An aliquot was periodically removed from the gelant and diluted with carrier solvent to six different evenly distributed concentrations from ~ 15 to ~ 120 mg/kg (polymer concentration). Then the six diluted samples were injected manually to load the sample loop in ascending order of the concentrations. The volume of the sample loop was 1.17 mL. When samples passed through the MALLS detector, the scattered light intensities and angles were recorded and processed by ASTRA software (Wyatt Technology Corporation, Santa Barbara, CA) to give the weight-average molecular weight. The processing parameters are: Zimm plot, Berry formalism, 4-12 detectors, second-order angle fit degree and first-order concentration fit degree.

Results and Discussion

Input parameters for the models, which are the initial conditions for the experimental gel system, are:

- Weight-average molecular weight of polymer, M_{w0}: 6.64×10^6 g/mol for polyacrylamide, AlcoFlood 935, Lot A2247BOV.
- Primary polymer follows Schulz-Zimm distribution with $\sigma = 1$ ("the most probable distribution" or Flory distribution).

$$w(0,x) = \frac{x}{P_{n0}^{\ 2}} \exp\left(-\frac{x}{P_{n0}}\right) \qquad \text{Eq. 3.25}$$

- Degree of hydrolysis of polymer, x_A: 10%.
- Concentration of polymer, c_A: 5000 mg/kg.
- Molecular weight of chromium trimer, M_B: $3 \times 52 = 156$ g/mol.
- Functionality of chromium trimer: $f_B = 2$.

– Concentration of chromium trimer, c_B: 100 mg/kg (95 mg/kg in the calculation, a 95% initial chromium concentration is used in the calculation to keep the consistency with the kinetic study [Chapter 2; Jain, et al., 2004]).

Experimental weight-average molecular weights of the pre-gel aggregates from this work and from Wang [2002] are plotted in Figure 3.5. Additional data taken at reaction times greater than 35 hours were not repeatable and consider unreliable, possibly due to difficulty in obtaining a representative diluted sample. Weight-average molecular weight of pre-gel aggregates calculated by the model is presented in Figure 3.5 as the solid line. The model results show the same trend as the data.

Viscosity of the gel system as a function of time is also shown in Figure 3.5. The calculated and experimental gel times were 36 hours and 31 hours, respectively. The development of the viscosity and the weight-average molecular weight are similar, increasing slowly in the initial stage, then increasing sharply near the gel time. During the gelation process, the larger the molecules become, the higher their expectancy for participation in further crosslinking by virtue of their high functionalities. That is, larger pre-gel aggregates are increasing in size faster than the small aggregates since the larger aggregates have more reactive sites. The rapid development and growth of large molecules as the gel time is approached results in an abrupt increase in the viscosity of the gelant (Note the log scale for viscosity in the figure). A relationship between viscosity and the weight-average molecular weight may provide a method to explain the viscosity behavior of gel system quantitatively in future work.

In Figure 3.6, the molecular weight (or degree of polymerization) distributions of the pre-gel aggregates calculated by Model II are shown as a function of conversion and time. The left axis goes with the bottom axis; the top axis goes with the right axis in Figure 3.6. The differential weight-fraction $w(\alpha, x)$ as functions of the degree of polymerization, x, and molecular weight, xM_0 (M_0 is the molecular weight of the monomer), at different reaction times are plotted. With increasing times, the weight fraction of "short" chains ($x < 1.5\times10^5$) decreases, while the weight fraction of the "mid-length" chains ($x = 1.5\times10^5 – 4\times10^5$) increases initially and then decreases, and the weight fraction of "long" chains ($x > 4\times10^5$) increases continually. Numerical values of selected fractions of chains are given in Table 3.2. The difference between one and the sum given in Table 3.2 indicates the weight fraction of chains with a degree of polymerization greater than 5×10^5. The model predicts a long "tail" of crosslinked molecules with high molecular weight. Further experiments are needed to validate the model. Experimental work is underway to determine the molecular weight and size distributions of pre-gel aggregates using a fractionator (separation of sample) with laser light scattering and refractive index detectors (measurement of molecular weight and size).

Conclusions

1. Two TBP models were developed to calculate the critical conversions of functional groups at the gel point and molecular weight averages and distributions of pre-gel aggregates as functions of conversion.
2. A relationship between the conversion of chromium functional groups and the reaction time was developed based on a previous kinetic study of the chromium-polymer uptake reaction for a polyacrylamide-chromium(III) acetate gel system [Jain, et al., 2004].

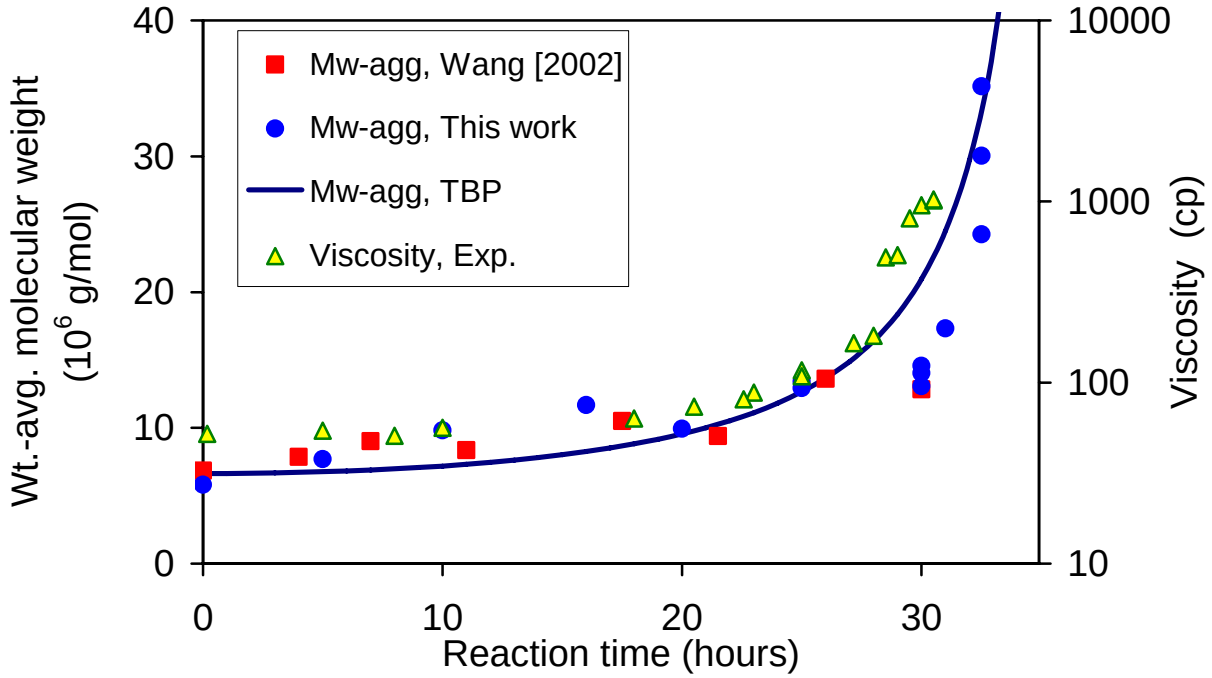

Figure 3.5 - Comparison of Model I and experimental data of weight-average molecular weight of pre-gel aggregates.

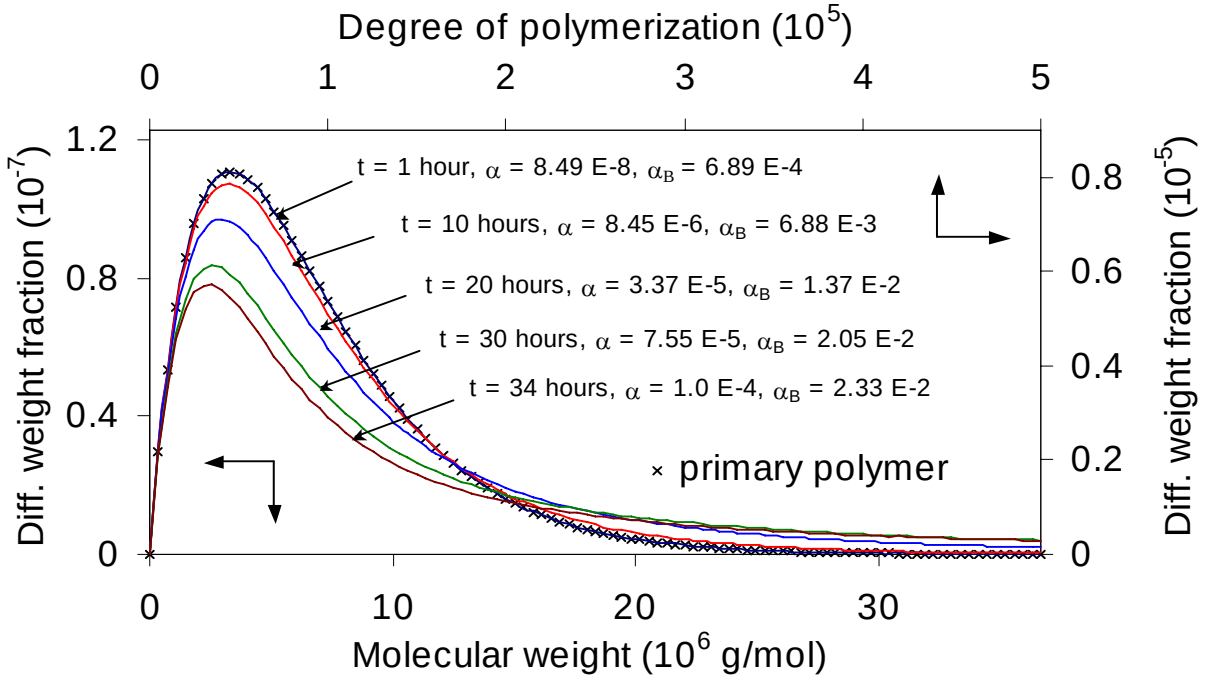

Figure 3.6 - Molecular weight distributions of pre-gel aggregates as functions of time and conversion (Model II).

Table 3.2 – Differential weight fraction distributions of pre-gel aggregates at different reaction times calculated by Model II. 5000 mg/kg polymer concentration and 100 mg/kg chromium concentration, 25 °C.

Degree of polymerization (10^5)	Molecular weight (10^6 g/mol)	weight fraction distribution					
		polymer	time (hours)				
			1	10	20	30	34
< 0.5	0 ~ 3.67	0.303	0.303	0.295	0.274	0.244	0.231
0.5 ~ 1.0	3.7 ~ 7.3	0.345	0.345	0.329	0.286	0.226	0.200
1.0 ~ 1.5	7.3 ~ 11.0	0.195	0.195	0.188	0.165	0.128	0.111
1.5 ~ 2.0	11.0 ~ 14.7	0.092	0.092	0.094	0.093	0.079	0.069
2.0 ~ 2.5	14.7 ~ 18.3	0.039	0.039	0.046	0.056	0.054	0.048
2.5 ~ 3.0	18.3 ~ 22.0	0.016	0.016	0.023	0.036	0.039	0.036
3.0 ~ 3.5	22.0 ~ 25.7	0.006	0.006	0.011	0.024	0.030	0.028
3.5 ~ 4.0	25.7 ~ 29.3	0.002	0.002	0.006	0.017	0.024	0.023
4.0 ~ 4.5	29.3 ~ 33.0	0.001	0.001	0.003	0.012	0.019	0.019
4.5 ~ 5.0	33.0 ~ 36.7	0.000	0.000	0.002	0.009	0.016	0.016
> 5.0	> 36.7	0.000	0.000	0.004	0.029	0.141	0.220
weight-average molecular weight (10^6 g/mol) ➔		6.64	6.65	7.19	9.56	20.9	53.4

3. The calculated weight-average molecular weights of pre-gel aggregates as a function of reaction time agree with the experimental data determined using a multi-angle laser light scattering technique. The development of viscosity shows a similar tendency with the calculated weight-average molecular weight.
4. The calculated molecular weight distributions of pre-gel aggregates predict a long "tail" of crosslinked molecules with high molecular weight with increasing reaction time.

Nomenclature

a, b	–	Reaction orders with respect to carboxylate group and chromium functional group
b_i	–	Number or weight fractions of chromium trimers which have i reacted functional groups, respectively. $i=0,2$
c_A, c_B	–	Initial mass concentrations of polymer and chromium trimer, respectively
f_B	–	Functionalities of chromium trimer, $f_B = 2$
n_A, n_B	–	Initial number fractions of polymer and chromium trimer, respectively.
k	–	Reaction rate constant at 25 °C, $k = 98.46\ h^{-1}\ (mol/kg)^{-2.30}$
r_A	–	The initial molar ratio of carboxylate groups to chromium functional groups.
t	–	Reaction time in hours
w_A, w_B	–	Initial weight fractions of polymer and chromium trimer, respectively.
$w(0,x)$	–	Initial weight fraction distribution (primary chain distribution) at $\alpha = 0$
$w(\alpha,x)$	–	Weight fraction distribution at conversion α
x	–	Degree of polymerization of an x-mer
x_A	–	Degree of hydrolysis of primary polymer, assuming $x_A = 10\%$
C_{Af}	–	Concentration of carboxylate group on polymer in mol/kg.

C_{Af0} – Initial concentration of carboxylate group on polymer in mol/kg.
C_{B0} – Initial chromium trimer concentration in mol/kg.
C_{Bf} – Concentration of chromium trimer functional group in mol/kg.
C_{Bf0} – Initial concentration of chromium trimer functional group in mol/kg
M_0 – Molecular weight of the monomer
M_B – Molecular weight of the chromium trimer
M_{n0} – Number-average molecular weight of the primary polymer
$M_{n\text{-}agg}$ – Number-average molecular weight of pre-gel aggregates
M_{w0} – Weight-average molecular weight of the primary polymer
M_w – Weight-average molecular weight of the entire gel system
$M_{w\text{-}agg}$ – Weight-average molecular weight of pre-gel aggregates
PI – Polydispersity index $PI = P_{w0}/P_{n0} = M_{w0}/M_{n0}$
P_{n0} – Number-average degree of polymerization of the primary polymer
P_{w0} – Weight-average degree of polymerization of the primary polymer

α – Conversions of carboxylate groups on polymer in Model II
α_{crit} – Critical conversions of carboxylate groups on polymer at gel point in Model II
α_A, α_B – Conversions of carboxylate groups on polymer and chromium functional groups, respectively, in Model I
$\alpha_{crit,A}$ $\alpha_{crit,B}$ – Critical conversions of carboxylate groups on polymer and chromium functional groups at gel point, respectively, in Model I
λ – An empirical parameter representing the effect of intra-molecular crosslinking.
σ – A parameter related to polydispersity index, $PI = (\sigma+1)/\sigma$

References

Bryant, S. L., Borghi, G. P., Bartosek, M. and Lockhart, T. P.: "Experimental Investigation on the Injectivity of Phenol-Formaldehyde/Polymer Gelants," paper SPE 37244 presented at the 1997 SPE International Symposium on Oilfield Chemistry, Houston, Texas, 18-21 Feb., 1997.

Dusek, K.: "Formation-Structure Relationships in Polymer Networks", *Br. Polym. J.*, **17** (1985), 185-189.

Dusek, K.: "Network Formation in Curing of Epoxy Resins", *Adv. Polym. Sci.,* **78** (1986) 1-57.

Dusek, K.: "Network Formation Involving Polyfunctionl Polymer Chains", Chapter 3 of *Polymer Networks: Principles of Their Formation Structure and Properties,* editor: R. F. T. Stepto, Thomson Science, London (1998).

Dusek K. and Duskova-Smrckova, M.: *Crosslinking and Polymer Networks*, DTW Associates Course (2002).

Huybrechts, J. and Dusek, K.: "Star Oligomers with Different Reactivity in Low VOC Polyurethane Coatings: Part III", *Surface Coating International*, **5** (1998) 234-239.

Jain, R., McCool, C.S., Green, D.W., Willhite, G. P., and Michnick, M.J.: “Reaction Kinetics of the Uptake of Chromium(III) Acetate by Polyacrylamide”, paper SPE 89399, presented at the 2004 SPE/DOE Fourteenth Symposium on Improved Oil Recovery, Tulsa, Oklahoma, U.S.A (17-21 April 2004).

McCool, C.S., Green, D.W. and Willhite, G. P.: “Permeability Reduction Mechanisms Involved in In-Situ Gelation of a Polyacrylamide/ Chromium (VI)/Thiourea System,” *SPE Reservoir Engineering*, **6**, No. 1 (Feb.1991) 77-83.

Vojta, V. and Dusek, K.: “Calculation of the Molecular Weight Distribution of Crosslinked Polymer Chains Using the Theory of Branching Processes”, *Br. Polym. J.*, **12** (1980) 1-4.

Wang, Chunyu: “The Rate of Pre-Gel Aggregate Growth in Gelled Polymer System used to Reduce Permeability of Porous Media,” MS thesis, The University of Kansas, 2002.

Willhite, G. P., Green, D.W. and McCool, C.S.: “Development of Polymer Gel Systems to Improve Volumetric Sweep and Reduce Producing Water/Oil Ratios” Annual Report for July 2003 – June 2004, Report No. 02NT15363-4, Contract No. DE-FC26-02NT15363, US DOE, Washington, DC (Dec 2004).

Chapter 4

Measurement of Molecular Weight and Size Distributions of Polymers and Pre-Gel Aggregates Using an SEC-MALLS-RI Apparatus

Graduate Research Assistant: Min Cheng

Introduction

Models presented in Chapter 3 are used to calculate molecular weight averages and distributions of pre-gel aggregates as functions of reaction time and initial conditions (concentrations of polymer and crosslinker, molecular weight and degree of hydrolysis of the polymer, *etc*). The models also predict a gel time for a particular system. Model calculations of the weight-average molecular weight of pre-gel aggregates as a function of reaction time agreed with experimental data as presented in Chapter 3. The objective of this work was to develop methods to measure the molecular weight and size *distributions* of pre-gel aggregates as a function of reaction time and to compare these types of data with model results. The model predicted a decreasing weight fraction of small molecules and an increasing weight fraction of big molecules, i.e., a long "tail" of crosslinked polymer molecules with high molecular weights.

An experimental apparatus with principle components of a size exclusion chromatography (SEC) column, a multi-angle laser light scattering (MALLS) detector and a refractive index (RI) detector was assembled. The apparatus was tested to determine the applicability to measure the distributions of absolute molecular weight and root mean square (rms) radius.

Experimental Equipment and Procedures

Polymers and Gel System. Bovine serum albumin (BSA, A-1900, Sigma Chemical Co., St. Louis, MO), which contained 98% BSA monomer, was used to determine the inter-detector delay volume. Three polyacrylamide samples were tested. One was a polyacrylamide standard, paam6000K (PSS-USA Inc., Warwick, RI). The others were polyacrylamide Alcoflood 935, Lots 7158 V and A2247 BOV. The number- and weight-average molecular weights, M_{n0} and M_{w0}, and the z-average rms radius, R_z, of these samples are listed in Table 4.1.

Table 4.1 – Molecular weight and size averages of samples.

	M_{n0} (g/mol)	M_{w0} (g/mol)	R_z (nm)	
BSA monomer	6.67×10^4	6.67×10^4	< 10	From Wyatt Tech. Corp.
paam6000K	2.46×10^6	5.55×10^6	/	Cited value (PSS-USA Inc.)
AlcoFlood 935, Lot 7158V	/	5.26×10^6	181.7	Measured in *batch* mode [Willhite et al.,2002]
AlcoFlood 935, Lot A2247BOV	/	6.64×10^6	216.8	

The gel system consisted of 5000 mg/kg polyacrylamide Alcoflood 935 (Lot A2247BOV) and 100 mg/kg chromium(III) at a temperature of 25 °C. The solvent used to prepare polymer and

chromium stock solution was a 1% KCl, 0.01% sodium azide (w/w) aqueous solution filtrated through a 0.02 μm membrane. The solvent was also used as the mobile phase (carrier solvent) in the measurement of the molecular weight and size distributions. A 6667 mg/kg polymer stock solution was prepared and filtrated through a 1μm screen filter. A 400 mg/kg chromium stock solution was diluted from an aqueous solution of 50% chromium(III) acetate (McGean-Rohco, Inc., Lot 40086816). The chromium stock solution was prepared and filtrated through a 0.02 μm filter immediately before mixing with the polymer stock. Then the polymer and chromium stock solutions were mixed at the ratio of 3:1 on a weight basis to form a gelant with 5000 mg/kg polymer and 100 mg/kg chromium(III) concentrations. The acetate-to-chromium(III) molar ratio was 3.0. The gelant was kept at 25 °C by a temperature-controlled water bath. The gel time of this gel system was 30 -31 hours as determined by the time the viscosity reached 1000 cp by periodic viscosity measurements.

Equipment. Polymer molecules in a sample need to be separated according to their size (or molecular weights) in order to determine the distributions of molecular weight and size. In this work a Shodex SUGAR KS 807 column and its guard column KS 807G (JMScience Inc., Grand Island, NY) were used as a fractionator. The SUGAR KS 807 column is a newly released SEC column which is designed to separate the water-soluble polymers with ultra-high molecular weights. The KS 807 column has an internal diameter of 8 mm and a length of 30 cm. The packing material is sulfonated polystyrene divinylbenzene copolymer with sulfo(Na^+) as the functional group. The particle size of the packing material is 30 μm and the average pore size is 4000 Å. The theoretical plate number of a KS 807 analytical column should be > 4000, and the exclusion limit is 200×10^6 g/mol tested with pullulan. The temperature of the column oven was set at 30 °C.

A DAWN EOS™ (Wyatt Technology Corporation, Santa Barbara, CA) detector was used to measure the absolute molecular weight distributions of polymers and the pre-gel aggregates. This instrument employs the multi-angle light scattering (MALLS) technique and the light scattering theory can be found elsewhere [Wyatt, 1993]. There are two operation modes: *batch mode* for measuring the weight-average molecular weight and z-average rms radius of unfractionated samples. This mode was employed in a previous study [Willhite, et al., 2002]; *inline mode* for measuring the molecular weight and size distributions of fractionated samples. This mode was used in this work. This MALLS detector does not have temperature control and was operated at room temperature (about 23 °C).

The mass detector used was an Optilab DSP (Wyatt Technology Corporation, Santa Barbara, CA) interferometer (refractive index [RI] detector). The Optilab was operated offline to determine the refractive index increment (dn/dc) of the polymer, which was required to compute the concentration of the polymer from the RI signals. The Optilab was also operated inline with the SEC column and the MALLS detector for the measurement of the concentrations of fractionated polymer fractions. The cell temperature of the RI detector was set at 35 °C in order to stabilize the RI baseline.

Procedures. A schematic of the SEC-MALLS-RI setup is shown in Figure 4.1. Mobile phase containing 1% KCl and 0.01% sodium azide was degassed and pumped at a flow rate of 0.5 mL/min from the solution reservoir through a digital pressure gauge, a 0.02 μm inline filter and

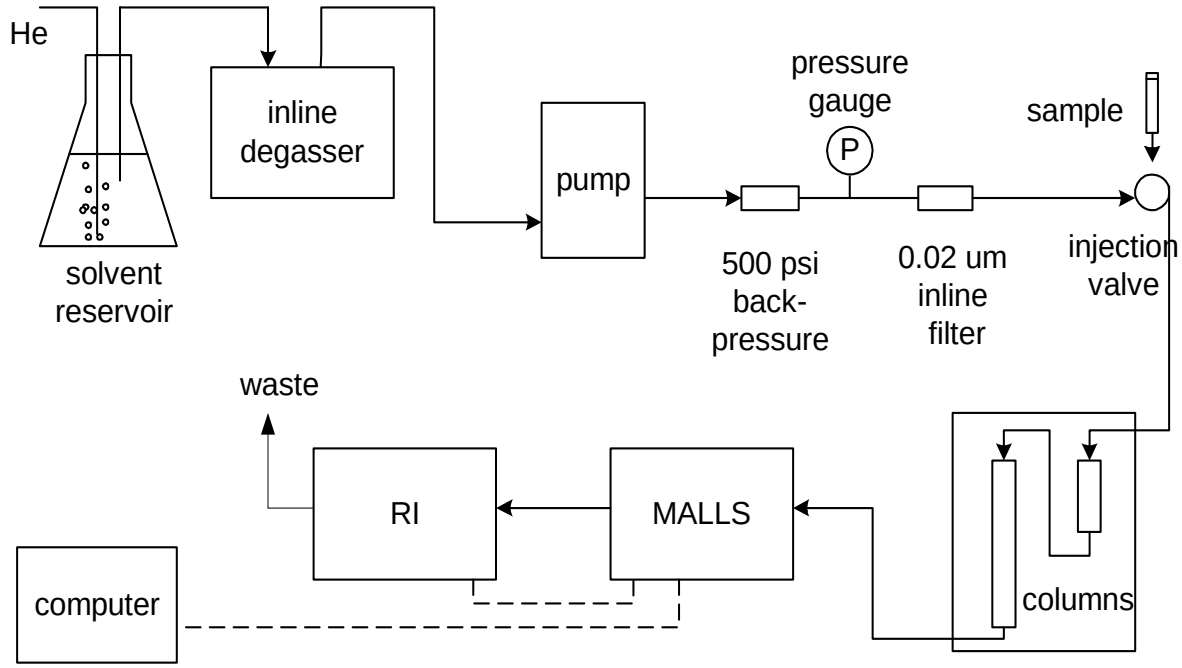

Figure 4.1 - Experimental schematic of a SEC-MALLS-RI Setup.

then through the sample injection valve, the SEC columns, MALLS and RI detectors sequentially. For the measurement of polyacrylamide samples, usually a 400 mg/kg polymer stock was prepared first then diluted to 200 mg/kg with the mobile phase. For the measurement of pre-gel aggregates, an aliquot was periodically removed from the gelant and diluted to 200 mg/kg (polymer concentration) with mobile phase. The diluted sample was injected manually to load a 100 μL sample loop and the sample was injected into the system and carried by the mobile phase through the column and detectors. Polydispersed polymer molecules were separated according to their sizes while passing through the SEC columns. The fractionated polymer then passed through the MALLS and RI detectors, and the corresponding signals were recorded and processed by ASTRA software (Wyatt Technology Corporation, Santa Barbara, CA) to give the molecular weight and size distributions.

Results and Discussion

dn/dc Measurements. The specific refractive index increment, dn/dc, is the change in the refractive index of a solution relative to the change of the solute (polymer) concentration. The dn/dc value depends on the wavelength of the incident light, the polymer-solvent pair and the molecular weight of the polymer. Generally, the dn/dc value increases with increasing molecular weight up to a certain value and then is constant at higher values [DAWN Course Manual, 1998]. The molecular weights of the polymers in this study are high and the dn/dc can be considered constant. Table 4.2 shows the dn/dc values of the samples used in this work. The dn/dc values are close for three polyacrylamide samples with weight-average molecular weights of about 5 ~ 6×10^6 g/mol.

The dn/dc values of the pre-gel aggregates were measured and are shown in Figure 4.2 as a function of reaction time. The dn/dc value of the gelant is a bit higher than that of the polymer,

Table 4.2 – Dn/dc of samples (25 °C; wavelength - 690 nm; in 1% KCl, 0.01% NaN_3 solution).

	dn/dc (mL/g)	
BSA	0.185	From Wyatt Tech. Corp.
paam6000K	0.178	[Wang, 2003]
AlcoFlood 935, Lot 7158V	0.182	[Wang, 2003]
AlcoFlood 935, Lot A2247BOV	0.179	this work

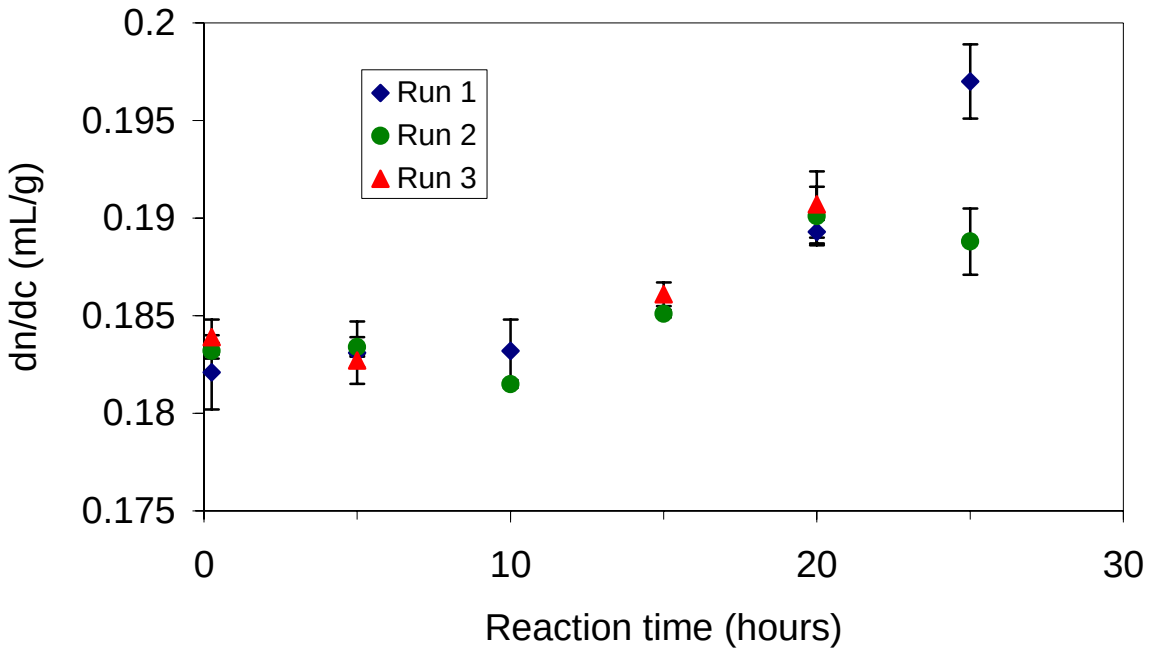

Figure 4.2 – dn/dc values of the gelant as a function of reaction time.

probably due to the presence of chromium(III) acetate in the solvent. The dn/dc values are constant up to 10 hours and then increase gradually.

Inter-detector Delay Volume. The delay volume between the MALLS and RI detectors is required to match the two measurements for the same sample. This was accomplished by running a monodispersed standard (polydispersity index < 1.05) of known molecular weight and with a known dn/dc value. A monodispersed BSA sample that contained 98% monomer, a molecular weight of 6.67×10^4 g/mol and a dn/dc value of 0.185 mL/g was used. Retention of BSA on the column was significant so the run was conducted with only the guard column to achieve a clear sample peak. Figure 4.3 shows the chromatogram for a BSA run. The MALLS peak is on the left side (lower elution time) of the RI peak due to the inter-detector volume. The peak maximum of the light scattering signal was aligned accurately with the peak maximum of the RI signal using an inter-detector delay volume of 0.148 mL as shown in Figure 4.4.

The BSA run was analyzed by the processing software ASTRA. The parameters used were: Debye plot, Zimm formalism, 4-18 detectors, detector fit degree = 1, result fit degree = 1. In Figure 4.5, the RI signal and molecular weight are plotted as a function of elution time. The RI

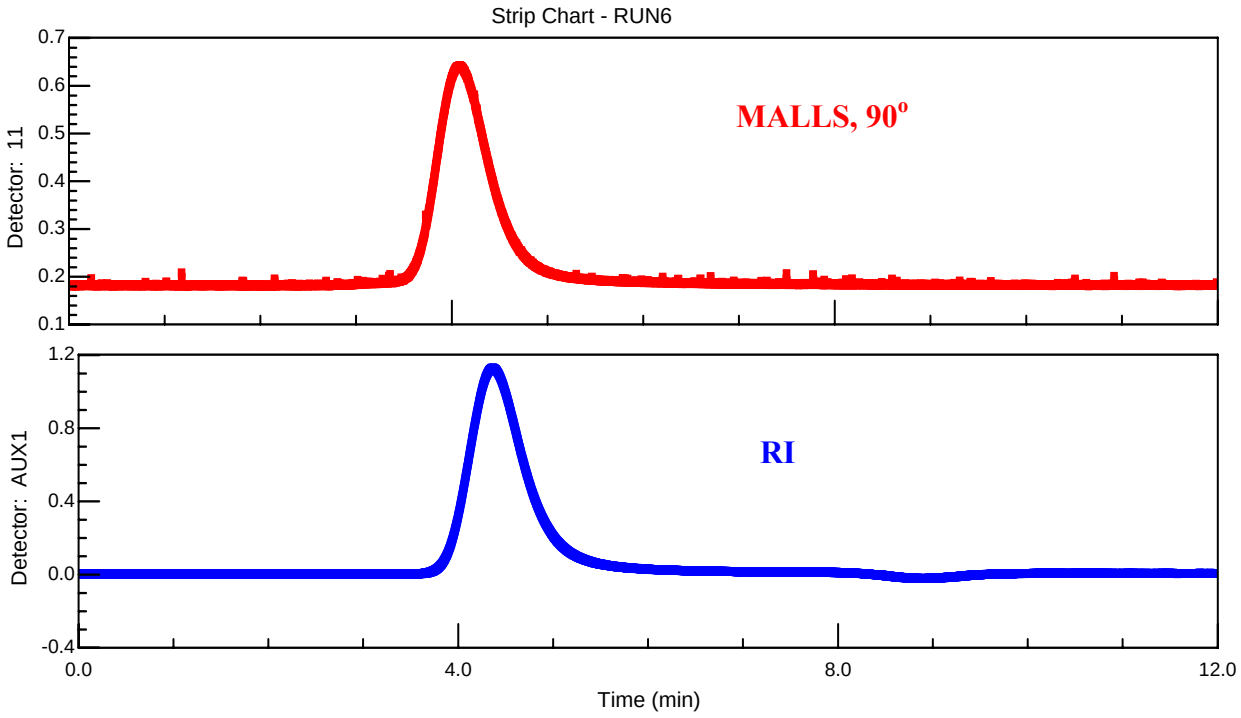

Figure 4.3 – Chromatograms for a monodispersed BSA run (1000 mg/kg, 100 µL).

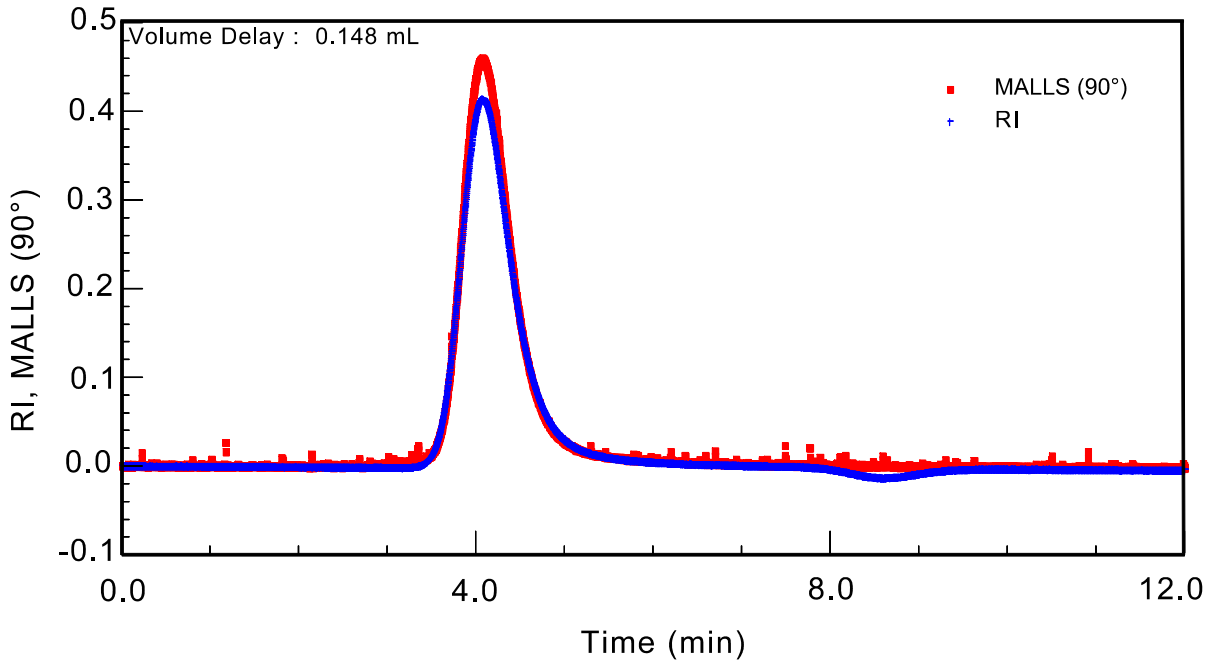

Figure 4.4 – MALLS and RI signals aligned for a monodispersed BSA run.

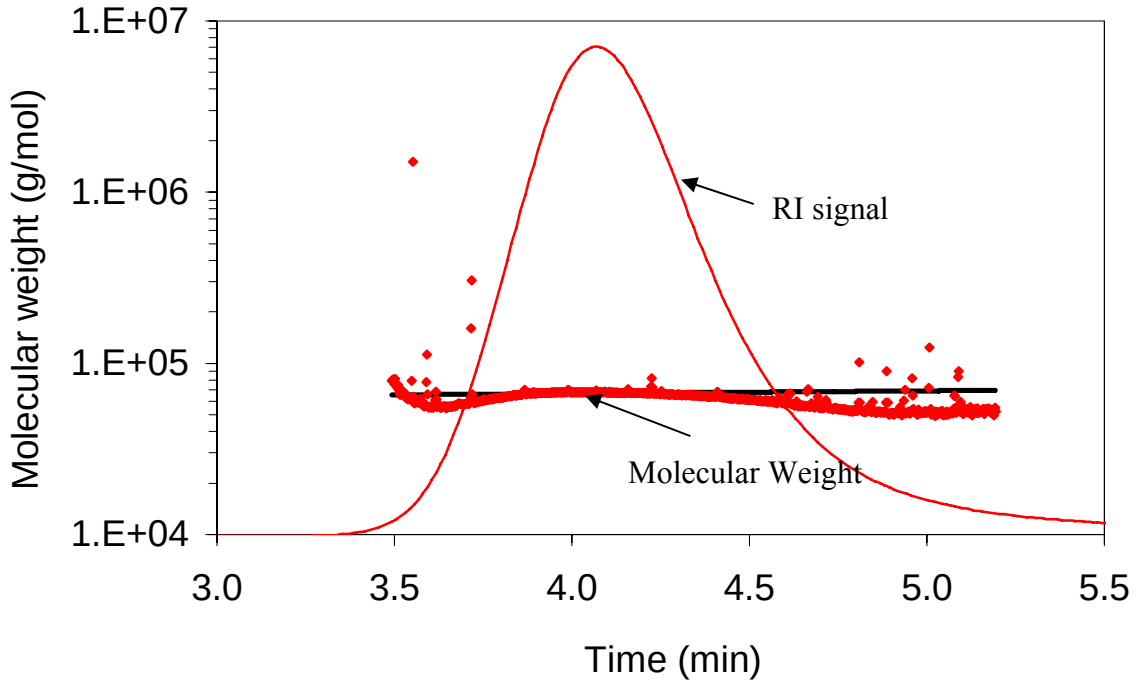

Figure 4.5 – Molecular weight versus elution time for a BSA run.

signal represents the mass eluted. The measured molecular weight is almost a flat horizontal line (the solid line represents the fitted data) indicating a monodispersed sample. The small curvatures at the ends of the molecular weight curve are due to band broadening caused by the delay volume between the detectors. The calculated number- and weight-average molecular weights were 6.701×10^4 and 6.702×10^4 g/mol, respectively, very close to the cited value. The measured polydispersity index was 1.000 ± 0.003. The molecular weight distribution of BSA is shown in the Figure 4.6. The distribution is very sharp indicating the monodispersity of the BSA sample. The measured size distribution is unreliable for the BSA sample since BSA is smaller than the MALLS detector can measure which is about 10 nm.

Molecular Weight and Size Distributions of Polymers

Polyacrylamide Standard. A polyacrylamide standard, paam6000K (PSS-USA Inc., Warwick, RI), was used to test the system using a high molecular weight polymer. Sample retention was also observed for this and other polymers. No sample peak appeared in the first 5-6 injections. Then the sample recovery or the area under the RI sample peak increased with successive injections. After about 15-20 injections, a stable RI sample peak was obtained.

The chromatogram for paam6000K is shown in Figure 4.7. There are two RI peaks and one MALLS peak. The second RI peak is negative and occurred near the end of the data collection. This peak is called a "salt peak" or a “solvent peak” and it appears at the total inclusion volume of the column. The RI detector is very sensitive to small changes in the inorganic salt content of the liquids and it is difficult to match the same salt content in the injected sample as in the mobile phase. The salt peak can be positive or negative. The salt peak overlapped a small portion of the polymer peak. During data processing, a small amount of the smaller sized polymer is

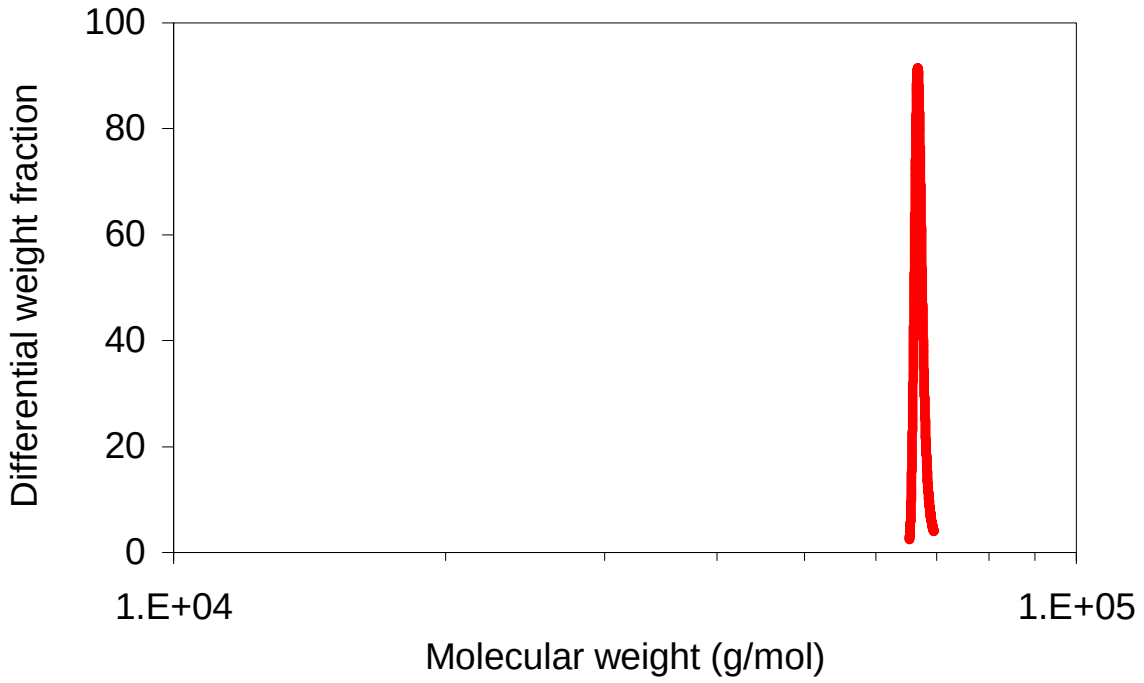

Figure 4.6 – Differential molecular weight distribution of BSA.

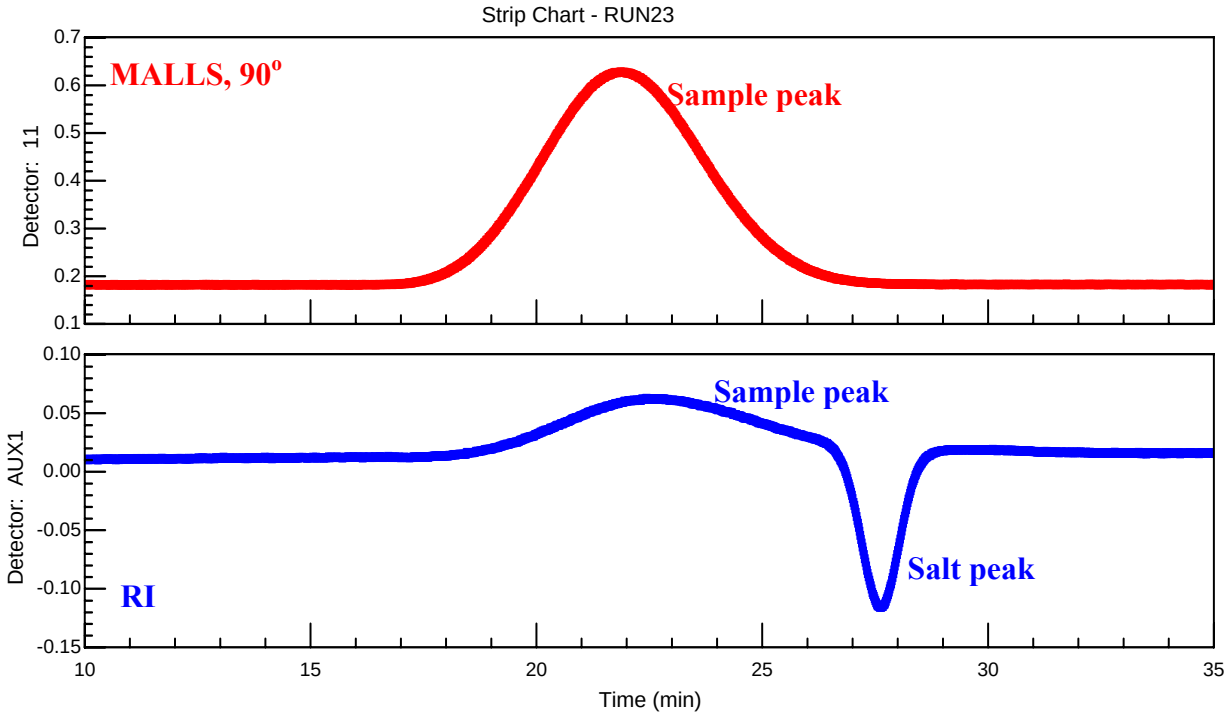

Figure 4.7 – Chromatograms for paam6000K (200 mg/kg, 100 μL).

excluded which also affects sample recovery calculation. The average sample recovery for the paam6000K was 77% after the columns were saturated.

The ASTRA processing parameters for paam6000K are the same with those for BSA: Debye plot, Zimm formalism, 4-18 detectors, detector fit degree = 1, result fit degree = 1. The measured number-average molecular weight (M_{n0}) was 2.47×10^6 g/mol (2.4%), the weight-average molecular weight (M_{w0}) was 4.83×10^6 g/mol (1.3%) and the z-average rms radius was 194.8 nm (1.1%). The value in parenthesis designates the relative standard deviation. The measured molecular weights were close to the cited values given in Table 4.1.

The measured molecular weight as a function of elution time and the molecular weight distributions of seven runs are shown in Figures 4.8 and 4.9. The corresponding graphs for the rms radius are shown in Figures 4.10 and 4.11. These results show the elution progression from big molecules with higher molecular weight and larger size through successively smaller molecules. The molecular weight of paam6000K ranges from ~ 0.5×10^6 g/mol to 50×10^6 g/mol. The rms radius ranges from ~ 40 nm to ~ 400 nm. Distribution curves of seven runs overlay well, indicating good data reproducibility.

The rms radii are plotted against molecular weight (log-log) for paam6000K in Figure 4.12. The slope gives information about the conformation of the molecules. For rod-like molecules, the slope should be approximately 1.0, for spherical molecules the slope is about 0.33, and for random coil molecules the slope ranges from 0.5 to 0.6. The average slope in Figure 4.12 is 0.56, which means that paam6000K molecules are random coils.

AlcoFlood 935. The molecular weight and size distributions of two lots (7158V and A2247BOV) of Alcoflood 935 were measured. Alcoflood 935 is a partially hydrolyzed polyacrylamide with the degree of hydrolysis about 10%.

The ASTRA processing parameters for Alcoflood 935 are: Debye plot, Berry formalism, 4-16 detectors, detector fit degree = 2, result fit degree = 1. The plotting formalism and the fit order were selected based on the appearance (how well the data is fit by looking at the Debye plot) and the uncertainty (which combination gives the lowest uncertainty). Table 4.3 gives the average sample recovery, weight-average molecular weight and z-averaged rms radius for these two polymer lots. The value in parenthesis designates the relative standard deviation. The weight-average molecular weights and z-averaged rms radii measured by the *inline* mode are comparable to the values measured by the *batch* mode that were given in Table 4.1.

Molecular weights of the two polymer lots as a function of the elution time is shown in Figure 4.13 and the molecular weight distribution curves are shown in Figure 4.14. Similar graphs of the rms radii are shown in Figures 4.15 and 4.16. Polymer Lot A2247BOV has a higher average molecular weight, a higher average rms radius, and a wider distribution than Lot 7158V.

The rms radii are plotted against molecular weight (log-log) for the two Alcoflood 935 lots in Figure 4.17.The slopes were 0.47 and 0.48 for Lots 7158V and A2247BOV, respectively, indicating the Alcoflood 935 polycarylamide is a random coil polymer with some branching since the slopes were just under 0.50.

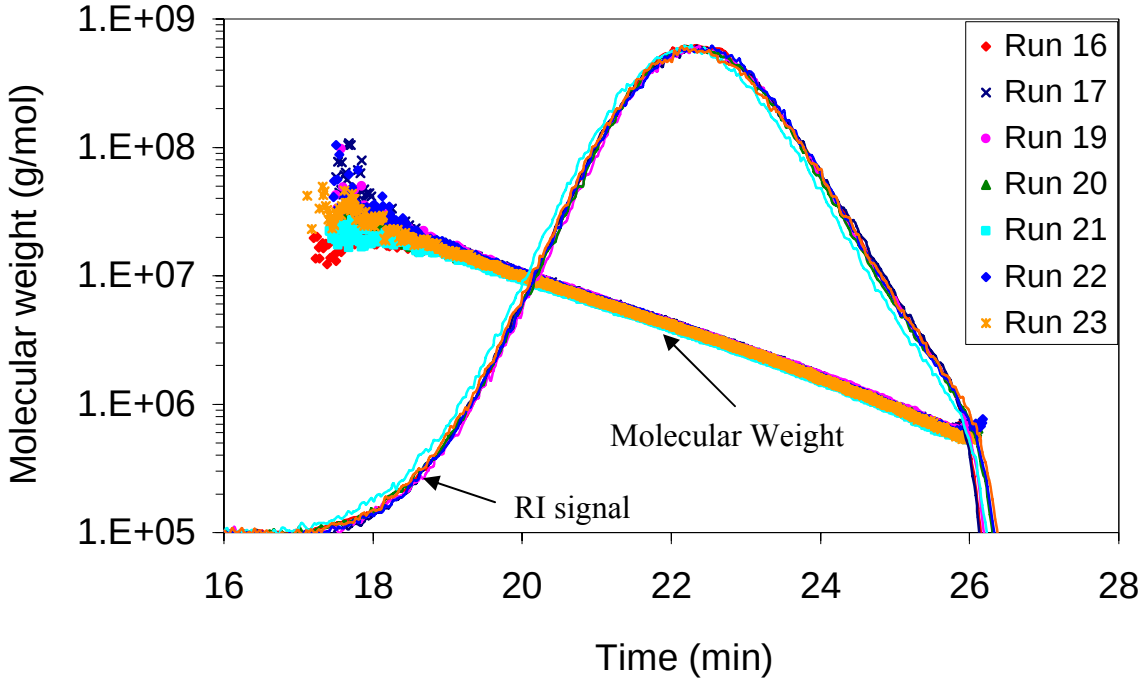

Figure 4.8 – Molecular weight versus elution time for paam6000K.

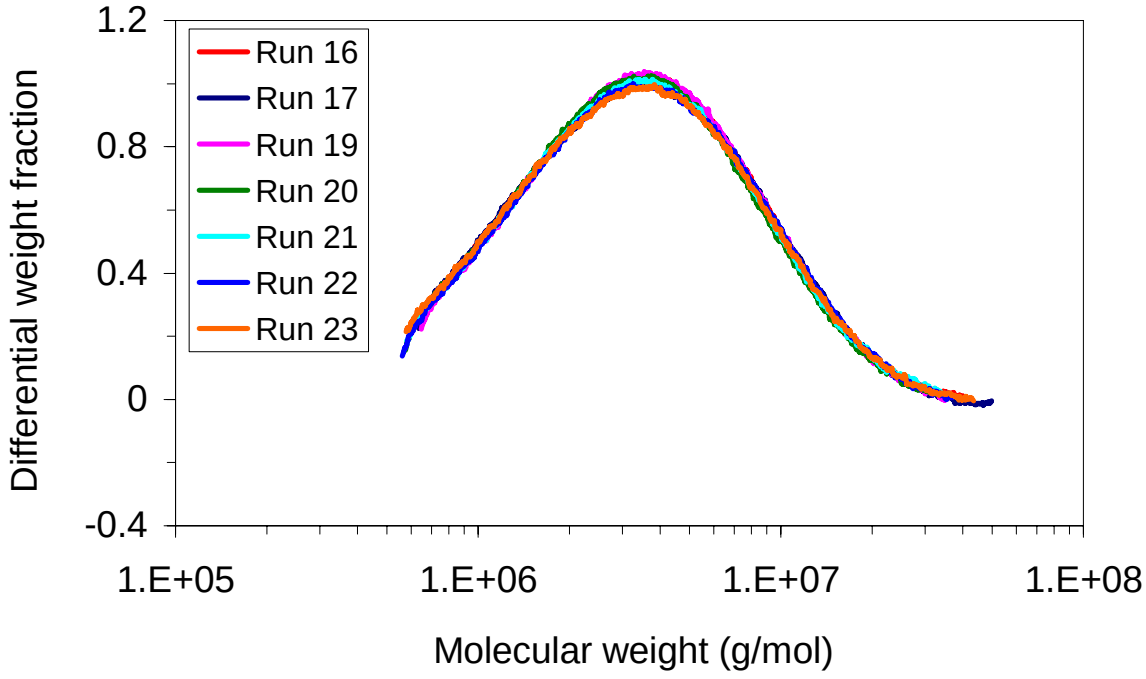

Figure 4.9 – Differential molecular weight distribution of paam6000K.

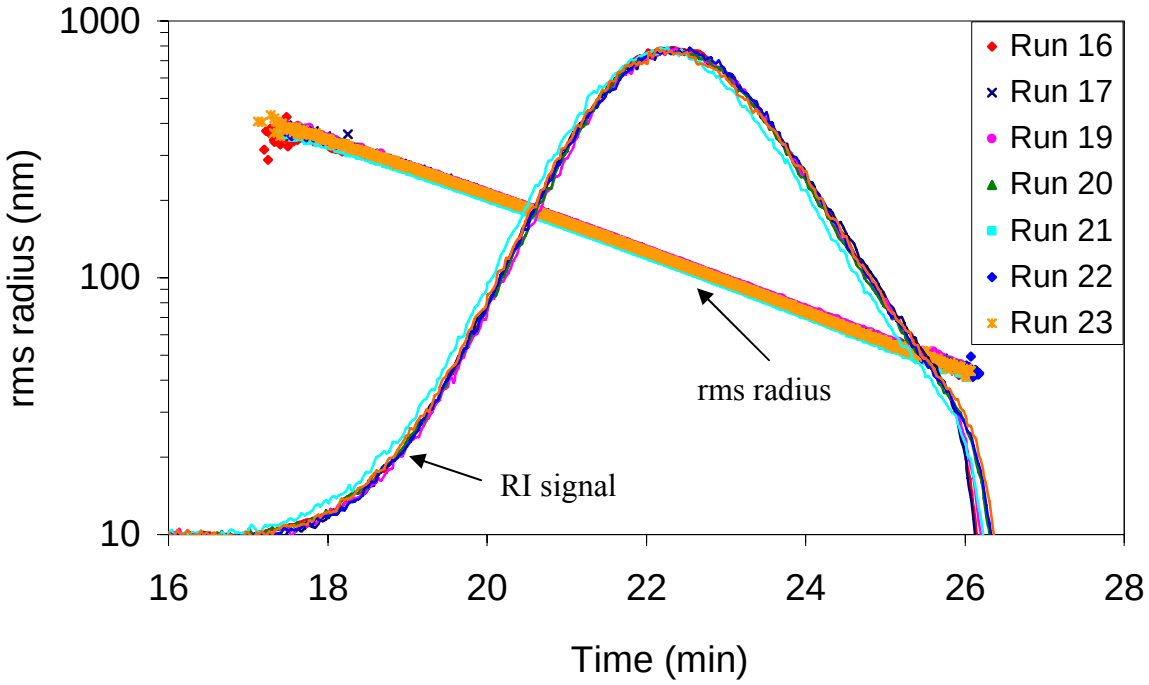

Figure 4.10 – Rms radius versus elution time for paam6000K.

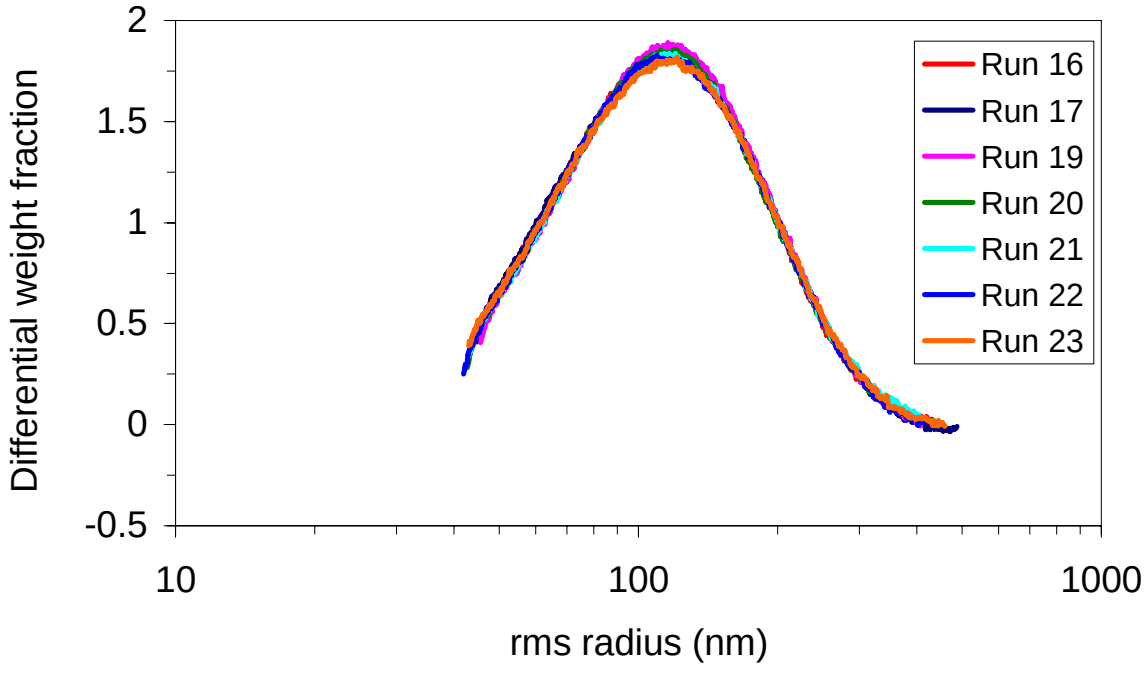

Figure 4.11 - Differential rms radius distribution of paam6000K.

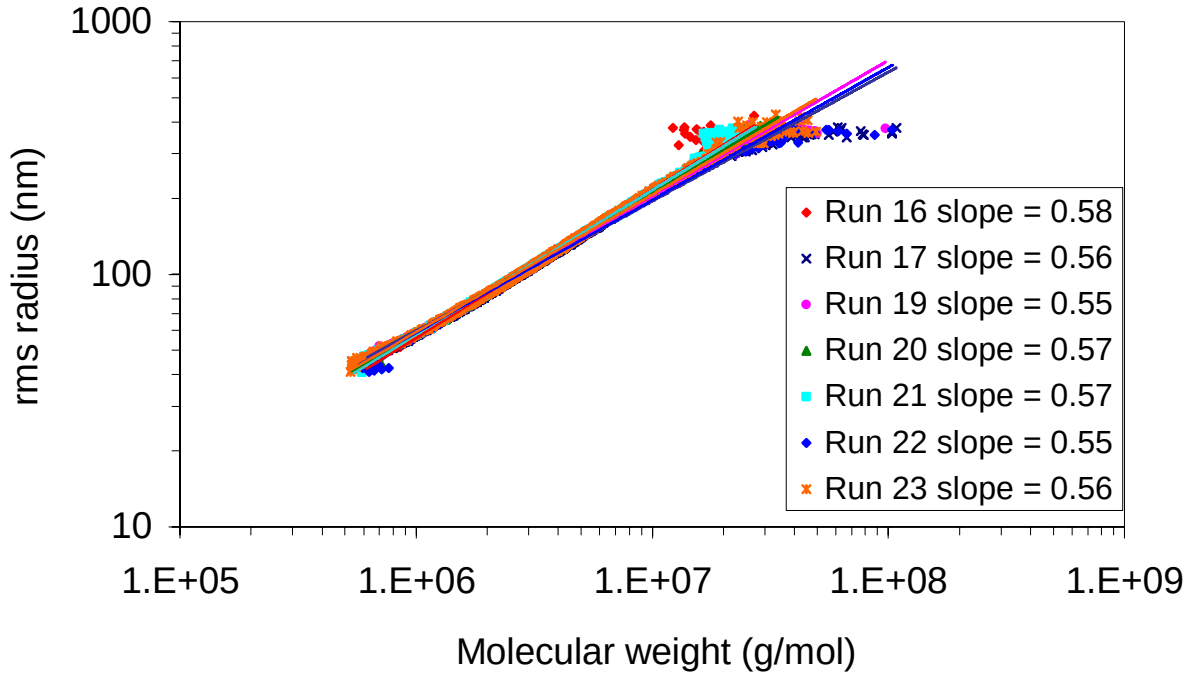

Figure 4.12 - Log-log plot of rms radius versus molecular weight for paam6000K.

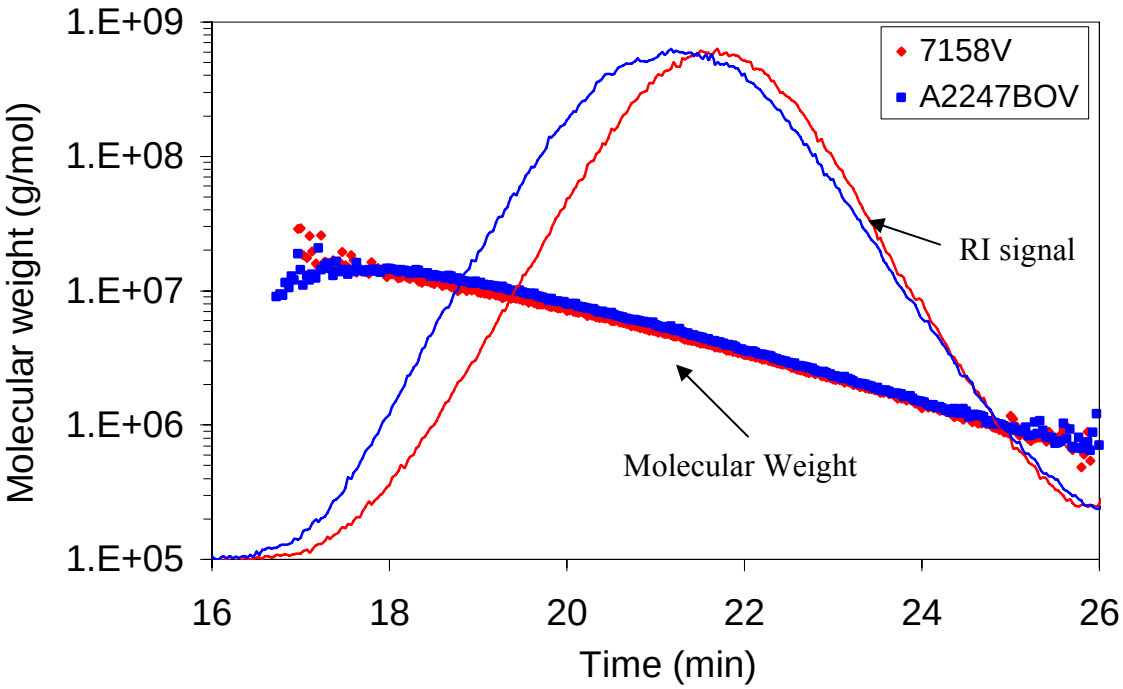

Figure 4.13 - Molecular weight versus elution time for two polymer lots of AlcoFlood 935.

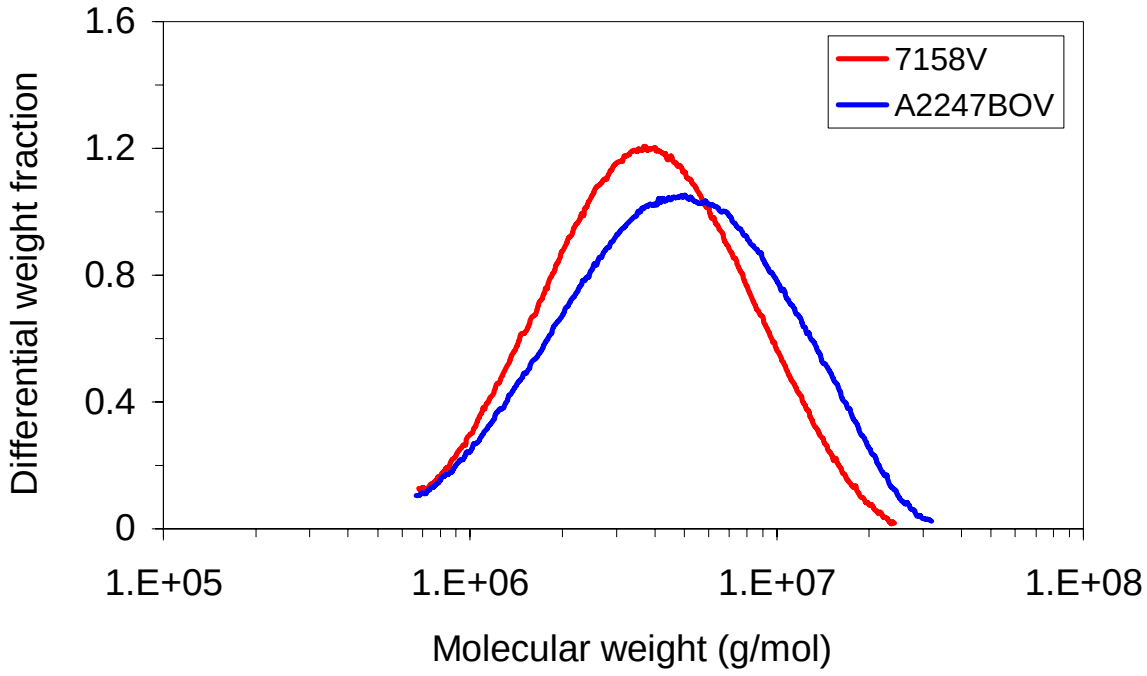

Figure 4.14 – Differential molecular weight distributions of two polymer lots of AlcoFlood 935.

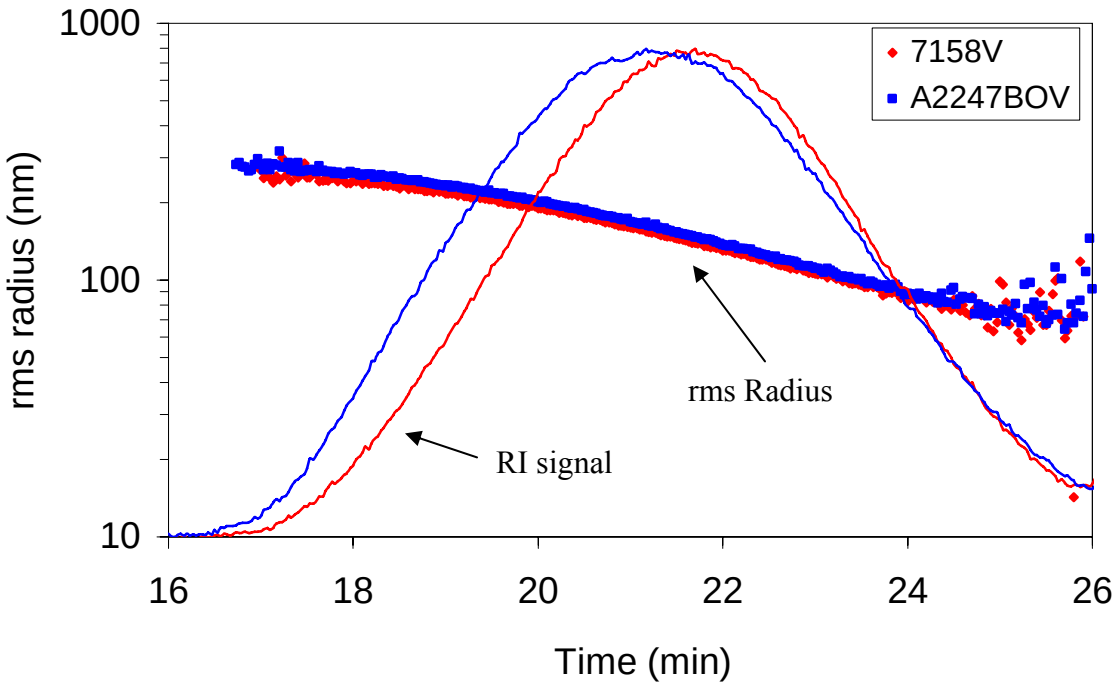

Figure 4.15 – Rms radius versus elution time for two polymer lots of AlcoFlood 935.

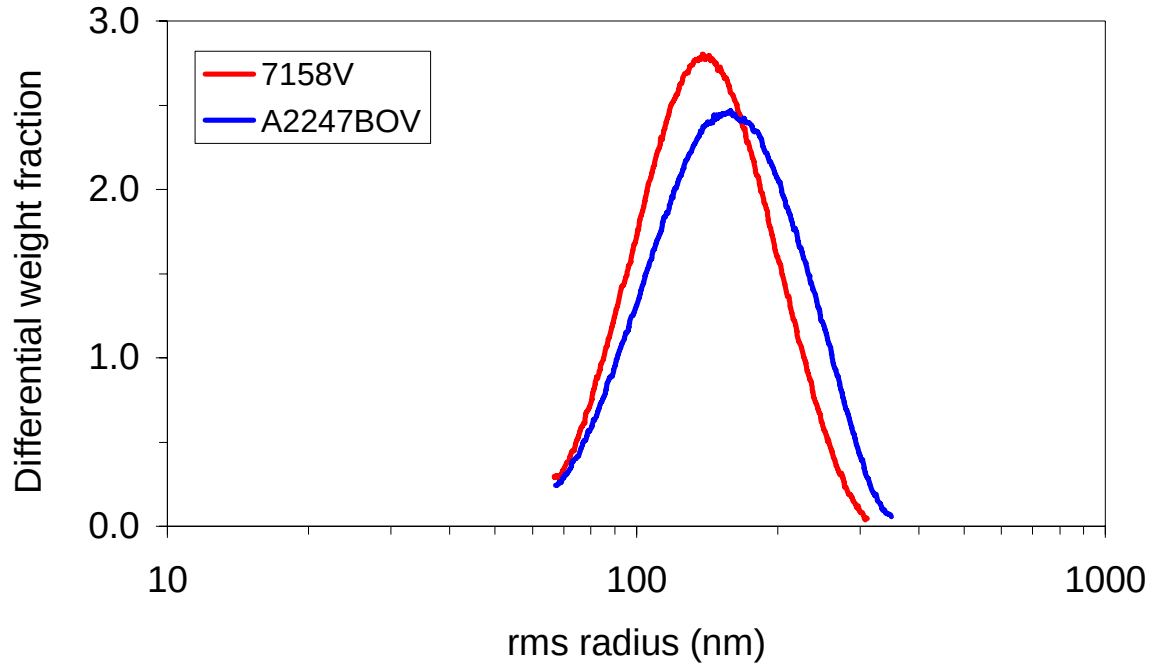

Figure 4.16 – Differential rms radius distributions of two polymer lots of AlcoFlood 935.

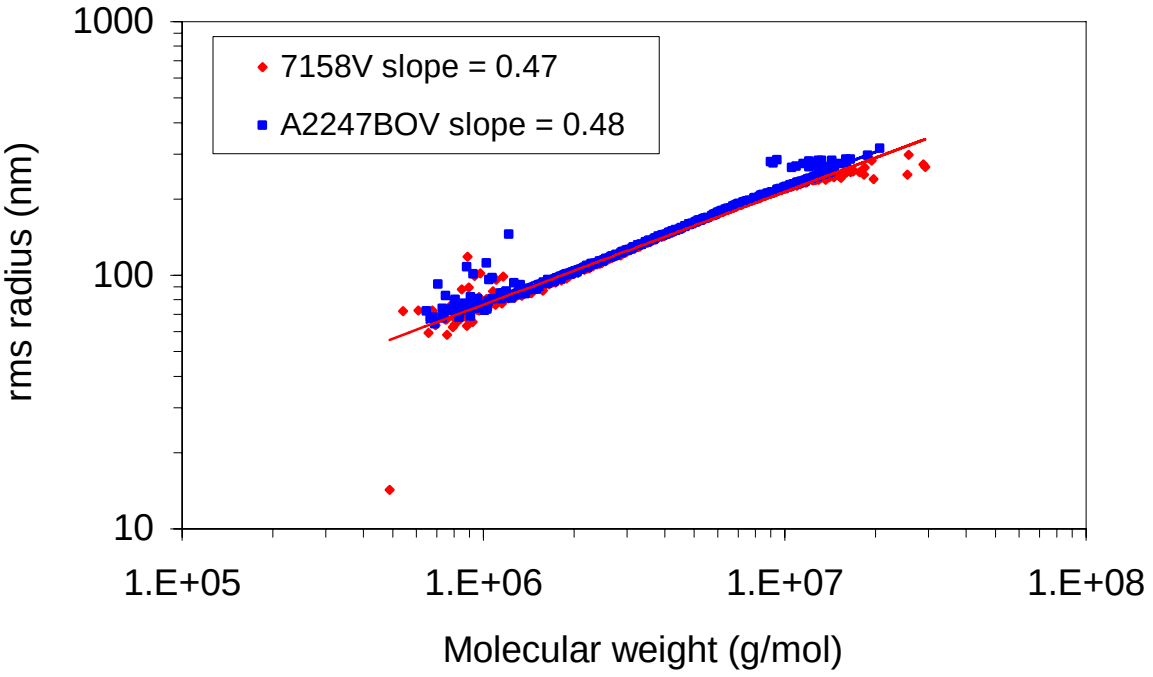

Figure 4.17 – Log-log plot of rms radius versus molecular weight for two lots of Alcoflood 935 polyacrylamide.

Table 4.3 – Sample recovery and measured molecular weight and size averages of polymer Alcoflood 935, Lot 7158V (12 runs) and Lot A2247BOV (9 runs).

	Sample recovery (%)	M_{w0} (g/mol)	R_z (nm)
AlcoFlood 935, Lot 7158V	83 (7.4%)	4.79×10^6 (2.7%)	189.0 (1.2 %)
AlcoFlood 935, Lot A2247BOV	89 (3.5%)	6.08×10^6 (2.8%)	207.6 (2.1%)

Numbers in parenthesis denote the relative standard deviation.

Molecular Weight and Size Distribution of Pre-Gel Aggregates

In mobile phase: 1% KCl, 0.01% NaN_3. A gel system containing 5000 mg/kg polyacrylamide (AlcoFlood 935, Lot. A2247BOV) and 100 ppm chromium(III) was prepared. Gelant was sampled periodically and immediately diluted from 5000 mg/kg (polymer concentration) to ~ 200 mg/kg by adding the mobile phase before injection into the columns. Polymer solutions were injected between gelant injections to keep the columns saturated and to test proper operation.

The RI chromatograms (proportional to mass) for a gelant at different reaction times are shown in Figure 4.18 and the corresponding chromatograms from the MALLS detector at the 90° angle are shown in Figure 4.19. The RI chromatograms of the gelant up to a reaction time of 5 hours were similar to the chromatograms for a polymer solution. At reaction times greater than 5 hours, the RI peak height decreased and the peak position shifted to the right (smaller molecules). The 90° LS signals showed the same trends. Recovery of the injected gelant decreased with reaction time as indicated by smaller areas under the chromatograms and the recovery values listed in Table 4.4.

Table 4.4 – Sample recovery of gelant runs (200 mg/kg polymer concentration, 100 μL).

Gelling time (hours)	Sample recovery (%)
0.08	84
5	84
10	82
16	68
20	69
25	59

Reduction of the peak height and the shift of the peak position to the right (smaller molecules) are consistent with results of the model presented in Chapter 2. However, the model predicts that the reduced mass on the left side of the chromatogram should form larger molecules that elute earlier, forming a leading edge on the chromatogram. The leading edge was not detected and presumably the large aggregates were retained in the columns. The columns were saturated with polymer during preliminary injections and additional retention occurred only when chromium was present. This indicated that the retention of aggregates was a result of their reactive nature after reaction with the chromium crosslinker.

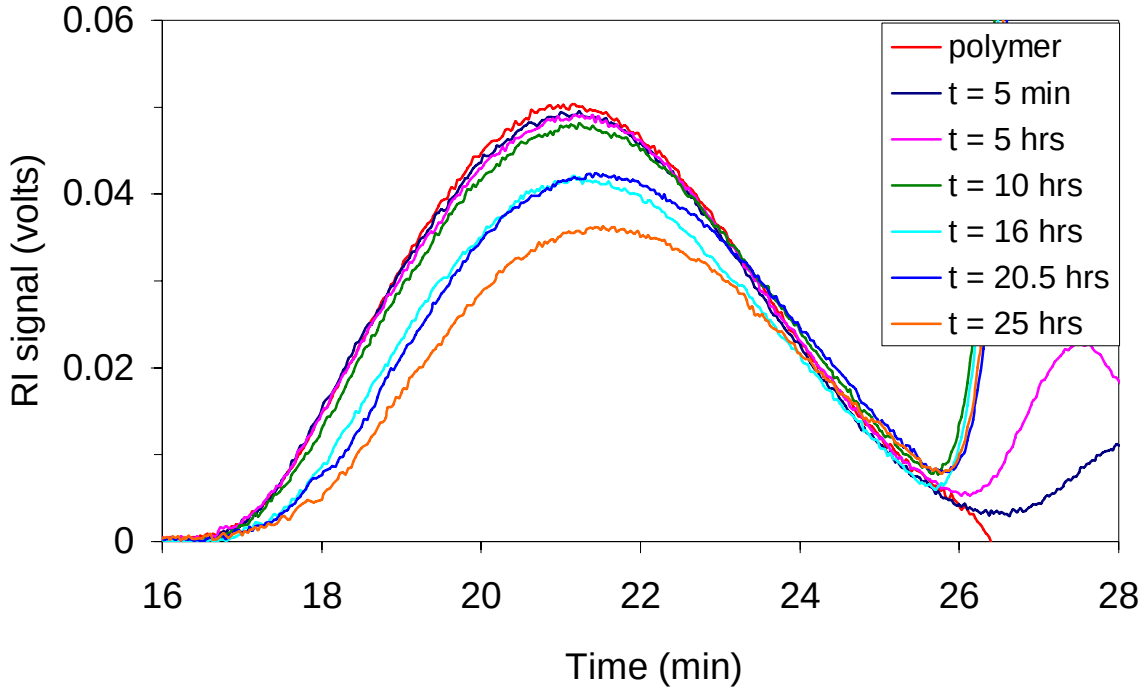

Figure 4.18 - RI chromatograms for gelant runs (Mobile phase: 1% KCl, 0.01% NaN_3).

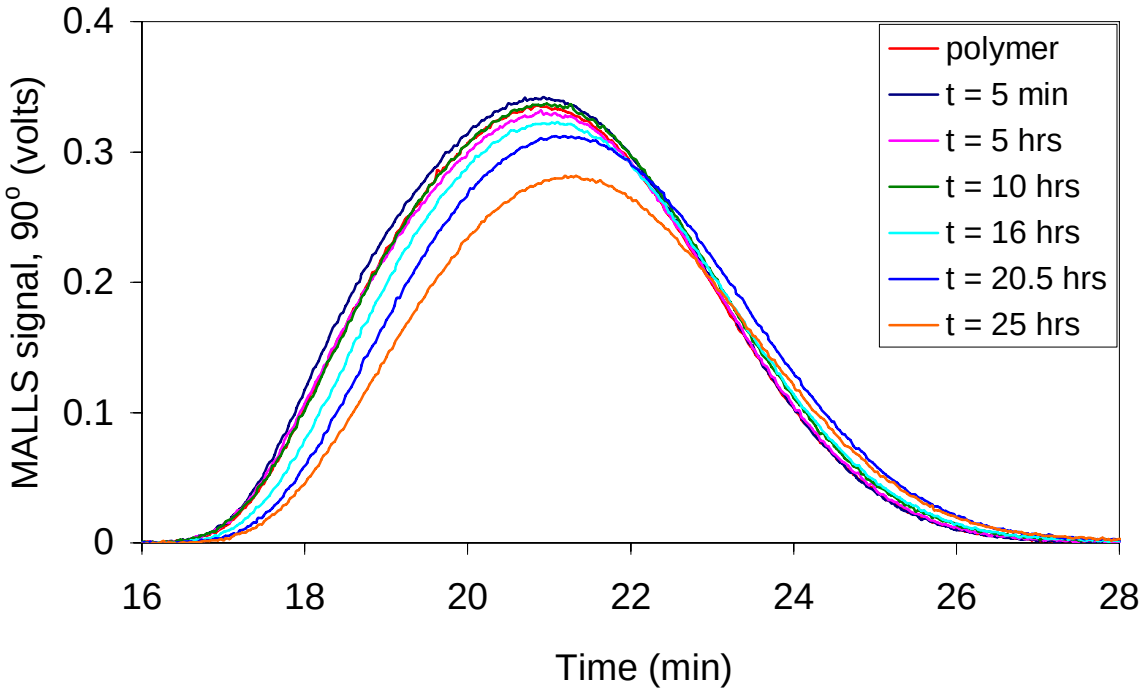

Figure 4.19 - MALLS chromatograms for gelant runs (Mobile phase: 1% KCl, 0.01% NaN_3).

The system pressure measured upstream of the columns (Figure 4.1) increased after injection of gelants that had reacted for 10 or more hours as shown in the second column in Table 4.5. The increased pressure indicated retention of material in the columns. The gel system was not injected at reaction times greater than 25 hours to prevent plugging of the columns. The columns required cleaning after the series of gelant injections. The mobile phase was changed to D.I. water and the columns were washed by injecting 50 μL of 1M NaOH solution repeatedly till the theoretical plate number increased to the original value of about 4000. The plate number was determined by glucose injections according to manufacture's procedure.

Table 4.5 – System pressure after gelant injections (200 mg/kg polymer concentration, 100 μL).

Reaction time (hours)	Pressure (psig)	
	Mobile phase: 1% KCl, 0.01% NaN_3	Mobile phase: 0.2 M NaOAc, 0.01% NaN_3
0.08	42.2	45.5
5	42.2	45.5
10	43.0	46.0
15-16	43.4	46.3
20	44.4	46.5
25	46.0	47.4

RI chromatograms for the injection of polymer solutions that were conducted between the gelant injections are shown in Figure 4.20. The chromatograms indicate proper operation.

In mobile phase: 0.2 M NaOAc, 0.01% NaN_3. In an effort to reduce the retention of aggregates in the column, a mobile phase containing 0.2 M sodium acetate was used. The additional acetate reduces chromium-polymer reaction rate. The pH of the NaOAc mobile phase was adjusted to 6.0 with acetic acid to prevent precipitation of chromium hydroxide. The chromium: acetate molar ratio was ~ 1: 2500.

A gel system was prepared and samples were injected as described above. The samples were diluted from 5000 mg/kg polymer concentration to 200 mg/kg by adding the new mobile phase. Between two gelant injections, polymers were injected to keep the columns saturated with polymer.

Results similar to runs with the KCl mobile phase were obtained as shown in Figure 4.21. Retention was indicated by the increased system pressure as shown in Table 4.5. The addition of acetate did not reduce the retention of aggregates. The Shodex column does not appear to be suitable for fractionating pre-gel aggregates.

Conclusions

1. Measurement of distributions of molecular weight and size of polymers was accomplished with a SEC-MALLS-RI setup.
2. The Shodex SUGAR KS 807 column separated polymers well, but was not suitable for gelants.

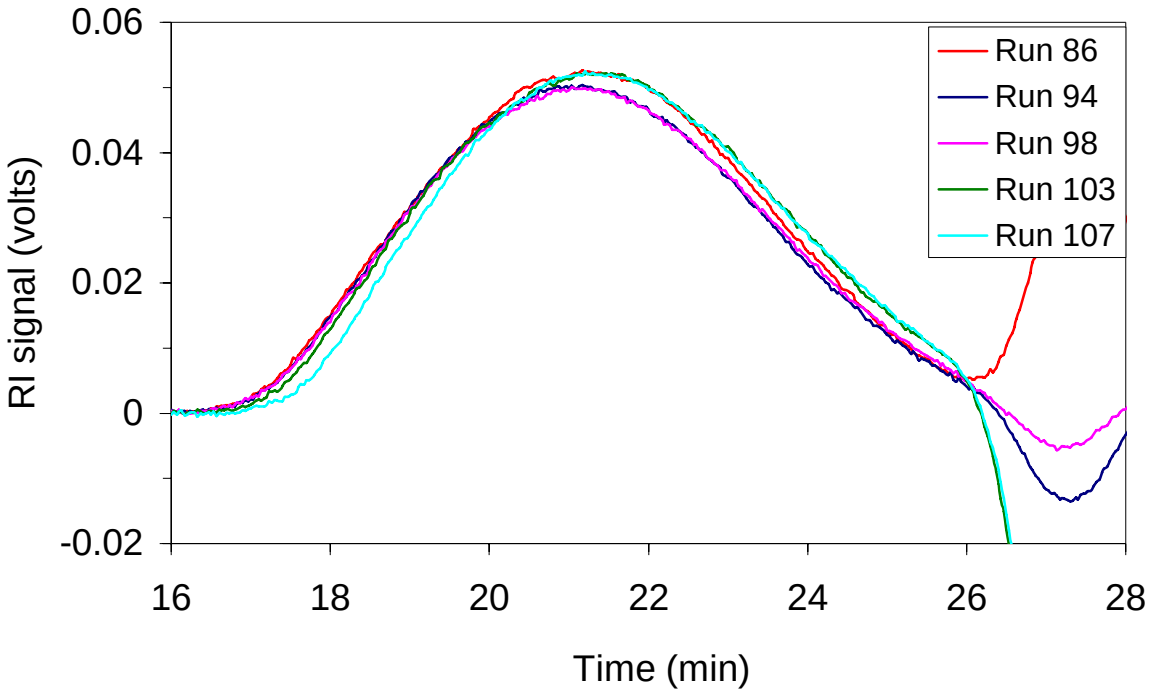

Figure 4.20 - RI chromatograms for polymer runs between the gelant injections.

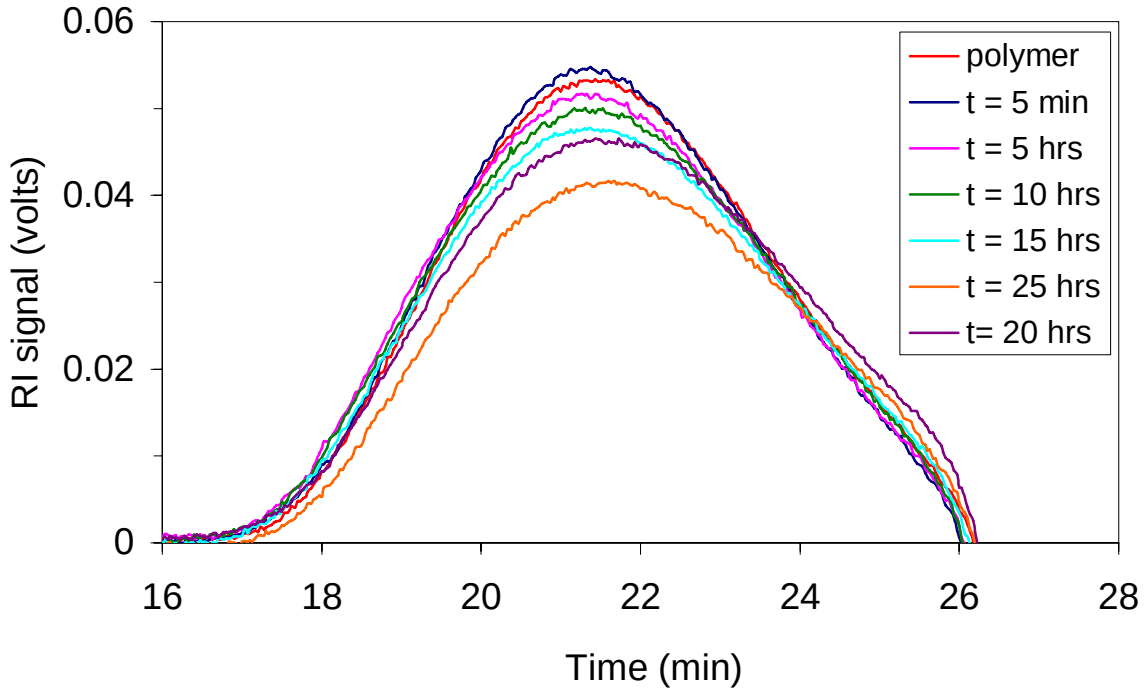

Figure 4.21 - RI chromatograms of gelant runs (Mobile phase: 0.2 M NaOAc, 0.01% NaN_3).

3. Larger, more reactive, gel-polymer aggregates were retained on the Shodex SUGAE KS 807 column after a period of reaction time that was much less than the gel time of the system.
4. Addition of acetate ion to the mobile phase of the measuring system did not reduce retention of the gel-polymer aggregates.

References

DAWN Course Manual, Light Scattering University Lectures, Wyatt Technology Corporation, Santa Barbara, CA (1998).

Wang, Tong: "Determination of Weight-average Molecular Weight and Z-average Root Mean Square Radius of Pre-gel Aggregates in a Polyacrylamide-chromium(III) Acetate System using a Multi-Angle Laser Light Scattering Technique," MS thesis, The University of Kansas, Lawrence, KS (2003).

Willhite, G. P., Green, D.W. and McCool, C.S.: "Increased Oil Recovery from Mature Oil Fields using Gelled Polymer Treatments," Annual Report for June 1999 – June 2002, Report No. 99BC15209-5, Contract No. DE-AC26-99BC15209, US DOE, Washington, DC (Dec 2002).

Wyatt, P.J.: "Light Scattering and the Absolute Characterization of Macromolecules", *Analytica Chimica Acta*, **272** (1993), 1-40.

Chapter 5

Measurement of the Distributions of Molecular Weight and Size of Polymers and Pre Gel Aggregates by an FFFF-MALLS-RI Apparatus

Graduate Research Assistant: Min Cheng

Introduction

Flow Field-Flow Fractionation (FFFF) is a technique applicable to the separation and characterization of particles and water-soluble polymer molecules. It is an open channel system containing no packing material. Compared with size exclusion chromatography (SEC), the sample molecules are supposed to have less chance to interact with the channel surface. The principle of FFFF can be found elsewhere [Giddings, J.C. *et al*, 1976; Willhite *et al*., 2002]. In this work an experimental apparatus composed of an FFFF channel, a multi-angle laser light scattering (MALLS) detector and a refractive index (RI) detector was developed to measure the distributions of the molecular weight and the root mean square (rms) radius of polymers.

Experimental Materials, Equipments and Procedures

Mobile Phase. In most of the experiments the mobile phase was 1% (weight fraction unless otherwise stated) potassium chloride aqueous solution, with 0.01% sodium azide as a bactericide. Fresh mobile phase was prepared every week to avoid contamination.

Some other kinds of mobile phase also found their applications:

(1) 0.01% sodium dodecyl sulfate (SDS) surfactant, 0.02% sodium azide solution.

(2) 1% potassium chloride solution, with pH = ~ 4.0 by adding 1 N hydrochloric acid.

Mobil phases were all filtered through 0.02 μm membranes under the vacuum.

Polymers and Gel System. Polystyrene particle size standards (Duke Scientific Co., Palo Alto, CA) were used to check the performance of the flow field-flow fractionator. The standards were narrowly distributed, and the particle sizes were certified by transmission electron microscopy (TEM) and photo correlation spectroscopy (PCS). Table 5.1 lists the particle sizes of three standards reported by the manufacturer. For ease of use, the polystyrene particles were packaged in a 1% aqueous suspension. They must be thoroughly dispersed in the bottle to assure statistically consistent samples. The bottle was gently inverted several times, and immersed in a low power ultrasonic bath for 30 seconds. Then the 1% polystyrene standards were further diluted to the desired concentrations with 0.01% SDS surfactant, 0.02% sodium azide solution. For particulate samples, a dilute surfactant solution is necessary to wet the particles, stabilize the dispersion and avoid the aggregation. The diluted samples also should be ultrasonicated for 30 seconds prior to the injections.

Four polyacrylamide samples were tested. Two were non-ionic polyacrylamide standards, paam1000K and paam6000K (Polymer Standards Service (PSS)-USA Inc., Warwick, RI) and two were partially hydrolyzed polyacrylamide Alcoflood 935, Lot 7158 V and Lot A2247 BOV (Ciba Specialty Chemicals Co., Suffolk, VA), with a degree of hydrolysis of 10%. The number- and weight-average molecular weights, M_{n0} and M_{w0}, and the z-average root-mean-square (rms) radius, R_z, of the polyacrylamide samples are listed in Table 5.2.

Table 5.1 – Manufacturer cited diameters of polystyrene particle standards.

Nominal diameter (nm)	TEM results Mean diameter (nm)	PCS results Hydrodynamic diameter (nm)
50	50 ± 2	54 ± 2.7
100	102 ± 3	102-109
300	300 ± 5	299-307

Table 5.2 – Molecular weight and size averages of samples.

	M_{n0} (g/mol)	M_{w0} (g/mol)	R_z (nm)	
paam1000K	4.65×10^5	1.14×10^6	/	PSS-USA Inc.
paam6000K	2.46×10^6	5.55×10^6	/	PSS-USA Inc.
AlcoFlood 935, Lot 7158V	/	5.26×10^6	181.7	[Wang, 2002]
AlcoFlood 935, Lot A2247BOV	/	6.64×10^6	216.8	[Wang, 2002]

A polyacrylamide - chromium(III) acetate gel system was prepared by mixing partially hydrolyzed polyacrylamide stock solution with chromium(III) acetate solution. The gel system used in this work consisted of 5000 mg/kg polyacrylamide Alcoflood 935, Lot A2247BOV and 100 mg/kg chromium(III). The solvent used to prepare polymer and chromium stock solutions was 1% potassium chloride, 0.01% sodium azide solution. A 6667 mg/kg polymer stock solution was prepared first. A 400 mg/kg chromium stock solution was diluted from a 50% chromium(III) acetate solution (McGean-Rohco, Inc., Lot No.40086816, Cleveland, OH; the chromium(III) concentration was 12.1 %). The chromium stock solution was freshly prepared and filtrated through a 0.02 μm filter prior to mixing with the polymer stock. Then the polymer and chromium stock solutions were mixed at the ratio of 3:1 on a weight basis to form a gelant with 5000 mg/kg polymer and 100 mg/kg chromium(III) concentrations. The acetate-to-chromium(III) molar ratio was 3.0. Then the gelant was kept in a temperature-controlled water bath at 25 °C. The gel time of this gel system was ~ 31 hours determined by the viscosity measurement.

Experimental Equipments. A Model F-1000-FIFO Universal Fractionator (Postnova Analytics, Salt Lake City, UT) was used to separate the polymers. The key of the fractionator is the FFFF channel.

This FFFF channel consists of two acrylic blocks with a polyester spacer and a membrane in between. Ceramic frits with average pore size of 5 μm were mounted in two channel blocks. There are three frit elements in the inlet block: the main frit, the frit inlet, and the frit outlet. The main frit allows the crossflow stream evenly distribute into the channel. The frit inlet is designed for the sample relaxation. In this study the frit inlet was disabled and a stopflow procedure was used. The frit outlet is designed for the sample enrichment. Mobile phase flowing above the

sample components exited through the frit outlet, leaving the samples concentrated in the channel outlet stream.

The channel dimension was cut from the spacer, which is 27.7 cm in length, 2.0 cm in width and 0.0254 cm in thickness. The membrane was placed below the spacer and on top of the channel outlet block. 10,000 molecular weight cutoff membranes, including regenerated cellulose (RGC) membranes and polyethersulfone (PES) membranes (Postnova Analytics, Salt lake city, UT), were used in the experiments.

In general, brine solutions are compatible with the components of the FFFF channel. Depending on the membrane installed, a mobile phase with pH ranging from 3.0 to 10.0 may be used. When changing the mobile phase, the FFFF system should first be flushed with at least 1 liter of water. Then the system should be purged overnight with the new mobile phase. The FFFF channel works under the room temperature. The maximum channel pressure is 150 psi, yet a minimum pressure of 50 psi in the channel must be guaranteed to prevent the liquid in the crossflow outlet from cavitating.

A DAWN EOS^{TM} (Wyatt Technology Corporation, Santa Barbara, CA) detector was used to measure the molecular weight and size distributions of polymers. This instrument employs the multi-angle laser light scattering (MALLS) technique. The main components of the DAWN EOS include a GaAs laser that emits light at the wavelength of 680- 690 nm, a K5-597 model flow cell, and 18 detectors placed at different angles around the flow cell assembly. There are two operation modes: *batch mode* for measuring the weight-average molecular weight and z-average rms radius of unfractionated samples; *inline mode* for measuring the molecular weight and size distributions of fractionated samples. The inline mode was used in this study. The flow cell can withstand up to 1000 psi back pressure. This MALLS detector does not have temperature control and was operated at room temperature (about 23 °C).

The mass detector used was an Optilab DSP (Wyatt Technology Corporation, Santa Barbara, CA) interferometer (refractive index [RI] detector). The Optilab DSP measures the difference in refractive index between the current solution in a sample cell and a clean solvent, usually used to prepare the sample solution, in a reference cell. A P10 cell was used in this study. The Optilab DSP can be operated offline to determine the refractive index increment (dn/dc) of the polymer, which is required to compute the concentration of the polymer from the RI signals. In this study the Optilab was also operated inline with the FFFF channel and the MALLS detector for the measurement of the concentrations of fractionated polymer fractions. The cell can withstand 200 psi back pressure, but the maximum back pressure that the Optilab DSP can withstand is only 30 psi limited by the solenoid purge valve. The cell temperature of the RI detector was set at 35 °C in order to stabilize the RI baseline.

Experimental Procedures. The experimental schematic for an FFFF-MALLS-RI setup is shown in Figure 5.1. The channel flow stream was pumped through a 0.5 μm slip-on inlet filter in the reservoir, an inline degasser, a 0.02 μm inline filter, a Rheodyne 7725i sample injector, then through the FFFF channel to the detectors. The flow direction of the channel flow stream was controlled by a two-position, ten-port Valco switching valve. The crossflow stream was also degassed and pumped through a 0.02 μm inline filter. It could flow in a recirculating mode or a

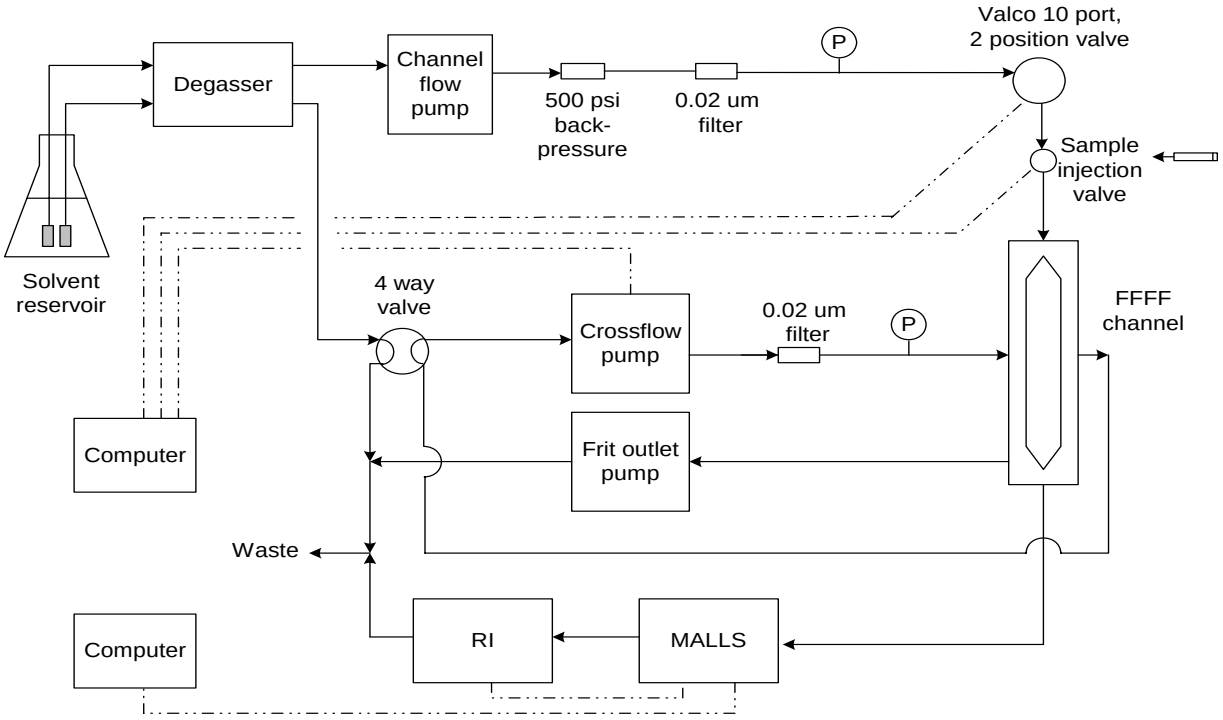

Figure 5.1 - Experimental schematic of an FFFF-MALLS-RI Setup.

non-recirculating mode, switched by a two-position four-port Hamilton valve. Two pressure gauges were used to monitor the pressures generated by the channel flow and crossflow respectively. A frit outlet pump controlled the flow rate of the frit outlet stream. The details of plumbing can be found in section 3.2.2 in FFFF user manual.

A 0.01″ID PEEK tubing was attached to the Optilab DSP outlet to artificially increase the channel pressure. The length of the tubing was carefully chosen to ensure the back pressure added to the Optilab DSP less than 30 psi at different channel flow rates.

Sample was injected to load a 20 or a 100 μL sample loop, and then carried by the mobile phase into the head of the channel. The channel flow stream was diverted after an injection delay time, leaving the channel bypassed. The channel flow was halted and only crossflow was maintained in the channel for the sample relaxation. The injection delay time is related to the channel flow rate and the void volume from the sample injector to the channel inlet, and the stopflow time depends on the crossflow rate and the channel void volume. After the stopflow period the channel flow was resumed in the channel to bring the samples out. Fractionated samples passed though the DAWN EOS and Optilab DSP detectors, and the corresponding MALLS and RI data were collected and processed by ASTRA (Wyatt Technology Corporation, Santa Barbara, CA).

In some experiments the FFFF channel was coupled with a Water 490 Multiwavelength Ultraviolet (UV) detector (Waters Associates Inc., Milford, MA). In this case a 40 psi back pressure regulator was attached after the UV detector to add pressure to the channel. The UV data were collected by a Flow 160 software and processed by the Analysis software, both provided by Postnova Analytics.

The Flow 160 software controlled the operation of the FFFF. The Rheodyne sample injector, the Valco switching valve, and the crossflow pump were all interfaced with the computer, so that the Flow 160 software could initiate and discontinue the stopflow period, and control the crossflow rate automatically. A power programmed crossflow rate was used in this study, *i.e.,* a high initial crossflow rate was applied first for a period of time, *t1*, and then decreased gradually.

The Optilab DSP is extremely sensitive. It can easily distinguish between solvent which has been open to the air overnight and solvent freshly prepared. A refractive index change due to a concentration difference of 1 mg/kg is easy to detect (~10 mV for a P10 cell). The use of "two or more pumps and a mixing chamber" is strongly unrecommended in the Optilab DSP user manual, because two streams often can not equilibrate thoroughly under such conditions and can easily cause the drift of the RI baseline. The Optilab DSP also responds to a slight change of the pressure or flow rate. The varying crossflow rate interferes with the stability of the RI baseline when a power programmed crossflow is applied. However, the Optilab DSP is still a more favorable concentration detector in this study due to its high performance and low level of noise. Every time when new solvent was added into the reservoir, the FFFF channel was flushed overnight with channel flow and non-recirculating crossflow at low flow rates to equilibrate these two streams in the channel.

Results and Discussion

Polystyrene Particle Size Standards. Polystyrene particle size standards were tested first on an FFFF-UV setup to check the performance of the FFFF channel. The mobile phase was 0.01% SDS surfactant, 0.02% sodium azide solution, and a 10,000 molecular weight cutoff regenerated cellulose (RGC) membrane was placed in the FFFF channel.

Experiments focused on the separation of the 50, 102 and 300nm polystyrene mixtures. Sample retention of 300 nm polystyrene was observed, especially when using the power programmed crossflow. Since the 300 nm polystyrene is bigger in size and closer to the membrane, it is easier to get retained on the membrane surface. The sample recovery of 300 nm polystyrene or the area under the UV sample peak kept increasing in the first several runs. Repeatable result was obtained after the membrane was conditioned. Figure 5.2 shows the fractograms of polystyrene mixtures with different compositions. Smaller particles eluted earlier under the same operating conditions, suggesting that the elution behavior of the polystyrene mixtures followed the normal mode of FFFF.

A better separation of the 50 nm and 102 nm polystyrene sample peaks was achieved when a higher initial crossflow rate was applied, as shown in Figure 5.3. Higher field strength enhances the resolution between these two species of small size. However the total elution time was elongated.

The preliminary experiments on the separation of the polystyrene particle size standards indicate the proper operation of the FFFF channel.

Polyacrylamide Standards. Non-ionic polyacrylamide standards paam1000K and 6000K were first tested on the FFFF-MALLS-RI setup. The FFFF system was flushed with at least one liter of water. A new RGC membrane was replaced in the channel. Then the mobile phase was

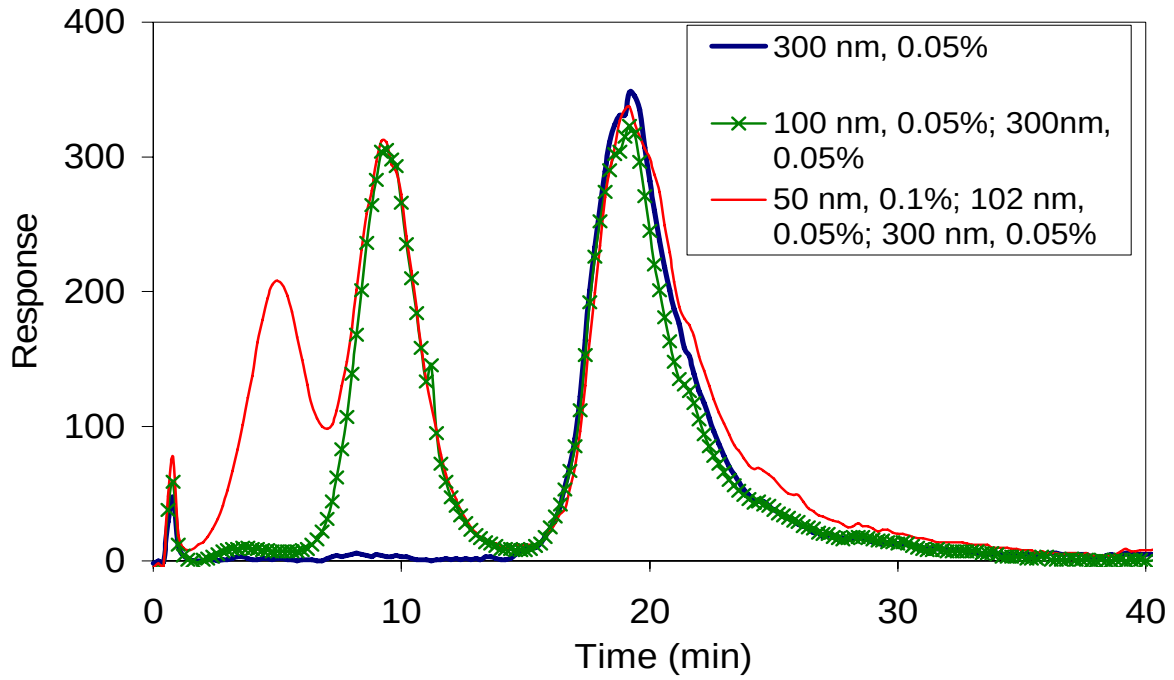

Figure 5.2 – Fractograms of polystyrene mixtures with different compositions (Sample loop: 20 µL, channel flow rate: 1.5 mL/min, frit outlet flow rate: 0.75 mL/min, cross flow rate: 0.6 → 0.1 mL/min, t1 = 6 min, UV wavelength = 254 nm).

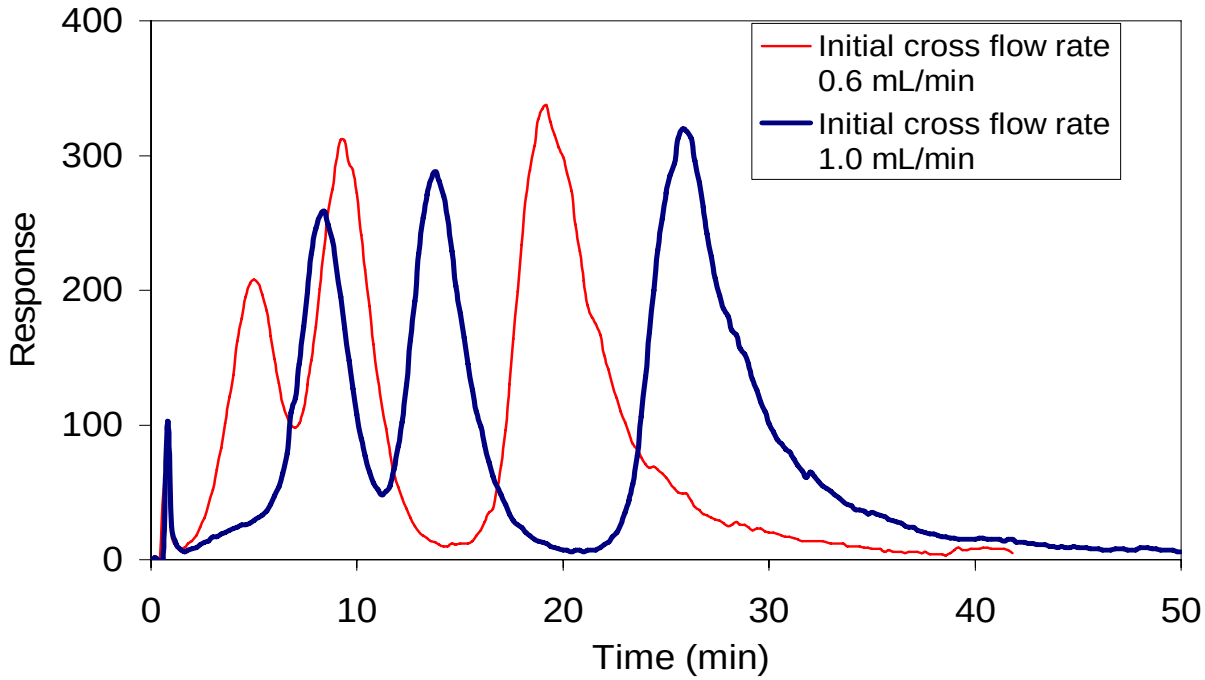

Figure 5.3 – Fractograms of polystyrene mixtures under different initial crossflow rates (Sample: 50 nm 0.1%, 102 nm 0.05%, 300 nm 0.05% polystyrene mixture, sample loop: 20 µL, channel flow rate: 1.5 mL/min, frit outlet flow rate: 0.75 mL/min, t1 = 6 min, UV wavelength = 254 nm).

changed to 1% potassium chloride, 0.01% sodium azide solution. The FFFF system was flushed with the new mobile phase thoroughly prior to the coupling with the MALLS and RI detectors.

Figure 5.4 shows the MALLS and RI fractograms of paam1000K. Contrary to SEC, it can be seen clearly that the RI peak top locates on the left side of the MALLS peak top, indicating that small molecules with low molecular weight elute earlier. The MALLS fractogram suggests the presence of large species with high molecular weight at longer elution time (≥ 40 minutes), which are not taken into account for the calculation of the molecular weight because of a too low RI response.

Sample overloading was not observed for paam1000K and 6000K. Under the same operating conditions, the RI chromatograms of paam1000K and 6000K are shown in Figure 5.5. The elution time remained unchanged when the injected mass was decreased by 50%. Paam6000K, with higher molecular weight, eluted later than paam1000K. The elution behaviors of these two polyacrylamide standards follow the normal mode of FFFF: smaller molecules elute faster than bigger ones.

The data processing methods were chosen as the same as in SEC runs: Debye plot, Zimm formalism, 4-18 detectors, detector fit degree = 1, result fit degree = 1. The measured molecular weight verses elution time of these two standards is shown in Figure 5.6. The differential molecular weight and the rms radius distributions are shown in Figures 5.7 and 5.8. Figure shows the elution progression from small molecules with lower molecular weight through successively bigger molecules.

The measured molecular weight averages and the z-average rms radius of these two standards are shown in Table 5.3. The FFFF results are comparable with the SEC results and the cited values. Figures 5.9 and 5.10 show the differential molecular weight and rms radius distributions of paam6000K measured by SEC and FFFF respectively. The rms radii are plotted against molecular weight (log-log) for paam6000K in Figure 5.11. Similar molecular weight and size distributions are obtained by means of two separation methods. The slopes of rms radius vs. molecular weight (log-log) plot are also identical. The separation of nonionic polyacrylamide standards is successful in FFFF.

Table 5.3 - Molecular weight and size averages of polyacrylamide standards measured by different methods.

	M_{n0} (10^6 g/mol)	M_{w0} (10^6 g/mol)	R_z (nm)	
paam1000K	0.85	1.77	111.8	FFFF
paam6000K	2.47	4.83	194.8	SEC
	2.66	4.76	195.7	FFFF

Polyacrylamide Alcoflood 935

In mobile phase: 1% potassium chloride, 0.01% sodium azide solution. The basic separating conditions for partially hydrolyzed polyacrylamide, AlcoFlood 935, were the same as those for the polyacrylamide standards paam1000K and 6000K: the mobile phase was 1% potassium

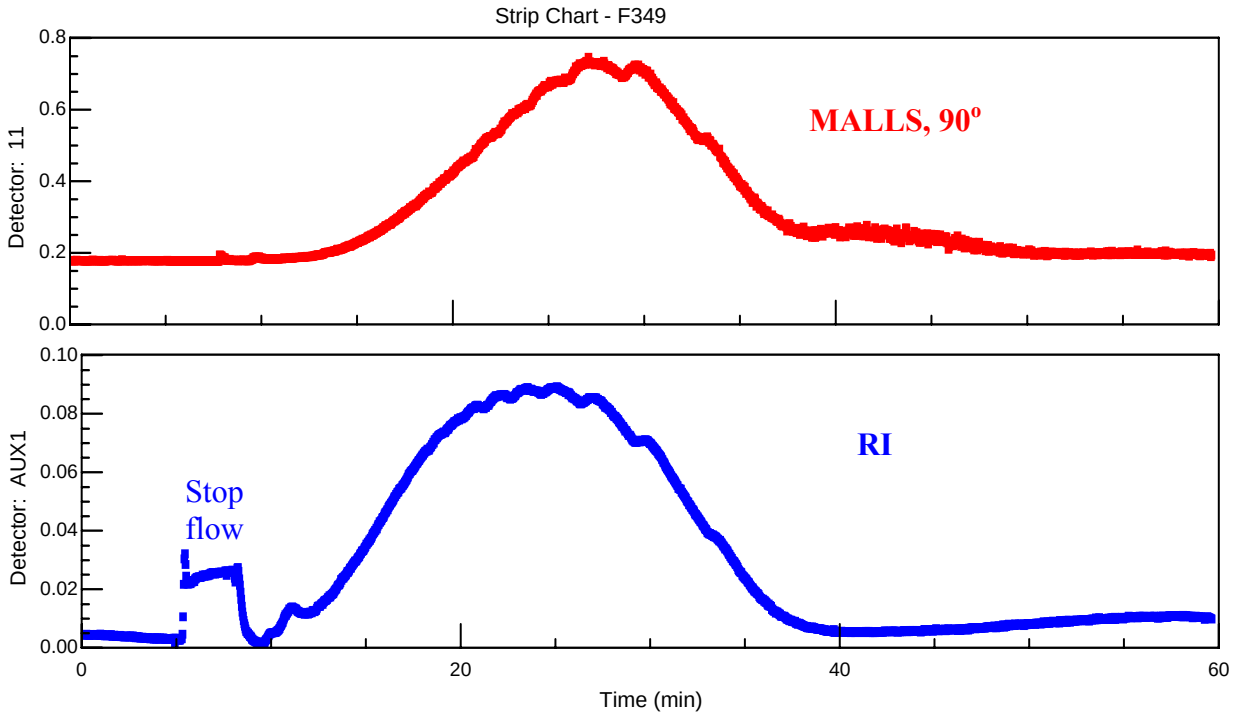

Figure 5.4 – MALLS and RI fractograms of paam1000K (Sample: paam1000K, 1000mg/kg, sample loop: 100 µL, channel flow rate: 0.5 mL/min, frit outlet flow rate: 0, cross flow rate: 0.7 → 0.05 mL/min, t1 = 4 min).

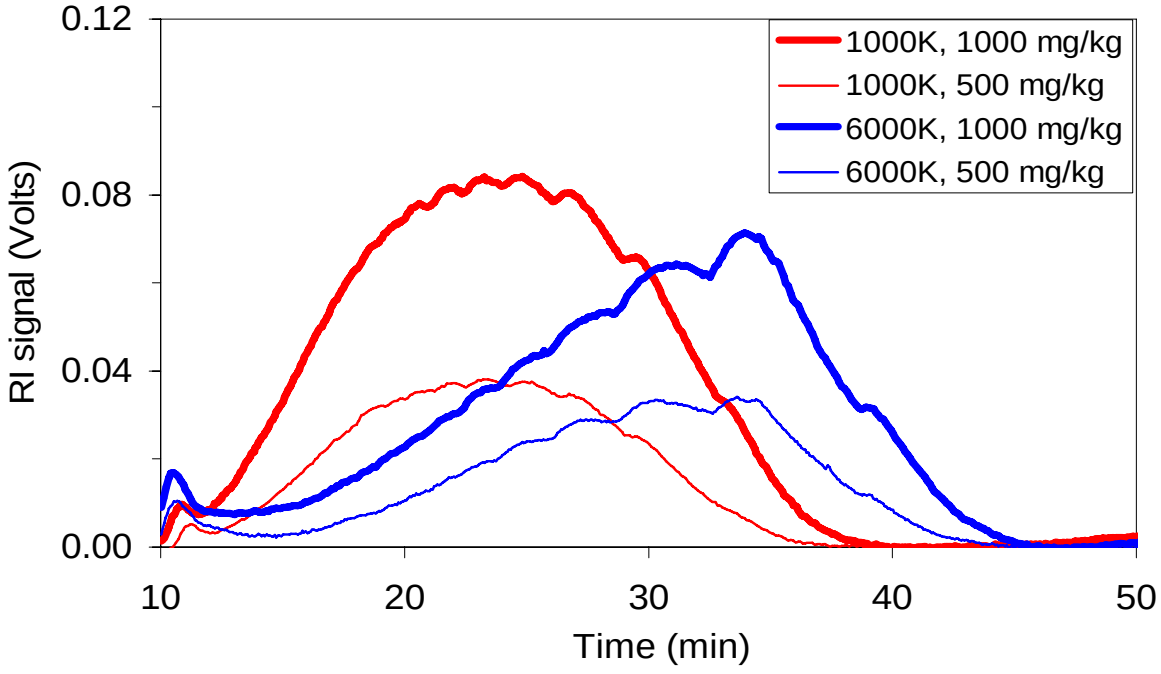

Figure 5.5 – RI fractograms of paam1000K and 6000K (sample loop: 100 µL, channel flow rate: 0.5 mL/min, frit outlet flow rate: 0, cross flow rate: 0.7 → 0.05 mL/min, t1 = 4 min).

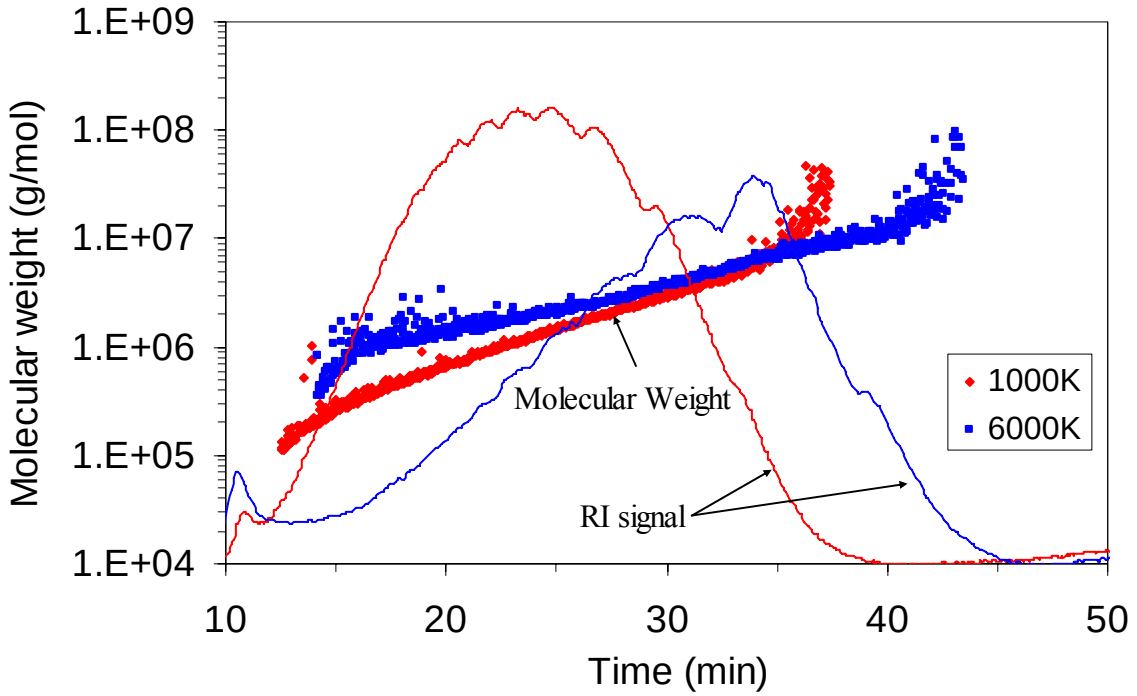

Figure 5.6 – Molecular weight versus elution time for paam1000K and 6000K.

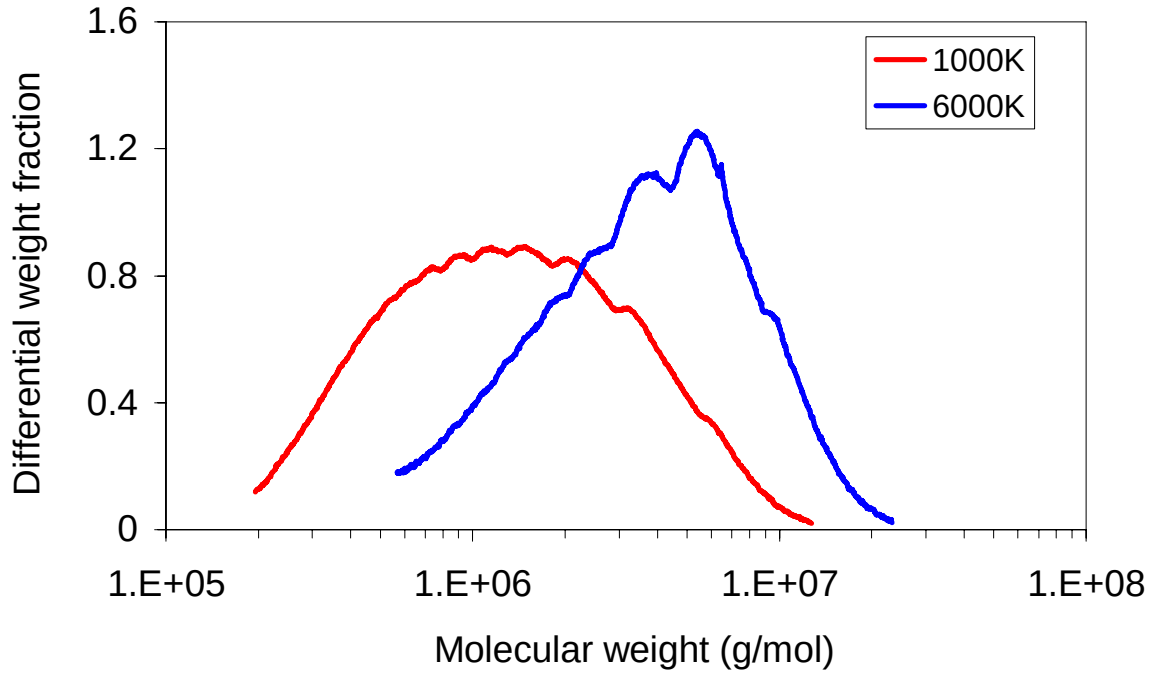

Figure 5.7 – Differential molecular weight distributions of paam1000K and 6000K.

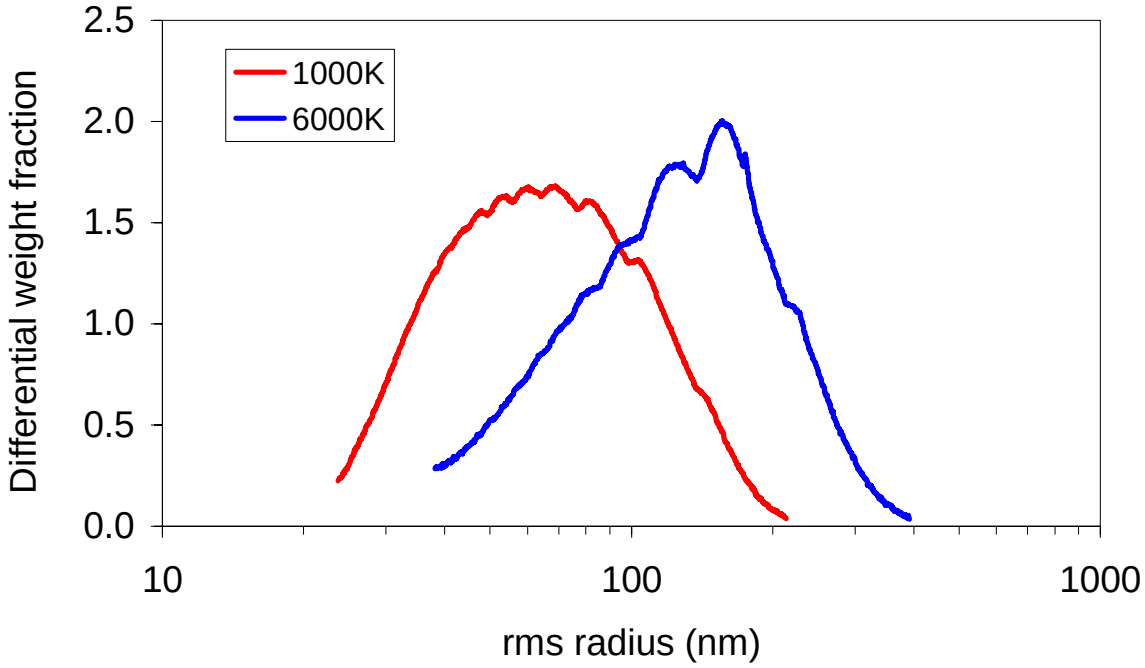

Figure 5.8 – Differential rms radius distributions of paam1000K and 6000K.

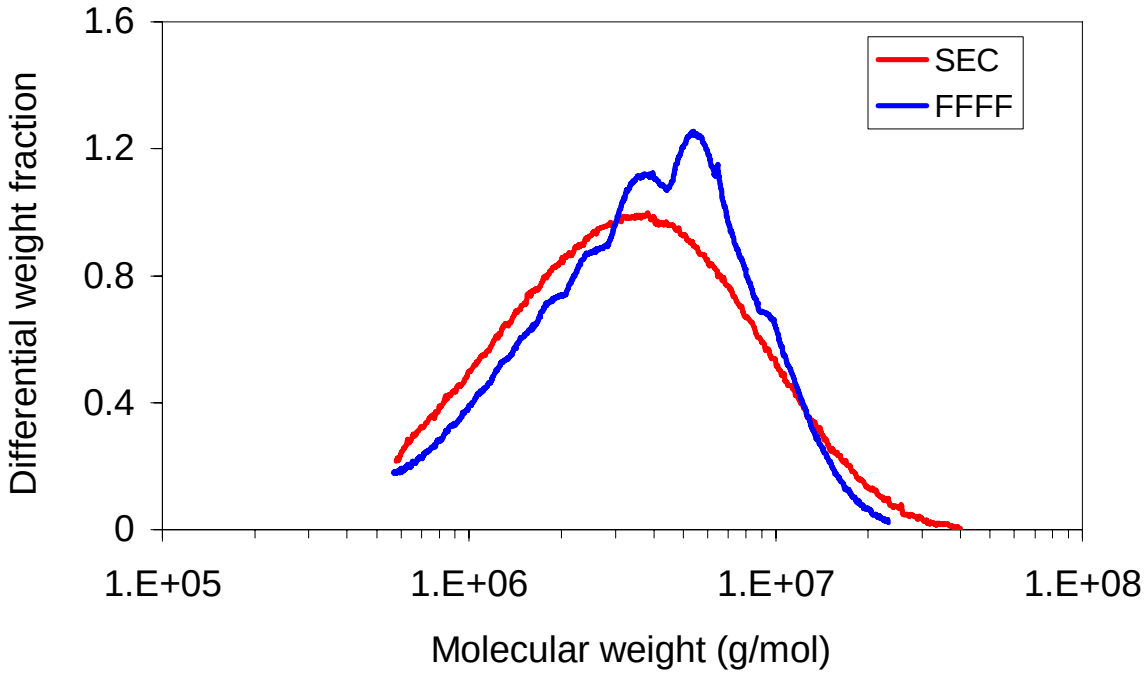

Figure 5.9 – Differential molecular weight distributions of paam6000K measured by SEC and FFFF.

.

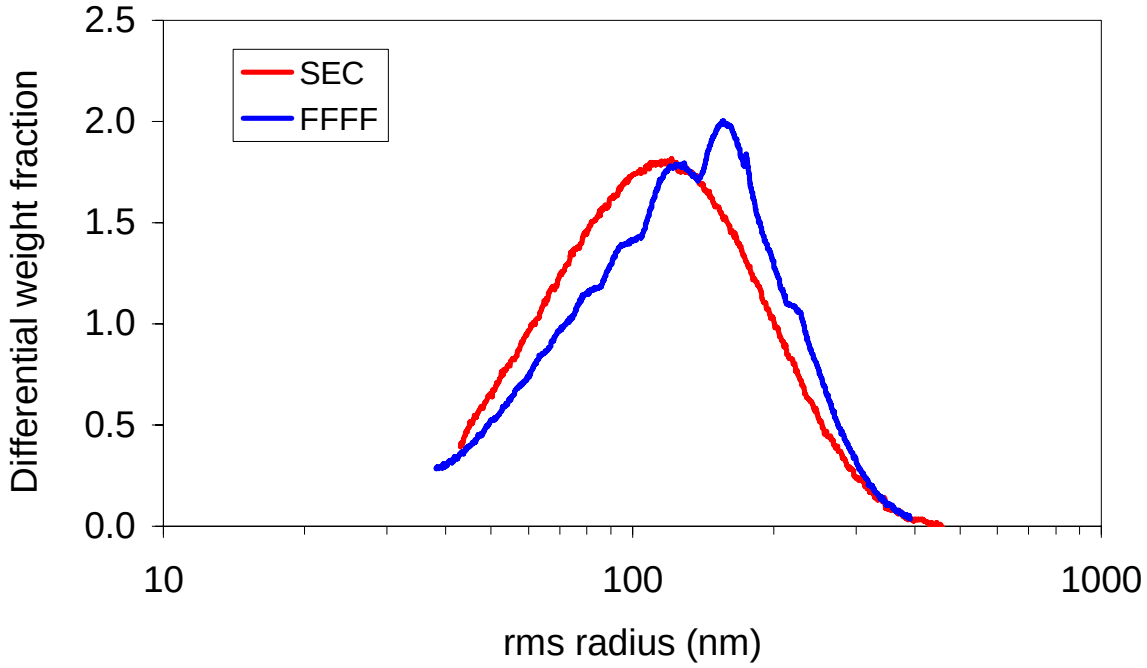

Figure 5.10 – Differential rms radius distributions of paam6000K measured by SEC and FFFF.

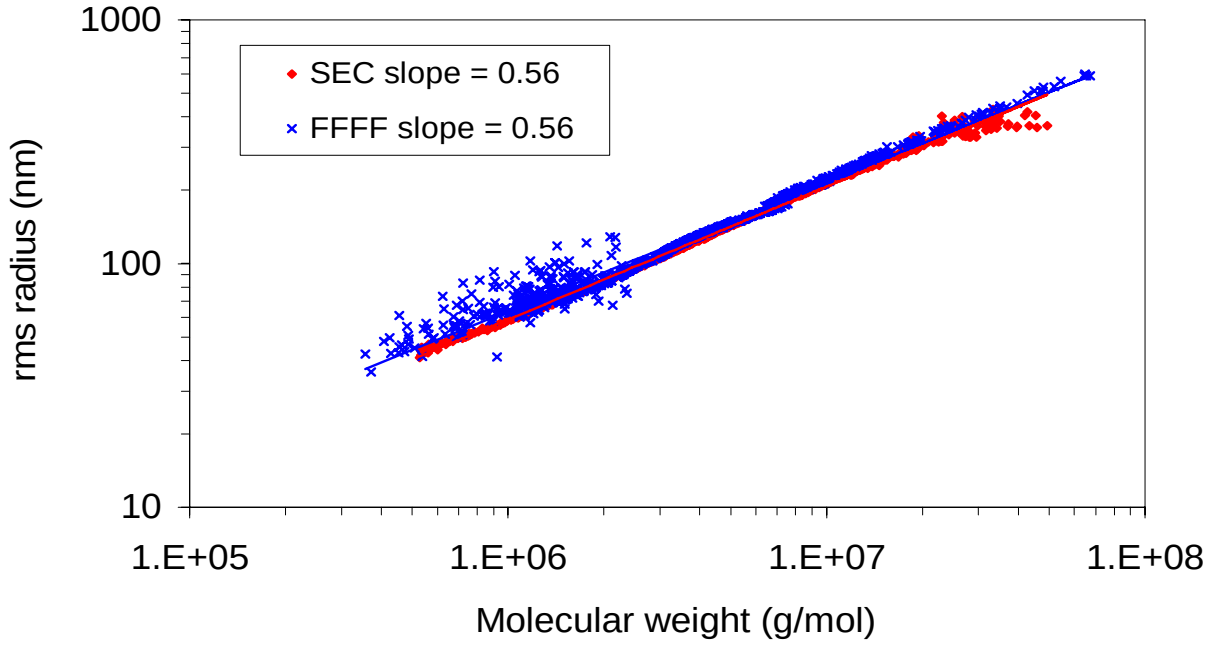

Figure 5.11 - Log-log plot of rms radius versus molecular weight for paam6000K measured by SEC and FFFF.

chloride, 0.01% sodium azide solution, and a RGC membrane with 10000 molecular weight cutoff was placed in the FFFF channel. Several problems were found for the separation of AlcoFlood 935.

Figure 5.12 shows the RI fractograms for AlcoFlood 935, Lots 7158V and A2247BOV, with different sample concentrations. Overloading was observed for Lot A2247BOV, but not for Lot 7158V. The RI peaks of Lot A2247BOV shifted towards earlier elution time with an increase in the sample load. Furthermore, Lot A2247BOV, with higher molecular weight and bigger size, eluted earlier than Lot 7158V.

It was also found that AlcoFlood 935 polymer molecules did not get separated successfully in FFFF. Because the MALLS signal is proportional to the product of the polymer concentration and the molecular weight, the RI peak will locate at the left side (FFFF) or the right side (SEC) of the MALLS peak even after the peak alignment. The MALLS and RI peaks of AlcoFlood 935 almost overlap after the alignment, as shown in Figure 5.13. That means AlcoFlood 935 behaves most likely monodispersed. Figures 5.14 and 5.15 show the differential molecular weight distributions of two polymer lots. Compared with SEC results, FFFF gives a much narrower molecular weight distributions. The calculated polydispersity index (PI) for the AlcoFlood 935 polymer is only about 1.0 ~ 1.1, much lower than SEC result, which is 1.7 ~ 1.8.

Several possible reasons could contribute to the abnormal elution behaviors and the underdetermined polydispersity index of AlcoFlood 935. In steric flow mode of FFFF, larger particles elute earlier than the smaller particles. In this case, a decreasing molecular weight versus elution time profile would be expected, like the one in a SEC run. However, it was found that the molecular weight still increased with the elution time across all the sample peaks in spite of the narrow distribution, as shown in Figure 5.16. It is unlikely for the AlcoFlood 935 polymers to experience steric flow mode of FFFF.

The optimization of the operating conditions, like the flow rates and the sample concentrations, is of great importance to obtain reliable separation results about the polymers. Slower channel flow rate can be used to increase the resolution between two species of similar size. At the same time the channel flow rate needs to be sufficiently large with respect to the crossflow rate so that the sample does not stick to the membrane. It was reported that a too small crossflow rate (a crossflow rate of 0.25 mL/min relative to a channel outlet flow rate of 1 mL/min) could lead to poor fractionation of the samples, resulting in a polydispersity index close to 1.0 for hydroxypropylmethylcelluloses [Wittgren, et al., 1997]. The use of higher crossflow fields leads to greater retention and fractionating power so that smaller species can be resolved. However, the concentration of the polymer molecules near the membrane is also increased at high crossflow. This could cause chain entanglement and change the elution behavior of the sample, resulting in a too short (repulsion) or too long (adsorption) retention time. With an initial crossflow rate of 1.0 mL/min and a channel flow rate of 0.3 mL/min, Duval et al. [2001] observed a polydispersity index of 1.0 for carboxymethylpullulan due to the over-retention of the high molecular weight fractions by the crossflow stream, while a polydispersity index of 1.5 was obtained when using SEC. In this work different combinations of the channel and crossflow rates were tried, but no improvement in the separation of AlcoFlood 935 was attained.

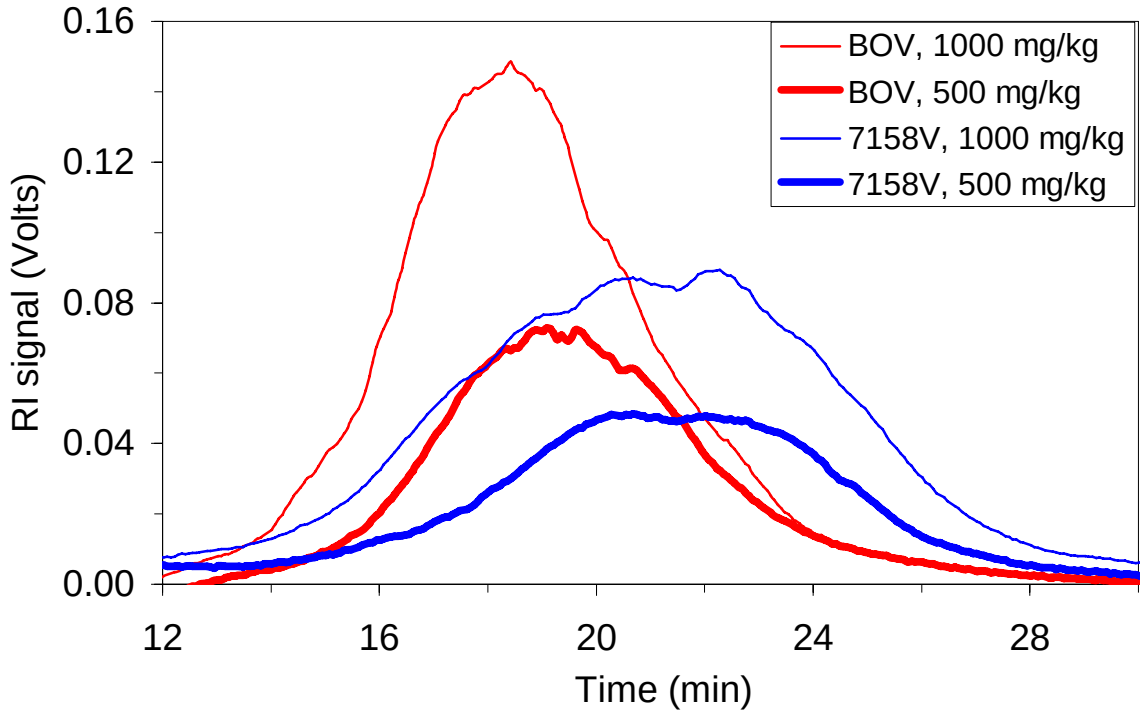

Figure 5.12 - RI fractograms of two polymer lots of AlcoFlood 935 (Sample loop: 100 µL, channel flow rate: 0.7 mL/min, frit outlet flow rate: 0, cross flow rate: 0.4 → 0.05 mL/min, t1 = 4 min).

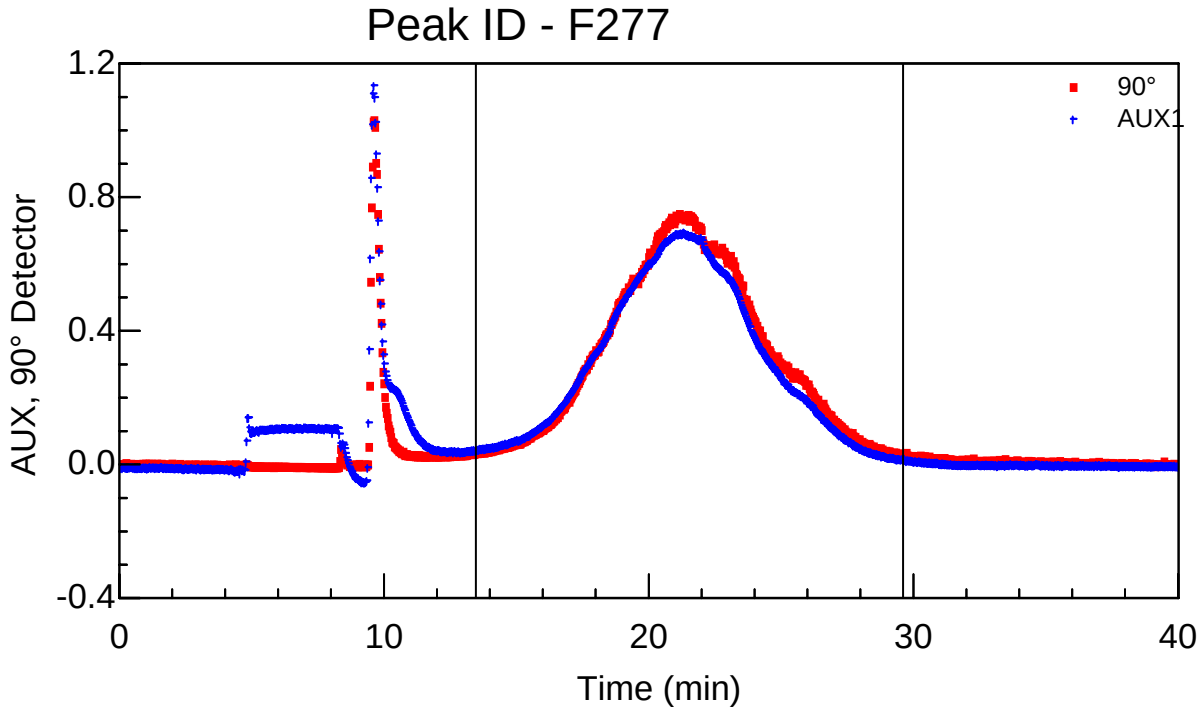

Figure 5.13 - MALLS and RI peaks almost overlap after the alignment (AlcoFLood 935, Lot 7158V).

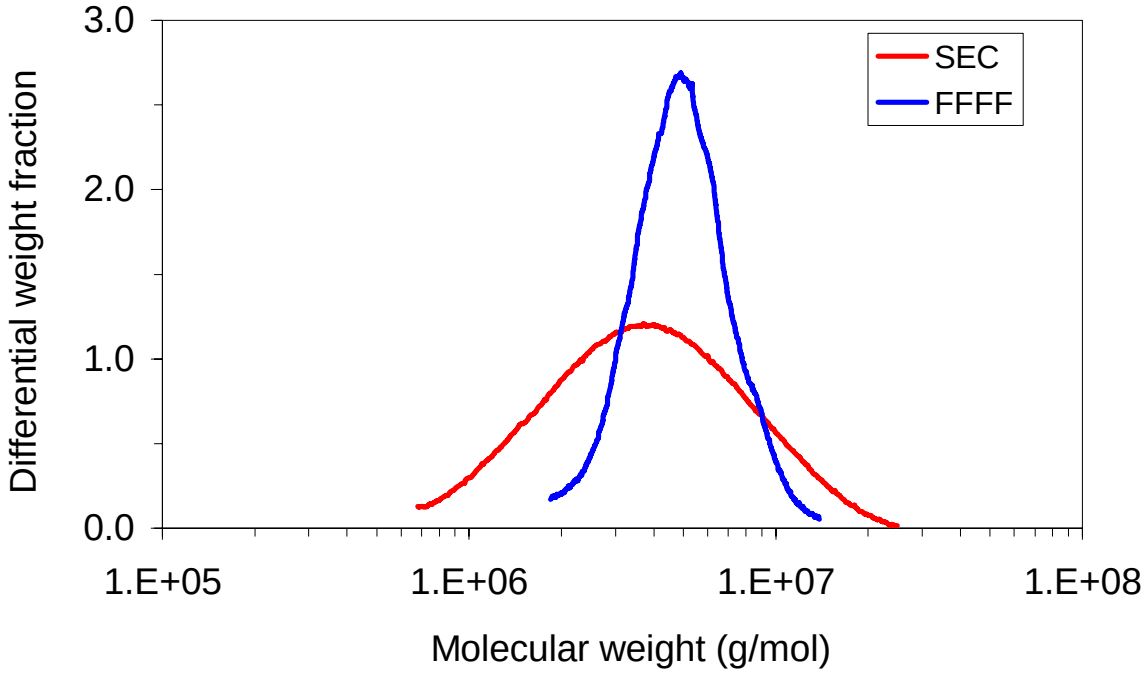

Figure 5.14 – Differential molecular weight distributions of AlcoFlood 935, Lot 7158V measured by SEC and FFFF.

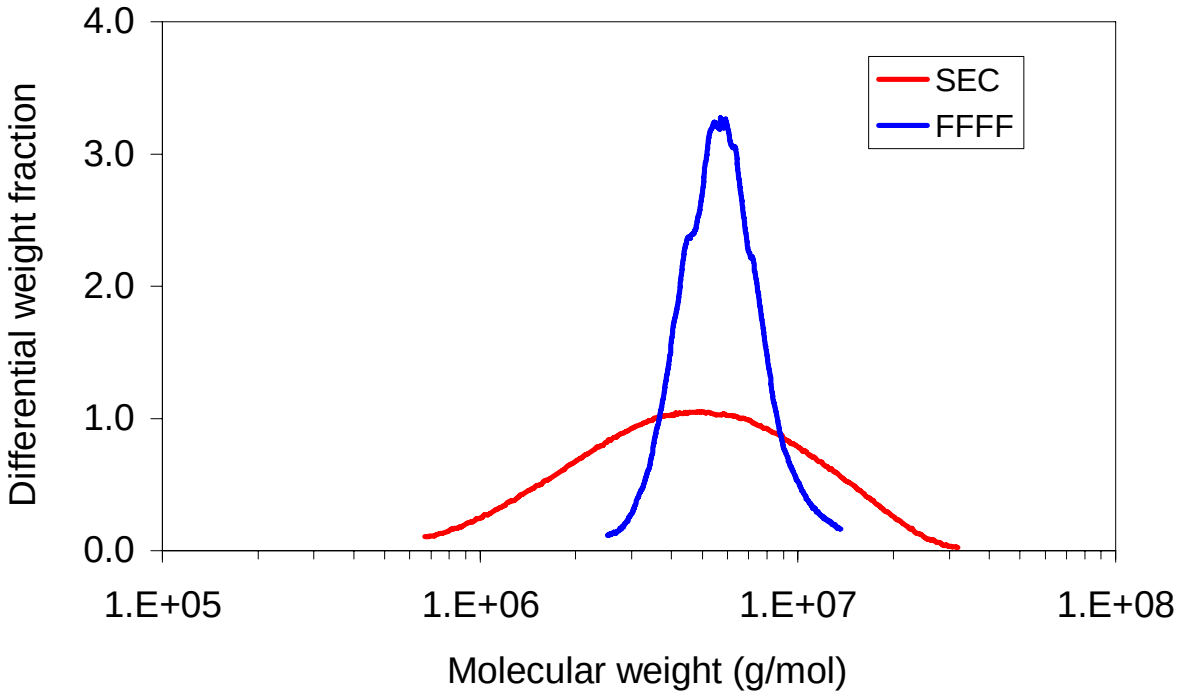

Figure 5.15 – Differential molecular weight distributions of AlcoFlood 935, Lot A2247BOV measured by SEC and FFFF.

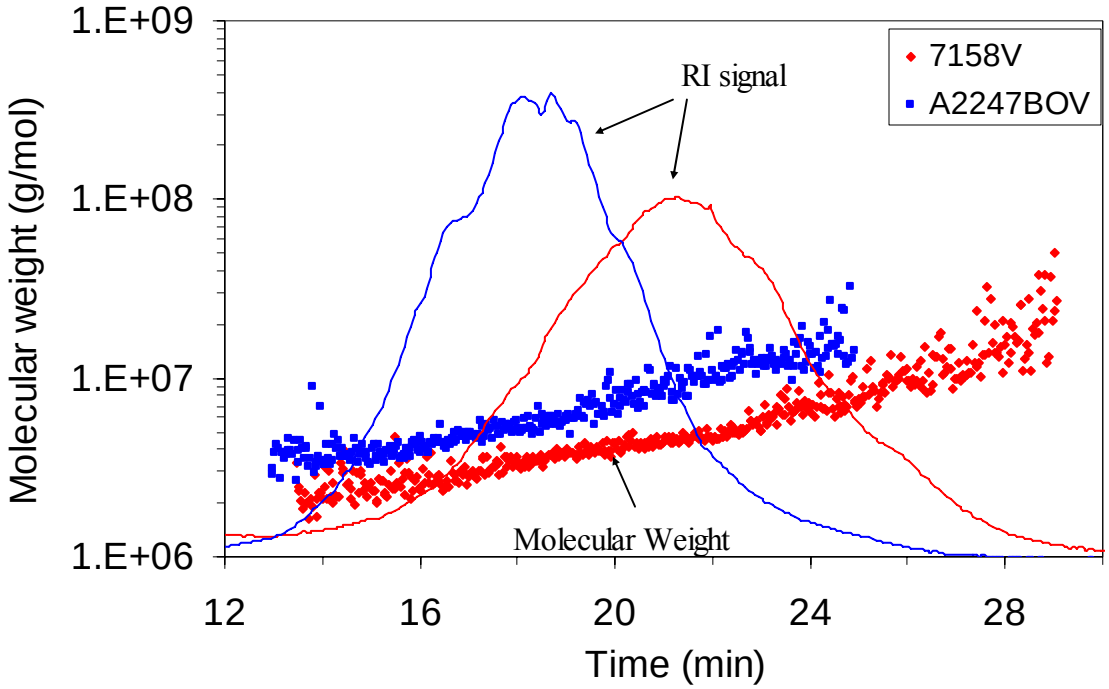

Figure 5.16 – Molecular weight versus elution time for two polymer lots of AlcoFlood 935.

High sample concentrations are beneficial in obtaining a clear sample peak, especially in detecting the molecules with low and high molecular weights (at the two ends of the peak). On the other hand, it will also lead to interactions between the polymer chains, causing sample overloading effect. This is crucial for the random coil like polyacrylamide molecules with high molecular weight and long chains, since they usually have a relatively low overlap concentration and are subject to entanglement. Injected sample concentrations lower than 500 mg/kg were also tested in this study. It was found that even a slight RI baseline drift would affect the data processing significantly when the polymer concentration was too low and so was the peak height. While the RI detector is very sensitive to any pressure or flow rate change, there was always a slight increase in the RI baseline due to the variance of the crossflow rate when power programmed crossflow was applied.

The frit outlet of the FFFF channel is designed to enrich the sample concentration in the channel outlet so as to enhance the detector response. However, a lower channel outlet flow rate will decrease the channel pressure, which is mostly generated by the pressure drop across the outlet tubings and the detectors. The channel pressure should be higher than 50 psi to keep the crossflow pump working properly. Band broadening or shear degradation to the samples may happen if back pressure regulators or small tubings are added between the FFFF channel and the detectors, yet the backpressure which can be added to the last detector, the Optilab DSP RI detector, is limited up to 30 psi. Therefore, the frit outlet function was not used in the FFFF-MALLS-RI setup.

For viscous polymer solutions, the sample viscosity increases with increasing sample concentration. If the viscosity effect is considered alone, the concentrated sample should elute later than the diluted sample because of the reduced velocity in the region near the membrane. While Figure 5.12 shows that there is a tendency for the high load peak of Lot A2247BOV to elute earlier, this phenomenon was attributed to the increase in charge interactions [Benincasa, et al, 1992, 1997; Lee, et al., 2003]. Unlike the non-ionic polyacrylamide standards paam1000K and 6000K, partially hydrolyzed AlcoFlood 935 polymers possess negatively charged carboxylate groups. When high crossflow applies, polymer molecules are pushed closer to the membrane and also move closer to each other. The ionic molecules will then tend to repel each other and move away from the membrane, and will elute earlier than they would in the absence of the charge interactions. Big molecules with long chains and more charged groups may be repelled further from the membrane, co-eluting with the small molecules and resulting in a low polydispersity index.

The charge repulsion could also exist between the polymer molecules and the membrane. The pH value of the 1% potassium chloride, 0.01% sodium azide mobile phase was around 7.0, while the charged sites on the membrane surface (e.g. hydroxyl group, sulfonic group) are also negatively charged at neutral pH or higher, but will lose their charges at acidic pH. Polyethersulfone (PES) membranes are known as less charged than RGC membranes. Thus a PES membrane with 10000 molecular weight cutoff was chosen to replace the RGC membrane.

Increasing the ionic strength of the mobile phase from 0.015 M to 0.15 M was found to be able to suppress the overloading effect due to the charge repulsion [Benincasa, et al., 1997], yet a considerable salt concentration (~ 0.134 M) had been used in this study. Decreasing the pH value of the polymer solution and the mobile phase also helps reduce the charge repulsion effect. It was reported that the viscosity of a pure polyacrylamide solution was independent of pH, while the viscosity of a partially hydrolyzed polyacrylamide solution increased as the pH value was increased from 3 to 10. The viscosity of a given partially hydrolyzed polyacrylamide solution also increased with increasing degree of hydrolysis when measured at pH = 8.4, but was constant when measured at pH = 4 with the same ionic strength [Langhorst et al., 1986]. The change in viscosity is caused by the transition of the hydrolyzed side groups from uncharged carboxylic acid at acidic pH to charged carboxylate ions at neutral pH or higher. Considering the compatibility of the materials in each component of the system, a new mobile phase with 1% potassium chloride at pH = 4.0 was used in an effort to decrease the charge repulsion effect.

In mobile phase: 1% potassium chloride, pH = 4.0 solution. The FFFF system was flushed with at least one liter water, then the channel was opened and the RGC membrane was replaced with a 10,000 molecular weight cutoff polyethersulfone (PES) membrane. The channel was reassembled and filled with water. Then the mobile phase was changed to 1% potassium chloride solution with the pH value of 4.0 ± 0.1 adjusted by adding 1N hydrochloric acid. The FFFF system was flushed with the new mobile phase thoroughly prior to the coupling with the MALLS and RI detectors.

Partially hydrolyzed polyacrylamide AlcoFlood 935 stock solutions were prepared by dissolving the polymer beads in the new mobile phase. The pH value was about 5.3 for a 1000 mg/kg AlcoFlood 935, Lot A2247BOV stock solution; while the pH of a 1000 mg/kg Lot 7158V

solution was about 4.7. More H+ ions were consumed in Lot A2247BOV solution, possibly due to a higher degree of hydrolysis, or a higher amount of sodium hydroxide residue.

Polymer Lot 7158V was tested first. The RI peak of each polymer run was almost repeatable, while the MALLS peaks were lower in the first a few runs than in the later runs. After ~ 15 consecutive injections repeatable results were obtained. The data processing methods were the same as in SEC runs: Debye plot, Berry formalism, 4-16 detectors, detector fit degree = 2, result fit degree = 1. The dn/dc of the polymer in the new mobile phase was assumed to be unchanged.

Figure 5.17 shows the measured molecular weight versus time for 4 runs conducted in three days. The differential molecular weight and the rms radius distributions of Lot 7158V are shown in Figures 5.18 and 5.19. The rms radii are plotted against molecular weight (log-log) in Figure 5.20. Comparing with SEC results, FFFF gives a similar polydispersity index (~ 1.70) and a comparable molecular weight distribution. The slopes of rms radius vs. molecular weight plot are also close. The size measured by FFFF is smaller, which means the conformation of the polymer molecules may become more compact since the polymer molecules are less charged therefore less "stretched out" in the new mobile phase.

A little improvement was achieved on the separation of AlcoFlood 935, Lot A2247BOV. Figure 5.21 shows the differential molecular weight distributions of Lot A2247BOV measured by SEC and FFFF. The polydispersity index was increased from 1.1 to 1.3, but still much lower than the SEC result, ~1.8. No further improvement was obtained in an attempt to adjust the pH values of the injected polymer samples to ~ 4.0.

The fact that Lot A2247BOV still can not get good separation in FFFF suggests that these two polymer lots of AlcoFlood 935 may have different degrees of hydrolysis. Samples of AlcoFlood 935, Lots 7158V and A2247BOV, were sent out to the Chemical Analysis Lab, University of Georgia, for C, H, N element analysis. Based on the analysis result, the degree of hydrolysis can be calculated according to Equation 4.1.

$$\text{Degree of hydrolysis} = 1.0 - \frac{3M_C}{M_N \cdot (C/N)} \qquad \text{Eq. 4.1}$$

where, M_C – molecular weight of C atom, 12.0107 g/mol
M_N – molecular weight of N atom, 14.00674 g/mol
C/N – C/N weight ratio

Table 5.4 shows the element analysis results. Lot A2247BOV indeed has higher degree of hydrolysis than Lot 7158V. After the acid treatment, that is, to prepare and run the polymer samples in an acidic environment (pH = 4.0), with the charged carboxylate groups turning into the uncharged carboxylic acid, the charge repulsion effect for Lot 7158V was significantly reduced. While for Lot A2247BOV with higher degree of hydrolysis, the acid treatment is not enough to shield all the charges, resulting in an unsuccessful separation in FFFF.

Pre-gel Aggregates

A gel system containing 5000 mg/kg polyacrylamide AlcoFlood 935, Lot A2247BOV and 100 mg/kg chromium(III) was prepared in 1% potassium chloride, 0.01% sodium azide solution.

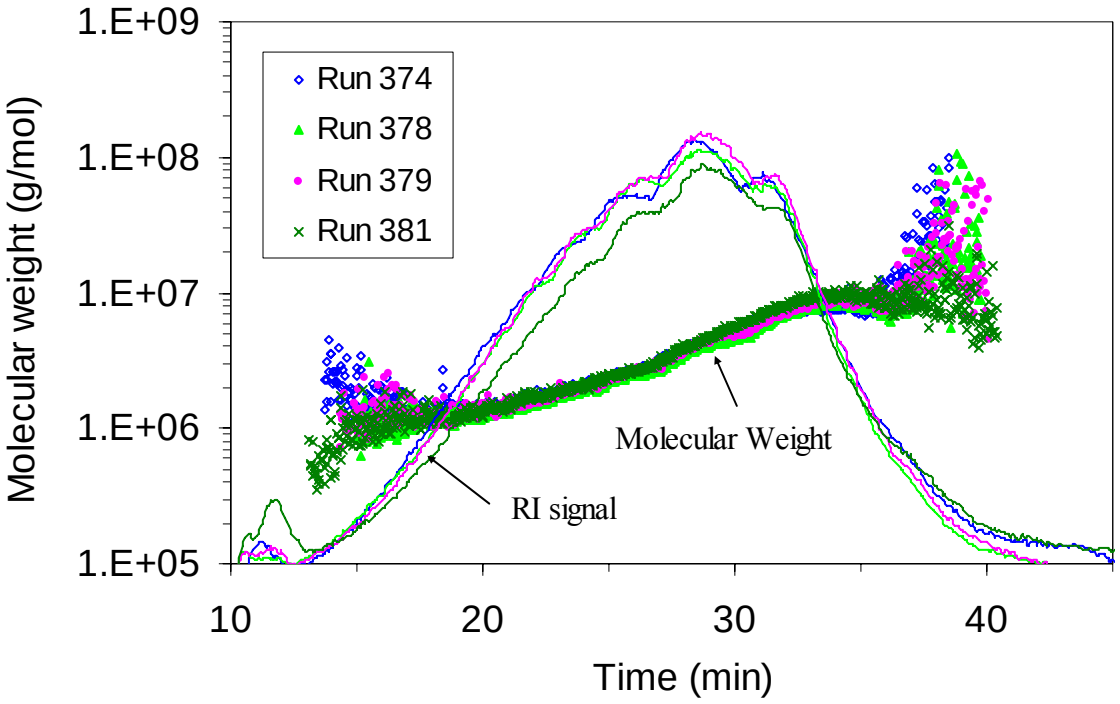

Figure 5.17 – Molecular weight versus elution time for AlcoFlood 935, Lot 7158V (Sample: Lot 7158V, 500mg/kg, sample loop: 100 µL, channel flow rate: 0.5 mL/min, frit outlet flow rate: 0, cross flow rate: 0.6 → 0.05 mL/min, t1 = 4 min).

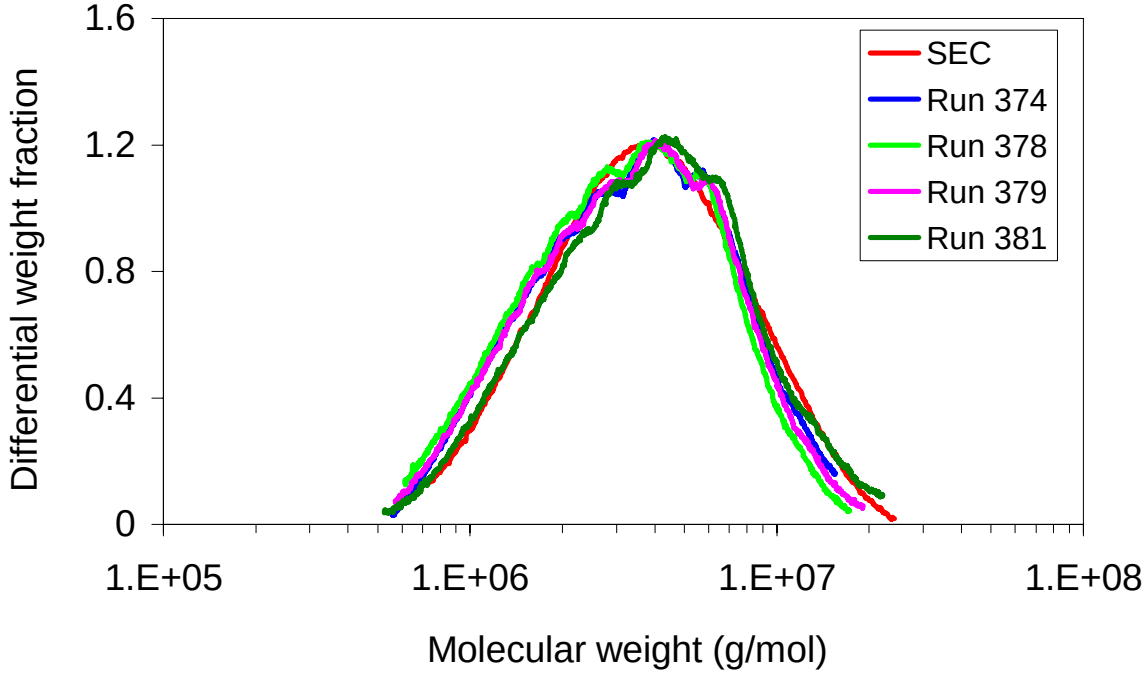

Figure 5.18 - Differential molecular weight distributions of AlcoFlood 935, Lot 7158V, measured by SEC and FFFF.

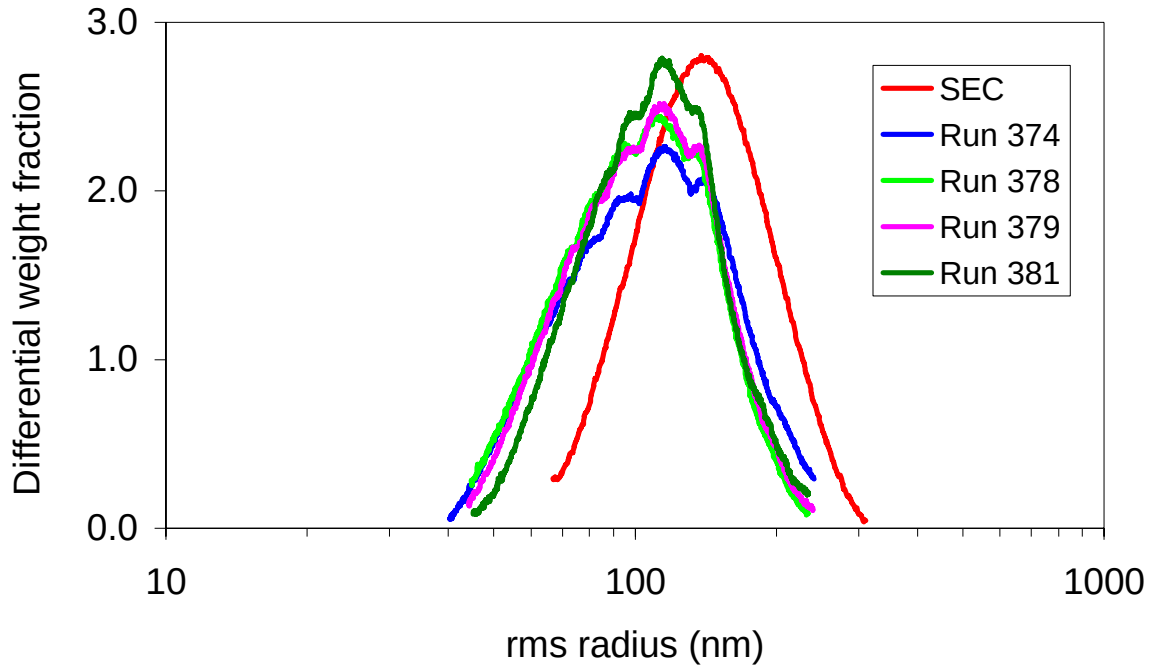

Figure 5.19 - Differential rms radius distributions of AlcoFlood 935, Lot 7158V, measured by SEC and FFFF.

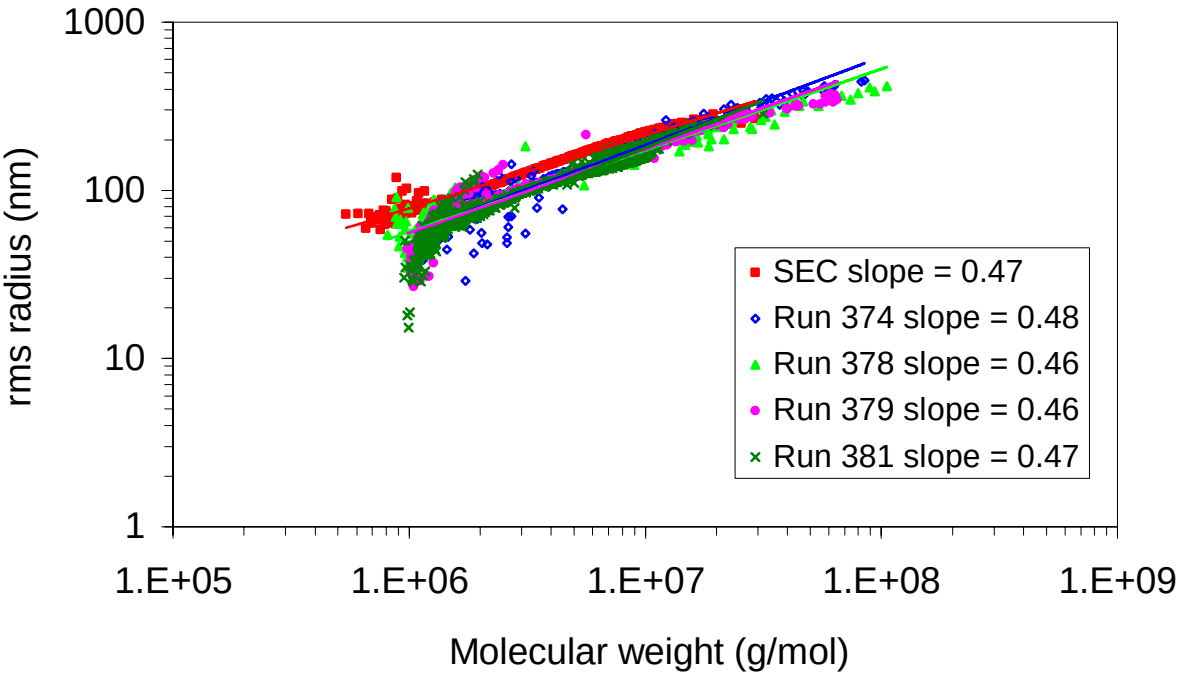

Figure 5.20 - Log-log plot of rms radius versus molecular weight for Alcoflood 935, Lot 7158V, measured by SEC and FFFF.

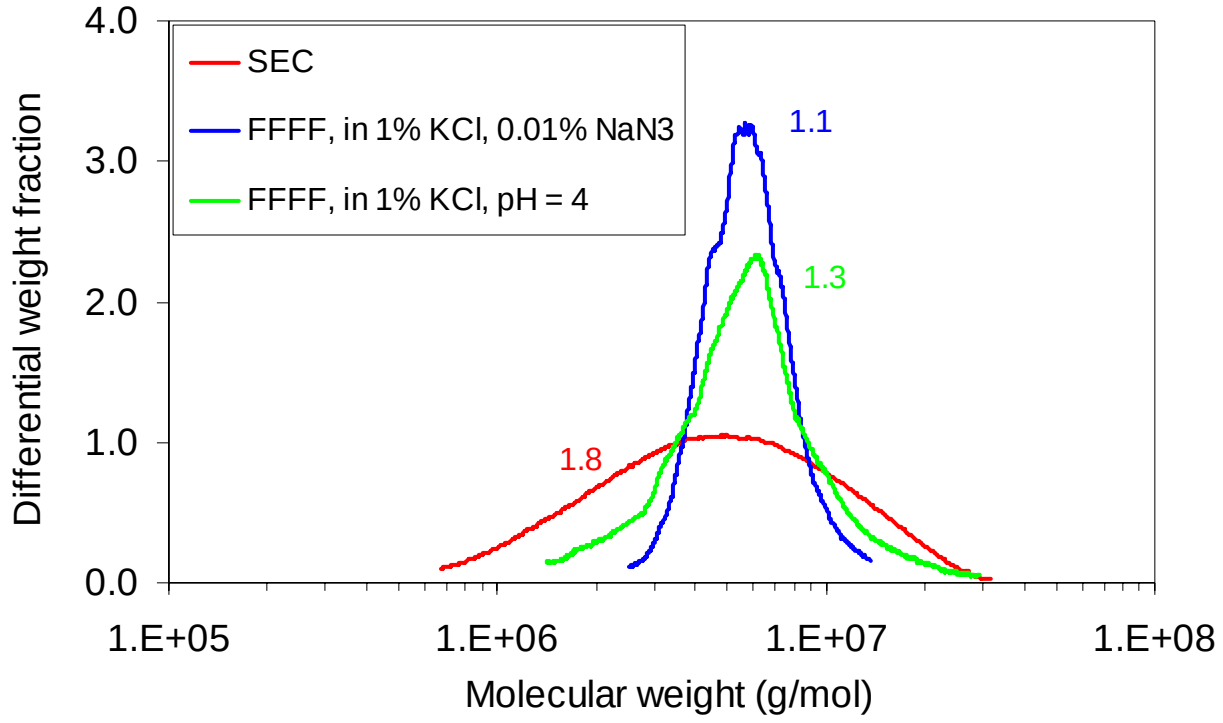

Figure 5.21 - Differential molecular weight distributions of AlcoFlood 935, Lot A2247BOV, measured by SEC and FFFF.

Table 5.4 - C, H, N analysis results and the degree of hydrolysis of two polymer lots of AlcoFlood 935.

	C, (wt.)%	N, (wt.)%	H, (wt.)%	C/N ratio	degree of hydrolysis, %
Lot 7158V	44.792	17.074	7.067	2.62	1.8
Lot A2247BOV	46.626	16.791	7.182	2.78	7.5

Gelant was sampled periodically and immediately diluted to 1000 mg/kg (polymer concentration) by adding the mobile phase prior to the injections. The mobile phase was 1% potassium chloride, 0.01% sodium azide solution, and a RGC membrane was used.

The RI and MALLS fractograms of gelant runs are shown in Figures 5.22 and 5.23. The fractograms keep shifting to earlier elution time with increasing reaction times. The same elution profile was also observed by Chong [2002] in an FFFF-UV setup. Without the aid of a MALLS detector, it was claimed that the gel aggregates became smaller as the reaction proceeded, conflicting with the results of equilibrium dialysis. From Figure 5.23 it can be seen that the MALLS peak heights increase with the reaction time, indicating bigger molecular weights and sizes. Figure 5.24 shows the calculated differential molecular weight distributions of the gelant runs. The molecular weight indeed increased, while a polydispersity index close to 1.0 was

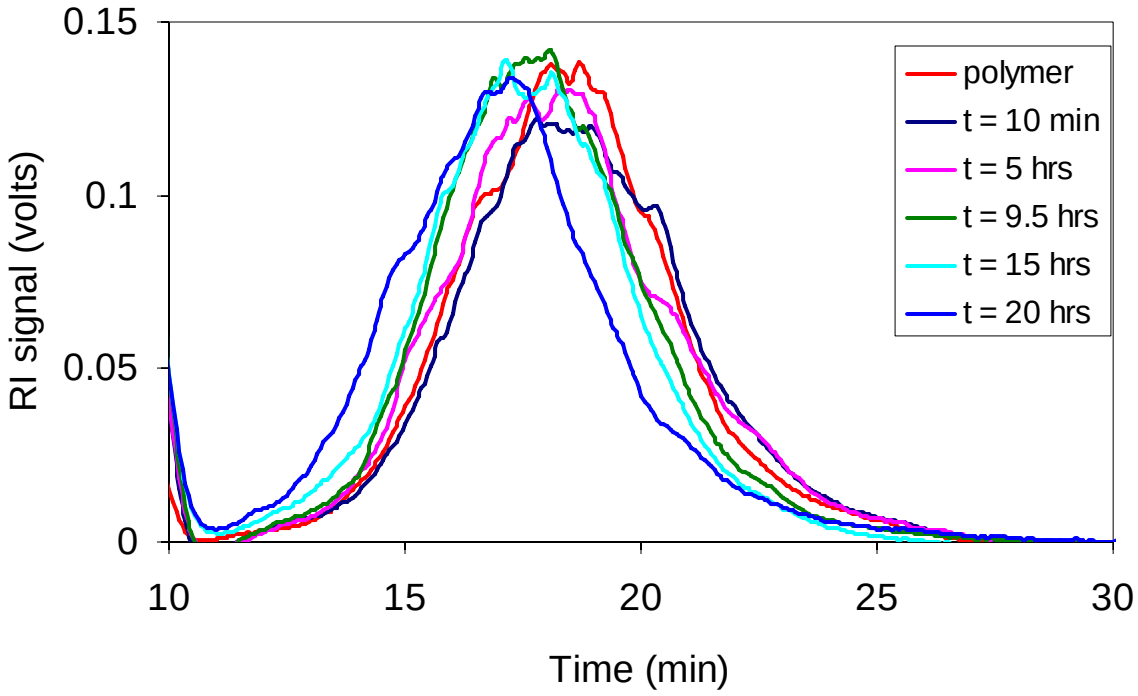

Figure 5.22 - RI fractograms of gelant runs (Sample loop: 100 µL, channel flow rate: 0.7 mL/min, frit outlet flow rate: 0, crossflow rate: 0.4 → 0.05 mL/min, t1 = 4 min).

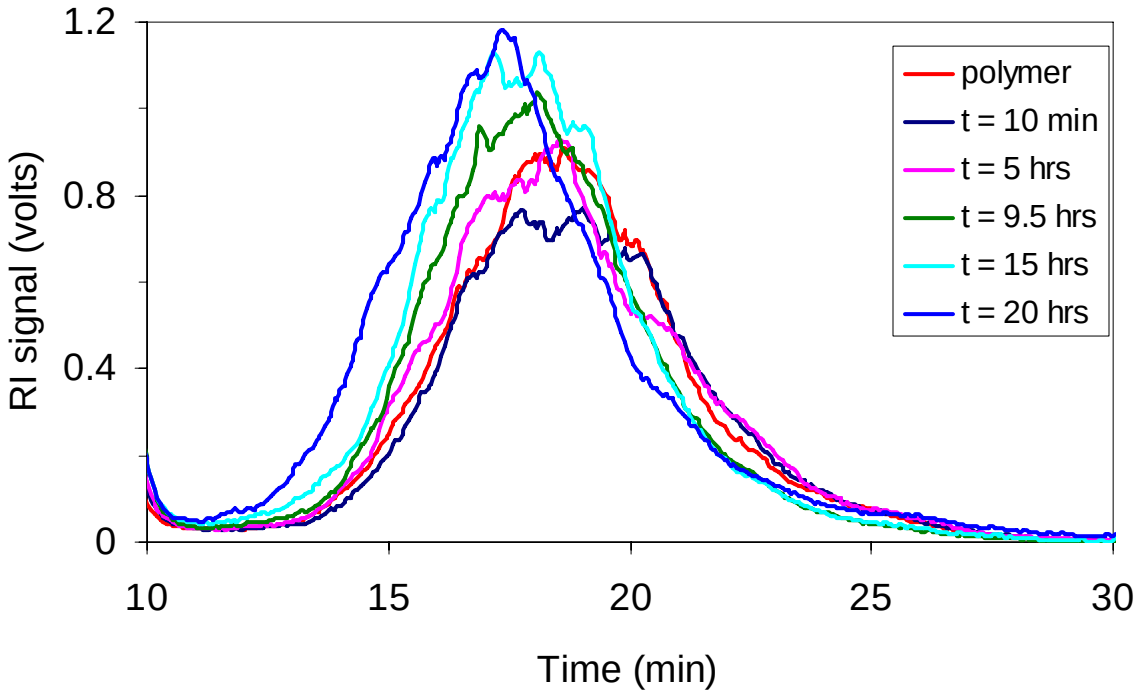

Figure 5.23 - MALLS fractograms of gelant runs.

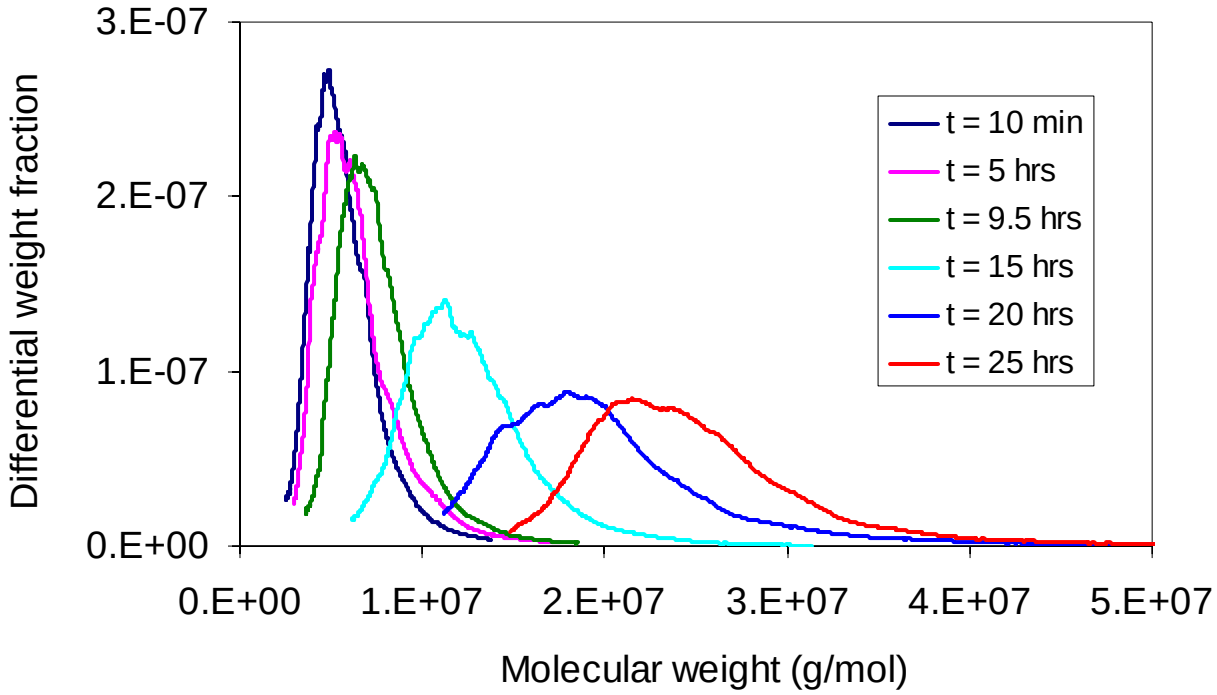

Figure 5.24 – Differential molecular weight distributions of gelant runs.

obtained for each run. Based on the previous discussions, this systematic shifting of the elution profile is mostly caused by charge repulsion and sample overloading. The conformation and distribution of the pre-gel aggregates were altered in the FFFF channel. Therefore the calculated molecular weight and size distributions of pre-gel aggregates are not reliable.

Conclusions

1. An FFFF-MALLS-RI setup was developed. The separation of the polystyrene particle size standards and the nonionic polyacrylamide standards was demonstrated successfully. The measured molecular weight and size distributions of the non-ionic polyacrylamide standards are comparable to the SEC results.
2. FFFF requires the optimization of the operating conditions. The operating conditions must be carefully chosen for separating the random-coil like and partially hydrolyzed (negatively charged) polyacrylamide molecules with high molecular weight and long chains.
3. Charge repulsion plays an important role in the separation of charged polymer molecules in FFFF. It was found that charge repulsion could cause an earlier elution time and a polydispersity index close to 1.0. An acidic pH helps reduce the charge effect. Further investigation in the separation of the polyacrylamide with higher degree of hydrolysis is needed.

References

Benincasa M. A. and Giddings J. C.: "Separation and Molecular Weight Distribution of Anionic and Cationic Water-Soluble Polymers by Flow Field-Flow Fractionation," *Anal. Chem.,* **64** (1992) 790-798.

Benincasa M. A. and Giddings J. C.: "Separation and Characterization of Cationic, Anionic, and Nonionic Water-Soluble Polymers by Flow FFF: Sample Recovery, Overloading, and Ionic Strength Effects," *J. Microcol. Sep.,* **9** (1997) 479-495.

Duval, C.; Le Cerf, D.; Picton, L.; Muller, G.: "Aggregation of Amphiphilic Pullulan Derivatives Evidenced by On-line Flow Field Flow Fractionation / Multi - Angle Laser Light Scattering," *Journal of Chromatography B,* **753** (2001) 115-122.

Giddings, J.C., Yang, F.J., Myers, M. N.: "Theoretical and Experimental Characterization of Flow Field-Flow Fractionation," *Anal. Chem.*, **48** (1976) 1126-1132.

Langhorst M. A., Stanley, Jr. F. W., Cutie S. S., Sugarman J.H., Wilson L. R., Hoagland, D.A., Prud'homme, R. K.. "Determination of Nonionic and Partially Hydrolyzed Polyacrylamide Molecular Weight Distributions Using Hydrodynamic Chromatography," *Anal. Chem.*, **58** (1986) 2242-2247.

Lee, S.; Nilsson, P.; Nilsson, G. S.; Wahlund, K.-G.: "Development of Asymmetrical Flow Field-Flow Fractionation – Multi-Angle Laser Light Scattering Analysis for Molecular Mass Characterization of Cationic Potato Amylopectin," *Journal of Chromatography A,* **1011** (2003) 111-123.

Willhite, G. P., Green, D.W. and McCool, C.S.: "Increased Oil Recovery from Mature Oil Fields using Gelled Polymer Treatments," Annual Report for June 1999 – June 2002, Report No. 99BC15209-5, Contract No. DE-AC26-99BC15209, US DOE, Washington, DC (Dec 2002).

Wittgren, B.; Wahlund, K.-G.: "Effects of Flow -rates and Sample Concentration on the Molar Mass Characterization of Modified Celluloses Using Asymmetrical Flow Field-Flow Fractionation – Multi-Angle Light Scattering," *Journal of Chromatography A,* **791** (1997) 135-149.

Chapter 6

Experimental and Modeling Study of the Transport of Chromium Acetate Solutions Through Carbonate Rocks

Graduate Research Assistant: Feiyen Chen

The transport of chromium acetate solutions through dolomite rock material was studied by injecting various solutions through short dolomite cores and measuring Cr, Mg, and Ca concentrations and pH in the effluent. A mathematical model was developed that describes convection, dispersion, kinetic reactions of carbonate dissolution and chromium precipitation, and chemical equilibrium for reactions between aqueous components. Experimental data and data taken from literature were simulated by the model.

Introduction

Gelled polymer systems are applied to oil reservoirs to reduce undesired fluid production and to increase sweep efficiencies in displacement processes. A common gel system consists of hydrolyzed polyacrylamide crosslinked by chromium(III) acetate. Transport of polymer and chromium through the reservoir rock are essential for a successful treatment. In carbonate reservoirs, dissolution of carbonate raises the pH of the gelant to levels where chromium precipitates, robbing the gelant of crosslinker. Precipitation has been identified as an important retention mechanism impeding the transport of chromium(III) in laboratory flow experiments [Seright, 1992; Stavland et al., 1993, 1995; Bartosek et al., 1994; McCool et al., 1995].
Zou et al. [2000b] measured the rate of chromium(III) precipitation in chromium(III) acetate solutions as a function of pH, temperature, salinity, chromium salt type, salt type and acetate-to-chromium(III) ratio. Chromium precipitation was characterized by an induction period followed by precipitation. An empirical kinetic model was developed that describes chromium precipitation from bulk solutions with 1.0% KCl as a function of chromium concentration, pH and acetate concentration at 25 °C.

The purpose of this work was to determine experimentally the transport of chromium acetate solutions through carbonate cores and to model that transport numerically. Retention of chromium(III) is a kinetic process, in that lower flow rates in dolomite cores, or longer residence times, result in larger amounts of retained chromium(III). The effect of residence time and injected chromium concentration were experimentally investigated. Results from flow experiments in carbonate cores using brines and a potassium acetate solution supported the interpretation of experiments using chromium acetate solutions. A mathematical model to simulate the transport of brine and chromium(III) acetate solutions through carbonate-containing rocks was developed by determining parameters in the rate equations for carbonate dissolution and chromium precipitation to fit the experimental data. Retention of chromium as measured by several investigators was matched by one set of parameters in the rate equation for chromium precipitation.

Mathematical Model Description

A mathematical model was developed to simulate the transport of 24 aqueous species through a one-dimensional, carbonate-containing porous medium. Convection, dispersion, kinetic reactions

of carbonate dissolution and chromium precipitation, and chemical equilibrium for reactions between aqueous components are represented in the model. It was assumed that the temperature remained constant at 25°C, the medium was homogenous with constant permeability and porosity, precipitated materials were retained without affecting flow properties and water activity was unity.

There are four types of components/species in the model which are listed in Table 6.1. Of the 24 aqueous species, ten are identified as independent and fourteen are identified as dependent. Concentrations of the dependent species are calculated explicitly from values of the independent species using equilibrium relationships. Additionally, there are nine material components that are used during the calculation procedure. Concentration of each material component is the sum of the concentrations of all the dependent and independent species that contain that transport component. For example, [Calcium] = $[Ca^{2+}]$ + $[CaOH^{+}]$ + $[CaCO_3^{0}]$ + $[CaHCO_3^{+}]$. Flow through the porous medium was modeled using the transport equation for the nine material components. The 24 aqueous species are determined from the concentrations of material components and a charge balance to determine the concentration of hydrogen ion.

Table 6.1 - Summary of the chemical species and components used in the model.

24 Aqueous species, 10 independent species + 14 dependent species.
Independent species: 1: Ca^{2+}, 2: Mg^{2+}, 3: CO_3^{2-}, 4: H^{+}, 5: K^{+}, 6: Cl^{-}, 7: Cr^{3+}, 8: OAc^{-}, 9: SO_4^{2-}, 10: H_2O
Dependent species: 11: OH^{-}, 12: $CaOH^{+}$, 13: $MgOH^{+}$, 14: $CaCO_3^{0}$, 15: $MgCO_3^{0}$, 16: $CaHCO_3^{+}$, 17: $MgHCO_3^{+}$, 18: HCO_3^{-}, 19: H_2CO_3, 20: $Cr(OH)^{2+}$, 21: $Cr(OH)_2^{+}$, 22: $Cr(OH)_3^{0}$, 23: $CrAc(OH)_2$, 24: HOAc
9 Material components: Calcium, Magnesium, Carbonate, Sulfate, Potassium, Chloride, Chromium, Acetate, Water
(Material components and hydrogen calculated by mass balances and a charge balance.)

Model equations. The transport equation for flow through the porous medium in the *x* direction is

$$\frac{\partial C_i}{\partial t} + \frac{v}{\phi}\frac{\partial C_i}{\partial x} - K_{di}\frac{\partial^2 C_i}{\partial x^2} = \sum_j R_i(C) \quad , \qquad \text{Eq. 6.1}$$

where

i represents the material component,
$R_i(C)$ is the rate of reaction per unit volume for each solid-liquid reaction *j*, moles/liter-PV/s,
C_i is the concentration in the fluid phase, moles/liter-PV,
v is the superficial velocity of the fluid, cm/s,
K_{di} is the dispersion coefficient, cm^2/s,
t is time, s,
x is length, cm.

The dispersion term in Eq. 6.1 was omitted and approximated by numerical dispersion during the solution procedure.

The general form for the rate of carbonate dissolution is described by

$$R_i = r_i \left(1 - \left(\frac{IAP}{K_{sp}} \right)^{m_2} \right)^{m_1} \frac{y_i \, S_0 (1-\phi)}{\phi} \quad , \qquad \text{Eq. 6.2}$$

where

r_i is the surface reaction rate of the mineral, mmol/cm^2/s.
IAP is the ion activity product of the mineral.
K_{sp} is the solubility product for the mineral.
m_1 and m_2 are fitting parameters.
y_i is the weight fraction of the mineral in the rock.

S_0 is specific surface area, calculated from the modified Kozeny-Carmen equation [Carman, 1937], cm^2/cm^3.

$$S_0 = \sqrt{C_0 \frac{\phi^3}{K(1-\phi)^2}} \quad , \qquad \text{Eq. 6.3}$$

where

C_0 is the Kozeny constant for which Carman [1937] suggested the value of 0.2,
K is permeability, cm^2
ϕ is the porosity, fraction.

Forms of the surface reaction rate, r_i, were taken from literature for dolomite and calcite and a similar form was used for anhydrite. The second term in Eq. 6.2,

$$\left(1 - \left(\frac{IAP}{K_{sp}} \right)^{m_2} \right)^{m_1} \quad , \qquad \text{Eq. 6.4}$$

was included to reduce the rate as the reaction approached the saturated condition. The last term in Eq. 6.2,

$$\frac{y_i \, S_0 (1-\phi)}{\phi} \quad , \qquad \text{Eq. 6.5}$$

is a material balance relating the surface area to the liquid volume.

R_i (mol/L/s) in Eq. 6.2 represents the change in concentration with time of the dissolved ions (independent species) from the mineral according to the stoichiometry of the dissolution. Using dolomite dissolution as an example, $CaMg(CO_3)_2 \rightarrow Mg^{2+} + Ca^{2+} + 2CO_3^{2-}$. The dissolved ions are added to the appropriate material component during the calculation procedure. The reaction rates of the material components involved in dolomite dissolution are described by

$$R_{dolomite} = R_{calcium} = R_{magnesium} = \frac{1}{2} R_{carbonate} \quad . \qquad \text{Eq. 6.6}$$

Dolomite dissolution was modeled by

$$R_{dolomite} = (k_1\{H^+\}^n + k_2\{H_2CO_3\}^n + k_3)\times \left(1-\left(\frac{\{Ca^{2+}\}\{Mg^{2+}\}\{CO_3^{2-}\}^2}{K_{sp\ Dolomite}}\right)^{m_2}\right)^{m_1} \frac{y_{dolomite} S_0(1-\phi)}{\phi} \quad \text{Eq. 6.7}$$

where

{ } stands for activity. S_0 the specific surface area of the solid, cm^2/cm^3.
k_1= 2.6x10^{-7}; k_2=2.0x10^{-7}; k_3=1.1x10^{-10}; n=0.75, m_1=2.0, m_2=0.25,
$K_{sp\ Dolomite}$ = 10$^{-17.2}$ [Sherman and Barak, 2000].

The form of the surface-reaction-rate portion of Eq. 6.7 was taken from the literature [Chou et al., 1989], but the constants k_1,k_2 *and* k_3 were used as parameters to fit the experimental data. m_1 and m_2 were also used as fitting parameters.

Eq. 6.8 was used to describe the rate of calcite dissolution. The form of the surface-reaction-rate portion of Eq. 6.8 was taken from the literature [Chou et al., 1989]. The parameters in the kinetic equation were adjusted to fit experimental data.

$$R_{calcite} = \left(k_4\{H^+\} + k_5\{H_2CO_3\} + k_6 - k_7\{Ca^{2+}\}\{CO_3^{2-}\}\right)\times \left(1-\frac{\{Ca^{2+}\}\{CO_3^{2-}\}}{K_{sp\ Calcite}}\right)\frac{y_{calcite} S_0(1-\phi)}{\phi} \quad \text{Eq. 6.8}$$

where

k_4 = 8.9x10^{-5}; k_5=5.0x10^{-8}; k_6=6.5x10^{-11}; k_7 =1.9,
$K_{sp\ Calcite}$ = 10$^{-8.31}$ [Bhuyan, 1989].

The rate of anhydrite dissolution is modeled by

$$R_{anhydrite} = k_8\left(1-\frac{\{Ca^{2+}\}\{SO_4^{2-}\}}{K_{sp\ Anhydrite}}\right) \quad \text{Eq. 6.9}$$

where k_8 includes the effect of surface dissolution rate, the specific surface area, and the material balance that relates the surface area to the liquid volume in the rock. k_8 is a fitting parameter and is equal to 3.2 x 10^{-6}. $K_{sp\ Anhydrite}$ is the solubility constant of anhydrite and is equal to 2.45 x 10^{-5} [Sillen L.G. and Martell A.E., 1964].

Zou et al. [2000b] modeled chromium precipitation in bulk experiments using two equations, one that described an induction time period with no precipitation followed by precipitation according to Eq. 6.10. Induction time periods were not observed in flow experiments, so chromium precipitation was modeled with Eq. 6.10 only. The rate constant, k_0 and the exponents, α, β, γ in the equation are fitting parameters. The following values were proposed by Zou et al. [2000b]: k_0 = 2.6x10^{-3} (min M$^{\alpha+\gamma+\beta-1}$)$^{-1}$, α = 1.0, β = 0.37, γ = -1.2. These parameters were adjusted to have a better match to the experimental data. A better match occurred when the chromium precipitation was modeled as second order in chromium concentration rather than first order as proposed by Zou et al.

$$R_{chromium} = -k_0([Cr_t] - [Cr_{eq}])^{\alpha}[OH^-]^{\beta}[Ac_t]^{\gamma}$$ Eq. 6.10

where

k_0 = 882.9 (min $M^{\alpha+\gamma+\beta-1}$)$^{-1}$,

α = 2.0,

β = 0.65,

γ = -0.75.

$[Cr_t]$is the total chromium concentration in the solution,

$[Ac_t]$ is the total acetate ions concentration in the solution,

$[Cr_{eq}]$ is the chromium(III) concentration at equilibrium of chromium(III) hydrolysis and was determined by Rai et al. [1987] as follows:

$$\left[Cr_{eq}\right] = 10^{\log k_{s1} - 2pH} + 10^{\log k_{s2}} + 10^{\log k_{s3} + pH}$$ Eq. 6.11

where $[Cr_{eq}]$ is the total chromium concentration in the solution including all possible mononuclear chromium species: Cr^{3+}, $Cr(OH)_2^+$, $Cr(OH)^{2+}$, $Cr(OH)_3^0$, and $Cr(OH)_4^-$.The constants have values of 5.96 for log k_{s1}, -6.84 for log $k_{s2,}$ and –18.25 for log k_{s3}.

Concentrations of the fourteen dependent species were calculated explicitly using the concentration values of the ten independent species, activity coefficients and the equilibrium relationships shown in Table 6.2. The equilibrium constants for those reactions are taken from literature. Equilibrium constants of K_5, K_6 and K_{13} were taken from the database of Minteq.v4.dat for PHREEQC model [Parkhurst and Appelo, 2005]. Non-ideal behavior of the solution was modeled using the Davies equation [Benjamin, 2002] to calculate activity coefficients for the equilibrium relationships as well as for solubility products and reaction rate equations.

Constraints on the solubility products for calcite and anhydrite were considered. The solubility product is given by

$$K_{sp,k} = \prod_{i}^{N_i} \{a_i\}^{q_{i,k}} \qquad for \qquad i = 1,.....,N_k$$, Eq. 6.12

where K_{sp} is the solubility product for the corresponding solid and is defined in terms of the activities of the aqueous species. α_i is the activity of species i, and $q_{i,k}$ is the stoichiometric coefficient for species i related to solid phase k. Supersaturation was not allowed.

For the study of the interaction between dolomite and the injected solution, which includes calcium ions, three cases for the solubility constraint of calcite are tested for the possibility of calcite precipitation from the solution. A solubility constraint was included in the model using the saturation index: $I_s = IAP/K_{sp} = [\{Ca^{2+}\}\{CO_3^{2-}\}]/K_{sp}$, where { } is the activity of the ion and K_{sp} is the solubility product of calcite. There is a critical supersaturation index, (I_s*), above which the secondary mineral starts to nucleate or form new crystals. Equal molar reductions in the Ca^{2+} and CO_3^{2-} concentrations were forced on the solution chemistry so that the saturation index did not exceed I_s*. Two values of I_s* were used in this work. A value of one was used to produce precipitation when the IAP equaled K_{sp} (Walsh M.P. [1983], Bhuyan D. [1989], and Nghiem L. et al. [2004]). A value of 4.93 was used as recommended for calcite by Araque-Martinez and Lake [2001]. In this case, supersaturation occurs and the activities of calcium ions

Table 6.2 - Equilibrium reactions and constants used in the model.

Equilibrium reactions	Equilibrium constants, K	Reference
$CO_3^{2-} + H^+ \overset{K_1}{\leftrightarrow} H_2CO_3^-$	2.138E+10	9
$CO_3^{2-} + 2H^+ \overset{K_2}{\leftrightarrow} H_2CO_3$	3.981E+16	9
$Ca^{2+} + H_2O \overset{K_3}{\leftrightarrow} CaOH^+ + H^+$	1.205E-13	9
$Mg^{2+} + H_2O \overset{K_4}{\leftrightarrow} MgOH^+ + H^+$	3.887E-12	9
$Ca^{2+} + CO_3^{2-} \overset{K_5}{\leftrightarrow} CaCO_3^0$	1.585E+03	12
$Mg^{2+} + CO_3^{2-} \overset{K_6}{\leftrightarrow} MgCO_3^0$	8.318E+02	12
$Ca^{2+} + H^+ + CO_3^{2-} \overset{K_7}{\leftrightarrow} CaHCO_3^+$	3.548 E+11	9
$Mg^{2+} + H^+ + CO_3^{2-} \overset{K_8}{\leftrightarrow} MgHCO_3^+$	5.888 E+11	9
$Cr^{3+} + H_2O \overset{K_9}{\leftrightarrow} Cr(OH)^{2+} + H^+$	1.000E-04	13
$Cr^{3+} + 2H_2O \overset{K_{10}}{\leftrightarrow} Cr(OH)_2^+ + 2H^+$	2.399E-10	13
$Cr^{3+} + 3H_2O \overset{K_{11}}{\leftrightarrow} Cr(OH)_3^0 + 3H^+$	1.778E-17	13
$Cr^{3+} + Ac^- + 2H_2O \overset{K_{12}}{\leftrightarrow} CrAc(OH)_2 + 2H^+$	6.900E-06	Fitting parameter
$H^+ + Ac^- \overset{K_{13}}{\leftrightarrow} HAc$	5.715E-04	12
$H_2O \overset{K_{14}}{\leftrightarrow} H^+ + OH^-$	1.009E-14	9

and carbonate ions in the solution are greater than what is allowed by being in equilibrium with calcite. Simulations were also conducted where there was no solubility constraint.

Calculation procedures. The mixing-cell concept was applied in the model to solve the transport equation (Eq. 6.1) for each material component. The mixing-cell concept is based on the conservation of mass and the assumption of complete mixing within a cell [Ommen, 1985; Midha, 1994; Wang and Chen, 1995]. The flow path was divided into a number of cells. Flow phenomena were regarded as a combination of two processes: complete mixing in each cell and translation at the average flow velocity from one cell to the next at each time step. Mathematically, the mixing-cell concept is equivalent to using the forward finite-difference approximation for the time derivative and the backward difference for the spatial derivative. Numerical dispersion was used to approximate the physical dispersion term in the transport equation. The advantages of using the mixing-cell concept are its simplicity to code and its flexibility.

The dimensionless variables

$$t_D = \frac{tv}{\phi L} \quad \text{and} \quad x_D = \frac{x}{L}, \qquad \text{Eq. 6.13}$$

were used to give the following form of the transport equation:

$$\frac{\partial C_i}{\partial t_D} + \frac{\partial C_i}{\partial x_D} - \frac{K_{di}\phi}{vL}\frac{\partial^2 C_i}{\partial {x_D}^2} - \frac{L\phi}{v}\sum_j R_i = 0 \qquad \text{Eq. 6.14}$$

Introducing an explicit finite-difference approximation for the time derivative and upstream finite difference for the spatial derivative for a non-reactive material component gives

$$\frac{C_{i,j}^{n+1} - C_{i,j}^{n}}{\Delta t_D} = -\left(\frac{C_{i,j}^{n} - C_{i,j-1}^{n}}{\Delta x_D}\right) + \left(\frac{\Delta t_D}{2} - \frac{\Delta x_D}{2} + \frac{K_{di}\phi}{vL}\right)\frac{\partial^2 C_i}{\partial {x_D}^2} \qquad \text{Eq. 6.15}$$

where the indices for the material component, the time step and the cell number are *i*, *n* and *j*, respectively.
Numerical dispersion was controlled by adjusting time and distance steps according to the relationship [Ommen, 1985; Midha, 1994; Wang and Chen, 1995].

$$\frac{\Delta t_D}{2} - \frac{\Delta x_D}{2} + \frac{K_{di}\phi}{vL} = 0 \qquad \text{Eq. 6.16}$$

The dispersion coefficient, K_{di}, was determined from a tracer test. The dispersion coefficient was assumed to be directly proportional to the velocity [Perkins and Johnston, 1963]. A value of 0.561 cm for K_{di}/v was used for all simulations.

The transport equation (Eq. 6.14) was solved using the mixing-cell concept according to the flow diagram shown in Figure 6.1. Initially, the equilibrium conditions for the injected solution and for the fluid resident in all mixing cells were determined. Compositions of these two fluids were calculated by auxiliary programs that are described below.

Steps 1 to 4 represent calculations for a time step, Δt_D. Material components were transferred between successive mixing cells in Step 1. This transfer was accomplished for each material component by

$$C_{i,j}^{n+1} = C_{i,j}^{n} - (\Delta t_D / \Delta x_D)(C_{i,j}^{n} - C_{i,j-1}^{n}) \qquad \text{Eq. 6.17}$$

Eq. 6.17 is a finite-difference representation of Eq. 6.14 when the dispersion and reaction terms are zero. The inlet boundary condition (j=1) consisted of the concentrations of the injected material components.

In the second step the equilibrium condition in each mixing cell for the 24 aqueous species was determined from the concentrations of the nine material components using a method given by Walsh [1983] and by Bhuyan [1989]. Concentration of each material component was written as the sum of the concentrations of all the aqueous species that contain that material component. For example, [Calcium] = $[Ca^{2+}]$ + $[CaOH^{+}]$ + $[CaCO_3^{0}]$ + $[CaHCO_3^{+}]$. Each dependent species

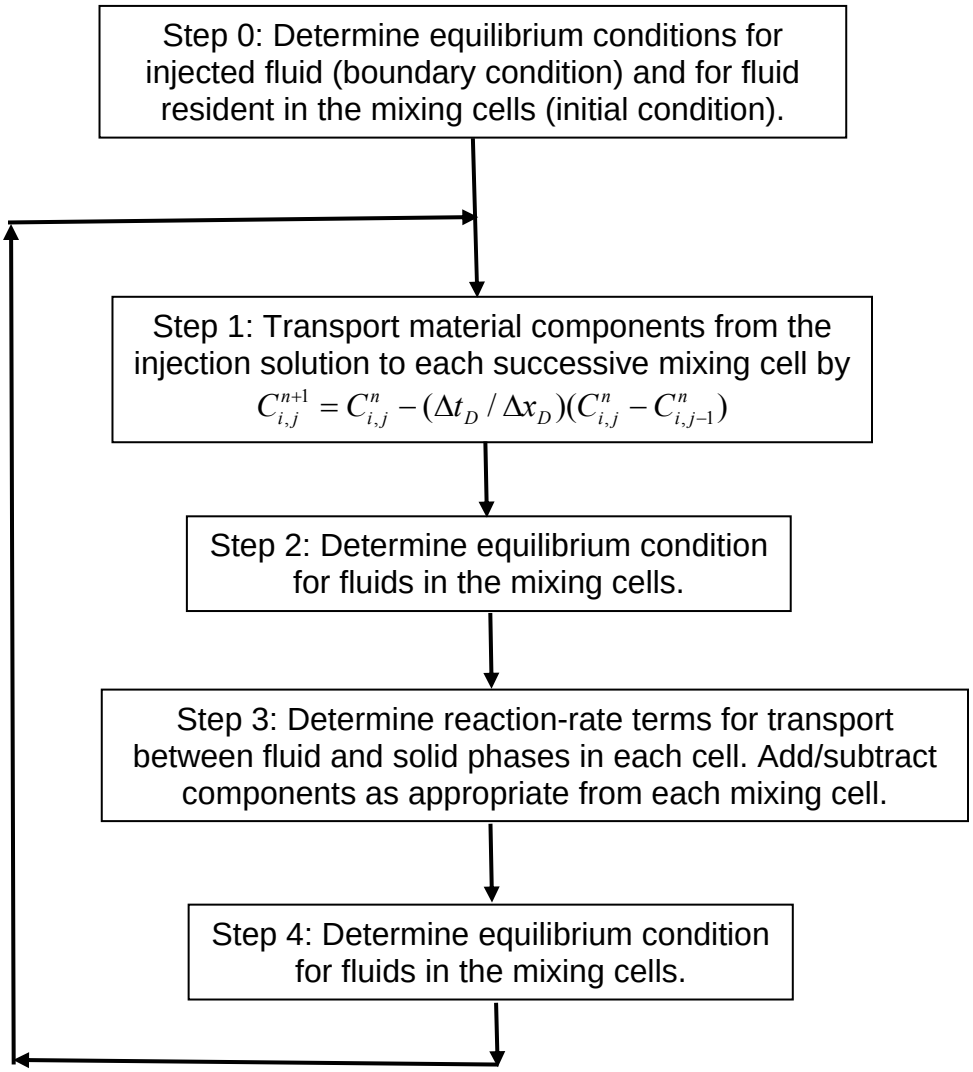

Figure 6.1 - Schematized flow chart of mixing-cell concept.

in these equations was expressed by the independent species using the appropriate equilibrium equation for the reactions given in Table 6.2. Concentration of the corresponding material component provided the concentration estimate for the independent species (i.e. $[Ca^{2+}]$ = [Calcium]) in the initial step of the Newton-Raphson procedure. A difference function was written for each material component. For calcium, this function was

$$F_1 = [\text{Calcium}] - \{[Ca^{2+}]+[CaOH^{+}]+[CaCO_3^{0}]+[CaHCO_3^{+}]\} \quad \text{Eq. 6.18}$$

A charge balance on all the aqueous species of the form

$$F_{10} = \{\text{sum of charge of positive ions}\} - \{\text{sum of charge of negative ions}\} \quad \text{Eq. 6.19}$$

provided a tenth equation for determining the hydrogen ion concentration. This set of nonlinear equations (9 material component equations and the charge balance) was solved by a Newton-

Raphson iteration method to determine the 10 independent species. Dependent species were then calculated explicitly by the equilibrium relationships given in Table 6.2. Convergence was specified to require that values of the 10 difference functions be less than 10^{-10}.

A nested iteration procedure using successive substitution was employed within the Newton-Raphson iteration to determine activity coefficients. Activity coefficients were initially assumed to be unity. The iterative procedure consisted of two steps. (1) Activities of the aqueous independent species were calculated and the activities of all the dependent species were determined from the equilibrium relationships (Table 6.2). (2) The ionic strength was calculated and activity coefficients for all the species were calculated using the Davies equation. This iterative process was continued until the relative change of the ionic strength between two iteration steps was less than 10^{-3}.

The reaction rate terms for each aqueous species, R_i, in each cell were calculated in Step 3, multiplied by the value of the time step (Δt), and the product was added to the appropriate material component in each cell that was determined in Step 2. In Step 4, the 24 aqueous species were again determined from the adjusted concentrations of the material components by the same procedure used in Step 2. Steps 1 through 4 were repeated for additional time steps.

Boundary and initial conditions for the flow model are represented by the solution injected into the first flow cell and the fluid resident in each mixing cell, respectively. A proper simulation requires that each of these fluids be in equilibrium. Auxiliary programs were written to determine the compositions. The injected solutions were KCl brines at selected pH values and chromium acetate solutions containing KCl. Addition of HCl or KOH were required to prepare KCl brines at selected pH values. One program determined the aqueous species concentrations (including the hydrogen concentration or pH) at an equilibrium condition for KCl solutions. Noting that hydrogen or hydroxide are not material components, different pH values were obtained by adding K or Cl to the material component compositions and then determining the equilibrium condition as described for Step 2 in the flow model. Only the water equilibrium relationship was required in this calculation. A second program solved the aqueous equilibrium relationships involving chromium and acetate species and water to provide equilibrated solutions at selected chromium concentrations for injection into the flow system. The value of K_{12} in Table 6.2 was adjusted from 3.45E-7 [Stavland et al., 1993] to 6.90E-6 to fit the measured pH values of the chromium(III) acetate solution. The pH value of the 200 ppm chromium(III) (acetate salt) solution was about 4.6, close to the measured value.

A third program determined the composition of the aqueous phase that results after a KCl brine has come to equilibrium after dissolution of the appropriate rock material (Baker dolomite ($CaMg(CO_3)_2$), San Andres dolomite ($CaMg(CO_3)_2$ and $CaSO_4$) and Brent sandstone ($CaCO_3$). A method similar to that describe for Step 2 of Figure 6.1 was used to solve a set of equations for the material components (and hydrogen) in one mixing cell. Mole-balance equations for the material components that are dissolved from the carbonate rocks followed the stoichiometry of the minerals and the K_{sp} expression for each mineral was applied. As an example, pH of the equilibrated KCl solution with Baker dolomite was about 10, consistent with laboratory measurements. The equilibrated solution was resident in each mixing cell of the model as an initial condition.

Experimental Details

Cylindrical cores were drilled from a block of Baker dolomite (Millersville, Ohio). Baker is a relatively pure dolomite as determined by chemical analysis [Meister, 1978]. The cores were washed with deionized water and dried in an oven at 105ºC for one day. End caps with grooves that allowed for distribution of fluids across the face were attached to the ends of the core and the cores were coated with epoxy. The cores were saturated with KCl brine and porosity and permeability values were determined. Tracer tests were conducted on each core to determine flow characteristics and dispersion coefficients by injecting a 0.1 mole/L KNO_3 solution and detecting nitrate concentration in the effluent by an in-line spectrophotometer. Cores with heterogeneous flow characteristics were discarded. Names and properties of the cores used for flow experiments are listed in Table 6.3. One flow experiment was conducted in Cores C1, C3, C4, C5, C6 and C7. Multiple flow experiments were conducted in Cores B and C2.

Table 6.3 - Properties of dolomite cores used in this project.

Core name	B	C1	C2	C3	C4	C5	C6	C7
Diameter (cm)	1.86	1.88	1.88	1.88	1.88	1.88	1.88	1.88
Length cm)	6.50	6.55	6.02	6.00	6.42	7.15	6.83	6.62
Porosity	0.23	0.22	0.23	0.22	0.23	0.22	0.21	0.21
Pore volume (mL)	4.14	4.06	3.83	3.61	4.13	4.34	4.03	3.94
Permeability (md)	42	30	27	23	55	24	17	36

Chromium(III) acetate salt (Alfa Chemicals) is a dark green powder with an empirical formula $Cr(OAc)_3 \cdot H_2O$. Solutions were prepared by dissolving chromium(III) acetate into 1% potassium chloride solutions and aging the solution for two weeks before use.

A schematic of the experimental apparatus used for the flow experiments is shown in Figure 6.2. Two pumps were used to inject solutions at constant volumetric flow rates. One pump was used for the injection of 1% KCl solution and the other was used for the injection of the selected solutions: chromium(III) acetate solution, tracer solution, etc. A four-way valve was positioned between the pumps and the core for switching between injected fluids. A six-way valve allowed for the injected solution to bypass the core for calibrations of inline UV/Vis spectrophotometer and the pH electrode and for shutting in the core without detaching connections. A transducer connected at both ends of the dolomite core was used to measure the differential pressure across the core. An in-line Varian spectrophotometer and pH meter were connected to the exit of the core to measure values of the effluent chromium or potassium nitrate tracer concentrations and pH. Potassium nitrate and chromium acetate were detected at the wavelengths of 302 nm and 575 nm, respectively. An automatic fraction collector was used at high flow rates to collect samples for the analysis of calcium, magnesium and chromium concentrations using atomic absorbance spectrometer. At low flow rates, samples were collected manually by inserting the effluent tube through a tight hole in the plastic caps of the sample vials to minimize evaporation. The experimental setup was enclosed in a constant temperature air bath maintained at 25°C.

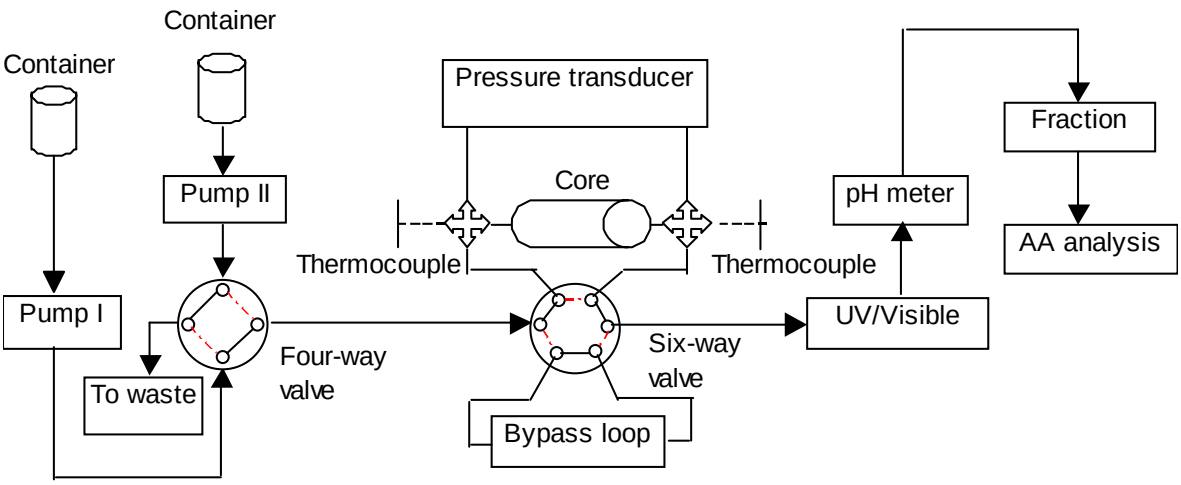

Figure 6.2 - Schematic of equipment used for the flow experiments.

Two types of displacements were conducted: (I) flow experiments, and (II) shut-in experiments. Flow experiments were conducted with KCl brines, a ptassium acetate solution and chromium acetate solutions. The procedure for a flow experiment was:

- Inject the selected solution at a constant injection rate through a dolomite core that was initially saturated with 1% KCl solution. About five to six pore volumes were injected for chromium(III) acetate solutions. The size of the effluent samples collected (0.25 or 0.5 pore volumes) was determined by the estimated calcium, magnesium and/or chromium concentrations and the concentration range required for analysis.
- Flush the core with 1% KCl at flow rates of 1.00 and 0.03 mL/min.

Chromium acetates solutions were used in shut-in experiments. The procedure for a shut-in experiment was:

- Inject the selected solution at a fast rate (1.00 to 2.00 mL/min) through a dolomite core that was initially saturated with 1% KCl brine solution. About five to six pore volumes were injected for chromium(III) acetate solutions. Effluent samples with volumes of about one pore volume were collected for calcium, magnesium and/or chromium analysis. This first step of a shut-in experiment also provided results of a "flow experiment" at a high flow rate.
- Shut-in the core by switching the six-way valve so the solution flowed through the bypass tubing instead of the core. Change the injected solution to 1% KCl brine solution and flush the bypass tubing and the in-line spectrophotometer and pH meter.
- After a selected shut-in period, switch the six-way valve to inject 1% KCl solution into the core at 1.00 mL/min to displace the shut-in fluid from the core. Effluent samples were collected during the first pore volume of brine injection to determine calcium, magnesium and/or chromium concentrations. Values at about 0.5 PV injected were assumed to be representative of the solution that was in contact with the rock for the shut-in (residence) time.
- Flush the core with 1% KCl at flow rates of 1.00 and 0.03 mL/min.

Calcium, magnesium and chromium concentrations in the effluent solutions were determined with an atomic absorption (AA) spectrophotometer (Perkin Elmer Aanalyst 300 with an AS 90 plus autosampler) using an air-acetylene flame. To minimize the matrix effects, AA analyses were conducted with standards containing similar compositions to that of the effluent solutions. A solution containing 2% nitric acid and 1% potassium chloride was used to prepare standard solutions and to dilute the effluent samples for chromium analysis. For magnesium and calcium analysis, 0.1% and 1.0% lanthanum was added to the solution containing 2% nitric acid and 1% KCl to minimize the interference from silica, aluminum, sulfate etc. Lanthanum solutions were prepared from $LaCl_3.7H_2O$ (Fisher Scientific). The AA was operated in the linear concentration range with the manufacturer's recommended operating parameters.

Results and Discussion

Flow experiments using brines and chromium acetate solutions in carbonate-containing rocks (Baker dolomite, San Andres dolomite, and Brent sandstone) under different conditions of injected solution pH, ionic concentration and flow rate were conducted and then simulated with the model. Successive simulations were conducted where fitting parameters were adjusted manually in order to closely match selected data. Comparison of the simulations and experimental results are presented in the following three sections for each type of carbonate rock.

Flow experiments were conducted in eight Baker dolomite cores. Core B was used to test a restoration process that would permit reuse of the medium. The restoration process was ineffective in that results from the flow experiments using chromium(III) acetate solutions were different in the virgin and "restored" cores. Therefore, new, or virgin, core material was used for injection of chromium(III) acetate solution in Cores C1 to C7. One core, C2, was used after the initial injection of chromium(III) acetate solution to conduct additional flow tests. The sequences of flow experiments in Cores B and C2 are shown in Tables 6.4 and 6.5, respectively.

Three general types of effluent data were considered during the adjustment of the parameters in the model to match the experimental data from flow experiments that are conducted at constant flow rate. The types of data are referred to as (a) transient, (b) steady-state, and (c) equilibrium. Transient data are the measured pH values and component concentrations in the effluent that vary with volume injected (or time) when the front of the injected fluid exits the core at about one PVI. Transient data include the mixing zone between the injected and displaced fluids as well as the other interactions between the rock and the injected fluid that cause changes in the effluent data. Following the transient period, the effluent data stabilize or become steady-state. Steady-state data are collected during flow experiments and during shut-in type experiments. The effluent solution is assumed to be in equilibrium with the rock when the flow rate is low (large resident times) and further reduction in the flow rate (larger resident times) does not appreciably change the pH and component concentrations in the effluent. Equilibrium data are also achieved when a solution saturates the medium and is shut-in for a sufficient time period to allow the system to approach to equilibrium.

Transport through Baker Dolomite Cores. Parameters for dolomite dissolution, Eq. 6.7, were established by fitting the model to flow experiments where brines at selected pH values were flowed through Baker dolomite cores. The fraction of dolomite, $y_{dolomite}$, in Eq. 6.7 was set to 1.0. Using these parameters for dolomite dissolution, adjustable parameters for chromium

Table 6.4 - Sequence of flow experiments in Baker dolomite Core B.

Flow experiment	Injected solution*	Flow rate(s) (mL/min)	Residence time (hours)	Volume injected (pore volumes)
B-Flow0.032-1	chromium acetate	0.032	2.2	5.8
Brine postflood	KCl brine	1.00	0.07	380
B-Flow0.032-2	chromium acetate	0.032	2.2	5.0
Brine postflood	KCl brine	1.00	0.07	440
B-Flow1-1	chromium acetate	1.00	0.07	5.0
B-Shutin2-1	chromium acetate	-	2.0	-
Brine postflood	KCl brine	0.10	0.69	70
B-Flow0.032-3	chromium acetate	0.03	2.3	5.1
Brine postflood	KCl brine	0.03, 1.00, 0.10	2.3, 0.07, 0.69	180
B-Flow1.5-2	chromium acetate	1.50	0.05	5.0
B-Shutin2-2	chromium acetate	-	2.0	-
Brine postflood	KCl brine	0.10	0.69	140
B-Flow1.5-3	chromium acetate	1.50	0.05	5.0
B-Shutin4-3	chromium acetate	-	4.0	-
Brine postflood	KCl brine	0.10, 0.03	0.69, 2.3	90
B-Flow0.032-4	chromium acetate	0.032	2.2	6.0
Brine postflood	KCl brine	1.00	0.07	6
B-Flow0.032-5	chromium acetate	0.032	2.2	4.2
Brine postflood	KCl brine	1.00	0.07	

* All solutions contained 1.0% KCl; Chromium acetate solutions contained 200 ppm Cr.

Table 6.5 - Sequence of flow experiments in Baker dolomite Core C2.

Flow experiment	Injected solution	Flow rate(s) (mL/min)	Residence time (hours)	Volume injected (pore volumes)
C2-Flow0.032-1	chromium acetate 200ppm Cr	0.032	2.0	5
Brine postflood	KCl brine	1.00, 0.03	0.06, 2.1	123
C2-pH2.1-Flow-2	KCl brine pH = 2.1	1.02, 0.10 0.032, 0.06, 1.02	0.06, 0.64 2.0, 1.1, 0.06	23
Brine postflood	KCl brine	1.00, 0.03	0.06, 2.1	350
C2-KOAc-Flow-3	0.0114 M potassium acetate pH 4.6	1.02, 0.134, 0.032	0.06, 0.5, 2.0	24
Brine postflood	KCl brine	1.00, 0.03	0.06, 2.1	78

precipitation, Eq. 6.10, were then established by fitting the model to the flow experiments where chromium acetate solutions were flowed through virgin Baker dolomite cores. Comparisons of the simulations with the best-fit parameters to the experimental data for Baker dolomite cores are presented in the following sections.

Brine transport. A 1.0% KCl brine at a pH of 2.1 was injected through Core C2 at several flow rates. The pH of the injected brine was adjusted so that the effluent pH from the dolomite core would be in the vicinity of 6.9, similar to the effluent pH value measured during injection of chromium acetate solutions. Concentrations of calcium and magnesium and the pH in the effluent and the corresponding simulated values from the model are shown in Figure 6.3. The pH values exhibit long transient times in that several PVI are required to approach a steady-state value. Effluent pH values are more closely simulated by the model at the lower injection rates or longer residence times. Simulated calcium and magnesium concentrations are somewhat higher than the experimental values, particularly at the higher flow rate.

Model simulations are compared to the experimental data from Zou et al. [2000a]. They conducted a series of brine injections through a Baker dolomite core where the pH of the injected brine (0.5% KCl) and the flow rate were varied. The Baker dolomite core used in these experiments was cut from the same block as used in this study. The core was 3.7 cm in diameter and 15 cm in length, and had a porosity of 0.25 and a permeability of 70 md.

The steady-state values of effluent pH for different pH values and flow rates of the injected brine are shown in Figure 6.4 as a function of the residence time in the core. A similar plot for the magnesium concentration in the effluent is shown in Figure 6.5. Also included in these figures are the steady-state data taken from Figure 6.3. The model results, shown by the continuous lines in Figures 6.4 and 6.5, match the steady-state data reasonably well for a wide variation of injected pH values and residence times greater than about 5 minutes. Values of the data and the model results for long residence times represent equilibrium values which are plotted in Figure 6.6 as a function of the pH of the injected solution. The equilibrium pH demonstrates a three-stage behavior when the injected pH increases from 2.1 to 10.9. The effluent pH increased with increase of the injected pH at values less than 4. The effluent pH is about 10 when the injected pH is between 4 and 10 due to the buffering effect of the carbonate-bicarbonate ions. The effluent pH is essentially the same as the injected pH when the injected pH is above 10. The flow model simulates the equilibrium experimental data well.

An experiment was conducted with a potassium acetate solution to test the model. A solution containing 0.0114 M potassium acetate and 1.0 % potassium chloride at an adjusted pH of 4.6 was injected through Core C2 at flow rates corresponding to residence times of 3.8, 28 and 120 minutes (Run C2-KOAc-Flow-3, Table 6.5). The solution contained the same amount of acetate and potassium chloride and was at the same pH as the chromium(III) acetate solutions (200 ppm Cr(III)) used in the flow experiments. Fitting parameters for dolomite dissolution in the model that were established for the KCl brine injections were used. The simulated effluent steady-state calcium and magnesium concentrations and pH matched the experimental steady-state data as shown in Figure 6.7 The mathematical model simulated the dolomite dissolution in the presence of acetate ions well.

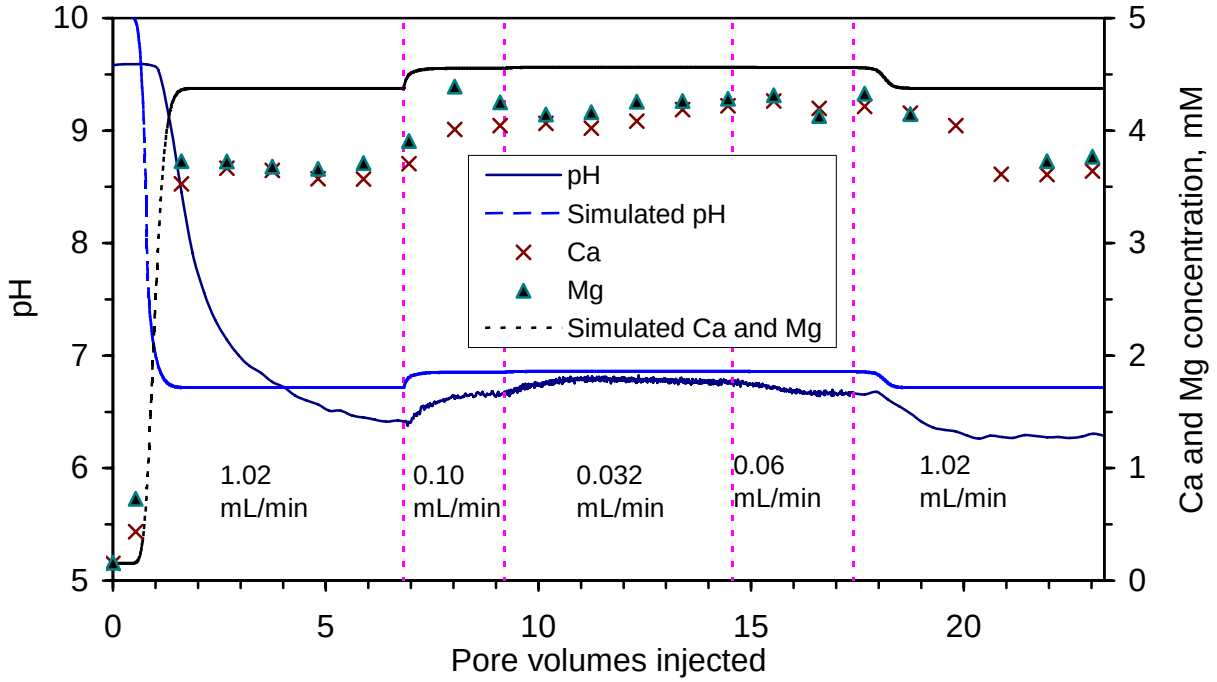

Figure 6.3 - Comparison of the effluent pH, calcium and magnesium concentrations for run C2-pH2.1-Flow-2 between experimental data and simulated results.

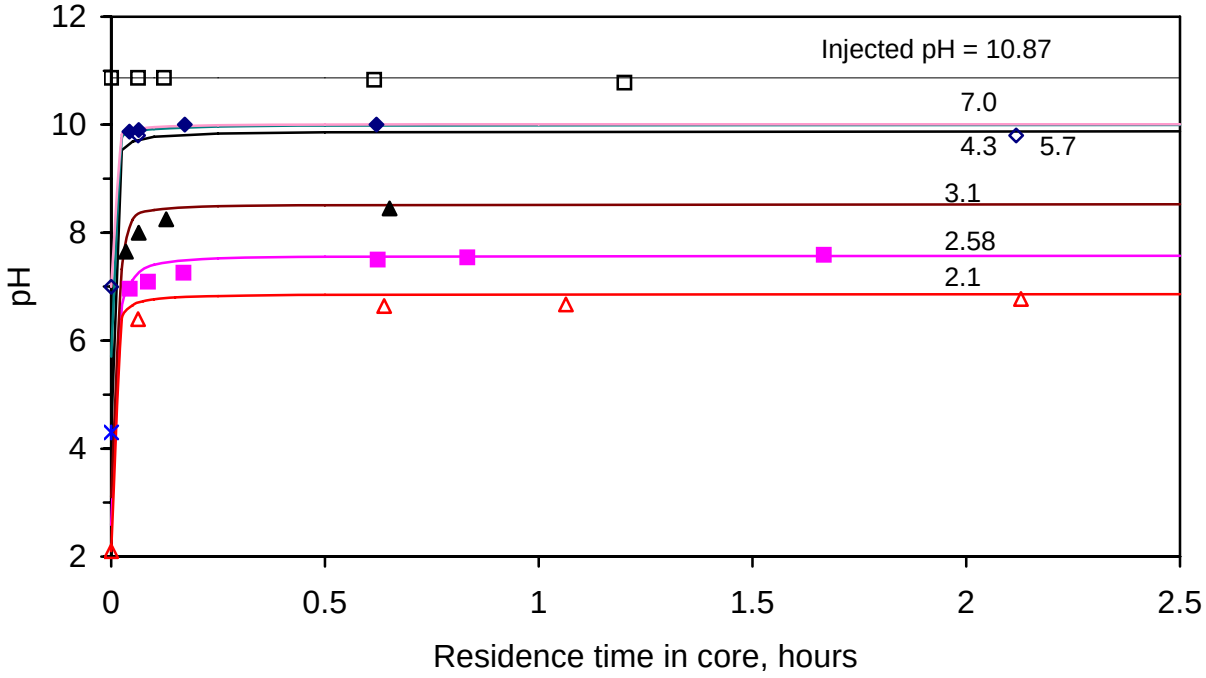

Figure 6.4 - Comparison of the effluent steady-state pH between experimental data and simulated results. Injected pH values are shown in the graph.

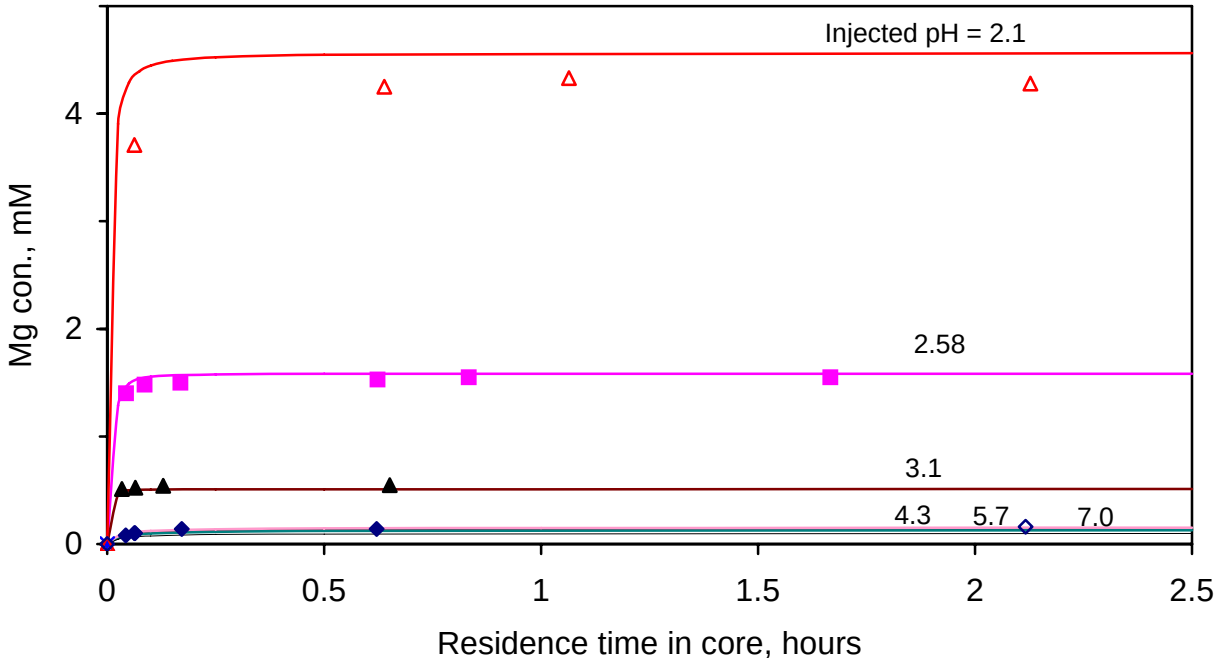

Figure 6.5 - Comparison of the effluent steady-state magnesium concentration between experimental data and simulated results. Injected pH values are shown in the graph.

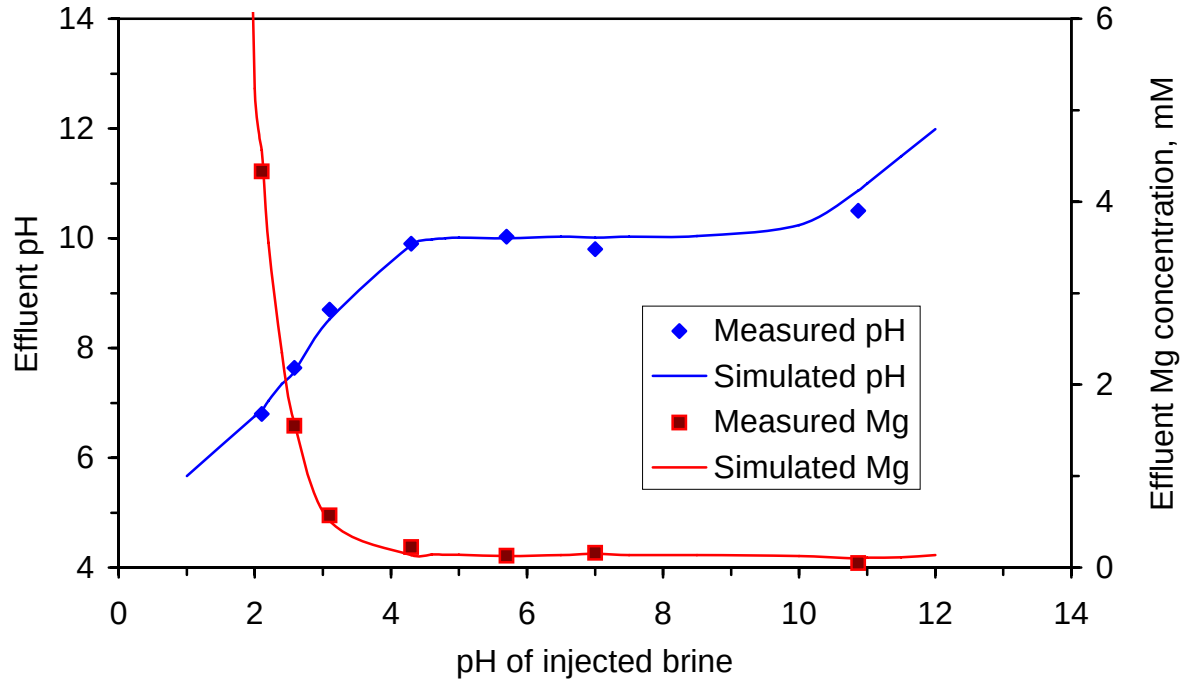

Figure 6.6 - Comparison of the effluent equilibrium pH and magnesium concentration between experimental data and simulated results.

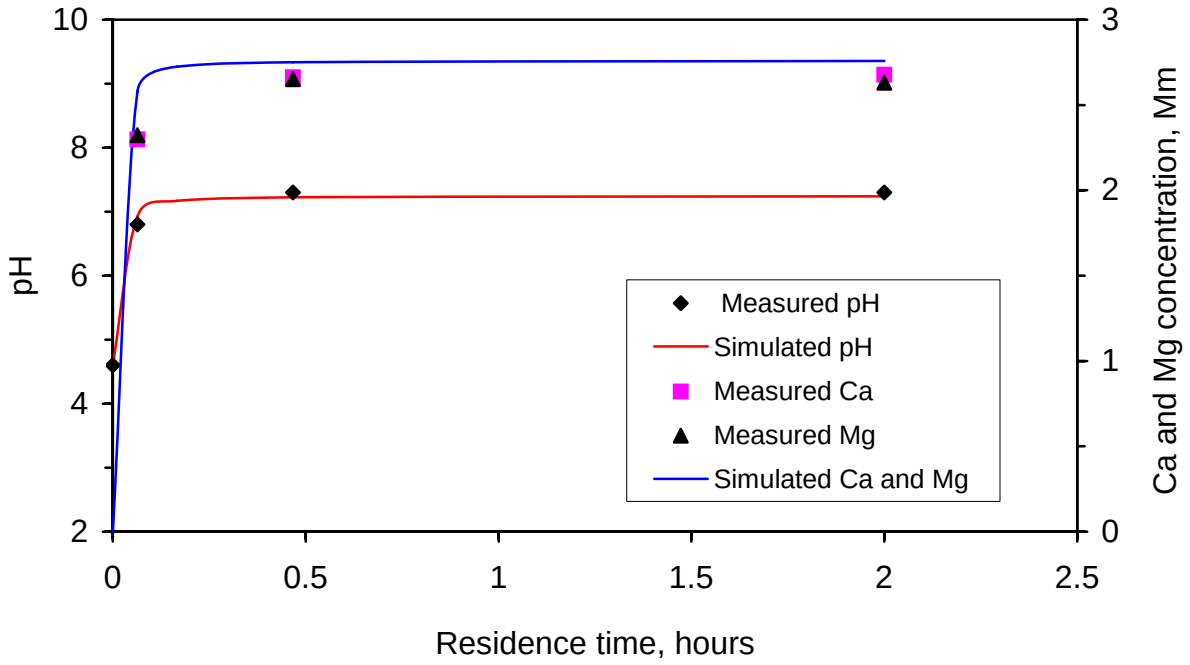

Figure 6.7 - Comparison of the effluent steady-state pH, calcium and magnesium concentrations for run C2-KOAc-Flow-3 between experimental data and simulated results.

Zou et al. [2000a] conducted additional experiments to investigate the effect of the calcium concentration in the injected fluid on the effluent pH and the dissolution of Baker dolomite. The injected solution contained 0.5% KCl at a pH of 5.0 with selected calcium concentrations (0.0025-0.25 mol/L). The injection rate was 1.1 ml/min (residence time 36.7 mins). The effluent data collected were the steady-state values and it is not known if the data represent equilibrium values. The same core that was described above was used.

The possibility of the precipitation of calcite occurs during the dissolution process of dolomite when there is another source of calcium ions in addition to that which is dissolved from the dolomite. These run in which calcium ions were contained in the injected fluid give rise to concentrations of Ca^{2+} and CO_3^{2-} whose product exceeds the K_{sp} of calcite. Three cases that describe the precipitation of calcite were studied in this work.

Case 1a: precipitation of calcite occurs at the saturation condition of $I_s^* = 4.93$.
Case 1b: precipitation of calcite occurs at the saturation condition of $I_s^* = 1.0$.
Case 2: precipitation of calcite is not considered.

In Cases1a and 1b, the precipitation rate of calcite is assumed very fast. Equilibrium between the solution and solid calcite is reached instantly.

Figure 6.8 shows the effluent calcium concentration versus injected calcium concentration. For all the three cases, the effluent calcium concentrations are close to the injected calcium concentration. The amount of calcium concentration changed due to dolomite dissolution or calcite precipitation is not significant compared to the calcium amount in the injected solution.

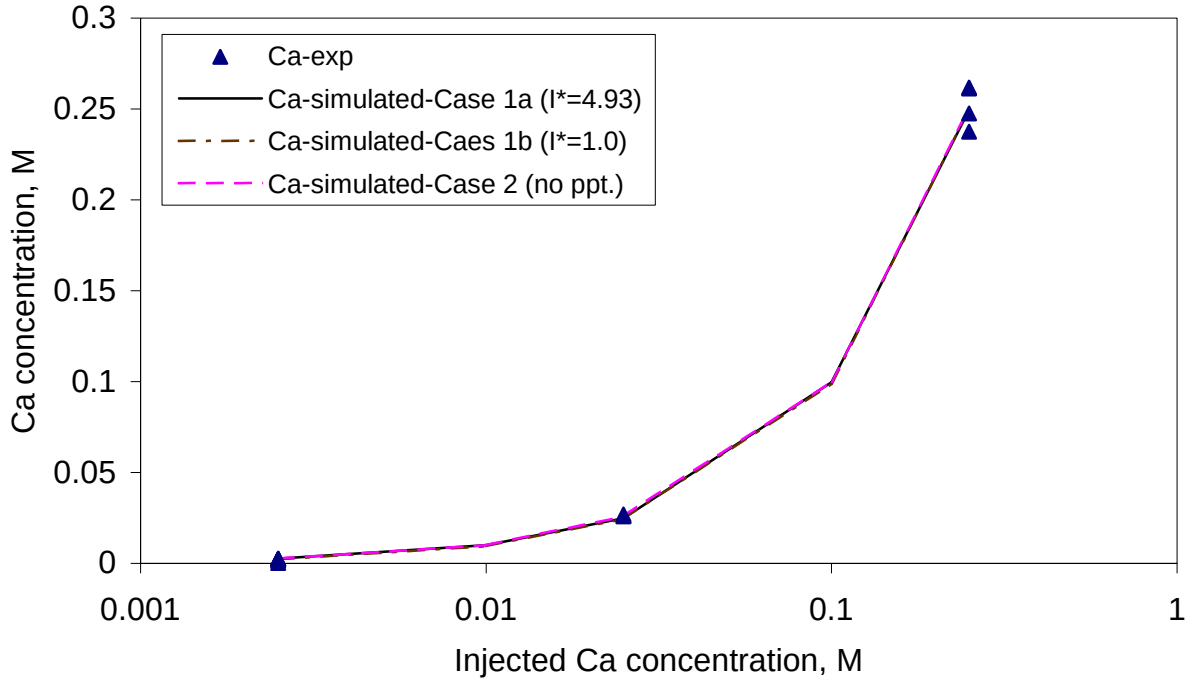

Figure 6.8 - Comparison between the simulated results and experimental data for the effluent steady-state Ca concentration versus injected Ca concentration.

Figure 6.9 shows the effluent magnesium concentration versus injected calcium concentration. Case 2 simulations are in best agreement with the experimental data. Figure 6.10 shows the effluent pH concentration versus injected Ca concentration. Case 1b simulations are in best agreement with the experimental data. For calcite precipitation in Case 1b, the simulated magnesium concentration is 3 to 4 times higher than the experimental data. Additional work is require in order to improve the model so that it can simulate the injection of common ions on dolomite dissolution.

Chromium transport. Seven experiments were conducted in which chromium acetate solutions were flowed through Baker dolomite cores that were previously only contacted by 1% KCl brine. Six experiments were conducted with solutions containing 200 ppm chromium and one was conducted with a 100 ppm chromium solution. About five pore volumes of chromium acetate solution were injected in each run. Experimental parameters and results are listed in Table 6.6. Residence times for the solution in the core ranged from 0.03 to 24 hours and were the primary parameter to correlate the results.

Fitting parameters established for dolomite dissolution during brine injections in Baker dolomite cores were used for simulating the flow of chromium acetate solution through virgin Baker cores. One set of parameters for chromium precipitation were fitted to match effluent chromium concentrations for the set of five flow experiments using solutions containing 200 ppm chromium. Effluent pH and concentrations of calcium and magnesium were not considered during the fitting process.

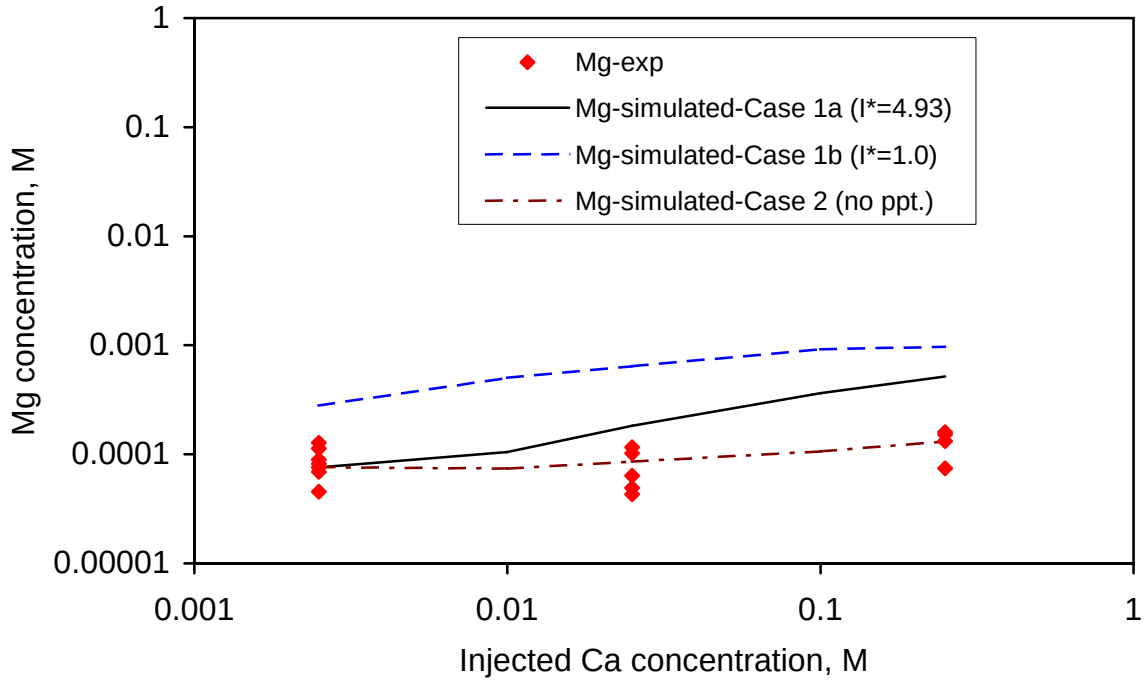

Figure 6.9 - Comparison between the simulated results and experimental data for the effluent steady-state Mg concentration versus injected Ca concentration.

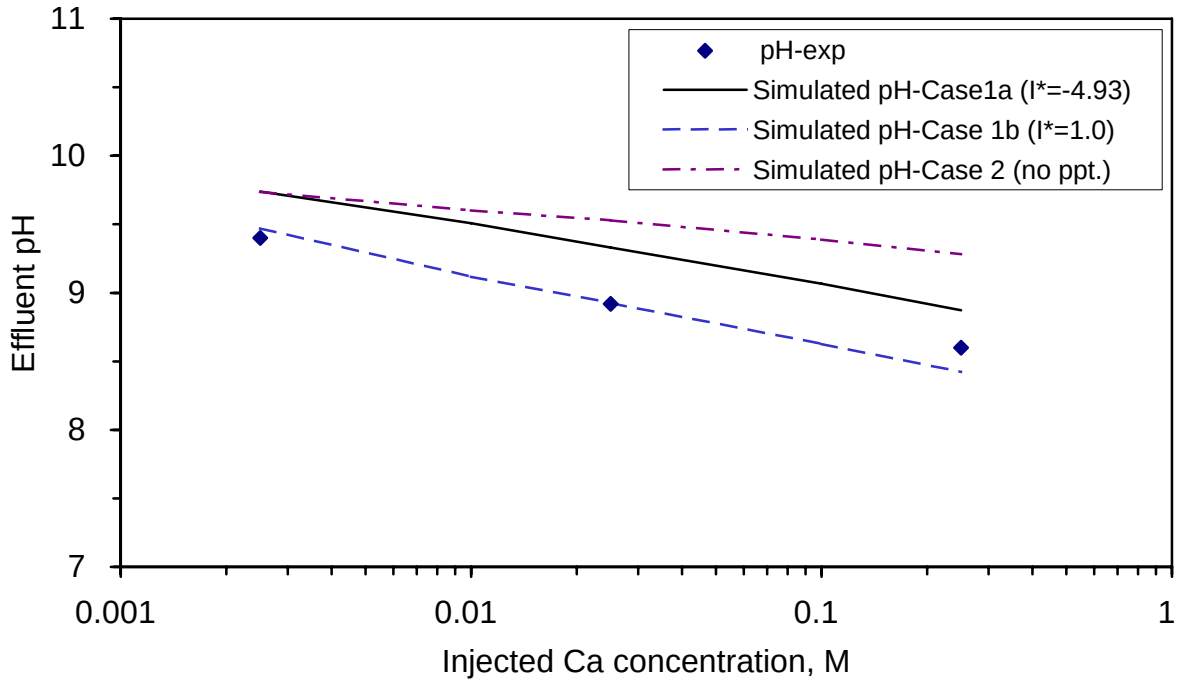

Figure 6.10 - Comparison between the simulated results and experimental data for the effluent steady-state pH versus injected Ca concentration.

Table 6.6 – Experimental parameters and results for flow experiments in virgin cores.

Run No.	C4-Flow2-1	C3-Flow1-1	C2-Flow0.032-1	C1-Flow0.032-1	C6-Flow0.0056-1	C5-Flow0.003-1	C7-Flow0.033-1
Chromium conc. (ppm)	200	200	200	200	200	200	100
Residence time (hours)	0.034	0.060	2.0	2.1	12.0	24.1	2.0
PV injected	4.8	5.7	5.01	4.74	5.94	5.43	5.02
Steady-state norm. Cr conc.	0.99	0.99	0.88	0.85	0.43	0.23	0.75
Steady-state pH	6.8	6.9	6.9	7.0	6.9	7.2	7.4
Steady-state Mg conc. (mM)	1.4	1.4	1.93	1.88	2.2	2.3	1.2
Steady-state Mg/Ca molar ratio	1.00	1.00	0.99	1.00	1.05	1.15	1.00
Amount of chromium retention* (mg)	-	-	0.903	0.888	3.469	3.660	0.711

* The amount of chromium retention = the amount of chromium injected – the amount of chromium detected by spectrophotometer.

Runs C4-Flow2-1 and C3-Flow1-1 were experiments with short residence times of 0.034 and 0.060 hours, respectively. Effluent chromium concentrations are shown in Figure 6.11 as a function of injected volume. Higher chromium concentrations were measured by the inline VIS spectrophotometer than by AA analysis during the transition period before steady state values were observed at about 4 to 5 PVI. The cause of the concentration differences between the two methods was not determined. Chromium concentrations during the steady-state period were close to the injected values and are matched by the simulation after about 2 PVI for the VIS data and after 4.5 PVI for the AA data. Relatively long transient periods were observed for the effluent pH values. Effluent pH values were approaching the simulated values at the end of injection at 5 PVI. Effluent calcium and magnesium concentrations stabilized at about 1.4 mM for both runs as shown in Figure 6.12. Simulated calcium and magnesium concentrations were considerably higher than the measured values.

Runs C1-Flow0.032-1 and C2-Flow0.032-1 with residence times of about 2.0 hours were conducted to test reproducibility of the flow experiments. Brine was injected at 1.00 mL/min immediately after injection of the chromium solution. Chromium concentrations and pH values in the effluent are shown in Figure 6.13. Starting at about one pore volume injected, a transient period occurred where the chromium concentration increased and the pH decreased to values that approached steady-state values. Chromium was continuously retained as shown by the almost steady chromium concentration which was about 170 ppm. Reproducible behavior was observed when the flow experiments were conducted in virgin cores.

When brine was injected at a faster rate at about 5 PVI, the chromium concentration increased and then decreased to zero. During the first PVI at the faster rate, the residence time the effluent experiences in the core decreases linearly between the values of the residence times at the two injection rates. The chromium concentration increases with shorter residence time (or PVI) until

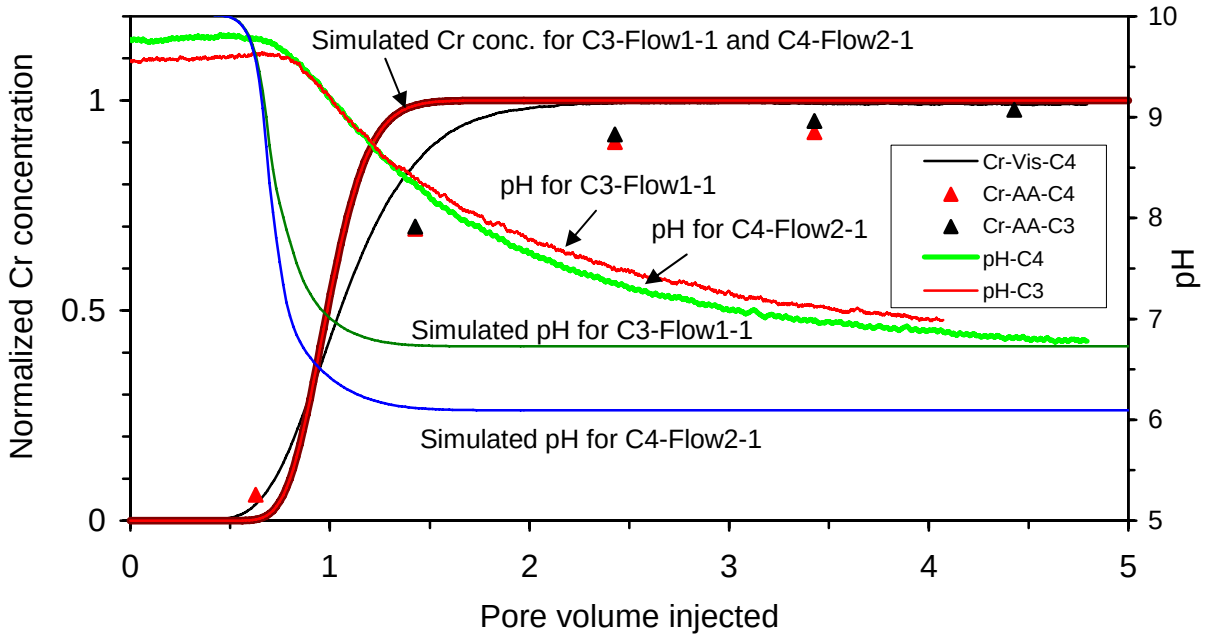

Figure 6.11 - Comparison of the effluent chromium concentration and pH for runs C3-Flow1-1 and C4-Flow2-1 between experimental data and simulated results.

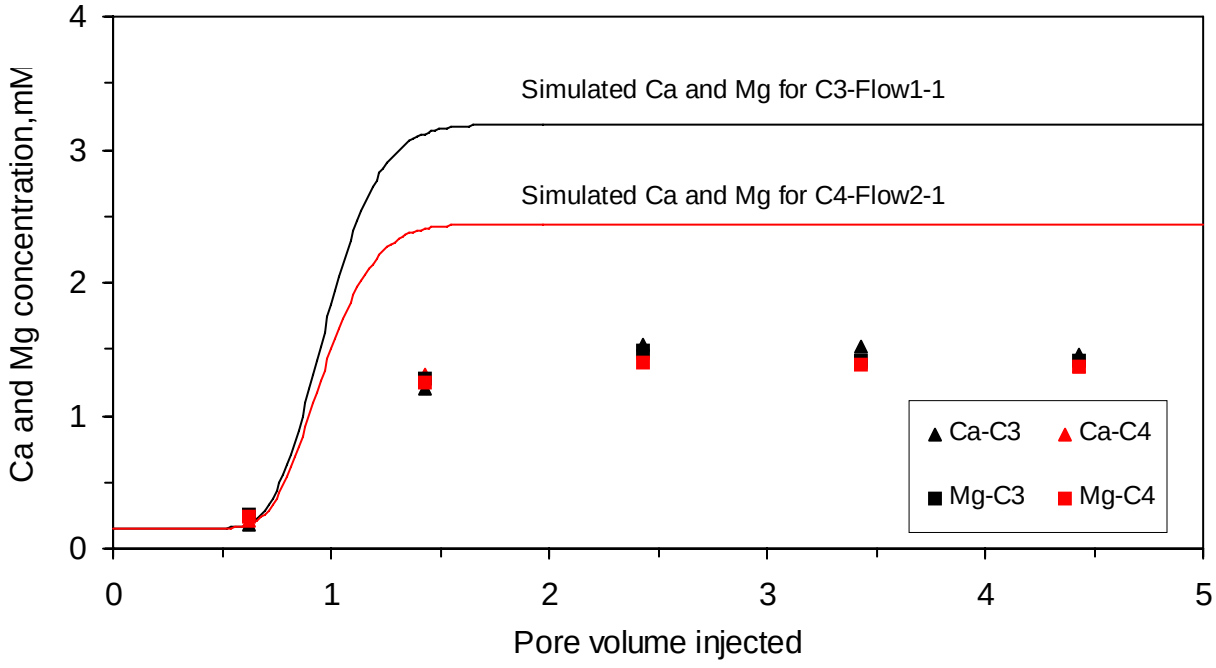

Figure 6.12 - Comparison of the effluent calcium and magnesium concentrations for runs C3-Flow1-1 and C4-Flow2-1between experimental data and simulated results.

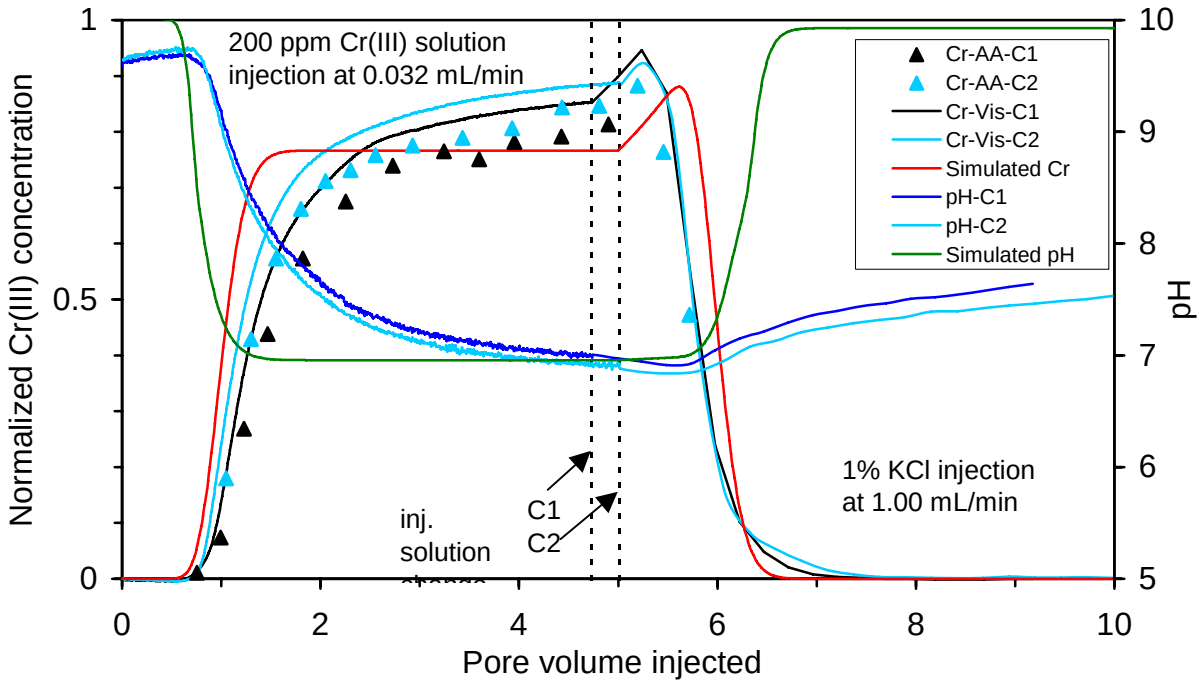

Figure 6.13 - Comparison of the effluent chromium concentration and pH for runs C1-Flow0.032-1 and C2-Flow0.032-1 and the following brine postflood between experimental data and simulated results.

the mixing zone between the brine and chromium solution elutes which then causes the concentration to go to zero. The model simulated trends of the effects of injecting brine at the higher rate well.

Calcium and magnesium concentrations in the effluent for the runs with residence times of about 2.0 hours are shown in Figure 6.14. Calcium and magnesium concentrations from Cores C1 and C2 were in good agreement. Magnesium concentrations were consistently higher than calcium concentrations in the transient period during the injection of chromium(III) acetate solutions and were less than the calcium concentrations during the brine postflush. Equimolar concentrations of calcium and magnesium were displaced from the cores during the steady-state periods between 2 and 5 PVI. Simulated calcium and magnesium concentrations are always equimolar and were about twice the measured values during the steady-state period.

Long resident times of 12 and 24 hours were tested in Runs C6-Flow0.0056-1Run C5-Flow0.003-1, respectively, and the effluent measurements and simulated values are shown in Figures 6.15 to 6.18. Longer transient periods for the measured chromium concentrations are observed with longer residence times. Measured chromium concentrations approached lower steady-state values with longer residence times. The model did not simulate well the transient period but matched the steady-state values of the chromium concentration.

Magnesium concentrations were higher than the calcium concentration in the transient and steady-state periods for the long residence times of 12 and 24 hours as shown in Figures 6.16 and 6.18. An opposite trend was observed during the brine post-flush for the run with a 12 hour

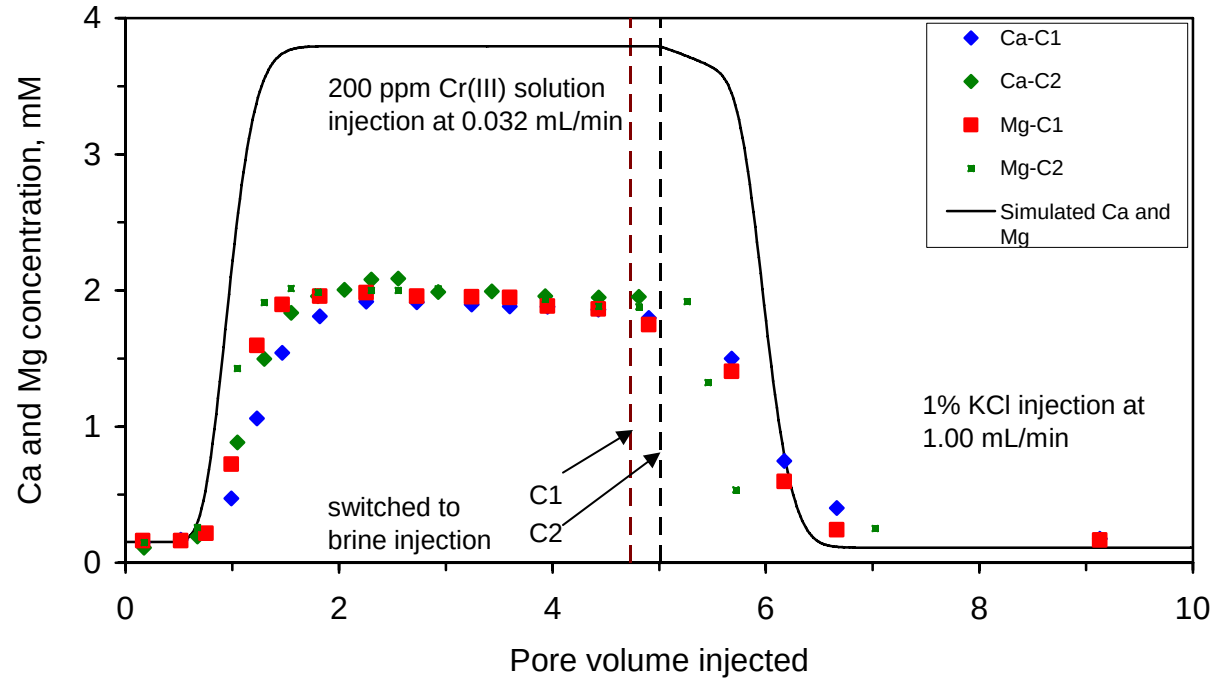

Figure 6.14 - Comparison of the effluent calcium and magnesium concentrations for runs C1-Flow0.032-1 and C2-Flow0.032-1 and the following brine postflood between experimental data and simulated results.

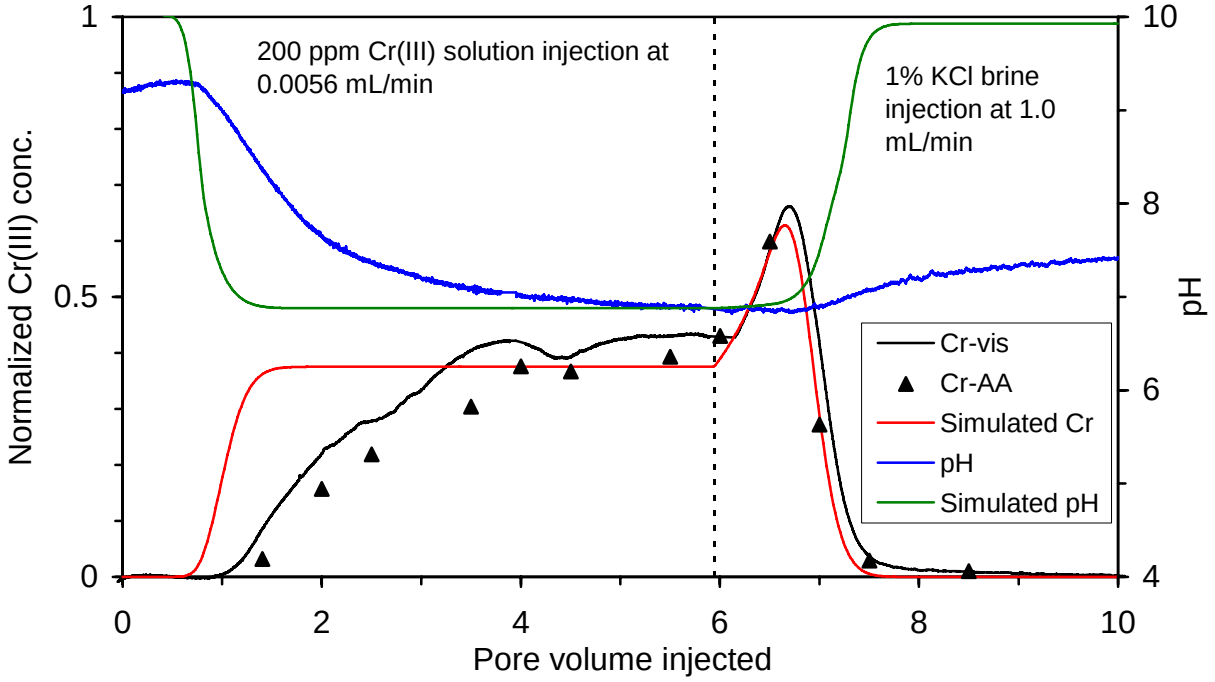

Figure 6.15 - Comparison of the effluent chromium concentration and pH for Run C6-Flow0.0056-1 and the following brine postflood between experimental data and simulated results.

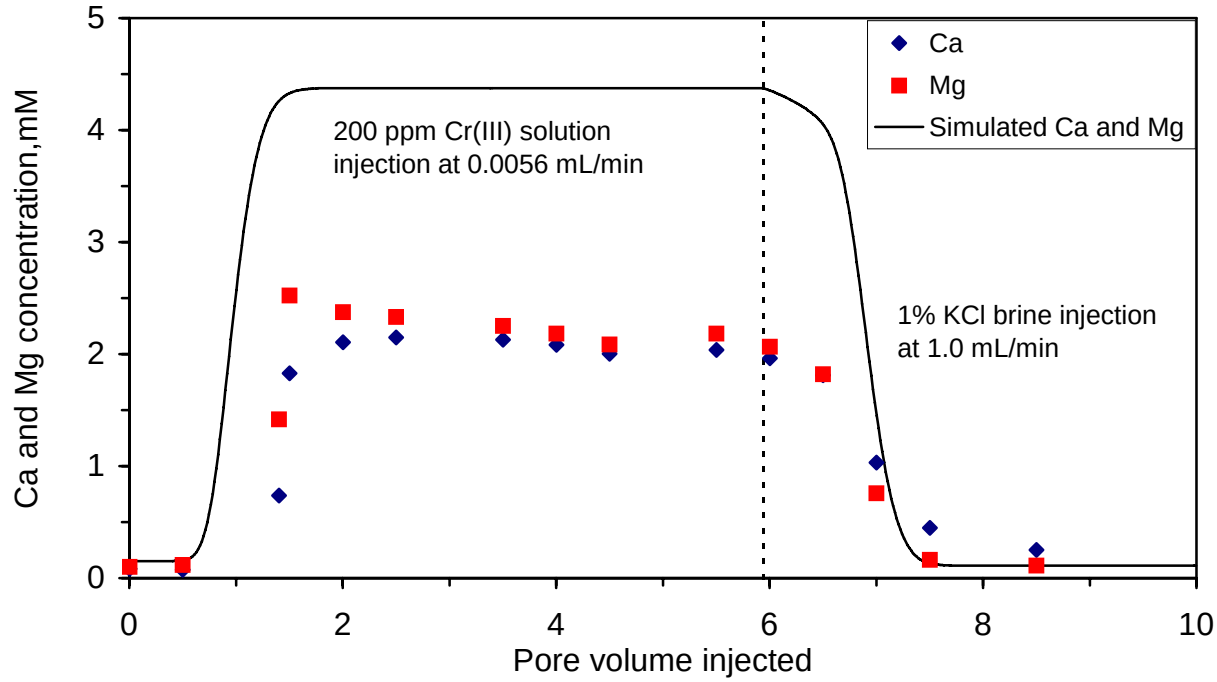

Figure 6.16 - Comparison of the effluent calcium and magnesium concentrations for Run C6-Flow0.0056-1 and the following brine postflood between experimental data and simulated results.

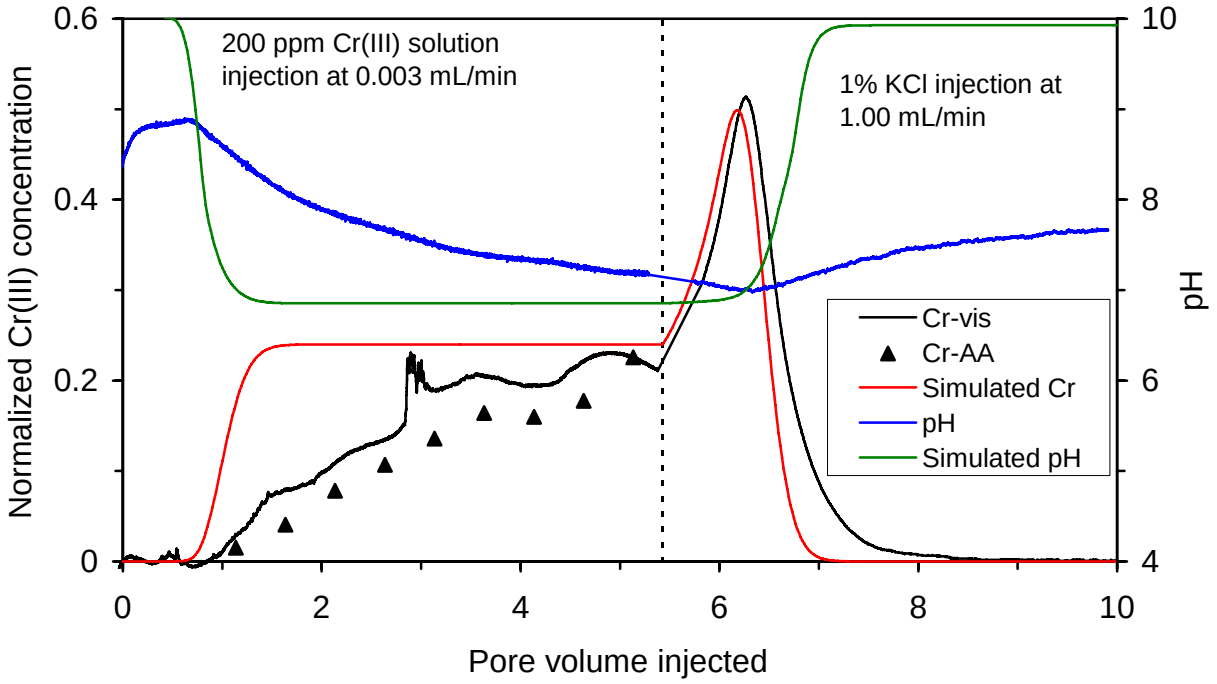

Figure 6.17 - Comparison of the effluent chromium concentration and pH for C5-Flow0.003-1 and the following brine postflood between experimental data and simulated results.

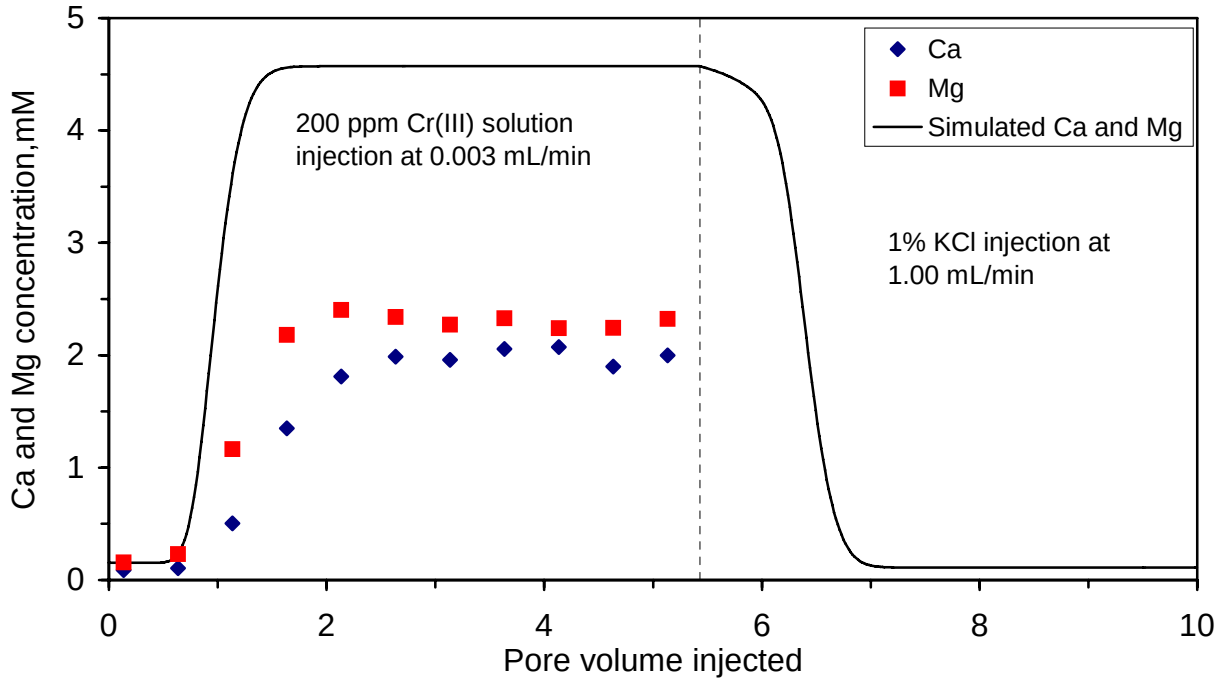

Figure 6.18 - Comparison of the effluent calcium and magnesium concentrations for C5-Flow0.003-1 between experimental data and simulated results.

residence time (Figure 6.16). Calcium and magnesium concentrations were not measured during the brine post flush for Run C5-Flow 0.003-1. The mole ratio of magnesium to calcium was about 1.15 for the 24 hour residence time (Figure 6.18). Simulated concentrations of calcium and magnesium were about twice the measured values during the steady-state period.

Transition periods when the chromium front arrived in the effluent spanned larger PVI than runs at shorter residence times and were not matched by the model. However, the model simulated the effluent steady-state chromium concentrations with one set of fitting parameters in Eq. 6.10. Steady-state values of the effluent measurements and the simulated values are presented in Figures 6.19 and 6.20. The simulated effluent chromium concentrations were matched reasonably well with the set of fitting parameters in Eq. 6.10. This set of parameters also matched the pH data during the steady-state period for all residence times (flow rates). Simulated effluent state-steady calcium and magnesium concentrations were much higher and did not match the experimental data as shown in Figure 6.20.

Jin et al. [2002] conducted a series of runs in which chromium acetate solutions (200 ppm Cr) were injected into Baker dolomite cores at two flow rates and for shut-in experiments at selected time periods. Effluent chromium concentrations are plotted in Figure 6.19 and are in reasonable agreement with results of this study. Additional results for shut-in experiments are presented in the following section.

The model does not predict correct values of calcium and magnesium concentrations in the effluent during the injection of chromium acetate although reasonable matches of these

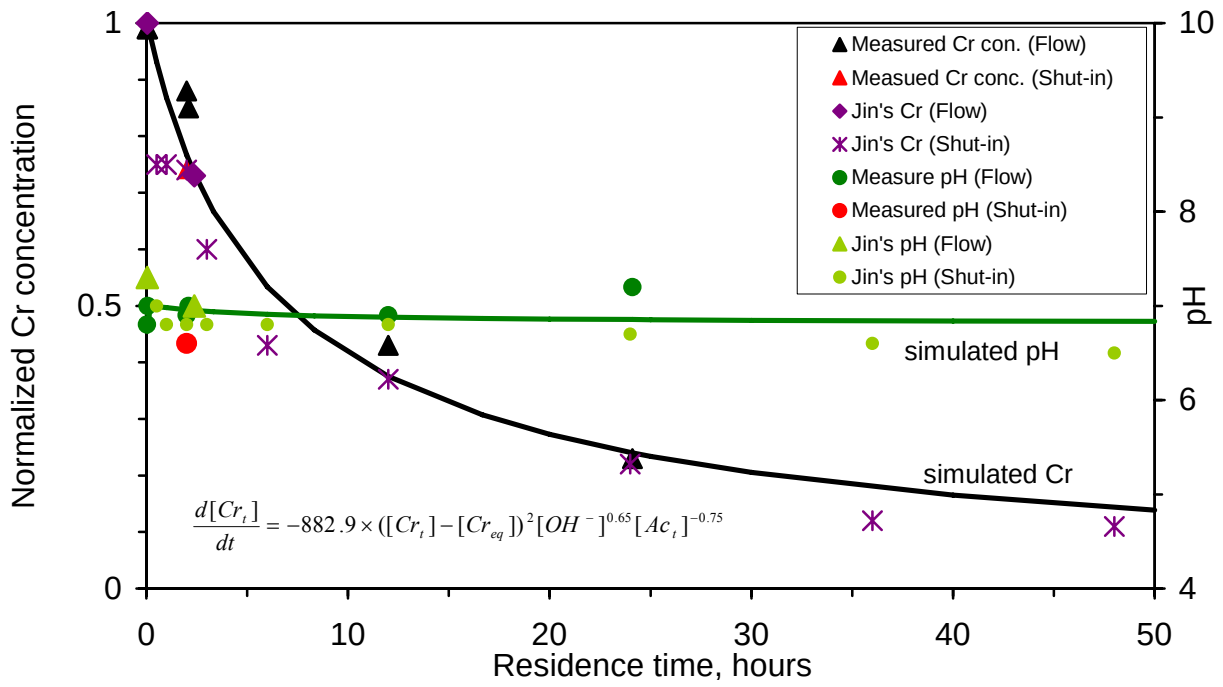

Figure 6.19 - Comparison of the simulated and measured steady-state Cr concentration and pH as functions of contact time.

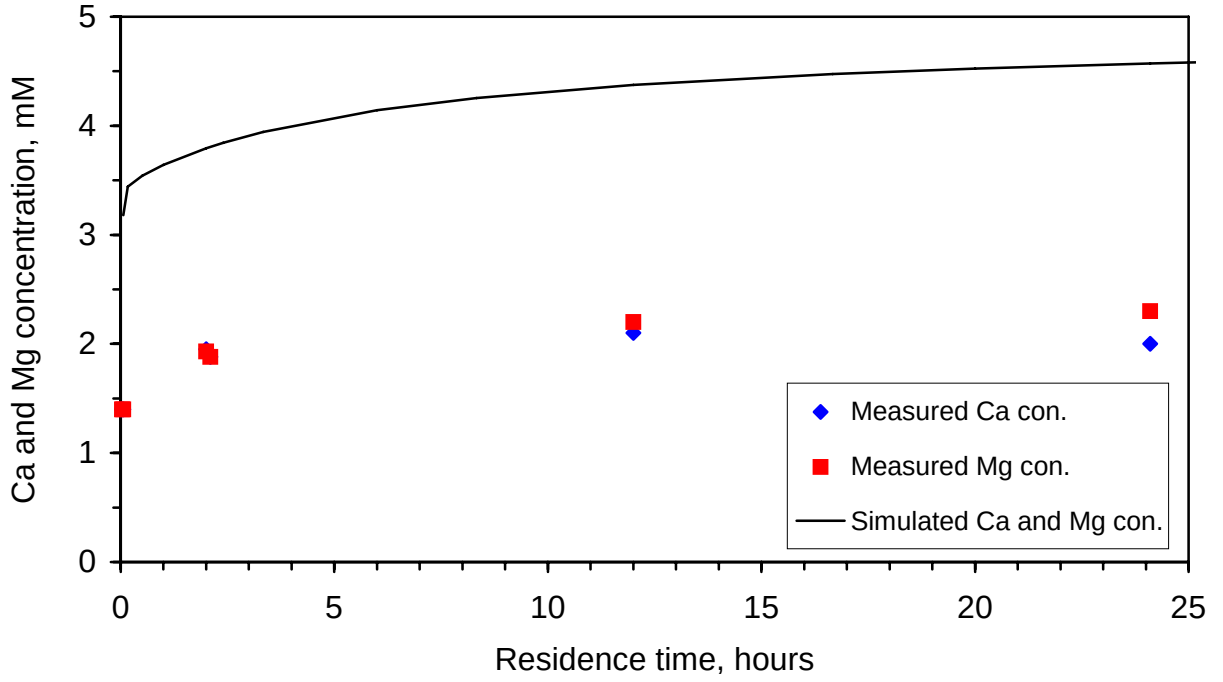

Figure 6.20 - Comparison of the simulated and measured steady-state Ca and Mg concentrations as functions of contact time.

concentrations were achieved during the injection of brine and sodium acetate solutions. The presence of chromium acetate reduces calcium and magnesium concentrations by some mechanism that is not incorporated in the model. One mechanism that was experimental tested is co-precipitation where calcium and magnesium are precipitated with chromium hydroxide. Co-precipitation is defined as the simultaneous precipitation of a normally soluble component with a macro-component from the same solution by the formation of mixed crystals, by adsorption, occlusion, or mechanical entrapment [McNaught and Wilkinson, 1997]. Erdey [1965] stated that chromium(III) hydroxide could be regarded as an amorphous gel. Precipitates of chromium(III) hydroxide in the presence of alkali can adsorb cations, especially magnesium ions.

Bottle tests were conducted to study the co-precipitation of calcium and/or magnesium ions with chromium(III) precipitation. Calcium chloride and/or magnesium chloride solutions were mixed with aqueous chromium(III) acetate solution. The pH of the solution was adjusted to around 9.0 by adding 0.1 N NaOH solution to induce chromium precipitation. The solutions were closed to the atmosphere. After 25 hours, the calcium and magnesium concentrations in the solutions were similar to the initial concentrations, while chromium concentration decreased to about half of the initial concentration for samples Nos. 1, 2 and 3 in Table 6.7. The pH decreased from about 9.05 to 6.55 because the precipitates consumed hydroxide ions. After 142 hours, the calcium and magnesium concentrations in the solutions still did not change significantly from the initial concentrations. Chromium precipitation continued and the chromium concentration in the solution was around 56 ppm for all the samples studied. About 72% of the total amount of chromium was precipitated and the pH of the solutions was about 6.05. The experimental results from bottle tests demonstrated that calcium and magnesium ions did not co-precipitate with chromium hydroxide under these experimental conditions.

Table 6.7 – Results of experiments to test for co-precipitation.

Sample No	Initial condition				Measured value after 25 hours				
	Cr conc. (ppm)	Ca conc. (mM)	Mg conc. (mM)	pH	Contact time (hrs)	Cr conc. (ppm)	Ca conc. (mM)	Mg conc. (mM)	pH
1	200	6.39	-	9.06	25	90	6.14	-	6.55
					142	56	6.19	-	6.04
2	200	-	5.51	9.07	25	94	-	5.21	6.54
					142	58	-	5.43	6.05
3	200	5.63	5.13	9.04	25	98	5.40	5.14	6.54
					142	58	5.46	5.13	6.01
4	200	2.21	1.78	9.05	142	56	2.20	1.78	6.06

Chromium(III) acetate solution at a concentration of 100 ppm chromium was injected in Run C7-Flow0.033-1 at a residence time of 2.0 hours to test the effect of initial chromium concentration on the transport of chromium through virgin dolomite cores. Measured and simulated values of the effluent concentrations are shown in Figures 6.21 and 6.22. Similar trends were observed except that the normalized chromium concentration at 5 PVI was lower and the pH was higher than the steady-state values measured during the injection of the 200 ppm chromium solution at

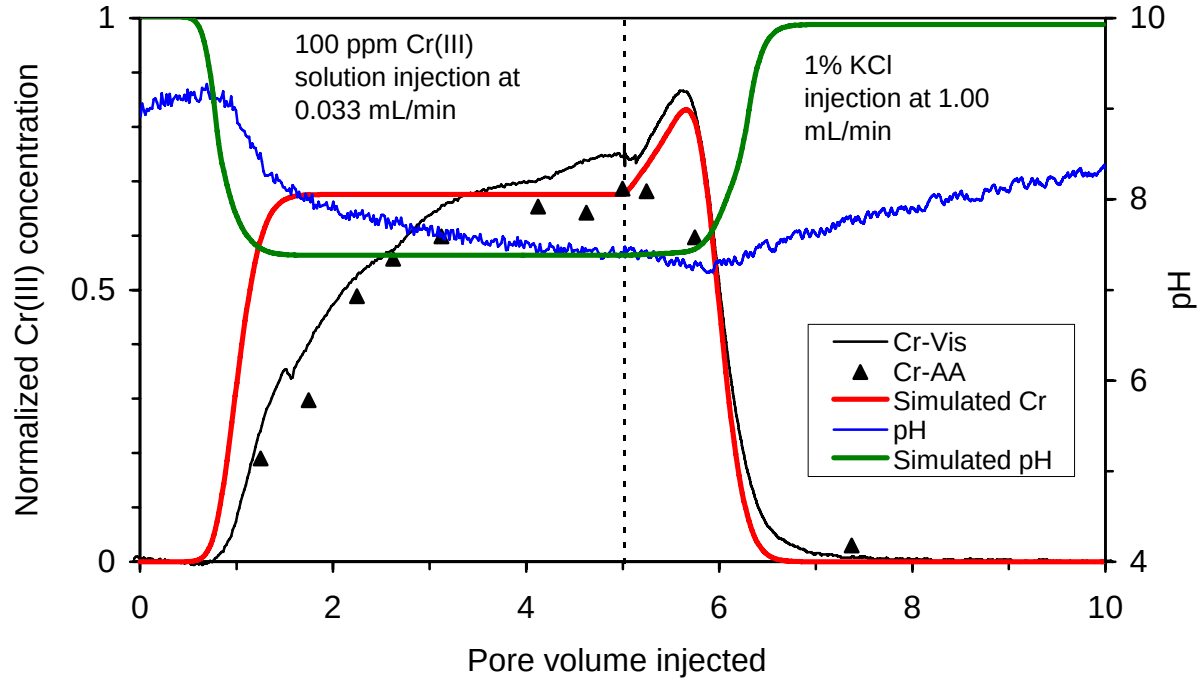

Figure 6.21 - Comparison of the effluent chromium concentration and pH for C7-Flow0.033-1 and the following brine postflood between experimental data and simulated results.

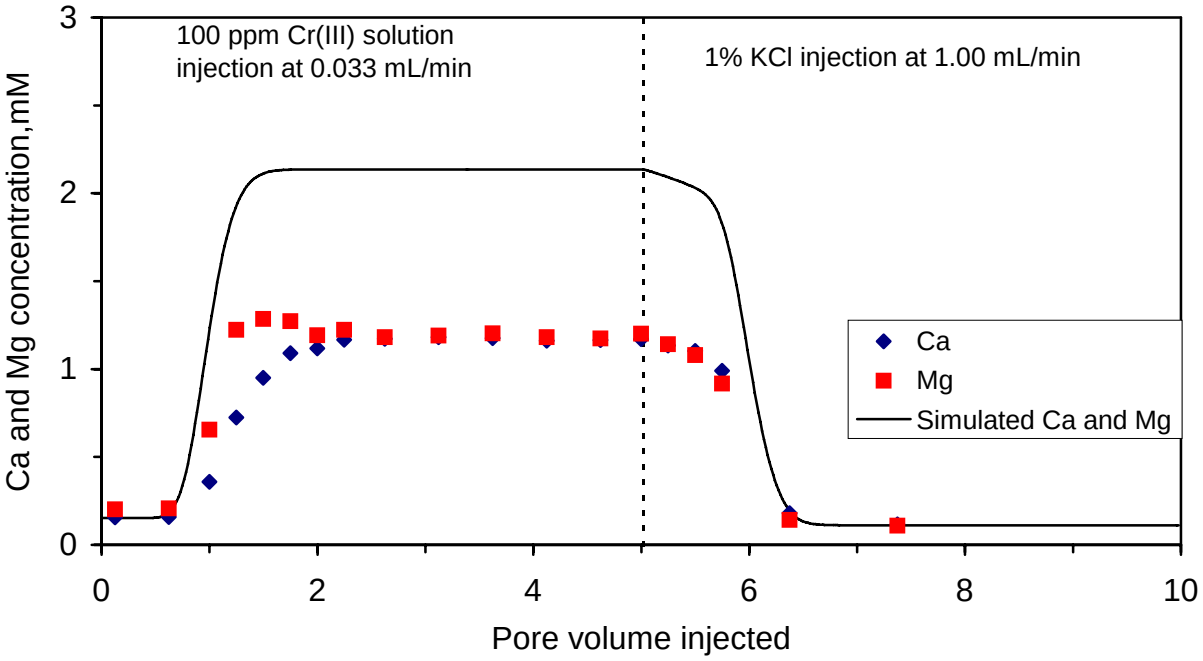

Figure 6.22 - Comparison of the effluent Ca and Mg concentrations for C7-Flow0.033-1 and the following brine postflood between experimental data and simulated results.

the same residence time. Lower concentration of chromium acetate resulted in less buffering capacity of the fluid which caused the pH to increase and a higher chromium precipitation rate. Simulations matched the steady-state chromium concentration and the steady-state pH values using the fitting parameters for dolomite dissolution and chromium precipitation that were established for the brine transport and the injection of 200 ppm chromium solutions.

Shut–in experiments. Shut-in experiments were designed to collect data on the retention of chromium(III) in an easy manner, particularly for long residence times when using small cores. The premise was that the chromium remaining in the solution after being in contact with the rock for a selected shut-in time would be equal to the chromium concentration in the effluent from a flow experiment that was conducted at a residence time equal to the shut-in time. Four shut-in runs were conducted at residence times of two hours. Several pore volumes of chromium acetate solution were injected at high flow rates to saturate the core. 1% KCl brine solution was used to displace the chromium acetate solution from the cores after the shut-in period. Measurements of effluent concentrations at 0.5 PVI of brine injection were considered to be representative of the resident fluid inside the cores at the end of the shut-in period.

Two shut-in runs, C3-Shutin2-2 and C4-Shutin2-2, were conducted in virgin cores and two runs, B-Shutin 2-1 and B-Shutin 2-2, were conducted in Core B that had been previously contacted by chromium acetate solutions. Parameters and results from the four shut-in runs and from two flow experiments conducted in virgin cores with residence times of two hours are listed in Table 6.8. The results from Cores C3 and C4 were in good agreement but some additional chromium was retained during the shut-in experiments as compared to the flow experiments. Also, more chromium was retained in the shut-in experiments in Core B than in Cores C3 and C4, possibly due to the greater volume of chromium solution that was injected through Core B prior to the run. The molar ratio of magnesium to calcium during shut-in experiments was greater than one, similar to flow experiments conducted at low flow rates.

Table 6.8 - Parameters and results of shut-in and flow experiments; chromium(III) acetate solution (200 ppm Cr, 1% KCl).

Run	Residence or shut-in time (hrs)	Volume of chromium acetate injected prior to exp (PV)	Norm. Cr conc.	Mg conc. (mM)	Ca conc. (mM)	Mg/Ca molar ratio	pH
C3-Shutin2-2	2.0	6.9	0.74	2.2	1.9	1.16	6.6
C4-Shutin2-2	2.0	5.0	0.74	2.2	1.8	1.22	6.6
B-Shutin2-1	2.0	15.8	0.67	2.4	-	-	6.9
B-Shutin 2-2	2.0	25.9	0.64	2.5	-	-	6.8
C1-Flow0.032-1	2.1	0	0.85	1.88	1.88	1.00	7.0
C2-Flow0.032-1	2.0	0	0.88	1.93	1.95	0.99	6.9

Transport of chromium(III) acetate in a used core. It was determined in previous work[Jin, 2001] that the injection of several hundred pore-volumes of brine was required before the

effluent pH would attain a value of about 9.8 after a chromium acetate solution was flowed through a dolomite core. A pH value of 9.8 is the "equilibrium" value that a 1% KCl brine (initial pH between 5 and 9) attains when in contact with dolomite rock [Zou et al., 2000a]. It was hypothesized that the core was restored to its initial condition when the "equilibrium" pH value was re-established. To test the restoration procedure, five primary flow experiments using chromium(III) acetate solutions (200 ppm chromium, 1.0% KCl) were conducted in the Core B at a flow rate of 0.032 mL/min. These experiments are listed as B-Flow0.032-(1, 2, 3, 4 or 5) in Table 6.4 No chromium was injected prior to Run B-Flow0.032-1. Prior to Runs 2, 3 and 4, many pore volumes of brine (70 to 380 pore volumes) were injected through the core to restore the effluent pH to approximately 9.5, the equilibrium value for the injection of brine with a neutral pH. Only 6 pore volumes of brine were injected prior to the Run 5 and the effluent pH attained a value of about 9.

Figure 6.23 presents the effluent chromium concentration as a function of volume of solution injected for the five primary flow experiments in Core B. Run B-Flow0.032-1 represents data from a virgin core. The chromium concentration increased just before one pore volume injected and then approached a steady-state normalized concentration of about 0.91. The amount of chromium retained increased with successive Runs 2, 3 and 4 as indicated by the delayed chromium front and the lower concentration values that was approached. Effluent analyses were not conducted during the brine post flushes so that the amount of chromium remaining in the core was not determined. The higher values of chromium retention with successive runs corresponded to higher effluent pH values as shown in Figure 6.24. These results showed that the history of the core plug significantly affected the retention behavior of chromium(III) and that the re-establishment of the effluent pH to about 9.5 did not correspond to the restoration of the core to a common initial condition. The data suggest that chromium remained in the pack after the brine post flush and affected the subsequent run. Also, the amount of chromium retained increased in each successive run. Additional chromium was injected in shut-in experiments conducted before Runs B-Flow0.032-3 and B-Flow0.032-4.

Run B-Flow0.032-5 was conducted after a brine pre-flush in which only six pore volumes of 1.0% KCl brine were injected and the effluent pH value was about 9. The pH dropped to about 7.3 at the start of Run B-Flow0.032-5 apparently due to the core being shut-in for a period of time between the runs. Less chromium was retained during the transition period (1 to 3 pore volumes injected) in Run 5 than in Runs 3 and 4 apparently due to the lower pH values experience by the injected solution. Thereafter, the chromium concentration appears to approach a steady-state value at approximately the same value as in Runs 3 and 4.

Bottle tests for chromium(III) precipitation in solutions with ground dolomite:
Chromium(III) precipitation in solutions with ground dolomite was studied. Results of the experiments are presented in Figures 6.25 and 6.26 for the reaction of chromium(III) acetate solutions (200 ppm Cr(III), 1% KCl) with ground dolomite. The weight ratio of solution to dolomite is around 11.5 except one ratio of 5.5 (contact time of 262 hrs). At 24 hours contact time, the measured pH was 6.4 and increased slowly to 6.8 at 450 hours. The chromium precipitation was much slower than the results from the flow experiments. This can be explained by the contact surface of dolomite with solutions. The weight ratio of dolomite to solution was much less in the bottle test than that in the flow experiments, in addition that the solutions and

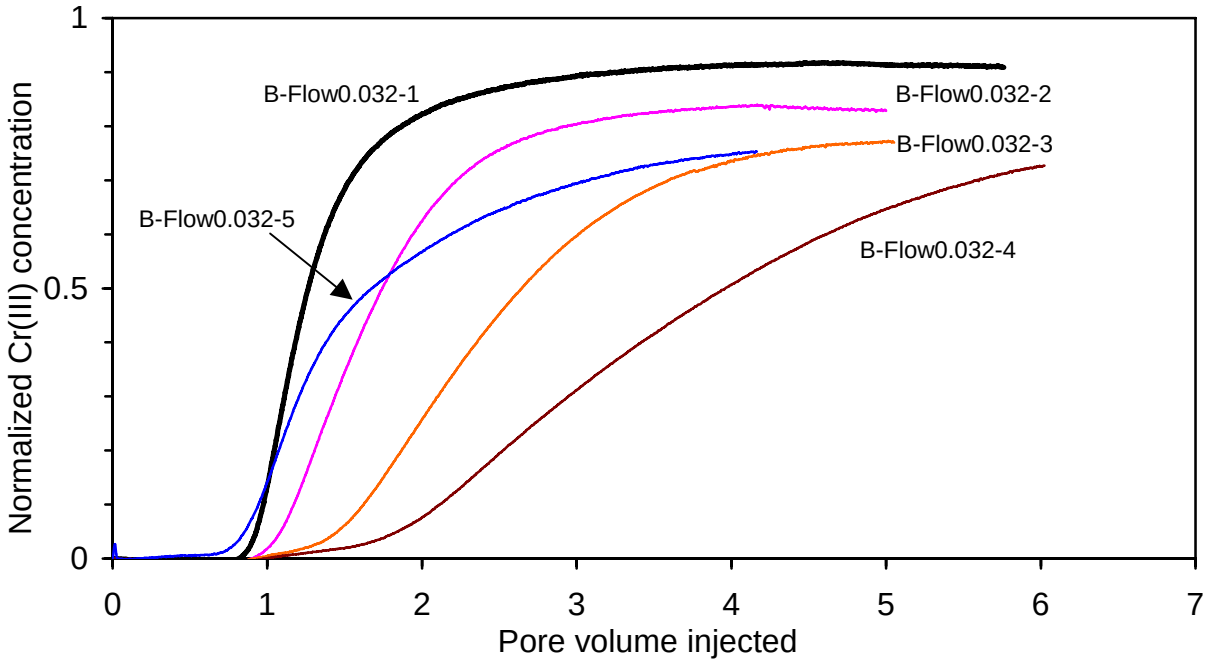

Figure 6.23 - The effluent chromium concentration when 200 ppm chromium solution (acetate ion) was injected through dolomite Core B at 0.032 mL/min.

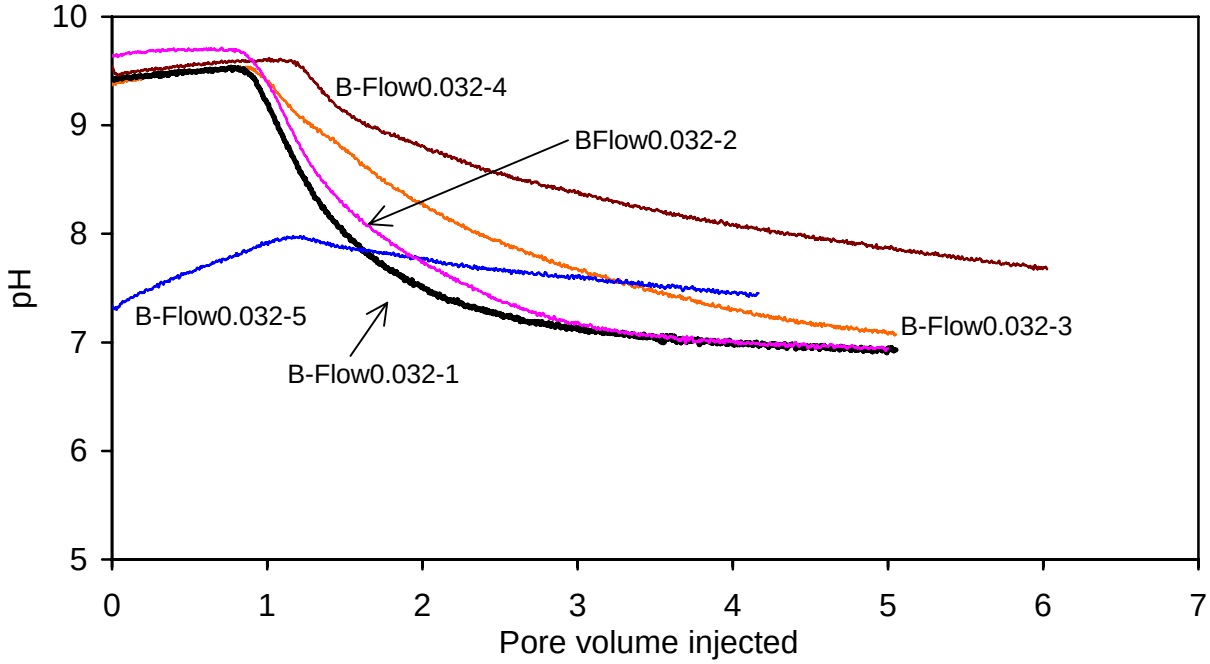

Figure 6.24 - The effluent pH when chromium acetate solutions (200 ppm chromium(III)) was injected through dolomite Core B at 0.032 mL/min.

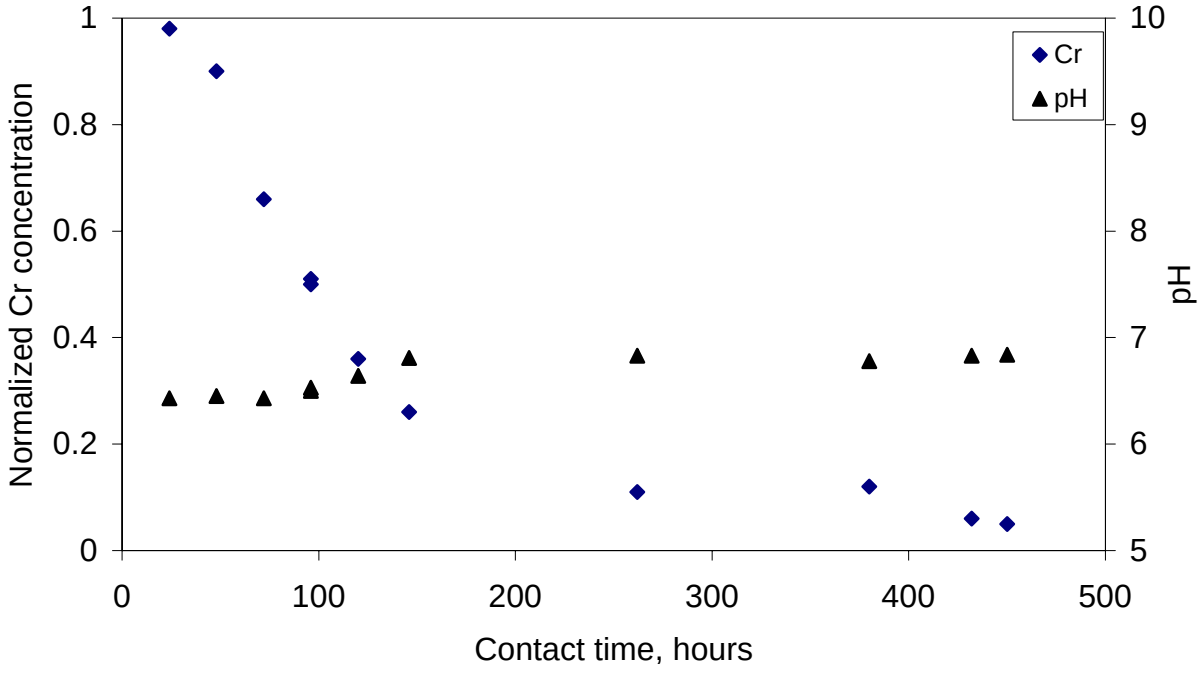

Figure 6.25 - The measured pH and chromium concentration for the reaction of 200 ppm chromium(III) (acetate salt) solution with ground dolomite.

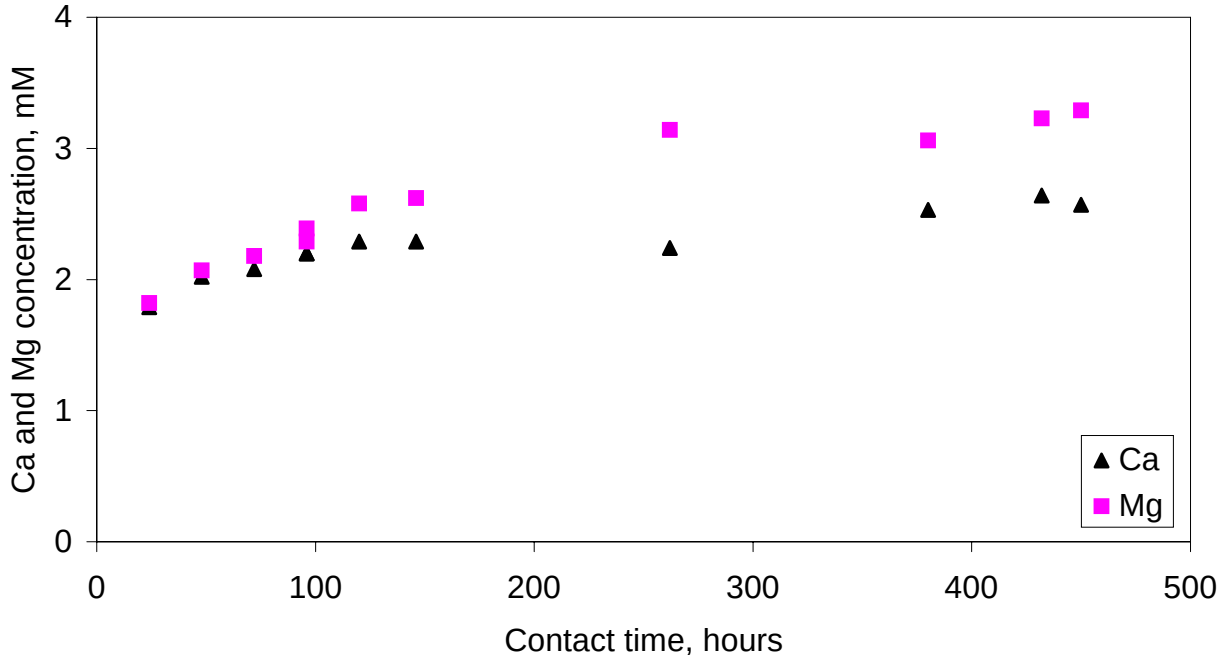

Figure 6.26 - The measured Ca and Mg concentrations for the reaction of 200 ppm chromium(III) (acetate salt) solution with ground dolomite.

ground dolomite were not well mixed. The surface area of dolomite in contact with the solutions was much less in the bottle tests, and thus the dolomite dissolution rate was much lower than that in the flow experiments. The lower dolomite dissolution rate accounted for lower pH, thus lower chromium precipitation rate. At 450 hours contact time, the chromium concentration was about 10 ppm. Calcium and magnesium concentrations were 2.6 and 3.3 mM. The Mg/Ca molar ratio was about 1.26, which was similar to that in the shut-in experiments and the flow experiments conducted at low flow rates.

Results of the experiments are presented in Table 6.9 for chromium(III) precipitation in solutions of different initial chromium concentration with ground dolomite. It showed that when most chromium in the solution was precipitated, the final pH was decreased and the concentrations of calcium and magnesium ions increased with increasing initial chromium concentration, which can be attributed to the consumption of hydroxide ions with the precipitation of chromium(III). The amount of hydroxide ions consumed increased with the increasing amount of chromium precipitated, thus decreased the pH of the solution and increased the amount of dolomite dissolved.

Table 6.9 - Results of bottle tests for chromium(III) precipitation in solutions of different initial chromium concentration with ground dolomite.

Initial Cr conc. (ppm)	Contact time (hrs)	Normalized Cr conc.	Measured pH	Mg conc. (mM)	Ca conc. (mM)	Mg/Ca ratio
50	432	0.01	7.50	1.02	0.89	1.15
100	432	0.04	7.24	1.86	1.62	1.15
147	262	0.09	7.03	2.44	2.13	1.15
200	432	0.06	6.83	3.23	2.64	1.22

The weight ratio of solution to rock is around 11.5.

Transport of brine and chromium(III) acetate solutions through San Andres dolomite cores. McCool et al. [2000] studied the transport of brine and chromium(III) acetate solutions through San Andres dolomite cores under different conditions of solution pH, injection rate, and ionic concentrations. Effluent samples during brine floods contained higher concentrations of calcium than magnesium. A mineralogy study showed that San Andres dolomite contained anhydrite ranging from 0.5-5% [Anderson, 1991]. Carbonate dissolution was modeled with both the dolomite dissolution equation (Eq.6.7 using $y_{dolomite} = 0.95$) and the anhydrite dissolution equation (Eq. 6.9). Supersaturation of calcite was not allowed. Chromium precipitation was modeled by Eq. 6.10. Core plugs of the San Andres dolomite were 5.08 cm in diameter and had porosity ranging from 0.13 to 0.18, and permeability between 3.6 and 10.4 md. An average specific surface area of 3677 cm^{-1} was used in the model.

3.0% KCl brine, two brine solutions #1 and #2 containing common ions, and two chromium acetate solutions were injected through San Andres dolomite cores. Experimental parameters, effluent measurements and simulation results for the runs are listed in Table 6.10. A few pore volumes of injection were required before chromium concentrations and effluent pH values stabilized due to transient behavior and heterogeneity of flow properties. Ranges of calcium and

Table 6.10 - Simulated and experimental results for the injection of brine and chromium(III) acetate solution through San Andres dolomite cores.

Injected solution and residence time	Effluent solution	
	Experimental data	Simulation results
3.0 % KCl pH = 6.9 residence time = 23 mins	pH = 9.5 Ca Conc. = 3.88-1.55 mM Mg Conc. = 0.20-0.10 mM	pH = 9.51 Ca Conc. = 4.14 mM Mg Conc. = 0.29 mM
Brine #1 pH = 7.1 ion conc. (ppm) Na^+ 20,700 Ca^{2+} 2,900 Mg^{2+} 250 Chloride salts residence time = 23 mins	pH = 7.8	pH = 8.75
Brine #2 pH = 5.0 ion conc. (ppm) Na^+ 20,700 Ca^{2+} 3,630 Mg^{2+} 313 Chloride salts residence time = 23 mins	pH = 7.6	pH = 8.52
3.0 % KCl, 50 ppm Cr pH = 7.0 residence time = 138.5 mins	pH = 7.9 Normalized Cr Conc. = 0.40	pH = 8.0 Normalized Cr Conc. = 0.39
3.0 % KCl, 215 ppm Cr pH = 4.4 residence time = 120 mins	pH = 6.8 Normalized Cr Conc. = 0.79	pH = 6.8 Normalized Cr Conc. = 0.79

magnesium were measured in the effluent during brine injection. Data for calcium and magnesium concentrations during injection of chromium acetate solution were not available.

Fitting parameters established for dolomite dissolution and chromium precipitation in Baker dolomite were used in the simulations for San Andres cores. Only one fitting parameter, k_8 in the anhydrite dissolution equation, was adjusted to match the effluent pH and calcium and magnesium concentrations during the injection of the 3.0% KCl brine. Addition of the anhydrite dissolution equation provided a higher concentration of calcium than magnesium and a reasonable match. For the injection of brine #1 and brine #2, the effluent pH values are higher than the experimental data. The common ion effect on dolomite dissolution needs further investigation. Simulations of the two flow experiments with chromium acetate solutions matched well the experimental data using established fitting parameters.

Transport of chromium(III) acetate solutions through Brent sandstone cores. The model was used to simulate flow experiments where chromium(III) acetate solutions were flowed through Brent sandstone cores [Stavland et al., 1993]. Brent sandstone contained 47.4% quartz,

42.7% clay, 6.9% K-Feldspar, and 2.4% carbonate with calcite the dominate form of carbonate in the reservoir cores. The cores used had a porosity of about 0.30, and permeabilities ranging from 60 to 500 md giving an average specific surface area of 1997 cm^{-1}.

Stock chromium acetate solutions were diluted with artificial seawater. For simplification, some components of the seawater were ignored in the simulation, such as 0.021 g/l $SrCl_2.6H_2O$ and 1.00 g/l HCHO. The simulated pH of the artificial seawater was 7.9, which was close to the measured pH of 7.8.

Two types of experiments, continuous flow and shut-in, were conducted by Stavland et al. [1993]. In the continuous-flow experiments, solutions containing 400 ppm chromium(III) (acetate salt) in artificial seawater were injected through the Brent sandstone cores. Experiments were conducted at flow rate of 0.2 mL/min, corresponding to a residence time in the core of 5 hours. After the effluent chromium concentration reached steady state, the effluent was injected through a second core of the same length. Effluent from the second core represented samples at a residence time of 10 hours. Steady-state values of chromium concentration and pH in the effluent (after more than 10 pore volumes injection) were used for comparison with the results of the model. In the shut-in experiments, several pore volumes of a solution containing 400 ppm chromium(III) (acetate salt) in artificial seawater were injected quickly through the cores and the cores were then shut in for a selected time period. This was followed by an injection of the artificial seawater to displace the resident chromium acetate solution from the core. Measured values of chromium concentration and pH in the effluent that represented values in the core after different contact times were compared to the results of the model.

It was shown in our experiments with Baker dolomite that steady-state chromium concentrations in the effluent during shut-in experiments were reduced by small amounts as compared to flow experiments in virgin cores, particularly at the lower residence times. Stavland et al. did not provide sufficient history of their cores to allow this comparison. Notwithstanding, it was assumed the discrepancy did not occur in Brent Sandstone and the data were simulated with the model.

Simulations were compared to the steady-state behavior because the transient behavior of the effluent pH and chromium concentrations were affected by adsorption of cations by clays [Stavland et al., 1993] and adsorption was not considered in the model. The effluent measurements approached steady-state values after adsorption reached maximum capacity. Carbonate dissolution was modeled with only the calcite rate equation (Eq. 6.8) with $y_{calcite}$ value of 0.024. Fitting parameters in calcite dissolution equation were adjusted to match the effluent steady-state pH values. Fitting constants for chromium precipitation that were established for the flow experiments in Baker dolomite were used.

Steady-state chromium concentration and pH from the two types of experiments and from the simulations are shown in Figure 6.27 as a function of residence time. Simulated steady state effluent pH values were about 5.7, consistent with the experimental data. Simulated chromium concentrations in the effluent were higher than the data for short residence times but matched the data at longer residence times.

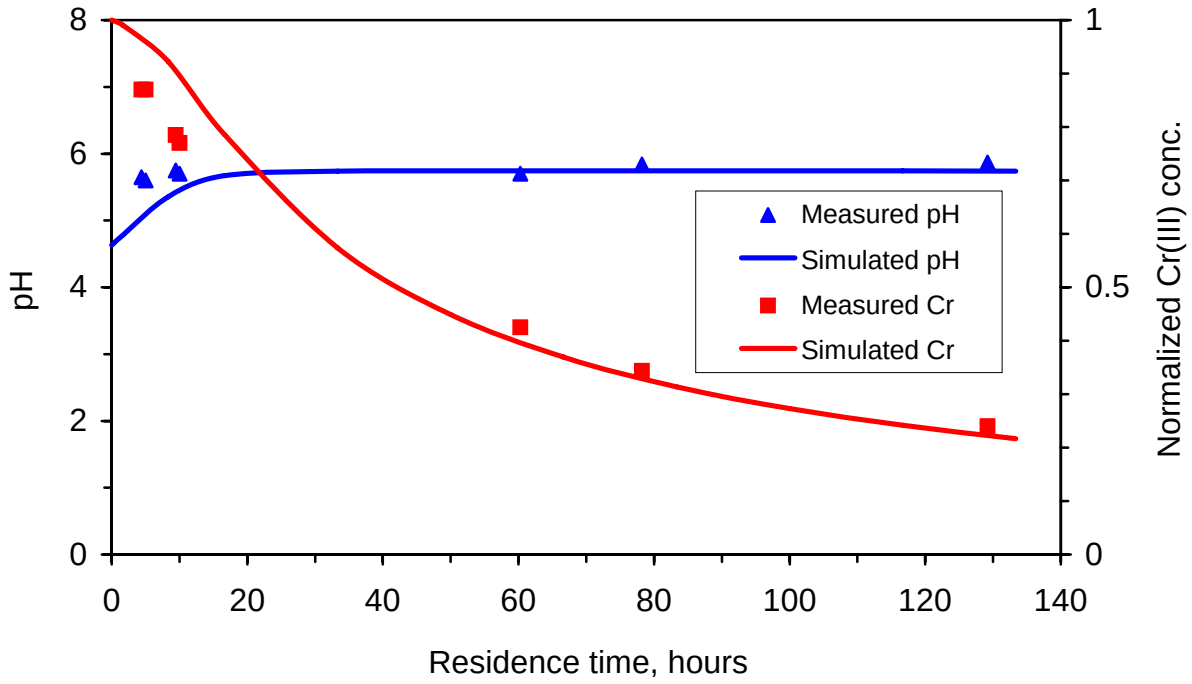

Figure 6.27 - Comparison of simulated and measured steady-state pH and chromium concentration as functions of contact time. Injected solution is 400 ppm chromium (acetate salt) in artificial seawater.

Conclusions

The conclusions are based on and are applicable to the experimental data and simulations of the transport of chromium acetate solutions through Baker dolomite and samples of San Andres dolomite and Brent sandstone.

1. Transport of chromium through three types of carbonate-containing rocks was characterized by one equation that describes a kinetic precipitation process that retained chromium in the rocks.
2. The mathematical model simulates the steady-state values of the measured chromium concentrations in the effluent for various experimental conditions. Measured and simulated chromium precipitation increased with increasing pH, increased residence time in the core and a decrease in the injected chromium acetate concentration. Matches between experimental and simulated effluent chromium concentrations were less satisfactory during the transient period when the injected solution front exits the cores.
3. Repeatable data were obtained in flow experiments in virgin Baker dolomite cores. Results from flow experiments in cores that were previously contacted with chromium acetate solutions exhibited greater chromium retention than in the flow experiments in virgin cores.
4. Results from shut-in experiments approximated the flow experiments at the same residence times.
5. The presence of chromium in fluids injected into Baker dolomite cores significantly reduced the dissolution of calcium and magnesium as compared to similar injected fluids

that contained no chromium. The mathematical model did not simulate dolomite dissolution when in contact with chromium acetate solutions well.

6. Magnesium and calcium were not removed from the Baker dolomite cores during transient periods in a mole ratio consistent with the stoichiometry of dolomite dissolution.

Nomenclature

Ac_t	-	Total acetate ions concentration in the solution, mol/L
C_i	-	Concentration of ith species in the fluid phase, moles/liter-PV
C_0	-	Kozeny constant
Cr_{eq}	-	Equilibrium chromium(III) concentration hydrolysis, mol/L
Cr_t	-	Total chromium concentration in the solution, mol/L
I	-	Ionic strength
IAP	-	Ion activity product
K	-	Permeability, cm^2
k_0	-	Rate constant in the rate equation of chromium precipitation, $(minM^{\alpha+\gamma+\beta-1})^{-1}$
K_d	-	Dispersion coefficient, cm^2/s
K_{sp}	-	Solubility product for the mineral
S_0	-	Specific surface area, cm^2/cm^3
r_i	-	Surface reaction rate of the mineral, $mol/cm^2.s$.
$R_i(C)$	-	Rate of reaction per unit volume, moles/liter-PV/s
t	-	Time, s
t_D	-	Dimensionless time, $tv/\phi L$
v	-	Superficial velocity of the injected fluid, cm/s
x	-	Length, cm
x_D	-	Dimensionless length, x/L
y_i	-	Weight fraction of the mineral in the rock.
α	-	Exponent of chromium concentration in the rate equation of chromium precipitation
β	-	Exponent of OH^- concentration in the rate equation of chromium precipitation
γ	-	Exponent of acetate ion concentration in the rate equation of chromium precipitation
ϕ	-	Porosity, fraction

References

Anderson, M.S.: "Reactivity of San Andres dolomite," *SPE Production Engineering*, **6** No. 2 (1991) 227-237.

Araque-Martinez, A. and Lake L.W.: "A simplified approach to geochemical modeling and its effect on mineral precipitation," *SPE Journal*, **6**, No.1 (2001) 98-107.

Bartosek, M., Mennella, A., and Lockhart, T. P.: "Polymer gels for conformance treatments: propagation of Cr(III) crosslinking complexes in porous media," paper SPE 27828, SPE/DOE Ninth Symposium on Improved Oil Recovery, Tulsa, OK (17-20 April 1994).

Benjamin, M.M.: "Water chemistry," McGraw-Hill, New York (2002).

Bhuyan, D.: "Development of an alkaline/surfactant/polymer compositional reservoir simulator," PhD dissertation, University of Texas, Austin, TX (1989).

Carman, P.C.: "Fluid flow through granular beds," *Transactions of the Institution of Chemical Engineers*, **15** (1937) 150-166.

Chou, L., Garrels, R.M., and Wollast, R.: "Comparative study of the kinetics and mechanisms of dissolution of carbonate minerals," C*hemical Geology*, **78** (1989) 269-282.

Erdey, L.: "Gravimetric analysis, Part II," Pergamon Press LTD. (1965).

Jin, H.: "Transport of chromium(III) acetate through dolomite rock," MS thesis, University of Kansas (2001).

Jin, H., McCool, C.S., Green, D.W., Willhite, G.P. and Michnick, M.J.: "Propagation of chromium(III) acetate solutions through dolomite rock," paper SPE 75159, SPE/DOE Thirteenth Symposium on Improved Oil Recovery, Tulsa, OK, (13-17 April 2002).

McCool, C.S., Green, D.W., and Willhite, G.P.: "Fluid/rock interactions between xanthan/chromium(III) gel systems and dolomite core materials," *SPE Production&Facilities*, **15**, No. 3 (2000).

McNaught, A.D. and Wilkinson, A.: "International union of pure and applied chemistry - compendium of chemical terminology," 2nd edition, Blackwell Science (1997).

Meister, J.J.: "A porous permeable carbonate for use in oil recovery experiments," *Journal of Petroleum Technology*, **30**, No. 11 (1978) 1632-1634.

Midha, V.: "Mathematical modeling of fluid-rock interactions during the flow of alkaline solutions through porous media," MS thesis, The University of Kansas, Lawrence, KS (1994).

Nghiem, L., Sammon, P., Grabenstetter, J., and Ohkuma, H.: "Modelling CO_2 storage in aquifers with a fully-coupled geochemical EOS compositional simulator," paper SPE 89474, SPE/DOE Fourteenth Symposium on Improved Oil Recovery, Tulsa, OK (17-21 April 2004).

Ommen, H.C.V.: "The 'mixing-cell' concept applied to transport of non-reactive and reactive components in soils and groundwater," *Journal of Hydrology*, **78**, (1985) 201-213.

Parkhurst, D.L., and Appelo, C.A.J.: "PHREEQC (version 2)-A hydrogeochemical transport model," http://wwwbrr.cr.usgs.gov/projects/GWC_coupled/phreeqc/ (2005).

Perkins, T.K. and Johnston, O.C.: "A review of diffusion and dispersion in porous media," *SPE, Trans., AIME*, **228** (1963) 70-81.

Rai, D., Sass, B.M., and Moore, D.A.: "Chromium(III) hydrolysis constants and solubility of chromium(III) hydroxide," *Inorganic Chemistry*, **26** (1987) 345-349.

Seright, R.S.: "Impact of permeability and lithology on gel performance," paper SPE 24190, Eighth Symposium on Enhanced Oil Recovery, Tulsa, OK (22-24 April 1992).

Sherman, L.A., and Barak, P.: "Solubility and dissolution kinetics of dolomite in Ca-Mg-HCO_3/CO_3 solutions at 25 ^oC and 0.1 MPa carbonate dioxide," *Soil Science Society of America Journal*, **64** (2000) 1959-1968.

Sillen, L.G. and Martell, A.E.: "Stability constants of metal-ion complexes," London, the Chemical Society, Burlington House (1964).

Stavland, A., Kvanvik, B.A. and Lohne, A.: "Evaluation of Xanthan-Cr(III) gels for deep emplacement: Retention of Cr(III) in North Sea sandstone reservoirs," Seventh European Symposium on Improved Oil Recovery, Moscow, Russia (27-29 Oct. 1993).

Walsh, M.P.: "Geochemical flow modeling," PhD dissertation, University of Texas, Austin, TX (1983).

Wang, G.T. and Chen, S.: "A new model describing convective-dispersive phenomena derived by using the mixing-cell concept," *Applied Mathematical Modelling*, **20** (April 1996) 309-320.

Zou, B., McCool, C.S., Green, D.W., and Willhite, G.P.: "A study of the chemical interactions between brine solutions and dolomite," *Reservoir Evaluation and Engineering,* **3**, No. 3, (200a) 209-215.

Zou, B., McCool, C.S., Green, D.W., Willhite, G.P and Michnick, M.J.: "Precipitation of chromium acetate solutions," *SPE Journal*, **5**, No. 3, (2000b) 324-330**.**

Appendix

A listing of the Fortran code of the program FLUIDROCKINTERACTION and an example of an input data set are presented.

Fortran code of program FLUIDROCKINTERACTION for the simulation of the transport of brine and chromium(III) acetate through carbonate rocks

```
Program fluidrockinteraction
C=======================================================================
C
C    A STUDY OF FLUID-ROCK INTERACTION.
C    08/29/2005

C    Feiyan Chen
C    Department of Chemical and Petroleum Engineering
C    University of Kansas
C    Lawrence, KS 66045
C
C=======================================================================
     IMPLICIT DOUBLE PRECISION (A-H,O-Z)
```

```
      PARAMETER (NEQ=10,NEQ1=24,NEQ2=NEQ-1,NNJ=1001)

C=======================================================================

C          PARAMETERS FOR DIMENSIONING OF THE VALUES USED IN THE PROGRAM.

C          NEQ: NO OF MATREIAL COMPONENTS PLUS HYDROGEN.
C          NEQ1: NO OF ALL CHEMICAL SPECIES.
C          NEQ2: NO OF MATERIAL COMPONENTS EXCEPT H2O, SINCE H2O IS CONSTANT C      IN THIS
PROGRAM.
C
      REAL*8 A(NEQ,NEQ),AA(NEQ,NEQ1),AR(NEQ2,NEQ1),AC(NEQ1,NNJ),
     & B(NEQ1,NEQ),C(NEQ1,NNJ),CLOG(NEQ),
     & F(NEQ),GAMMA(NEQ1),IFLAG(2),TOT(NEQ),
     & TOT1(NEQ,NNJ),TOT10(NEQ,NNJ),XK(NEQ1),IMINERAL(3)
      Integer z(NEQ1)
          LOGICAL FLAG

      REAL*8 RDOL(NNJ),RANH(NNJ),RCAL(NNJ),
     &     RCR(NNJ),RCA(NNJ),RMG(NNJ),RCO3(NNJ),RSO4(NNJ)
C

      COMMON/M1/ N,NJ
      COMMON/M2/ CONV,CONV2,ZERO,XLN
      COMMON/M3/ XK,Z,AR,B
      COMMON/M4/ C,AC
          COMMON/M5/ TOT1,H2O
          COMMON/M6/ FLAG
          COMMON/M7/ DOLKSP,CALKSP,ANHKSP

C-----------------------------------------------------------------------
C          NOTATION USED IN THE WHOLE PROGRAMS.
C-----------------------------------------------------------------------

C          A(I,M):  ELEMENTS OF JOCABI MATRIX.
C          AA(I,M): COEFFICIENT OF FLUID AFTER ALGEBRAIC MANIPULATION OF THE C
           MASS BALANCE AND CHARGE BALANCE.
C          AR(I,M): STOICCHIOMETRIC COEFFICIENT OF ELEMENT I IN FLUID SPECIES M.
C          AC(I,J): ACTIVITY OF CHEMCIAL SPECIES I AT NODE POINT J.
C          B(I,M);  EXPONENT OF THE INDENPENDT FLUID SPECIES CONCENTRATION
C                     WHEN FLUID SPECIES I IS EXPRESSED IN Ms.
C          C(I,J):  CONCENTRATION OF ALL CHEMCIAL SPECIES AT NODE POINT J.
C          CLOG(I): LOG10(C(I)).
C          DELX(I): X(N+1)-X(N) FROM LU DECOMPOSITION TO CALCULATE SETS OF C
           LINEAR EQUATION.
C          F(I):    RIGHT HAND SIDE OF VECTORS (RESIDUAL).
C          GAMMA(I): ACTIVITY COEFFICIENT.
C          IFLAG(I): OPTION FLAGS:(0,1).
C          RDOL(J):  DOLOMITE DISSOLUTION RATES.
C          RCR(J):   CHROMIUM PRECIPITATION RATES.
C          TOT(I):  THE TOTAL CONCENTRATION OF MATERIAL COMPONENTS USED IN
C            SUBROUTINE EQUILIBIRUM(PHIN,J) AND DOLDISSEQUIL(PHIN,J) FOR
C                     TEMPERATORY SAVING OF TOT1(I,J).
C          TOT1(I,J): THE TOTAL CONCENTRATION OF MATERIAL COMPONENTS AT NODE C
           POINT J.
C          TOT10(I,J):TEMPORARY SAVING FOR TOT1(I,J).
```

```
C       XK(I):   EQUILIBRIUM CONSTANS.
C       XI(I):   THE IONIC STRENGTH.
C       Z(I):    THE CHARGE OF THE AQUEOUS SPECIES I.

C       AQUEOUS PHASE SPECIES

C        1: Ca2+                                                    K=1
C        2: Mg2+                                                    K=1
C        3: CO3,2-                                                  K=1
C        4: H+                                                      K=1
C        5: K+                                                      K=1
C        6: Cl-                                                     K=1
C        7: Cr3+                                                    K=1
C        8: Ac-                                                     K=1
C        9: SO4,2-                                                  K=1
C        10: H2O                                                    K=1
C        11: OH-          {OH-}=K/{H+}                              K=1.009E-14
C        12: CaOH+        {CaOH+}=K{Ca2+}/{H+}                      K=1.205E-13
C        13: MgOH+        {MgOH+}=K{Mg2+}/{H+}                      K=3.887E-12
C        14: CaCO3,0      {CaCO3,0}=K{Ca2+}{CO3,2-}                 K=1.585E+03
C        15: MgCO3,0      {MgCO3,0}=K{Mg2+}{CO3,2-}                 K=8.318E+02
C        16: CaHCO3,+     {CaHCO3,+}=K{Ca2+}{CO3,2-}{H+}            K=3.548E+11
C        17: MgHCO3,+     {MgHCO3,+}=K{Mg2+}{CO3,2-}{H+}            K=5.888E+11
C        18: HCO3,-       {HCO3-}=K{CO3,2-}{H+}                     K=2.138E+10
C        19: H2CO3        {H2CO3}=K{CO3,2-}{H+}^2                   K=3.981E+16
C        20: Cr(OH),2+    {Cr(OH),2+}=K{Cr3+}/{H+}                  K=1.000E-04
C        21: Cr(OH)2,+    {Cr(OH),2+}=K{Cr3+}/{H+}^2                K=2.399E-10
C        22: CrAc(OH)2    {CrAc(OH)2}=K{Cr3+}{Ac-}/{H+}^2           K=6.900E-06
C        23: HAc          {HAc}=K{H+}{Ac-}                          K=5.715E+04
C        24: Cr(OH)3,0    {Cr(OH),2+}=K{Cr3+}/{H+}^3                K=1.778E-17


      OPEN (FILE='INPUT.DAT',UNIT=10,STATUS='OLD')
!     OPEN (FILE='INPUTZOU.DAT',UNIT=20,STATUS='OLD')
!     OPEN (FILE='INPUTHONGTRACER.DAT',UNIT=20,STATUS='OLD')
!     OPEN (FILE='INPUTHONG.DAT',UNIT=20,STATUS='OLD')
!     OPEN (FILE='INPUTCHEN.DAT',UNIT=20,STATUS='OLD')
      OPEN (FILE='INPUTCHEN200ppm.DAT',UNIT=20,STATUS='OLD')
!     OPEN (FILE='INPUTCHEN100ppm.DAT',UNIT=20,STATUS='OLD')
!     OPEN (FILE='INPUTSTANBRINE.DAT',UNIT=20,STATUS='OLD')
!     OPEN (FILE='INPUTSTANBRINE1.DAT',UNIT=20,STATUS='OLD')
!     OPEN (FILE='INPUTSTANBRINE2.DAT',UNIT=20,STATUS='OLD')
!     OPEN (FILE='INPUTSTAN50PPM.DAT',UNIT=20,STATUS='OLD')
!     OPEN (FILE='INPUTSTAN215PPM.DAT',UNIT=20,STATUS='OLD')
!     OPEN (FILE='INPUTSTAVLAND200PPM.DAT',UNIT=20,STATUS='OLD')
!     OPEN (FILE='INPUTSTAVLAND400PPM.DAT',UNIT=20,STATUS='OLD')
!     OPEN (FILE='INPUTCHENtracer.DAT',UNIT=20,STATUS='OLD')
!     OPEN (FILE='INPUTCHENKAC.DAT',UNIT=20,STATUS='OLD')

      OPEN (FILE='EFFLUENT.DAT',UNIT=3,STATUS='UNKNOWN')
      OPEN (FILE='PROFILES.DAT',UNIT=4,STATUS='UNKNOWN')
      OPEN (FILE='SOLUTIONOUTPUT.DAT',UNIT=11,STATUS='UNKNOWN')
C         INPUT.DAT IS FOR MATRIX AR, B, Z AND XK.
C         INPUT???.DAT (for example, INPUTZOU.DAT) IS FOR NJ, TIME, S0,
C                   PHI,DT,THKX,RESIDENCETIME (in mins) AND
C                   INITIAL AND INJECTED SOLUTIONS.
```

```
C       EFFLUENT.DAT IS FOR THE EFFLUENT CONCENTRATIONS AT DIFFERENT TIME. C
        (CA AND MG IN mM).
C       PROFILES.DAT IS FOR THE CONCENTRATIONS ALONG THE CORE AT SELECTED C
        TIME. (CA AND MG IN mM).
C       SOLUTIONOUTPUT.DAT IS FOR ALL THE SPECITES IN THE SOLUTION AT C
        EQUILBRIUM CONDITIONS.

!   OPEN (FILE='OUTPUT.DAT',UNIT=2,STATUS='UNKNOWN')
C
C
C   N:      ACTUAL NUMBER OF UNKNOWNS.
C   NJ:     ACTUAL NUMBER OF NODE POINTS.
C   CONV:   CRITERIAL FOR CONVERGENCE FOR DABS(F(I)).
C   CONV2:  CRITERIAL FOR CONVERGENCE FOR DELX(I)/CLOG(I).

        N=NEQ
        CONV=1.E-10
        CONV2=1.0E-3
        XLN=10.
        XLN=DLOG(XLN)
        ZERO=1.E-30
        H2O=111.11

C       MINERAL SOLUBILITY PRODUCTS.
        DOLKSP=10**(-17.2)   ! DOLOMITE
        CALKSP=10**(-8.31)   ! CALCITE
        ANHKSP=2.45E-5       ! ANHYDRITE



        READ (10,*) ((AR(I,J),J=1,NEQ1),I=1,N-1)
        READ (10,*) ((B(I,J),J=1,N),I=1,NEQ1)
        READ (10,*) (Z(I),I=1,NEQ1)
        READ (10,*) (XK(I),I=1,NEQ1)

C       S0:   SPECIFIC SURFACE AREA.
C       PHI:  POROSITY.
C       TIME: TOTAL PORE VOLUME SIMULATED.
C       DT:   TIME STEP.
C       THKX: LENGTH OF CORE IN CM.
C       DX:   STEP SIZE.
C       V:    FINAL V IS VEOLCITY IN CM/S.
C       RETIME: RESIDENCE TIMEIN MINUTES

        READ (20,*) NJ,TIME,S0,PHI,DT,THKX,RETIME
        READ (20,*) CAINJ,XMGINJ,CO3INJ,XKINJ,CLINJ,CRINJ,ACINJ,SO4INJ,PHINJ
        READ (20,*) CAINI,XMGINI,CO3INI,XKINI,CLINI,CRINI,ACINI,SO4INI,PHINI
        READ (20,*) IFLAG(2)
        READ (20,*) IFLAG(1)
        READ (20,*) IMINERAL(1),IMINERAL(2),IMINERAL(3)
        READ (20,*) CM1SET


!       CLINJ=XKINJ+2.*(CAINJ+XMGINJ)
!       CLINI=XKINI+2.*(CAINI+XMGINI)
!       ACINJ=CRINJ*3.
```

```
!           ACINI=CRINI*3.


      S=S0*(1-PHI)/PHI
      DX= 1./(NJ-1)
      TWODX= 2.*DX
      DXSQ=DX*DX
      V=THKX/(RETIME*60.)
!           dispersion coefficient for tracer test.
            Dis=3.3e-3/(THKX/(2.9*60.))*V
            vxx=Dis*(RETIME*60.)/THKX**2.

!           print *, vxx
C           IF INPUT THE VELOCITY IN ML/MIN, USE THE FOLLOW THREE LINES.
            DIAMETER=1.88  !CORE Cs
!           DIAMETER=3.7   !ZOU'S CORE
!           V=1.02
!           V=V/3.142/(DIAMETER/2.)**2./60/PHI

C           THE PORE VOLUMES SWITCHED FROM CHROMIUM SOLUTION TO BRINE
            SWITCHFLUIDPV=5.94

C----------------------
C     Initializing
C----------------------
            TIME1 = 0.
            M=1
            MM=1
C           TIME1 IS THE CURRENT TIME IN PORE VOLUME.
C           M AND MM IS FOR PRINTING SELECTED TIME FOR OUTPUT.


!             WRITE(*,*)'PLEASE MAKE THE FOLLOWING CHOICE.'
!5            WRITE (*,*)'IF PH OF INITIAL SOLUTION IS KNOWN,INPUT 1,
!     1   OTHERWISE, INPUT 0'
!       WRITE(*,*)

!             IF ((IFLAG(1) .NE. 0) .AND. (IFLAG(1) .NE. 1)) THEN
!              WRITE(*,*)'YOUR INPUT IS INVALID! INPUT 1 or 0 ONLY.'
!              GO TO 5
!       ENDIF
            J=1
            TOT1(1,J)=CAINI
            TOT1(2,J)=XMGINI
            TOT1(3,J)=CO3INI
            TOT1(5,J)=XKINI
            TOT1(6,J)=CLINI
            TOT1(7,J)=CRINI
            TOT1(8,J)=ACINI
            TOT1(9,J)=SO4INI

            CALL EQUILIBRIUM(PHINI,J)
            pH=-DLOG10(AC(4,J))

            IF (IFLAG(1) .EQ. 1) THEN
```

```
          CALL ADJUSTPH(CAINI,XMGINI,CO3INI,XKINI,CLINI,CRINI,ACINI,
     &    SO4INI,PHINI,J)
          PH=PHINI

          ENDIF
          WRITE(*,805) TOT1(1,1),TOT1(7,J),TOT1(8,J)

          print*,'PHINI',pH
          write(11,*) "INITIAL SOLUTION"
          WRITE(11,*) 'pHINI=',pH
          PAUSE
          WRITE(11,806) "CA","MG","CO3","CR","OAC"
          WRITE(11,805) TOT1(1,J),TOT1(2,J),TOT1(3,J),TOT1(7,J),TOT1(8,J)
C-----------------------------------------------------------------
!         write(*,*) clini

          write(11,806) 'Ca2+','Mg2+','CO32-','H+','K+','Cl-','Cr3+','Ac',
     & 'SO4,2-','H2O','OH-','CaOH+','MgOH+','CaCO30','MgCO30','CaHCO3+',
     & 'MgHCO3+','HCO3-','H2CO3',
     & 'Cr(OH)2+','Cr(OH)2,+','CrAc(OH)2','HAc','Cr(OAc)3,0'
          WRITE(11,*) 'CONCENTRATION'

          WRITE(11,807) (C(I,J),I=1,NEQ1)

          WRITE(11,*) 'ACTIVITY'

          WRITE(11,807)(AC(I,J),I=1,NEQ1)

!         WRITE(11,807) (GAMMA(I),I=1,NEQ1)

!         WRITE(11,807) (TOT1(I,J),I=1,NEQ)

C-------------------------------------------------------------------------
C         CALCULATION OF EQUILIBRIUM REACTION OF INITIAL SOLUTION WITH C
          DOLOMITE

          IF (IMINERAL(1) .EQ. 1) THEN
          CALL DOLDISSEQUIL(PHINI,J)
          ENDIF

          IF (IMINERAL(2) .EQ. 1) THEN
          CALL CALDISSEQUIL(PHINI,J)
          ENDIF

          IF (IMINERAL(3) .EQ. 1) THEN
          CALL CASO4DOLDISSEQUIL(PHINI,J)
          ENDIF
 !    STOP
C-------------------------------------------------------------------------
          pH=-DLOG10(AC(4,J))

          WRITE(3,804)'TIME1','pH','CA (mM)','MG (mM)','CR (mM)',
     &         'NorCR','NorK','Tracer analy'
          WRITE(3,805) TIME1,pH,TOT1(1,J)*1.E3,TOT1(2,J)*1.E3,TOT1(7,J),
     &    TOT1(7,J)/CRINJ,TOT1(5,NJ)/XKINJ,TOTk
```

```
!           WRITE(2,804)'TIME1','PH=', 'CaTOT=','Mgtot=','CRTOT=','NorCr='
!           WRITE(2,805) TIME1,pH,TOT1(1,J),TOT1(2,j),TOT1(7,J),TOT1(7,J)/crinj
!           WRITE(2,*)


            DO I=1,NEQ1
            DO J=1,NJ
            C(I,J)=C(I,1)
            AC(I,J)=AC(I,1)
            ENDDO
            ENDDO

            DO I=1,NEQ2
            DO J=1,NJ
            TOT1(I,J)=TOT1(I,1)
            ENDDO
            ENDDO



!             WRITE(*,*)'PLEASE MAKE THE FOLLOWING CHOICE.'
!15          write (*,*)'IF PH OF INJECTED SOLUTION IS KNOWN,INPUT 1,
!    1   OTHERWISE, INPUT 0'
!       WRITE(*,*)
!             IF ((IFLAG(2) .NE. 0) .AND. (IFLAG(2) .NE. 1)) THEN
!              WRITE(*,*)'YOUR INPUT IS INVALID! INPUT 1 or 0 ONLY.'
!              GO TO 15
!      ENDIF
            J=1
            TOT1(1,J)=CAINJ
            TOT1(2,J)=XMGINJ
            TOT1(3,J)=CO3INJ
            TOT1(5,J)=XKINJ
            TOT1(6,J)=CLINJ
            TOT1(7,J)=CRINJ
            TOT1(8,J)=ACINJ
            TOT1(9,J)=SO4INJ
            CALL EQUILIBRIUM(PHINJ,J)
            pH=-DLOG10(AC(4,J))

            IF (IFLAG(2) .EQ. 1) THEN
            CALL ADJUSTPH(CAINJ,XMGINJ,CO3INJ,XKINJ,CLINJ,CRINJ,ACINJ,
     &      SO4INJ,PHINJ,J)
            PH=PHINJ

            ENDIF
!           print*,'ok'
!            pause 1111

            print*,'PHINJ',pH
            PAUSE
            write(11,*)
            write(11,*) "INJECTED SOLUTION"
            write(11,*),'PHINJ',pH
            WRITE(11,806) "CA","MG","CO3","CR","OAC"
            WRITE(11,805) TOT1(1,J),TOT1(2,J),TOT1(3,J),TOT1(7,J),TOT1(8,J)
```

```
            write(11,806) 'Ca2+','Mg2+','CO32-','H+','K+','Cl-','Cr3+','Ac',
     & 'SO4,2-','H2O','OH-','CaOH+','MgOH+','CaCO30','MgCO30','CaHCO3+',
     & 'MgHCO3+','HCO3-','H2CO3',
     & 'Cr(OH)2+','Cr(OH)2,+','CrAc(OH)2','HAc','Cr(OAc)3,0'

            WRITE(11,*) 'CONCENTRATION'

            WRITE(11,807) (C(I,J),I=1,NEQ1)

            WRITE(11,*) 'ACTIVITY'

            WRITE(11,807)(AC(I,J),I=1,NEQ1)

!           WRITE(11,807) (GAMMA(I),I=1,NEQ1)


!           write(*,*) pH
!           pause 200

            do I=1,NEQ
            TOT10(I,1)=TOT1(I,1)
            enddo

!           PRINT*,((TOT1(I,J),J=1,NJ),I=1,NEQ2)
!           stop
            print*,time

C-------------------------------------------------------------------

            Do while (time1 .LE. (time + 1.E-6))

C-----------------------------------------------------------------
C           THE FOLLOWING LINES ARE FOR INJECTING AT DIFFERENT FLOW RATES.
C-----------------------------------------------------------------
!           if (time1 .ge. 2.0 .and. time1 .lt. 4.0) then
!           V=0.1
!           V=V/3.142/(DIAMETER/2.)**2./60./PHI
!           else if (time1 .ge. 4.0 .and. time1 .lt. 6.0) then
!           V=0.03
!           V=V/3.142/(DIAMETER/2.)**2./60./PHI
!           else if (time1 .ge. 6.0 .and. time1 .lt. 8.0) then
!           V=0.06
!           V=V/3.142/(DIAMETER/2.)**2./60./PHI
!           else if (time1 .ge. 4.0) then
!           V=1.02
!           V=V/3.142/(DIAMETER/2.)**2./60./PHI
!           endif
C-----------------------------------------------------------------
C-------------------------------------------------------------------------
C       THE FOLLOWING LINES ARE FOR POST FLOODING USING 1% KCL AT 1.0 ML/MIN
C-------------------------------------------------------------------------
!           TIME10=TIME1

            if (TIME1 .ge. SWITCHFLUIDPV) then
            V=1.0
```

```
          V=V/3.142/(DIAMETER/2.)**2./60/PHI
!         POST=1 GO TO 20
!         POST = 0
!20       IF (POST .EQ. 1) THEN
          J=1
          TOT1(1,J)=CAINI
          TOT1(2,J)=XMGINI
          TOT1(3,J)=CO3INI
          TOT1(5,J)=XKINI
          TOT1(6,J)=CLINI
          TOT1(7,J)=CRINI
          TOT1(8,J)=ACINI
          TOT1(9,J)=SO4INI

          CALL EQUILIBRIUM(PHINI,J)
          pH=-DLOG10(AC(4,J))

          IF (IFLAG(1) .EQ. 1) THEN

          CALL ADJUSTPH(CAINI,XMGINI,CO3INI,XKINI,CLINI,CRINI,ACINI,
     &    SO4INI,PHINI,J)
          PH=PHINI
          ENDIF
!         TIME10=0.
          do I=1,NEQ
          TOT10(I,1)=TOT1(I,1)
          enddo

          endif
C-------------------------------------------------------------------------
!         EXPLICIT METHOD
          DO J=2,NJ
          DO I=1,NEQ
          TOT10(I,J)=TOT1(I,J)
          ENDDO
          ENDDO

C --------------
C Iteration loop
C --------------

!         PRINT*,((TOT1(I,J),J=1,NJ),I=1,NEQ2)

C ================
C FOR 2 TO NJ,
C ================
!         PRINT*,(TOT10(8,J),J=1,NJ)
!         PRINT*,'RCR'
!         PRINT*,(RCR(J),J=1,NJ)

     DO J=2,NJ


     TOT1(1,J)=TOT10(1,J)-DT/DX*(TOT10(1,J)-TOT10(1,J-1))
     TOT1(2,J)=TOT10(2,J)-DT/DX*(TOT10(2,J)-TOT10(2,J-1))
     TOT1(3,J)=TOT10(3,J)-DT/DX*(TOT10(3,J)-TOT10(3,J-1))
```

```
      TOT1(5,J)=TOT10(5,J)-DT/DX*(TOT10(5,J)-TOT10(5,J-1))
      TOT1(6,J)=TOT10(6,J)-DT/DX*(TOT10(6,J)-TOT10(6,J-1))
      TOT1(7,J)=TOT10(7,J)-DT/DX*(TOT10(7,J)-TOT10(7,J-1))
      TOT1(8,J)=TOT10(8,J)-DT/DX*(TOT10(8,J)-TOT10(8,J-1))
      TOT1(9,J)=TOT10(9,J)-DT/DX*(TOT10(9,J)-TOT10(9,J-1))

            PHIN=7.0

            CALL EQUILIBRIUM(PHIN,J)


!           PRINT*,IMINERAL(3)

            IF (IMINERAL(1) .EQ. 1) THEN
            DOLK1=1.3E-7*2.
            DOLK2=1.0E-7*2.
            DOLK3=5.5E-11*2.
            DOLPN1=0.75
            DOLPM1=2.0
            DOLPM2=0.25
            DOLPERCEPT=1.0

            DOLS=1-(AC(1,J)*AC(2,J)*AC(3,J)**2./DOLKSP)
            IF (DOLS .LT. 0.) then
            DOLS=0.
            ELSE
      DOLS=(1-(AC(1,J)*AC(2,J)*AC(3,J)**2./DOLKSP)**DOLPM2)
            ENDIF
            RDOL(J)=(DOLK1*AC(4,J)**DOLPN1+DOLK2*AC(19,J)**DOLPN1
     & +DOLK3)*DOLS**DOLPM1*S*DOLPERCEPT
!           PM2=1.9
!           XKC1=6.3E-10/1.
!           XKC2=3.5E-5/1.
!           XKC3=4.5E-5/1.
!           RDOL(J)=S*XKC1*(xkc2*xkc3/(xkc2*xkc3+XKC3*AC(3,J)+AC(1,j)
!    & *AC(3,j)))**1.9*DOLS
            ENDIF

            IF (IMINERAL(2) .EQ. 1) THEN
            CALK1=8.9E-5
            CALK2=5.E-8
            CALK3=6.5E-11
            CALK4=1.9
            CALPERCEPT=0.024


      CALS=1-AC(1,J)*AC(3,J)/CALKSP
            IF (CALS .LT. 0.)           CALS=0.
            RCAL(J)=(CALK1*AC(4,J)+CALK2*AC(19,J)+CALK3-CALK4*AC(1,J)*AC(3,J))
     & *CALS*S*CALPERCEPT
            ENDIF

            IF (IMINERAL(3) .EQ. 1) THEN
            RANH(J)=3.2E-6*(1-AC(1,J)*AC(9,J)/ANHKSP)
            ENDIF
```

```
          RCA(J)=RDOL(J)+RCAL(J)+RANH(J)
          RMG(J)=RDOL(J)
          RCO3(J)=2.*RDOL(J)+RCAL(J)
          RSO4(J)=RANH(J)

          pH=-DLOG10(AC(4,J))
C         CEQ IS TO CALCULATE THE EQUILIBRIUM CHROMIUM CONCENTRATION AT
C                   GIVEN PH
          CEQ=10.**(5.96-2.*PH)+10.**(-6.84)+10.**(-18.25+PH)
          IF (TOT1(7,J) .lT. CEQ) THEN
          RCR(J)=0.
          ELSE

          RCR(J)=-882.9/60.*(TOT1(7,J)-CEQ)**2.0
     &              *AC(11,J)**0.65*TOT1(8,J)**(-0.75)
!         RCR(J)=-2.6E-3/60.*(TOT1(7,J)-CEQ)**1.0
!    &              *AC(11,J)**0.37*TOT1(8,J)**(-1.2)
          ENDIF
      TOT1(1,J)=TOT1(1,J) +RCA(J)*DT*THKX/V
      TOT1(2,J)=TOT1(2,J) +RMG(J)*DT*THKX/V
      TOT1(3,J)=TOT1(3,J) +RCO3(J)*DT*THKX/V
      TOT1(5,J)=TOT1(5,J)
      TOT1(6,J)=TOT1(6,J)
      TOT1(7,J)=TOT1(7,J) +RCR(J)*DT*THKX/V
      TOT1(8,J)=TOT1(8,J)
      TOT1(9,J)=TOT1(9,J) +RSO4(J)*DT*THKX/V
          PHIN=7.0

          DO I=1,NEQ2
          IF (TOT1(I,J) .LT. 0.) TOT1(I,J)=ZERO
          ENDDO

          CALL EQUILIBRIUM(PHIN,J)


!         if ( time1 .gt. 0.1 .and. j .eq.          3) then
!         if (  j .eq. 3) then
!         PRINT *, rdol(j-1), -dlog10(ac(4,j-1)),tot1(2,j-1)
!         PRINT *, rdol(j), -dlog10(ac(4,j)),tot1(2,j),tot10(2,j)
!         pause 13
!         endif

!         PRINT *, J, TOTCA,TOT10(1,J),RDOL(J)
!         PRINT *, J, TOTCR,TOT1(7,J),TOT1(7,J-1)

!         PRINT *, FLAG
!         IF (FLAG .EQ. .FALSE.)  THEN
!         PRINT *,FLAG
!         TOTCR=TOTCR*1.03
!         GO TO 29
!         ENDIF
          IF (FLAG .EQ. .FALSE.)  THEN
          PRINT *,FLAG, "EQUILIBRIUM IS NOT CONVERGEN AT J"
          PRINT *, J, (TOT10(I,J),I=1,8)

          CALL EQUILIBRIUM(PHIN,J)
```

```
            pause 1
            ENDIF

            CALL CALCITE(DP,J,CM1SET)

            ENDDO


C --------------
C IF CONVERGED,
C --------------

!     WRITE(8,*) ' AT CONVERGENCE, RES & JCOUNT =',RES,JCOUNT
!     WRITE(8,*)


            TIME1 = TIME1 + dt

            TOTk=1.0*(0.5*derfc((1-time1)/2/(vxx*time1)**0.5)
     &      +0.5*dexp(1./vxx)*derfc((1+time1)/2/(vxx*time1)**0.5))

     WRITE(*,*) 'TIME1=',TIME1
!           WRITE(*,809) -DLOG10(AC(4,NJ)),TOT1(1,NJ),TOT1(7,NJ)

!           J=1
!           pH=-DLOG10(AC(4,J))

!           WRITE(2,*) 'TIME=',time1

!           WRITE(2,804)'pH=','J=', 'CaTOT=','CRTOT=','ACTOT='

!           WRITE(2,808) pH, J, TOT1(1,J),TOT1(7,J),TOT1(8,J)
!           WRITE(2,*)

!           J=2
!           pH=-DLOG10(AC(4,J))

!           WRITE(2,808) pH, J, TOT1(1,J),TOT1(7,J),TOT1(8,J)
!           WRITE(2,*)

!           J=NJ
!           pH=-DLOG10(AC(4,J))

!           WRITE(2,808) pH, J, TOT1(1,J),TOT1(7,J),TOT1(8,J)
!           WRITE(2,*)

!
            IF (DABS((TIME1+1.E-8)/(10*dt)-MM) .LT. DT) THEN
            MM=MM+1
            WRITE(3,805) TIME1,pH,TOT1(1,NJ)*1.E3,TOT1(2,NJ)*1.E3,TOT1(7,NJ),
     &      TOT1(7,NJ)/CRINJ,TOT1(5,NJ)/XKINJ, TOTk
            ENDIF

            IF (DABS((TIME1+1.E-5)/0.5-M) .LT. DT) THEN
            M=M+1
            WRITE(4,*) time1
```

```
          WRITE (4,806) 'Ca2+','Mg2+','CO32-','H+','K+','Cl-','Cr3+','Ac',
     &'SO4,2-','H2O','OH-','CaOH+','MgOH+','CaCO30','MgCO30','CaHCO3+',
     & 'MgHCO3+','HCO3-','H2CO3',
     & 'Cr(OH)2+','Cr(OH)2,+','CrAc(OH)2','HAc','Cr(OH)30'

          WRITE(4,*) 'CONCENTRATION'

          WRITE(4,807) ((C(I,J),I=1,NEQ1),J=1,NJ)

          WRITE(4,*) 'ACTIVITY'

          WRITE(4,807)((AC(I,J),I=1,NEQ1),J=1,NJ)

          WRITE(4,*)
          WRITE(4,*) 'tD','pH=','TOTCa= IN mM','TOTMG=IN mM','CR=','NORCR='

          WRITE(4,809) ((J-1)*DX*THKX/V/60, -DLOG10(AC(4,J)),TOT1(1,J)*1.E3,
     &    TOT1(2,j)*1.E3,TOT1(7,J),TOT1(7,J)/CRINJ,J=1,NJ)

          ENDIF

          enddo
!         END OF TIME ITERATION

804       FORMAT(4X,A,4X,A,4X,A,4X,A,4X,A,4X,A,4X,A)

805       FORMAT(1X,F11.6,1X,E11.4,1X,E11.4,1X,E11.4,1X,E11.4,1X,E11.4,1x,
     & E11.4,1x,E11.4)

806       FORMAT(4X,24(A,8X))

807   FORMAT(24(E11.4,2X))
808       FORMAT(1X,E11.4,1X,I4,1X,E11.4,1X,E11.4,1X,E11.4)
809   FORMAT(6(E11.4,2X))
C
  28 CONTINUE
C
     STOP
     END
C
C ----- END OF MAIN -----
C=======================================================================
          SUBROUTINE EQUILIBRIUM(PHIN,J)

C    THIS SUBROUTINE CALCULATES THE EQUILIBRIUM CCONCENTRATIONS OF ALL
C         REACTIVE CHEMICAL SPECIES IN ONE CELL. THE INPUT DATA ARE THE TOTAL
C         CONCENTRATIONS OF ALL MATERIAL COMPONENTS EXCEPT HYDROGEN.
C         PHIN IS ESTIMATED PH VALUE
C         THE OUTPUT IS C,AC,TOT1.
C=======================================================================
     IMPLICIT DOUBLE PRECISION (A-H,O-Z)
     PARAMETER (NEQ=10,NEQ1=24,NEQ2=NEQ-1,NNJ=1001)
C
C   NEQ= Maximum number of EQUATIONS
C   NEQ1= NUMBER of UNKNOWNS
```

```
C      (USING EQUILIBRIUM RELATIONSHIP TO MINIMIZE THE EQUAIONS)

      REAL*8 A(NEQ,NEQ),AC(NEQ1,NNJ),AA(NEQ,NEQ1),AR(NEQ2,NEQ1),
     & B(NEQ1,NEQ),C(NEQ1,NNJ),CLOG(NEQ),DELX(NEQ),F(NEQ),GAMMA(NEQ1),
     & TOT(NEQ),TOT1(NEQ,NNJ),CLOG0(NEQ),XK(NEQ1)
      Integer z(NEQ1)
            LOGICAL FLAG

C
      COMMON/M1/ N,NJ
      COMMON/M2/ CONV,CONV2,ZERO,XLN
      COMMON/M3/ XK,Z,AR,B
      COMMON/M4/ C,AC
            COMMON/M5/ TOT1,H2O
            COMMON/M6/ FLAG
            COMMON/M7/ DOLKSP,CALKSP,ANHKSP
!     OPEN(11,file='EQUILIBRIUMOUT.dat')
!     OPEN(12,file='AA.dat')

            FLAG = .TRUE.

!           PRINT*, TOTCA,TOTMG,TOTCO3,TOTK,TOTCL,PHIN,
!     &     TOTCR,TOTAC,H2O,J

            DO I=1,N
            TOT(I)=TOT1(I,J)
            ENDDO
            TOT(4)=H2O
            TOT(10)=0.


            DO I=1,NEQ2
            DO M=1,NEQ1
            AA(I,M)=AR(I,M)
            ENDDO
            ENDDO
            DO M=1,NEQ1
            AA(NEQ,M)=Z(M)
            ENDDO



C---------------------
C     Initializing
C---------------------
C
C           INITIAL GUESS VALUE
            DO I=1,NEQ2
            CLOG(I)=DLOG10(TOT(I))
            ENDDO

            CLOG(4)=-PHIN
            CLOG(10)=DLOG10(H2O/2.)
```

```
            DO I=1,N
            C(I,J)=10.**CLOG(I)
            ENDDO

C           REFERENCE:BHUYAN,1989,PAGE282

            DO I=N+1,NEQ1
            DUMMY=XK(I)
            DO M=1,N-1
            IF (B(I,M) .NE. 0.) DUMMY=DUMMY*C(M,J)**B(I,M)
            ENDDO
            C(I,J)=DUMMY
            ENDDO

!           write(*, *) C(3,J),C(13,J),C(14,J),C(15,J),C(16,J),C(17,J),C(18,J)
!           PAUSE

!           PAUSE 11
!1          FORMAT(6(1X,F10.0))
!           STOP
!           write(2, *)

            JCOUNT=0
1000  JCOUNT=JCOUNT+1
C =======================================
C           INITIALISATION OF JACOBIAN
C =======================================

        DO I=1,N
                    CLOG0(I)=CLOG(I)
           DO K=1,N
           A(I,K)= 0.0D0
            ENDDO
            ENDDO
C
C           CALCULATE PARTIALS OF MATERIAL BALANCE EQUATIONS.
C
            DO I=1,N
            DO M=1,N
            SUM=0.0
            DO K=1,NEQ1
            SUM=SUM+B(K,M)*AA(I,K)*C(K,J)
            ENDDO
            A(I,M)=XLN*SUM
            ENDDO
            ENDDO

!           write (*,*) 'A'
!           write (*,*) ((A(I,J),J=1,N),I=1,N)
!           PAUSE
!           write(2, *) 'B'
!           write (2,3) ((B(I,J),J=1,N),I=1,NEQ1)
!           write(2, *) 'C'
!           write(2, *) (C(I),I=1,NEQ1)
```

```
!          write(2, 1) ((A(i,J),J=1,9),I=1,9)
!1         FORMAT(9(1X,E12.5))
!2         FORMAT(22(1X,F4.0))
!3         FORMAT(9(1X,F4.0))
!          write(2, *)
!          PAUSE

           DO I=1,N
           SUM=0.0
           DO M=1,NEQ1
           SUM=SUM+AA(I,M)*C(M,J)
           ENDDO
           F(I)=TOT(I)-SUM
!          TEST(I,J)=SUM
           ENDDO
!          PRINT*,'TOT1',TOT1(7,J),TOT1(8,J)
!          PAUSE 10
!          write(*, *) C(3,J),C(13,J),C(14,J),C(15,J),C(16,J),C(17,J),C(18,J)
!          FF3=C(3,J)+C(13,J)+C(14,J)+C(15,J)+C(16,J)+C(17,J)+C(18,J)
!          write(*, *) 'F3',F(3),FF3
!          WRITE(*,*) 'F',F(1),F(2),F(3),F(9),F(5),F(6),F(7),f(8)
!          PAUSE 9
!          WRITE(*,*) 'A1',(A(8,J),J=1,8)
!          PAUSE 0
!          PRINT*,'F4',F(4),TOT1(4,J),TOT(4)
!          PAUSE 10

C=========================

    RES10= 0.0D0
C
C          CALCULATE RESIDUALS
C
    DO I=1,N
                    RES11=DABS(F(I))
           IF (RES11 .GT. RES10) THEN
           RES10=RES11
           ENDIF
           ENDDO
    IF(RES10.LT.CONV) GO TO 28

!          write (*,*) 'A'
!          write (*,*) ((A(I,J),J=1,N),I=1,N)
!          WRITE(*,*) 'F',(F(J),J=1,9)
C
C          CALCULATE THE NEW INDEPENDENT SPECIES.
C
    Call LUD(n,A,F,DELX)

!          write(*, *) 'DELX',(DELX(i),I=1,N),CLOG(7)
!          PAUSE 1
!          write(2, *) 'CLOG',(CLOG(i),I=1,N)
!          IF (JCOUNT .GT. 30) THEN
!          DO i=1,n
!          DELX(7)=0.5*DELX(7)
!          ENDDO
```

```
!       ENDIF
C
C       DAMPEN THE NEWTON-PAPHSON ITERATION.
C

        DO i=1,n
        IF (DELX(I) .GE. 2.)      DELX(I)=2.
        IF (DELX(I) .LE. -2.)     DELX(I)=-2.
C
C       CALCULATE THE CONCENTRATIONS OF INDEPENDENT SPECIES.
C
        CLOG(I)=DELX(I)+CLOG0(I)
        C(I,J)=10.**CLOG(I)
        ENDDO
!       write(*, *) (C(i,M),I=1,22)
C
C       CALCULATE ACTIVITY COEFFICIENTS AND THE CONCENTRATIONS OF
C               DEPENDENT SPECIES.
C
        CALL GAMMA1(GAMMA,J)


C
C       CHECK CONVERGENCE.
C
    RES= 0.0D0
    DO I=1,N
!               RES1=DABS(F(I))
                RES1=DABS(DELX(I)/CLOG0(I))
!               RES1=DABS(DELX(I)/MAX(DABS(CLOG(I)),1.))
        IF (RES1 .GT. RES) THEN
        RES=RES1
        ENDIF
        ENDDO

!       IF (TIME1 .GT. 0.50) THEN

!       WRITE(*,*) TIME1, (DELX(I),I=1,N)
!       WRITE(*,*) 'Equilibrium:J,JCOUNT,RES= ',J,JCOUNT,RES,RES10
!       ENDIF



    IF(JCOUNT.GE.500) THEN
    IF(RES.LT.CONV2) THEN
!       PRINT*, 'F',(F(J),J=1,9)
!       PAUSE
        GO TO 28
        ENDIF
        GO TO 2000
        ENDIF

        GO TO 1000


C ----------
```

```
C ---------------------
C Not converged
C ---------------------
2000      CONTINUE
!         IF (RES .LT. 1.E-3) THEN
!         WRITE(*,*) 'SATISFACTORY CONVERGENCE!!!!!!!!!!!!!!'
!         PAUSE 1
!         GO TO 28
!         ENDIF

          WRITE(*,*) 'Equilibrium:PROGRAM DOES NOT CONVERGE AFTER ITERATION'
     &    ,JCOUNT
          stop
!       GOTO 28
!         STOP
          FLAG = .FALSE.
          return
!     ENDIF

C --------------
C IF CONVERGED,
C --------------
C =========================
  28 CONTINUE
          pH=-DLOG10(AC(4,J))

!         IF (TIME1 .GT. 0.548) THEN
!         PRINT*, (TEST(I,J),I=1,N)
!         PRINT*, (TOT(I),I=1,N)
!         PRINT*, (F(I),I=1,N)
!         ENDIF
!         write(11,806) 'Ca2+','Mg2+','CO32-','H+','K+','Cl-','Cr3+','Ac',
!    &'SO4,2-','H2O','OH-','CaOH+','MgOH+','CaCO30','MgCO30','CaHCO3+',
!    & 'MgHCO3+','HCO3-','H2CO3',
!    & 'Cr(OH)2+','Cr(OH)2,+','CrAc(OH)2','HAc','Cr(OH)30'

!         WRITE(11,*) 'CONCENTRATION'

!         WRITE(11,807) (C(I,J),I=1,NEQ1)

!         WRITE(11,*) 'ACTIVITY'

!         WRITE(11,807)(AC(I,J),I=1,NEQ1)

!         WRITE(11,*) 'GAMMA'

!         WRITE(11,807) (GAMMA(I),I=1,NEQ1)

!         WRITE(11,*)
!         WRITE(11,*) 'pH=','TOTCa= IN mM','TOTMG=IN mM','CR=','NORCR='

!         WRITE(11,807)  -DLOG10(AC(4,J)),TOT1(1,J)*1.E3,
!    &    TOT1(2,j)*1.E3,TOT1(7,J),TOT1(7,J)/CRINJ,J=1,NJ)
!         WRITE(21,*) 'TOTCA','TOTMG','TOTCO3','H2O','TOTK','TOTCl','TOTCr',
!    &          'TOTAc','TOTSO4','CB'
!         WRITE(11,807) (TOT1(I,J),I=1,NEQ)
```

```
806       FORMAT(4X,24(A,8X))

807       FORMAT(24(E11.4,2X))

C
C
      END

C=======================================================================
SUBROUTINE ADJUSTPH(CAIN,XMGIN,CO3IN,XKIN,CLIN,CRIN,ACIN,SO4IN,PHIN,J)

C    THIS SUBROUTINE CALCULATES THE EQUILIBRIUM CCONCENTRATIONS OF ALL
C   REACTIVE CHEMICAL SPECIES IN ONE CELL AT KNOWN PH.
C   THIS IS FOR KNOWN PH AND ASSUME PH IS ADJUSTED BY ADDING KOH OR HCL.
C   THE INPUT DATA ARE THE TOTAL CONCENTRATIONS
C   OF ALL MATERIAL COMPONENTS EXCEPT HYDROGEN. K AND CL ARE FROM KCL.
C   PHIN IS KNOWN PH VALUE
C   THE OUTPUT IS C, AC, TOT1. K AND CL ARE ADJUSTED TO FIT CHARGE BALANCE.

C-----------------------------------------------------------------------
C   THIS PROGRAM CAN USED FOR DOLOMITE DISSOLUTION IN KCL SOLUTION WITH
C   KNOWN PH. THE VALUE ADDED TO XKINI OR CLINI IS ADJUSTED.
C-----------------------------------------------------------------------

C=======================================================================

      IMPLICIT DOUBLE PRECISION (A-H,O-Z)
      PARAMETER (NEQ=10,NEQ1=24,NEQ2=NEQ-1,NNJ=1001)
C
C   NEQ= Maximum number of EQUATIONS
C   NEQ1= NUMBER of UNKNOWNS
C      (USING EQUILIBRIUM RELATIONSHIP TO MINIMIZE THE EQUAIONS)

      REAL*8 A(NEQ,NEQ),AC(NEQ1,NNJ),AA(NEQ,NEQ1),AR(NEQ2,NEQ1),
     & B(NEQ1,NEQ),C(NEQ1,NNJ),CLOG(NEQ),DELX(NEQ),F(NEQ),GAMMA(NEQ1),
     & TOT(NEQ),TOT1(NEQ,NNJ),CLOG0(NEQ),XK(NEQ1)
      Integer z(NEQ1)
            LOGICAL FLAG

C
      COMMON/M1/ N,NJ
      COMMON/M2/ CONV,CONV2,ZERO,XLN
      COMMON/M3/ XK,Z,AR,B
      COMMON/M4/ C,AC
            COMMON/M5/ TOT1,H2O
            COMMON/M6/ FLAG
            COMMON/M7/ DOLKSP,CALKSP,ANHKSP

            TOT1(1,J)=CAIN
            TOT1(2,J)=XMGIN
            TOT1(3,J)=CO3IN
            TOT1(5,J)=XKIN
            TOT1(6,J)=CLIN
            TOT1(7,J)=CRIN
```

```
          TOT1(8,J)=ACIN
          TOT1(9,J)=SO4IN

          CALL EQUILIBRIUM(PHINI,J)
          pH=-DLOG10(AC(4,J))


1         TOT1(1,J)=CAIN
          TOT1(2,J)=XMGIN
          TOT1(3,J)=CO3IN
          TOT1(5,J)=XKIN
          TOT1(6,J)=CLIN
          TOT1(7,J)=CRIN
          TOT1(8,J)=ACIN
          TOT1(9,J)=SO4IN

          CALL EQUILIBRIUM(PHIN,J)
          PH0=-DLOG10(AC(4,J))
!         write(*,*) pH
!         pause 2


          PH1=(pH0-PHIN)

          IF (PHIN .lE. PH) THEN
          IF (PH1 .gt. 0.005) THEN
          CLIN=CLIN+10.**(-PHIN)-10.**(-PH0)
          GOTO 1
          ELSE IF (ph1 .lt.-0.005) THEN
          CLIN=CLIN-(10.**(-PHIN)-10.**(-PH0))
          GOTO 1
          ELSE
          ENDIF
          ENDIF

          IF (PHIN .gt. PH) THEN
          IF (PH1 .gt. 0.005) THEN
          XKIN=XKIN-10.**(PH0-14.)
          GOTO 1
          ELSE IF (PH1 .lt.-0.005) THEN
          XKIN=XKIN+10.**(PH0-14.)
          GOTO 1
          ELSE
          ENDIF
          ENDIF


          PHIN=-DLOG10(AC(4,J))
!         PRINT*,PHIN
          END
C
C=======================================================================
          SUBROUTINE DOLDISSEQUIL(PHIN,J)
C    THIS SUBROUTINE IS FOR THE DOLOMITE DISSOLUTION EQUILIBRIUM
C         CALCULATION AT GIVEN INITIAL CONDITIONS. THE INPUT DATA ARE THE
C                   INITIAL CONCENTRATIONS:
```

```
C          TOTAL CA, MG, CO3. K CL, CR, AC, AND PH VALUE. K OR CL IS ADJUSTED TO
C          FIT THE CHARGE BALANCE AT KNOWN PH BY SUBROUTINE
C          ADJUSTPH(CAIN,XMGIN,CO3IN,XKIN,CLIN,CRIN,ACIN,SO4IN,PHIN,J).
C          THE OUTPUT IS C,AC,TOT1.
C=======================================================================
C
      IMPLICIT DOUBLE PRECISION (A-H,O-Z)
      PARAMETER (NEQ=10,NEQ1=24,NEQ2=NEQ-1,NNJ=1001)
C
C
C   NEQ= Maximum number of EQUATIONS
C   NEQ1= NUMBER of UNKNOWNS
C      (USING EQUILIBRIUM RELATIONSHIP TO MINIMIZE THE EQUAIONS)
C   NNJ= Maximum number of node points (NJ in model)
C
       REAL*8 A(NEQ,NEQ),AC(NEQ1,NNJ),AA(NEQ,NEQ1),AR(NEQ2,NEQ1),
     & B(NEQ1,NEQ),C(NEQ1,NNJ),CLOG(NEQ),DELX(NEQ),F(NEQ),GAMMA(NEQ1),
     & TOT(NEQ),TOT1(NEQ,NNJ),CLOG0(NEQ),XK(NEQ1)
      Integer z(NEQ1)
            LOGICAL FLAG

      COMMON/M1/ N,NJ
      COMMON/M2/ CONV,CONV2,ZERO,XLN
      COMMON/M3/ XK,Z,AR,B
      COMMON/M4/ C,AC
            COMMON/M5/ TOT1,H2O
            COMMON/M6/ FLAG
            COMMON/M7/ DOLKSP,CALKSP,ANHKSP

C
      OPEN(21,file='DOLDISSEQUIL.dat')


C----------------------
C     Initializing
C----------------------
C           INITIAL GUESS VALUE
            DO I=1,N
            TOT(I)=TOT1(I,J)
            ENDDO
            TOT(4)=H2O
            TOT(10)=0.

            CLOG(1)=-5.
            CLOG(2)=-5.
            CLOG(3)=-5.
            CLOG(4)=-5.
            CLOG(5)=DLOG10(TOT1(5,J))
            CLOG(6)=DLOG10(TOT1(6,J))
            CLOG(7)=DLOG10(TOT1(7,J))
            CLOG(8)=DLOG10(TOT1(8,J))
            CLOG(9)=DLOG10(TOT1(9,J))
            CLOG(10)=DLOG10(H2O/2.)

            DO I=1,N
            C(I,J)=10.**CLOG(I)
```

```
            ENDDO
            DO I=N+1,NEQ1
            DUMMY=XK(I)
            DO M=1,N-1
            IF (B(I,M) .NE. 0.) DUMMY=DUMMY*C(M,J)**B(I,M)
            ENDDO
            C(I,J)=DUMMY
            ENDDO

            DO I=1,NEQ2
            DO M=1,NEQ1
            AA(I,M)=AR(I,M)
            ENDDO
            ENDDO
            DO M=1,NEQ1
            AA(NEQ,M)=Z(M)
            ENDDO

            DO I=1,NEQ1
            GAMMA(I)=1.0
            ENDDO


C ---------------
C Iteration loop
C ---------------


            JCOUNT=0
1000  JCOUNT=JCOUNT+1
C ========================================
        DO I=1,N
            DO K=1,N
           A(I,K)= 0.0D0
            ENDDO
            ENDDO

            DO I=1,N
            SUM=0.0
            DO M=1,NEQ1
            SUM=SUM+AA(I,M)*C(M,J)
            ENDDO
            F(I)=TOT(I)-SUM
            TOT1(I,J)=SUM
            ENDDO

!           PRINT*, GAMMA(1)
     F(1)=(TOT(1)-TOT1(1,J))-(TOT(2)-TOT1(2,J))
     F(2)=(TOT(3)-TOT1(3,J))-2.*(TOT(1)-TOT1(1,J))
     F(3)=CLOG(1)+CLOG(2)+2.*CLOG(3)
    &      +DLOG10(GAMMA(1)*GAMMA(2)*GAMMA(3)**2.)-DLOG10(DOLKSP)
!     F(3)=C(1,M)*C(2,M)*C(3,M)**2.
!    &     *(GAMMA(1)*GAMMA(2)*GAMMA(3)**2.)-DOLKSP
            F(3)=-F(3)

!           WRITE(*,*) 'F',F(1),F(2),F(3),F(9),F(5),F(6),F(7),f(8)
```

```
!         PAUSE 0

!         A(3,1)=XLN*C(1,M)*C(2,M)*C(3,M)**2.
!    &    *(GAMMA(1)*GAMMA(2)*GAMMA(3)**2.)
!         A(3,2)=XLN*C(1,M)*C(2,M)*C(3,M)**2.
!    &    *(GAMMA(1)*GAMMA(2)*GAMMA(3)**2.)
!         A(3,3)=2.0*XLN*C(1,M)*C(2,M)*C(3,M)**2.
!    &    *(GAMMA(1)*GAMMA(2)*GAMMA(3)**2.)

          DO I=1,N
          DO M=1,N
          SUM=0.0
          DO K=1,NEQ1
          SUM=SUM+B(K,M)*AA(I,K)*C(K,J)
          ENDDO
          A(I,M)=XLN*SUM
          ENDDO
          ENDDO

          DO I=1,3
          DO M=1,N
          A(I,M)=0.
          ENDDO
          ENDDO

          A(1,1)=XLN*(C(1,J)+C(11,J)+C(13,J)+C(15,J))
          A(1,2)=-XLN*(C(2,J)+C(12,J)+C(14,J)+C(16,J))
          A(1,3)=XLN*(C(13,J)+C(15,J)-C(14,J)-C(16,J))
          A(1,4)=XLN*(-C(11,J)+C(15,J)+C(12,J)-C(16,J))


          A(2,1)=XLN*(C(13,J)+C(15,J))-2.*XLN*(C(1,J)+C(11,J)+C(13,J)+C(15,J))
          A(2,2)=XLN*(C(14,J)+C(16,J))
          A(2,3)=XLN*(C(3,J)+C(13,J)+C(14,J)+C(15,J)+C(16,J)+C(17,J)+C(18,J))
     &     -2.*XLN*(C(13,J)+C(15,J))
          A(2,4)=XLN*(C(15,J)+C(16,J)+C(17,J)+2.*C(18,J))
     &    -2.*XLN*(-C(11,J)+C(15,J))

          A(3,1)=1.0
          A(3,2)=1.0
          A(3,3)=2.0


!         WRITE(*,*) 'A9',(A(6,J),J=1,9)
!         PAUSE 1


!         PRINT*,'TOT3',TOT(3),F(3),F(1)
!         PAUSE
!         write(2, *) (F(i),I=1,N)

C=========================
     Call LUD(n,A,F,DELX)

     RES= 0.0D0
     DO 50 I=1,N
```

```
                    RES1=DABS(F(I))
!                   RES1=DABS(DELX(I)/CLOG(I))
          IF (RES1 .GT. RES) THEN
          RES=RES1
          ENDIF
 50  CONTINUE

!    WRITE(*,*) 'DOLDISSOLUTION:JCOUNT,RES= ',JCOUNT,RES

     IF(RES.LT.CONV) GO TO 28

     IF(JCOUNT.GE.155) GO TO 2000

!         PRINT*,'22', c(8,1)
!    Call LUD(n,A,F,DELX)
!         write(2, *) 'DELX',(DELX(i),I=1,N)
!         write(2, *) 'CLOG',(CLOG(i),I=1,N)
          DO i=1,n
          IF (DELX(I) .GE. 2.)       DELX(I)=2.
          IF (DELX(I) .LE. -2.)      DELX(I)=-2.
          CLOG(I)=DELX(I)+CLOG(I)
          C(I,J)=10.**CLOG(I)
          ENDDO

          CALL GAMMA1(GAMMA,J)


!         DO I=N+1,NEQ1
!         DUMMY=XK(I)
!         DO J=1,N-1
!         IF (B(I,J) .NE. 0.) DUMMY=DUMMY*C(J,M)**B(I,J)
!         ENDDO
!         C(I)=DUMMY
!         ENDDO

          GO TO 1000
C -------------
C Not converged
C -------------
2000  WRITE(*,*)'DOLDISSEquiL:PROGRAM DOES NOT CONVERGE AFTER ITERATION'
     &     ,JCOUNT
!       GOTO 28
          STOP


C ---------------
C IF CONVERGED,
C ---------------

c ==========================
  28 CONTINUE
          pH=-DLOG10(AC(4,J))
!         TOT(1)=C(1,M)+C(11,M)+C(13,M)+C(15,M)
!         TOT(2)=C(2,M)+C(12,M)+C(14,M)+C(16,M)
!         TOT(3)=C(3,M)+C(13,M)+C(14,M)+C(15,M)+C(16,M)+C(17,M)+C(18,M)
```

```
!          PRINT*,TOT(1),TOT1(1)

           WRITE(21,*) 'pH=',pH
           write(21,806) 'Ca2+','Mg2+','CO32-','H+','K+','Cl-','Cr3+','Ac',
     &'SO4,2-','H2O','OH-','CaOH+','MgOH+','CaCO30','MgCO30','CaHCO3+',
     & 'MgHCO3+','HCO3-','H2CO3',
     & 'Cr(OH)2+','Cr(OH)2,+','CrAc(OH)2','HAc','Cr(OH)3'

           WRITE(21,*) 'CONCENTRATION'

           WRITE(21,807) (C(I,J),I=1,NEQ1)

           WRITE(21,*) 'ACTIVITY'

           WRITE(21,807)(AC(I,J),I=1,NEQ1)

           WRITE(21,*) 'GAMMA'

           WRITE(21,807) (GAMMA(I),I=1,NEQ1)

           WRITE(21,*) 'TOTCA','TOTMG','TOTCO3','H2O','TOTK','TOTCl','TOTCr',
     &          'TOTAc','TOTSO4','CB'
           WRITE(21,807) (TOT1(I,J),I=1,NEQ)

804        FORMAT(4X,A,4X,A,4X,A)


806        FORMAT(4X,24(A,8X))

807   FORMAT(24(E11.4,2X))
808        FORMAT(1X,E11.4,1X,I4,1X,E11.4)

C
C
      END
C
C
C=======================================================================
           SUBROUTINE CALDISSEQUIL(PHIN,J)
C          THIS SUBROUTINE IS FOR THE CALCITE DISSOLUTION EQUILIBRIUM
C          CALCULATION AT GIVEN INITIAL CONDITIONS. THE INPUT DATA ARE THE
C          INITIAL CONCENTRATIONS:
C          TOTAL CA, MG, CO3. K CL, CR, AC, AND PH VALUE. K OR CL IS ADJUSTED TO
C          FIT THE CHARGE BALANCE AT KNOWN PH BY SUBROUTINE
C          ADJUSTPH(CAIN,XMGIN,CO3IN,XKIN,CLIN,CRIN,ACIN,SO4IN,PHIN,J).
C          THE OUTPUT IS C,AC,TOT1.
C=======================================================================
C
      IMPLICIT DOUBLE PRECISION (A-H,O-Z)
      PARAMETER (NEQ=10,NEQ1=24,NEQ2=NEQ-1,NNJ=1001)
C
C
C   NEQ= Maximum number of EQUATIONS
C   NEQ1= NUMBER of UNKNOWNS
C      (USING EQUILIBRIUM RELATIONSHIP TO MINIMIZE THE EQUAIONS)
C   NNJ= Maximum number of node points (NJ in model)
```

```
C
      REAL*8 A(NEQ,NEQ),AC(NEQ1,NNJ),AA(NEQ,NEQ1),AR(NEQ2,NEQ1),
     & B(NEQ1,NEQ),C(NEQ1,NNJ),CLOG(NEQ),DELX(NEQ),F(NEQ),GAMMA(NEQ1),
     & TOT(NEQ),TOT1(NEQ,NNJ),CLOG0(NEQ),XK(NEQ1)
      Integer z(NEQ1)
            LOGICAL FLAG

      COMMON/M1/ N,NJ
      COMMON/M2/ CONV,CONV2,ZERO,XLN
      COMMON/M3/ XK,Z,AR,B
      COMMON/M4/ C,AC
            COMMON/M5/ TOT1,H2O
            COMMON/M6/ FLAG
            COMMON/M7/ DOLKSP,CALKSP,ANHKSP

C
      OPEN(21,file='CALDISSEQUIL.dat')
!           H2O=111.11
C---------------------
C     Initializing
C---------------------
C           INITIAL GUESS VALUE
            DO I=1,N
            TOT(I)=TOT1(I,J)
            ENDDO
            TOT(4)=H2O
            TOT(10)=0.

            CLOG(1)=-5.
            CLOG(2)=DLOG10(TOT1(2,J))
            CLOG(3)=-5.
            CLOG(4)=-10.
            CLOG(5)=DLOG10(TOT1(5,J))
            CLOG(6)=DLOG10(TOT1(6,J))
            CLOG(7)=DLOG10(TOT1(7,J))
            CLOG(8)=DLOG10(TOT1(8,J))
            CLOG(9)=DLOG10(TOT1(9,J))
            CLOG(10)=DLOG10(H2O/2.)


            DO I=1,N
            C(I,J)=10.**CLOG(I)
            ENDDO
            DO I=N+1,NEQ1
            DUMMY=XK(I)
            DO M=1,N-1
            IF (B(I,M) .NE. 0.) DUMMY=DUMMY*C(M,J)**B(I,M)
            ENDDO
            C(I,J)=DUMMY
            ENDDO

            DO I=1,NEQ2
            DO M=1,NEQ1
            AA(I,M)=AR(I,M)
            ENDDO
            ENDDO
```

```
            DO M=1,NEQ1
            AA(NEQ,M)=Z(M)
            ENDDO

            DO I=1,NEQ1
            GAMMA(I)=1.0
            ENDDO


C ---------------
C Iteration loop
C ---------------


            JCOUNT=0
1000  JCOUNT=JCOUNT+1
C =======================================
        DO I=1,N
            DO K=1,N
           A(I,K)= 0.0D0
            ENDDO
            ENDDO

            DO I=1,N
            SUM=0.0
            DO M=1,NEQ1
            SUM=SUM+AA(I,M)*C(M,J)
            ENDDO
            F(I)=TOT(I)-SUM
            TOT1(I,J)=SUM
            ENDDO

!           PRINT*, GAMMA(1)
     F(1)=(TOT(3)-TOT1(3,J))-(TOT(1)-TOT1(1,J))
     F(3)=CLOG(1)+CLOG(3)
    &      +DLOG10(GAMMA(1)*GAMMA(3))-DLOG10(CALKSP)
            F(3)=-F(3)

!           WRITE(*,*) 'F',F(1),F(2),F(3),F(9),F(5),F(6),F(7),f(8)
!           PAUSE 0


            DO I=1,N
            DO M=1,N
            SUM=0.0
            DO K=1,NEQ1
            SUM=SUM+B(K,M)*AA(I,K)*C(K,J)
            ENDDO
            A(I,M)=XLN*SUM
            ENDDO
            ENDDO


            DO M=1,N
            A(1,M)=0.
            A(3,M)=0.
```

```
            ENDDO

            A(1,1)=XLN*(C(13,J)+C(15,J))-XLN*(C(1,J)+C(11,J)+C(13,J)+C(15,J))
            A(1,2)=XLN*(C(14,J)+C(16,J))
            A(1,3)=XLN*(C(3,J)+C(13,J)+C(14,J)+C(15,J)+C(16,J)+C(17,J)+C(18,J))
     &       -XLN*(C(13,J)+C(15,J))
            A(1,4)=XLN*(C(15,J)+C(16,J)+C(17,J)+2.*C(18,J))
     &      -XLN*(-C(11,J)+C(15,J))

            A(3,1)=1.0
            A(3,3)=1.0

!           WRITE(*,*) 'A9',(A(6,J),J=1,9)
!           PAUSE 1


!           PRINT*,'TOT3',TOT(3),F(3),F(1)
!           PAUSE
!           write(2, *) (F(i),I=1,N)

C=========================
      Call LUD(n,A,F,DELX)

      RES= 0.0D0
      DO 50 I=1,N
                        RES1=DABS(F(I))
!                       RES1=DABS(DELX(I)/CLOG(I))
            IF (RES1 .GT. RES) THEN
            RES=RES1
            ENDIF
   50  CONTINUE

      WRITE(*,*) 'CALDISSOLUTION:JCOUNT,RES= ',JCOUNT,RES

      IF(RES.LT.1.0E-8) GO TO 28

      IF(JCOUNT.GE.155) GO TO 2000

!           PRINT*,'22', c(8,1)
!     Call LUD(n,A,F,DELX)
!           write(2, *) 'DELX',(DELX(i),I=1,N)
!           write(2, *) 'CLOG',(CLOG(i),I=1,N)
            DO i=1,n
            IF (DELX(I) .GE. 2.)        DELX(I)=2.
            IF (DELX(I) .LE. -2.)       DELX(I)=-2.
            CLOG(I)=DELX(I)+CLOG(I)
            C(I,J)=10.**CLOG(I)
            ENDDO

            CALL GAMMA1(GAMMA,J)


!           DO I=N+1,NEQ1
!           DUMMY=XK(I)
!           DO J=1,N-1
!           IF (B(I,J) .NE. 0.) DUMMY=DUMMY*C(J,M)**B(I,J)
```

```
!           ENDDO
!           C(I)=DUMMY
!           ENDDO

            GO TO 1000
C -------------
C Not converged
C -------------
2000  WRITE(*,*)'CALDISSEquiL:PROGRAM DOES NOT CONVERGE AFTER ITERATION'
     &      ,JCOUNT
!       GOTO 28
            STOP


C ---------------
C IF CONVERGED,
C ---------------

c ==========================
  28 CONTINUE
            pH=-DLOG10(AC(4,J))
!           TOT(1)=C(1,M)+C(11,M)+C(13,M)+C(15,M)
!           TOT(2)=C(2,M)+C(12,M)+C(14,M)+C(16,M)
!           TOT(3)=C(3,M)+C(13,M)+C(14,M)+C(15,M)+C(16,M)+C(17,M)+C(18,M)

!           PRINT*,TOT(1),TOT1(1)

            WRITE(21,*) 'pH=',pH
            write(21,806) 'Ca2+','Mg2+','CO32-','H+','K+','Cl-','Cr3+','Ac',
     &'SO4,2-','H2O','OH-','CaOH+','MgOH+','CaCO30','MgCO30','CaHCO3+',
     & 'MgHCO3+','HCO3-','H2CO3',
     & 'Cr(OH)2+','Cr(OH)2,+','CrAc(OH)2','HAc','Cr(OH)3'

            WRITE(21,*) 'CONCENTRATION'

            WRITE(21,807) (C(I,J),I=1,NEQ1)

            WRITE(21,*) 'ACTIVITY'

            WRITE(21,807)(AC(I,J),I=1,NEQ1)

            WRITE(21,*) 'GAMMA'

            WRITE(21,807) (GAMMA(I),I=1,NEQ1)

            WRITE(21,*) 'TOTCA','TOTMG','TOTCO3','H2O','TOTK','TOTCl','TOTCr',
     &          'TOTAc','TOTSO4','CB'
            WRITE(21,807) (TOT1(I,J),I=1,NEQ)

804         FORMAT(4X,A,4X,A,4X,A)


806         FORMAT(4X,24(A,8X))

807   FORMAT(24(E11.4,2X))
808         FORMAT(1X,E11.4,1X,I4,1X,E11.4)
```

```
C
C
      END
C

C=======================================================================
            SUBROUTINE CASO4DOLDISSEQUIL(PHIN,J)
C     THIS SUBROUTINE IS FOR THE ANHYDRITE DISSOLUTION EQUILIBRIUM
C           CALCULATION AT GIVEN INITIAL CONDITIONS. THE INPUT DATA ARE THE
C           INITIAL CONCENTRATIONS:
C           TOTAL CA, MG, CO3. K CL, CR, AC, AND PH VALUE. K OR CL IS ADJUSTED TO
C           FIT THE CHARGE BALANCE AT KNOWN PH BY SUBROUTINE
C           ADJUSTPH(CAIN,XMGIN,CO3IN,XKIN,CLIN,CRIN,ACIN,SO4IN,PHIN,J).
C           THE OUTPUT IS C,AC,TOT1.
C=======================================================================
C
      IMPLICIT DOUBLE PRECISION (A-H,O-Z)
      PARAMETER (NEQ=10,NEQ1=24,NEQ2=NEQ-1,NNJ=1001)
C
C
C   NEQ= Maximum number of EQUATIONS
C   NEQ1= NUMBER of UNKNOWNS
C      (USING EQUILIBRIUM RELATIONSHIP TO MINIMIZE THE EQUAIONS)
C   NNJ= Maximum number of node points (NJ in model)
C
       REAL*8 A(NEQ,NEQ),AC(NEQ1,NNJ),AA(NEQ,NEQ1),AR(NEQ2,NEQ1),
     & B(NEQ1,NEQ),C(NEQ1,NNJ),CLOG(NEQ),DELX(NEQ),F(NEQ),GAMMA(NEQ1),
     & TOT(NEQ),TOT1(NEQ,NNJ),CLOG0(NEQ),XK(NEQ1)
      Integer z(NEQ1)
            LOGICAL FLAG

      COMMON/M1/ N,NJ
      COMMON/M2/ CONV,CONV2,ZERO,XLN
      COMMON/M3/ XK,Z,AR,B
      COMMON/M4/ C,AC
            COMMON/M5/ TOT1,H2O
            COMMON/M6/ FLAG
            COMMON/M7/ DOLKSP,CALKSP,ANHKSP

C
      OPEN(21,file='CASO4DISSEQUIL.dat')

            PRINT*,PH,'PH',h2o
!           PAUSE 1111
!           H2O=111.11
C---------------------
C     Initializing
C---------------------
C           INITIAL GUESS VALUE
            DO I=1,N
            TOT(I)=TOT1(I,J)
            ENDDO
            TOT(4)=H2O
            TOT(10)=0.
```

```
            CLOG(1)=-5.
            CLOG(2)=DLOG10(TOT1(2,J))
            CLOG(3)=-5.
            CLOG(4)=-10.
            CLOG(5)=DLOG10(TOT1(5,J))
            CLOG(6)=DLOG10(TOT1(6,J))
            CLOG(7)=DLOG10(TOT1(7,J))
            CLOG(8)=DLOG10(TOT1(8,J))
            CLOG(9)=DLOG10(TOT1(9,J))
            CLOG(10)=DLOG10(H2O/2.)


            DO I=1,N
            C(I,J)=10.**CLOG(I)
            ENDDO
            DO I=N+1,NEQ1
            DUMMY=XK(I)
            DO M=1,N-1
            IF (B(I,M) .NE. 0.) DUMMY=DUMMY*C(M,J)**B(I,M)
            ENDDO
            C(I,J)=DUMMY
            ENDDO

            DO I=1,NEQ2
            DO M=1,NEQ1
            AA(I,M)=AR(I,M)
            ENDDO
            ENDDO
            DO M=1,NEQ1
            AA(NEQ,M)=Z(M)
            ENDDO

            DO I=1,NEQ1
            GAMMA(I)=1.0
            ENDDO


C ---------------
C Iteration loop
C ---------------


            JCOUNT=0
1000  JCOUNT=JCOUNT+1
C =======================================
          DO I=1,N
             DO K=1,N
            A(I,K)= 0.0D0
             ENDDO
             ENDDO

            DO I=1,N
            SUM=0.0
            DO M=1,NEQ1
            SUM=SUM+AA(I,M)*C(M,J)
            ENDDO
```

```
          F(I)=TOT(I)-SUM
          TOT1(I,J)=SUM
          ENDDO

!         F(9)=F(9)+so4(j)*2.
!         SO4(J)=(-TOT(1)+TOT1(1,J))-(-TOT(2)+TOT1(2,J))

!         PRINT*, GAMMA(1)
     F(1)=C(1,J)*C(9,J)*GAMMA(1)*GAMMA(9)-ANHKSP
     F(2)=(-TOT(3)+TOT1(3,J))-2.*(-TOT(2)+TOT1(2,J))
     F(3)=CLOG(1)+CLOG(2)+2.*CLOG(3)
    &     +DLOG10(GAMMA(1)*GAMMA(2)*GAMMA(3)**2.)-DLOG10(DOLKSP)
!     F(3)=C(1,M)*C(2,M)*C(3,M)**2.
!    &     *(GAMMA(1)*GAMMA(2)*GAMMA(3)**2.)-XKSP
          F(9)=(-TOT(1)+TOT1(1,J))-(-TOT(2)+TOT1(2,J))-(-TOT(9)+TOT1(9,J))

          DO I=1,3
          F(I)=-F(I)
          ENDDO
          F(9)=-F(9)
!         WRITE(*,*) 'F',F(1),F(2),F(3),F(9),F(5),F(6),F(7),f(8)
!         PAUSE 0

!         A(3,1)=XLN*C(1,M)*C(2,M)*C(3,M)**2.
!    &     *(GAMMA(1)*GAMMA(2)*GAMMA(3)**2.)
!         A(3,2)=XLN*C(1,M)*C(2,M)*C(3,M)**2.
!    &     *(GAMMA(1)*GAMMA(2)*GAMMA(3)**2.)
!         A(3,3)=2.0*XLN*C(1,M)*C(2,M)*C(3,M)**2.
!    &     *(GAMMA(1)*GAMMA(2)*GAMMA(3)**2.)

          DO I=1,N
          DO M=1,N
          SUM=0.0
          DO K=1,NEQ1
          SUM=SUM+B(K,M)*AA(I,K)*C(K,J)
          ENDDO
          A(I,M)=XLN*SUM
          ENDDO
          ENDDO

          DO I=1,3
          DO M=1,N
          A(I,M)=0.
          ENDDO
          ENDDO

          DO M=1,N
          A(9,M)=0.
          ENDDO

          A(1,1)=XLN*C(1,J)*C(9,J)*GAMMA(1)*GAMMA(9)
          A(1,9)=XLN*C(1,J)*C(9,J)*GAMMA(1)*GAMMA(9)

          A(2,1)=XLN*(C(13,J)+C(15,J))
          A(2,2)=XLN*(C(14,J)+C(16,J))-2.*XLN*(C(2,J)+C(12,J)+C(14,J)+C(16,J))
          A(2,3)=XLN*(C(3,J)+C(13,J)+C(14,J)+C(15,J)+C(16,J)+C(17,J)+C(18,J))
```

```
     &      -2.*XLN*(C(14,J)+C(16,J))
            A(2,4)=XLN*(C(15,J)+C(16,J)+C(17,J)+2.*C(18,J))
     &      -2.*XLN*(-C(12,J)+C(16,J))

            A(3,1)=1.0
            A(3,2)=1.0
            A(3,3)=2.0

            A(9,1)=XLN*(C(1,J)+C(11,J)+C(13,J)+C(15,J))
            A(9,2)=-XLN*(C(2,J)+C(12,J)+C(14,J)+C(16,J))
            A(9,3)=XLN*(C(13,J)+C(15,J)-C(14,J)-C(16,J))
            A(9,4)=XLN*(-C(11,J)+C(15,J)+C(12,J)-C(16,J))
            A(9,9)=-XLN*C(9,J)


!           WRITE(*,*) 'A9',(A(6,J),J=1,9)
!           PAUSE 1


!           PRINT*,'TOT3',TOT(3),F(3),F(1)
!           PAUSE
!           write(2, *) (F(i),I=1,N)

C==========================
      Call LUD(n,A,F,DELX)

      RES= 0.0D0
      DO 50 I=1,N
                        RES1=DABS(F(I))
!                       RES1=DABS(DELX(I)/CLOG(I))
            IF (RES1 .GT. RES) THEN
            RES=RES1
            ENDIF
   50  CONTINUE

      WRITE(*,*) 'CASO4DISSOLUTION:JCOUNT,RES= ',JCOUNT,RES

      IF(RES.LT.1.0E-8) GO TO 28

      IF(JCOUNT.GE.155) GO TO 2000

!           PRINT*,'22', c(8,1)
!     Call LUD(n,A,F,DELX)
!           write(2, *) 'DELX',(DELX(i),I=1,N)
!           write(2, *) 'CLOG',(CLOG(i),I=1,N)
            DO i=1,n
            IF (DELX(I) .GE. 2.)        DELX(I)=2.
            IF (DELX(I) .LE. -2.)       DELX(I)=-2.
            CLOG(I)=DELX(I)+CLOG(I)
            C(I,J)=10.**CLOG(I)
            ENDDO

            CALL GAMMA1(GAMMA,J)


!           DO I=N+1,NEQ1
```

```
!           DUMMY=XK(I)
!           DO J=1,N-1
!           IF (B(I,J) .NE. 0.) DUMMY=DUMMY*C(J,M)**B(I,J)
!           ENDDO
!           C(I)=DUMMY
!           ENDDO

            GO TO 1000
C -------------
C Not converged
C -------------
2000  WRITE(*,*)'CASO4DISSEQ:PROGRAM DOES NOT CONVERGE AFTER ITERATION'
     &      ,JCOUNT
!       GOTO 28
            STOP


C --------------
C IF CONVERGED,
C --------------

c ==========================
   28 CONTINUE
            pH=-DLOG10(AC(4,J))
!           TOT(1)=C(1,M)+C(11,M)+C(13,M)+C(15,M)
!           TOT(2)=C(2,M)+C(12,M)+C(14,M)+C(16,M)
!           TOT(3)=C(3,M)+C(13,M)+C(14,M)+C(15,M)+C(16,M)+C(17,M)+C(18,M)

!           PRINT*,TOT(1),TOT1(1)

            WRITE(21,*) 'pH=',pH
            write(21,806) 'Ca2+','Mg2+','CO32-','H+','K+','Cl-','Cr3+','Ac',
     &'SO4,2-','H2O','OH-','CaOH+','MgOH+','CaCO30','MgCO30','CaHCO3+',
     & 'MgHCO3+','HCO3-','H2CO3',
     & 'Cr(OH)2+','Cr(OH)2,+','CrAc(OH)2','HAc','Cr(OH)3'

            WRITE(21,*) 'CONCENTRATION'

            WRITE(21,807) (C(I,J),I=1,NEQ1)

            WRITE(21,*) 'ACTIVITY'

            WRITE(21,807)(AC(I,J),I=1,NEQ1)

            WRITE(21,*) 'GAMMA'

            WRITE(21,807) (GAMMA(I),I=1,NEQ1)

            WRITE(21,*) 'TOTCA','TOTMG','TOTCO3','H2O','TOTK','TOTCl','TOTCr',
     &          'TOTAc','TOTSO4','CB'
            WRITE(21,807) (TOT1(I,J),I=1,NEQ)

804         FORMAT(4X,A,4X,A,4X,A)


806         FORMAT(4X,24(A,8X))
```

```
807   FORMAT(24(E11.4,2X))
808       FORMAT(1X,E11.4,1X,I4,1X,E11.4)

C
C
      END
C
C ==============================
      SUBROUTINE GAMMA1(GAMMA,J)
C ==============================
C           INPUT    C(I,J)
C           OUTPUT   AC(I,J),Gamma
C ==============================
      IMPLICIT DOUBLE PRECISION (A-H,O-Z)
      PARAMETER (NEQ=10,NEQ1=24,NEQ2=NEQ-1,NNJ=1001)
C
C   NEQ= Maximum number of EQUATIONS
C   NEQ1= NUMBER of UNKNOWNS
C      (USING EQUILIBRIUM RELATIONSHIP TO MINIMIZE THE EQUAIONS)

      REAL*8 A(NEQ,NEQ),AC(NEQ1,NNJ),AA(NEQ,NEQ1),AR(NEQ2,NEQ1),
     & B(NEQ1,NEQ),C(NEQ1,NNJ),CLOG(NEQ),DELX(NEQ),F(NEQ),GAMMA(NEQ1),
     & TOT(NEQ),TOT1(NEQ,NNJ),XK(NEQ1)
      Integer z(NEQ1)
C
      COMMON/M1/ N,NJ
      COMMON/M2/ CONV,CONV2,ZERO,XLN
      COMMON/M3/ XK,Z,AR,B
      COMMON/M4/ C,AC
            COMMON/M5/ TOT1,H2O
            COMMON/M6/ FLAG
            COMMON/M7/ DOLKSP,CALKSP,ANHKSP


c---------------------------------------
!           write(*, *) (C(i,J),I=1,22)
            XI=0.
            do I=1,NEQ1
            GAMMA(I)=1.0
            enddo

            DO I=NEQ+1,NEQ1
            DUMMY=XK(I)
            DO M=1,NEQ-1
            IF (B(I,M) .NE. 0.) DUMMY=DUMMY*C(M,J)**B(I,M)
            ENDDO
            C(I,J)=DUMMY
            ENDDO

            Icount=0
1           Icount=Icount+1

            XII=XI

            DO I=1,NEQ1
```

```
          AC(I,J)=C(I,J)*GAMMA(I)
          ENDDO

          DO I=NEQ+1,NEQ1
          DUMMY=XK(I)
          DO M=1,NEQ-1
          IF (B(I,M) .NE. 0.) DUMMY=DUMMY*AC(M,J)**B(I,M)
          ENDDO
          AC(I,J)=DUMMY
          ENDDO


          DO I=1,NEQ1
          C(I,J)=AC(I,J)/GAMMA(I)
          ENDDO
!   &     T(16,1),T(17,1),T(18,1),T(19,1),T(20,1),T(21,1)


          XI=0.

          DO i=1,NEQ1
          XI=XI+0.5*(C(i,J)*Z(i)**2.)
          ENDDO

!         PRINT*,XI(J)

          IF (XI .LT. 2.) THEN
          DO I=1,NEQ1
          GAMMA(I)=
     &    10**(-0.5*Z(i)**2.*(XI**0.5/(1+XI**0.5)-0.2*XI))

          ENDDO
          ELSE
          GO TO 28
          ENDIF

!         PRINT*,xi, 'OK'

          RES2=DABS((XI-XII)/XI)

!    WRITE(*,*) ' ICOUNT,RES2= ',ICOUNT,RES2

     IF (RES2 .GT. CONV2) THEN
     IF(ICOUNT.LE.150) GO TO 1
          WRITE(*,*) 'PROGRAM DOES NOT CONVERGE FOR INTERNAL ITERNATIVE
     &    AFTER ITERATION',ICOUNT
          STOP
          ENDIF
28        CONTINUE
!         write(*, *) (C(i,j),I=1,22),GAMMA(21),GAMMA(1),C(21,J),AC(21,J)
!         PAUSE 2
          END


C=======================================================================
          SUBROUTINE CALCITE(DP,J,CM1SET)
```

```
C    THIS SUBROUTINE CONSIDERS THE CALCITE SOLUBILITY CONSTRAINT. CM1SET IS
C    THE CRITICAL SUPERSATURATION INDEX.

C          THE OUTPUT IS DP FOR PRECIPIATED AMOUNT OF CA AND CO3,2-.


C=======================================================================

      IMPLICIT DOUBLE PRECISION (A-H,O-Z)
      PARAMETER (NEQ=10,NEQ1=24,NEQ2=NEQ-1,NNJ=1001)
C
C   NEQ= Maximum number of EQUATIONS
C   NEQ1= NUMBER of UNKNOWNS
C      (USING EQUILIBRIUM RELATIONSHIP TO MINIMIZE THE EQUAIONS)

      REAL*8 A(NEQ,NEQ),AC(NEQ1,NNJ),AA(NEQ,NEQ1),AR(NEQ2,NEQ1),
     & B(NEQ1,NEQ),C(NEQ1,NNJ),CLOG(NEQ),DELX(NEQ),F(NEQ),GAMMA(NEQ1),
     & TOT(NEQ),TOT1(NEQ,NNJ),XK(NEQ1)
      Integer z(NEQ1)
            LOGICAL FLAG

C
      COMMON/M1/ N,NJ
      COMMON/M2/ CONV,CONV2,ZERO,XLN
      COMMON/M3/ XK,Z,AR,B
      COMMON/M4/ C,AC
            COMMON/M5/ TOT1,H2O
            COMMON/M6/ FLAG
            COMMON/M7/ DOLKSP,CALKSP,ANHKSP

!           CM1SET=1.1
!           CALKSP=10**(-8.31)
!           XMGKSP=10**(-8.2115)
            mcount=0

1           mcount=mcount+1
            CM=AC(1,J)*AC(3,J)
!           PRINT *, CM,J
!           PAUSE 2
            CP=AC(1,J)+AC(3,J)
            DP=0.
!
            CM1=CM/CALKSP
!           write(*,*) cm1
!           pause 1

!           CM1=(CM-CALKSP)/CALKSP
            IF (CM1 .lT. CM1SET) go to 28
!           SUPERSATURATION IS NEEDED TO GET PRECIPITATION!

!           IF (TIME1 .GT. 1.0E-3) THEN
!           PRINT *, j,mcount,cm1,time1
!           PAUSE 1
!           ENDIF
```

```
          DP1=(CP+(CP**2.-4.*(CM-CALKSP))**0.5)/2.
          DP2=(CP-(CP**2.-4.*(CM-CALKSP))**0.5)/2.
          IF (DP2 .GT. 0. .AND. DP2 .LT. AC(1,J) .AND. DP2 .LT. AC(3,J))
     &    DP=DP2
          IF (DP1 .GT. 0. .AND. DP1 .LT. AC(1,J) .AND. DP1 .LT. AC(3,J))
     &    DP=DP1
!         PRINT*,'OK',J,DP1,DP2,AC(1,J),AC(3,J),cm1,dp,-dlog10(ac(4,j))
!         PAUSE 22
!         GO TO 28

!         IF (TIME1 .GT. 1.0E-3) THEN
!         PRINT*, TIME1,DP
!         PAUSE 1
!         ENDIF
          AC(1,J)=AC(1,J)-DP
          AC(3,J)=AC(3,J)-DP

!         IF (J .EQ. 2) THEN
!         PRINT*, DP
!         ENDIF
          DELDP1=DP/AC(1,J)
          DELDP3=DP/AC(3,J)
          DELDP=MAX(DELDP1,DELDP3)

          IF (DELDP .lT. CONV2) go to 28
!         PRINT*,J,AC(1,J),AC(3,J),-DLOG10(AC(4,J))
          TOT1(1,J)=TOT1(1,J)-DP
          TOT1(3,J)=TOT1(3,J)-DP
          CALL EQUILIBRIUM(PHIN,J)
!         PRINT*,AC(1,J),AC(3,J),-DLOG10(AC(4,J))
!         PAUSE 33

          IF(mCOUNT.LE.1550)   GO TO 1


     WRITE(*,*)'DOES NOT CONVERGE for sub calcite',mcount,j,cm1
          stop
28    CONTINUE
          END

C         ------------------------------------------------------
!
     Subroutine LUD(n,A,B,X)

     PARAMETER (NEQ=10)

! LU Decomposition for the Solution of [A]{X}={B}
!
! Global Varibles
!
! n     = maximun value of i and j
! A(n,n)= Coefficient Matrix
! B(n)  = RHS vector
! X(n)  = Solution Vector
!
! Local Variable
```

```
!
!  O(n)  = equation order vector (pointer)
!  C(n)  = [L]-1(superscript){B}
!
     Integer n
     Integer,dimension(NEQ)::O
     Real*8,dimension(NEQ)::B,X,S
     Real*8,dimension(NEQ,NEQ)::A
!
     Call ORDER(n,A,O,S)
     Call Decomp(n,A,O,S)
             Call SOLVE(n,A,B,X,O)

     Return
     End subroutine LUD
!
!-----------------------------------------------
!
     Subroutine Decomp(n,A,O,S)
     PARAMETER (NEQ=10)
!
!  Performing LUD Composition of A, Using A's space to Restore L and U
!
!  Global Varibles
!
!  n     = maximun value of i and j
!  A(n,n)= Coefficient Matrix
!  O(n)  = equation order vector (pointer)
!
!  Local Variables
!  i     = row index
!  j     = column index
!  k     = pivot index
!  S(n)  = scaling coefficient vector
!
     Integer,dimension(NEQ)::O
     Real*8,dimension(NEQ)::S
     Real*8,dimension(NEQ,NEQ)::A
!
     Integer i,j,n,k
     Real*8 Sum
!
!
             J=1
     Call pivot(n,A,O,S,J)
!
!  Calculate Row 1 of U
!
     Do j=2,n
     A(O(1),j)=A(O(1),j)/A(O(1),1)
     End Do
!
     Do j=2,n-1
!
!  Calculate Column j of L
!
```

```
      Do i=j,n
      Sum=0.
               Do k=1,j-1
                        Sum=Sum+A(O(i),k)*A(O(k),j)
        End Do
      A(O(i),j)=A(O(i),j)-Sum
            End Do
!
      Call pivot(n,A,O,S,j)
!
!  Calculate Row j of U
!
      Do k=j+1,n
               Sum=0.
                     Do i=1,j-1
                       Sum=Sum+A(O(j),i)*A(O(i),k)
        End Do
      A(O(j),k)=(A(O(j),k)-Sum)/A(O(j),j)
            End Do
!
      End Do
!
!  Caluculate Column n of L
!
      Sum=0.
      Do k=1,n-1
      Sum=Sum+A(O(n),k)*A(O(k),n)
      End Do
      A(O(n),n)=A(O(n),n)-Sum
!
      Return
      End Subroutine Decomp
!
!-------------------------------------------------
!
      Subroutine SOLVE(n,A,B,X,O)
      PARAMETER (NEQ=10)
!
!  Program does forward substitution to solve [L]{C}={B}
!
!  Global Varibles
!
!  n     = maximun value of i and j
!  A(n,n)= Coefficient Matrix
!  B(n)  = RHS vector
!  X(n)  = SOLUTION VECTOR
!  O(n)  = equation order vector (pointer)
!
!  Local Variables
!  i     = row index
!  j     = column index
!
      Integer,dimension(NEQ)::O
      Real*8,dimension(NEQ)::B,X
      Real*8,dimension(NEQ,NEQ)::A
      Integer i,j,n,K
```

```
      Real*8 Sum
!
      X(1)=B(O(1))/A(O(1),1)
      Do i=2,n
      Sum=0.0
            Do j=1,i-1
        Sum=Sum+A(O(i),j)*X(j)
      End Do
      X(i)=(B(O(i))-Sum)/A(O(i),i)
      End Do
!
!  Program does Backward substitution to solve [U]{X}={C}
!
      Do i=n-1,1,-1
      Sum=0.0
            Do j=i+1,n
        Sum=Sum+A(O(i),j)*X(j)
      End Do
      X(i)=X(i)-Sum
      End Do
!

      Return
      End Subroutine SOLVE
!
!-------------------------------------------------
!
!-------------------------------------------------
!
      Subroutine Order(n,A,O,S)
      PARAMETER (NEQ=10)
!
!  Program establishes the equation order and scaling constants
!
!  Global Variables
!
!  n     = maximun value of i and j
!  A(n,n)= Coefficient Matrix
!  O(n)  = equation order vector (pointer)
!  S(n)  = scaling coefficient vector
!
!  Local Variables
!  i     = row index
!  j     = column index
!
      Integer i,j,n
      Integer,dimension(NEQ)::O
      Real*8,dimension(NEQ)::S
      Real*8,dimension(NEQ,NEQ)::A
!
      Do i=1,n
      O(i)=i
            S=DABS(A(i,1))
            Do j=2,n
              If(DABS(A(i,j)).GT.S(i)) Then
                        S(i)=DABS(A(i,j))
```

```
                    End if
      End Do
      End Do
      Return
      End Subroutine Order
!
!-----------------------------------------------
!
      Subroutine Pivot(n,A,O,S,k)
      PARAMETER (NEQ=10)
!
!  Program performs partial (row) pivoting using a pointer vector
!
!  Global Variables
!
!  n     = maximun value of i and j
!  k     = equation index
!  A(n,n)= Coefficient Matrix
!  O(n)  = equation order vector (pointer)
!  S(n)  = scaling coefficient vector
!
!  Local Variables
!  i     = row index
!  ip    = pivot index
!
      Integer n,i,ip,k,idum
      Integer,dimension(NEQ)::O
      Real*8 big,dum
      Real*8,dimension(NEQ)::S
      Real*8,dimension(NEQ,NEQ)::A
!
            ip=k
      big=DABS(A(O(k),k)/S(O(k)))
      Do i=k+1,n
      dum=DABS(A(O(i),k)/S(O(i)))
            If(dum.GT.big) Then
               big=dum
                     ip=i
            End if
      End Do
      idum=O(ip)
      O(ip)=O(k)
      O(k)=idum
      Return
      End Subroutine Pivot


      FUNCTION derfc(x)
      DOUBLE PRECISION derfc,x
CU    USES dgammp,dgammq
      DOUBLE PRECISION dgammp,dgammq
      if(x.lt.0.d0)then
        derfc=1.d0+dgammp(.5d0,x**2)
      else
        derfc=dgammq(.5d0,x**2)
      endif
```

```
      return
      END

      FUNCTION dgammp(a,x)
      DOUBLE PRECISION a,dgammp,x
CU    USES dgcf,dgser
      DOUBLE PRECISION gammcf,gamser,gln
      if(x.lt.0.d0.or.a.le.0.d0)pause 'bad arguments in dgammp'
      if(x.lt.a+1.d0)then
        call dgser(gamser,a,x,gln)
        dgammp=gamser
      else
        call dgcf(gammcf,a,x,gln)
        dgammp=1.d0-gammcf
      endif
      return
      END

      FUNCTION dgammq(a,x)
      DOUBLE PRECISION a,dgammq,x
CU    USES dgcf,dgser
      DOUBLE PRECISION gammcf,gamser,gln
      if(x.lt.0.d0.or.a.le.0.d0)pause 'bad arguments in dgammq'
      if(x.lt.a+1.d0)then
        call dgser(gamser,a,x,gln)
        dgammq=1.d0-gamser
      else
        call dgcf(gammcf,a,x,gln)
        dgammq=gammcf
      endif
      return
      END


      SUBROUTINE dgcf(gammcf,a,x,gln)
      INTEGER ITMAX
      DOUBLE PRECISION a,gammcf,gln,x,EPS,FPMIN
      PARAMETER (ITMAX=100,EPS=3.d-7,FPMIN=1.d-30)
CU    USES dgammln
      INTEGER i
      DOUBLE PRECISION an,b,c,d,del,h,dgammln
      gln=dgammln(a)
      b=x+1.d0-a
      c=1.d0/FPMIN
      d=1.d0/b
      h=d
      do 11 i=1,ITMAX
        an=-i*(i-a)
        b=b+2.d0
        d=an*d+b
        if(dabs(d).lt.FPMIN)d=FPMIN
        c=b+an/c
        if(dabs(c).lt.FPMIN)c=FPMIN
        d=1.d0/d
        del=d*c
        h=h*del
```

```
      if(dabs(del-1.d0).lt.EPS)goto 1
11    continue
      pause 'a too large, ITMAX too small in dgcf'
1     gammcf=dexp(-x+a*dlog(x)-gln)*h
      return
      END

      SUBROUTINE dgser(gamser,a,x,gln)
      INTEGER ITMAX
      DOUBLE PRECISION a,gamser,gln,x,EPS
      PARAMETER (ITMAX=100,EPS=3.d-7)
CU    USES dgammln
      INTEGER n
      DOUBLE PRECISION ap,del,sum,dgammln
      gln=dgammln(a)
      if(x.le.0.d0)then
        if(x.lt.0.d0)pause 'x < 0 in dgser'
        gamser=0.d0
        return
      endif
      ap=a
      sum=1.d0/a
      del=sum
      do 11 n=1,ITMAX
        ap=ap+1.d0
        del=del*x/ap
        sum=sum+del
        if(dabs(del).lt.dabs(sum)*EPS)goto 1
11    continue
      pause 'a too large, ITMAX too small in dgser'
1     gamser=sum*dexp(-x+a*dlog(x)-gln)
      return
      END


      FUNCTION dgammln(xx)
      DOUBLE PRECISION dgammln,xx
      INTEGER j
      DOUBLE PRECISION ser,stp,tmp,x,y,cof(6)
      SAVE cof,stp
      DATA cof,stp/76.18009172947146d0,-86.50532032941677d0,
     *24.01409824083091d0,-1.231739572450155d0,.1208650973866179d-2,
     *-.5395239384953d-5,2.5066282746310005d0/
      x=xx
      y=x
      tmp=x+5.5d0
      tmp=(x+0.5d0)*dlog(tmp)-tmp
      ser=1.000000000190015d0
      do 11 j=1,6
        y=y+1.d0
        ser=ser+cof(j)/y
11    continue
      dgammln=tmp+dlog(stp*ser/x)
      return
      END
```

Input data set used to simulate the transport of 200 ppm chromium (acetate ion) solution through dolomite core

To illustrate the program's input requirements, input data set to simulate the transport of 200 ppm chromium (acetate ion) solution through dolomite core are given below.

In data set of Input.dat, parameters of AR(I,J), B(I,J), Z(I), XK(I) are given, where
AR(I,M): STOICCHIOMETRIC COEFFICIENT OF ELEMENT I IN FLUID SPECIES M.
B(I,M); EXPONENT OF THE INDENPENDT FLUID SPECIES CONCENTRATION WHEN FLUID SPECIES I IS EXPRESSED IN Ms.
Z(I): THE CHARGE OF THE AQUEOUS SPECIES I.
XK(I): EQUILIBRIUM CONSTANS.
Those parameters are constant.

Input.dat

```
1. 0. 0. 0. 0. 0. 0. 0. 0. 0. 0. 1. 0. 1. 0. 1. 0. 0. 0. 0. 0. 0. 0. 0.
0. 1. 0. 0. 0. 0. 0. 0. 0. 0. 0. 0. 1. 0. 1. 0. 1. 0. 0. 0. 0. 0. 0. 0.
0. 0. 1. 0. 0. 0. 0. 0. 0. 0. 0. 0. 0. 1. 1. 1. 1. 1. 1. 0. 0. 0. 0. 0.
0. 0. 0. 1. 0. 0. 0. 0. 0. 2. 1. 1. 1. 0. 0. 1. 1. 1. 2. 1. 2. 2. 1. 3.
0. 0. 0. 0. 1. 0. 0. 0. 0. 0. 0. 0. 0. 0. 0. 0. 0. 0. 0. 0. 0. 0. 0. 0.
0. 0. 0. 0. 0. 1. 0. 0. 0. 0. 0. 0. 0. 0. 0. 0. 0. 0. 0. 0. 0. 0. 0. 0.
0. 0. 0. 0. 0. 0. 1. 0. 0. 0. 0. 0. 0. 0. 0. 0. 0. 0. 0. 1. 1. 1. 0. 1.
0. 0. 0. 0. 0. 0. 0. 1. 0. 0. 0. 0. 0. 0. 0. 0. 0. 0. 0. 0. 1. 1. 0.
0. 0. 0. 0. 0. 0. 0. 0. 1. 0. 0. 0. 0. 0. 0. 0. 0. 0. 0. 0. 0. 0. 0. 0. (*AR*)

1.  0.  0. 0. 0. 0. 0. 0. 0. 0.
0.  1.  0. 0. 0. 0. 0. 0. 0. 0.
0.  0.  1. 0. 0. 0. 0. 0. 0. 0.
0.  0.  0. 1. 0. 0. 0. 0. 0. 0.
0.  0.  0. 0. 1. 0. 0. 0. 0. 0.
0.  0.  0. 0. 0. 1. 0. 0. 0. 0.
0.  0.  0. 0. 0. 0. 1. 0. 0. 0.
0.  0.  0. 0. 0. 0. 0. 1. 0. 0.
0.  0.  0. 0. 0. 0. 0. 0. 1. 0.
0.  0.  0. 0. 0. 0. 0. 0. 0. 1.
0.  0.  0. -1. 0. 0. 0. 0. 0. 0.
1.  0.  0. -1. 0. 0. 0. 0. 0. 0.
0.  1.  0. -1. 0. 0. 0. 0. 0. 0.
1.  0.  1. 0. 0. 0. 0. 0. 0. 0.
0.  1.  1. 0. 0. 0. 0. 0. 0. 0.
1.  0.  1. 1. 0. 0. 0. 0. 0. 0.
0.  1.  1. 1. 0. 0. 0. 0. 0. 0.
0.  0.  1. 1. 0. 0. 0. 0. 0. 0.
0.  0.  1. 2. 0. 0. 0. 0. 0. 0.
0.  0.  0. -1. 0. 0. 1. 0. 0. 0.
0.  0.  0. -2. 0. 0. 1. 0. 0. 0.
0.  0.  0. -2. 0. 0. 1. 1. 0. 0.
0.  0.  0. 1. 0. 0. 0. 1. 0. 0.
0.  0.  0. -3. 0. 0. 1. 0. 0. 0. (*B*)

+2 +2 -2 +1 +1 -1 +3 -1 -2 0 -1 1 1 0 0 1 1 -1 0 2 1  0 0 0 (*Z:CHARGE*)
1. 1. 1. 1. 1. 1. 1. 1. 1. 1. 1.009E-14 1.205E-13 3.887E-12 1.585E+3 8.318E+2 3.548E+11 5.888E+11 2.138E+10
3.981E+16 1.0E-4 2.399E-10 6.9E-6 5.715E+4  1.778E-17 (*XK:KEQ*)
```

In data set of Inputchen200ppm.dat, users define the following parameters:
The physical parameters of the core used which include length, porosity, specific surface area and the compositions of the core.
The experimental conditions which include the compositions of the initial and injected solutions, the injected pore volumes, the residence time.
The node points and the time step size.
The notation of the parameters are shown below:
NJ: ACTUAL NUMBER OF NODE POINTS.
TIME: TOTAL PORE VOLUME SIMULATED.
S0: SPECIFIC SURFACE AREA.
PHI: POROSITY.
DT: TIME STEP.
THKX: LENGTH OF CORE IN CM.
RETIME: RESIDENCE TIME IN MINUTES**.**
CAINJ, XMGINJ, CO3INJ, XKINJ, CLINJ, CRINJ, ACINJ, SO4INJ, PHINJ: the Composition of the injected solutions. PHINJ could be estimated value if pH is unknown.
CAINI, XMGINI, CO3INI, XKINI, CLINI, CRINI, ACINI, SO4INI, PHINI: the Composition of the initial solutions. PHINI could be estimated value if pH is unknown.

Inputchen200ppm.dat

```
25  2.0  3859.  0.23  0.0017  6.5  120. (*NJ, TIME(PV), S0, PHI,DT,THKX,RETIME (in mins)*)

1.E-30 1.E-30 1.E-30 0.1345 0.1345 3.864E-3 1.1538E-2 1.E-30 7.0
(*CAINJ,XMGINJ,CO3INJ,XKINJ,CLINJ,CRINJ,ACINJ,SO4INJ,PHINJ*)
1.E-30 1.E-30 1.E-30 0.1345 0.1345 1.E-30 1.E-30 1.E-30 7.0
(*CAINI,XMGINI,CO3INI,XKINI,CLINI,CRINI,ACINI,SO4INI,PHINI*)


0 (*.IFLAG(2),PH FOR INJECTED SOLUTION. 1, PH KNOWN,0, PH UNKNOWN*)
0 (*.IFLAG(1),PH FOR INITIAL SOLUTION. 1, PH KNOWN,0, PH UNKNOWN*)

1 0 0 (*IMINERAL(1):DOLOMITE, IMINERAL(2):CALCITE, IMINERAL(3):ANHYDRITE. 1 INCLUDES
SPECIFIED MINERALS, 0 NO THIS MINERALS)

1.0 (*CM1SET FOR CALCITE SUPERSATURATION INDEX*)
```

Chapter 7

Effects of Gelant Composition and Pressure Gradients of Water and Oil on Disproportionate Permeability Reduction of Sandpacks Treated with Polyacrylamide-Chromium Acetate Gels

Graduate Research Assistant: Tuan Nguyen

Introduction

High water production is a major concern in mature hydrocarbon reservoirs. Costs of handling and disposing of water produced from oil reservoirs often shorten the life of a production well. Disposal of the water is also an environmental concern. In order to reduce water production, polymer gels have been used to modify the mobility of water and oil in petroleum reservoirs.

When some gels are placed in a petroleum reservoir, permeability reduction occurs to a much greater extent for water than for oil. This phenomenon is known as favorable DPR. Reduced permeability to water can lead to decreased production of water, and sometimes increased oil production, thereby prolonging the useful life of the reservoir. Results reported in the literature have shown that the application of several polymer gel systems can result in DPR. Mechanisms for DPR have been debated, and the magnitude of the effect has been unpredictable from one application to another. Mechanisms for DPR that have been proposed and studied by several researchers are shown in Table 7.1.

The usual method to study DPR is to saturate a porous medium with gelant, allow time for gelation to occur, and then inject oil and water to steady-state conditions and determine permeabilities at 100% fractional flow of each fluid. One aspect of this procedure that most of these experimental works do not describe or examine is the process that occurs when oil or water is first injected into the gel-treated porous media. It is our experience that the medium has very little permeability at the start of injection and that considerable time is required for the injected fluid to develop channels or flow paths through the system before a steady state is approached. Several mechanisms might be involved to produce flow channels. Dawe and Zhang [1994[visually observed the process for the injection of oil and water through a gel placed in a porous micromodel. For a water-wet micromodel, they described water breaking the gel in the center of the pores and most of the gel adhering to the pore walls. Oil similarly flowed through the channels in the center of the pores and was accompanied by “water inside the gel…being pressed out of the gel structure” which widened the channel. They also observed that “some gel was destroyed and became fiber-like…and was easily washed away by the flowing oil.” In our experiments, oil is first injected into gel-filled sandpacks, and flow channels are formed over the time period of several days and the channels occupy a considerable portion of the initial gel volume. It is thought that the channel volume is formed by both displacement and dehydration of portions of the gel in accordance with the visual observations of Dawe and Zhang [1994]. Permeabilities to both oil and water are reduced as compared to their permeabilities prior to gel treatment. High oil saturations in the channels during water flow cause the water permeability to be reduced by a significant factor while during oil flow the oil saturates most of the channel volume resulting in a much smaller reduction in the oil permeability [Willhite et al. 2002]. Presumably the flow channels through the gel have smoother walls and are more water-wet than

Table 7.1 – Proposed mechanisms for disproportionate permeability reduction.

1	Gels swell in water but shrink in oil.	Dawe and Zhang (1994); Gales et al. (1994); Liang et al. (1995); Sparlin and Hagen (1984)
2	Gravity affects gel locations in pores.	Liang et al. (1995)
3	Lubrication effects.	Sparlin and Hagen (1984) Zaitoun and Kohler (1988)
4	Gels constrict water pathways more than oil pathways in a given pore (wall effects).	Liang and Seright (1997); Liang et al. (1995); Zaitoun et al. (1998)
5	Segregated pathway theory.	Liang and Seright (1997); Liang et al. (1995); Nilson et al. (1998); White et al. (1973)
6	Effect of capillary forces and gel elasticity on oil and water flow.	Al-Sharji et al. (1999); Liang and Seright (1997)
7	During brine injection, polymer leaches from the gel and significantly decreases the brine mobility.	Liang and Seright (1997)
8	Gels alter rock wettability.	Zaitoun et al. (1998)
9	Pore blocking by gel droplets.	Liang and Seright (2001); Nilson et al. (1998)
10	Channels for oil and water flow are created by gel dehydration and displacement.	Dawe and Zhang (1994); Green et al. (1998); Willhite et al. (2002)
11	High residual oil saturations in flow channels during water flow and low residual water saturations in flow channels during oil flow.	Green et al. (1998); Willhite et al. (2002)

the sandpack before the gel treatment. These factors are likely responsible in part for the observed changes in residual fluid saturations and endpoint permeabilities.

This chapter presents the results of a study on the effects of gel composition and applied pressure gradients on the magnitude of residual resistance factors and DPR during the flow of water and oil through gel-treated sandpacks. Additionally, material balances on the phases and components in the sandpacks during flow experiments were conducted to give insights into mechanisms that are responsible for channel development and for permeability reduction.

Experimental Equipment, Materials, and Procedures

A schematic of the experimental setup to conduct flow experiments is displayed in Figure 7.1. Pumps injected fluids at constant pressure or flow rate through the sandpacks, and effluent was collected in fractions. Pressure drops across the entire sandpack length and each of the six, 2-in.-long sections were monitored and recorded by pressure transducers and a data acquisition system. The experimental system was maintained at 30°C.

Various compositions of Cr(III)-acetate-polyacrylamide gelant were injected into the sandpacks that contained brine at residual oil saturations and allowed to gel. Oil was then injected into the sandpacks at a constant pressure drop to develop channels through the gel. Brine- and oilfloods

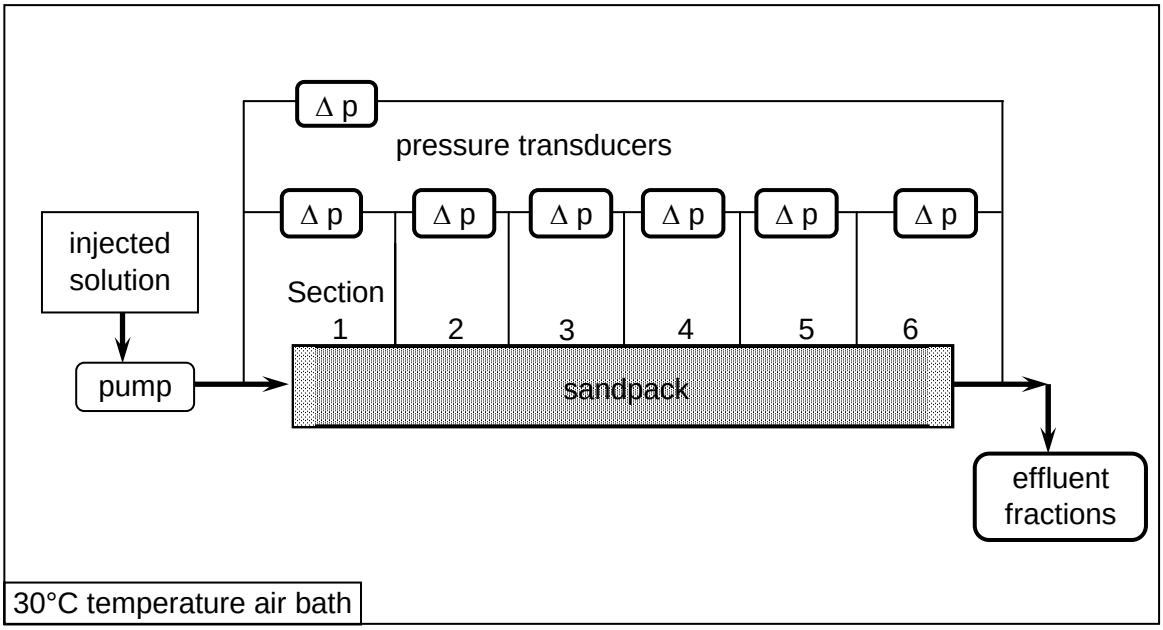

Figure 7.1 - Schematic of equipment for flow experiments.

were then conducted to determine endpoint permeabilities, residual resistance factors, and selectivity. Additional experimental details can be found in Nguyen [2003].

Sandpacks. Sandpacks were prepared by packing silica sand (F110, U.S. Silica Co.) in 1-ft-long holders. The sand holders were fabricated from acrylic tubes with an ID of 1.5 in. End caps were attached to both ends of the holder body and sealed with O-rings. The end caps had fittings at the center to allow fluid to flow in and out. Grooves cut on the inner face of the end caps provided a more uniform distribution of fluid across the entrance and exit faces of the sandpacks. Fine (330-mesh) and coarse (37-mesh) screens were placed at the end caps to prevent sand from exiting the pack. Fine F110 sand, grain size from 50 to 270 mesh, was acid-washed before packing. The sand was manually packed using a vibrator. A 1.5-cm length of coarse sand was packed adjacent to the screens in Sections 1 and 6. Plastic screens of 215-mesh were placed in pressure ports to prevent sand particles from entering tubing connections to the transducers.

Sections 1 and 6 were partially packed with coarse sand so the average values of the internal sections, Sections 2 through 5, were used to calculate permeability and quantities derived from permeabilities (residual resistance factors and selectivity). Values determined for the entire sandpack volume were used for pore volume, porosity, and saturations.

Injected Liquids. The gelants were prepared using partially hydrolyzed polyacrylamide and chromium(III) acetate. The polymer was Alcoflood 935 (Ciba Specialty Chemicals, Lot No. A2247 BOV. The molecular weight of this polymer was around 6 million daltons. Cr(III) stock solution was prepared from a Cr(III) acetate solution that contained 12.4% Cr(III) and 42.2% acetate by weight (McGean Rohco, Lot No. 40086816). The acetate-to-Cr(III) mole ratio was 3:1. The polymer-to-Cr(III) mass ratio in the gelants was maintained at 40:1. All gelants

contained 1.0% KCl and 10 ppm sodium azide (bactericide).

The oil used was n-dodecane. Stilbene tracer at a concentration of 100 ppm was in the residual oil phase prior to gelant injection into the sandpacks. Stilbene tracer was also used at a concentration of 10 ppm to determine mobile oil volume in the pack after gel treatment. The brine was a 1% KCl solution. KNO_3 was used as a tracer in water or brine at a concentration of 0.1 moles/L.

Procedures for Flow Experiments. The sequence of runs conducted in each sandpack is listed in Table 7.2. The prepared sandpack was saturated with water and porosity was determined by weight. Water was injected and permeabilities determined. Porosity was verified using an aqueous tracer. Oil with a 100-ppm stilbene tracer was then injected at a constant flow rate of 21 mL/min to achieve and determine a residual water saturation (S_{wr}), and the permeability to oil (k_o) at S_{wr}. The stilbene tracer in the oil allowed for the determination of the amount of residual oil that was displaced from the pack during injections after the gel treatment. Brine was then injected at 21 mL/min to achieve and determine the residual oil saturation (S_{or}) and the permeability to water (k_w) at S_{or}. S_{or} was determined both by weight and volume methods and verified by tracer tests. S_{or} determined by tracer tests was used because it was deemed to be the most accurate of the three methods. Sandpack properties were consistent as shown by the range of property values listed for Runs 0 to 6 in Table 7.2.

Gelants were bulk mixed and immediately injected into the sandpacks by a transfer cylinder. Approximately three pore volumes of gelant were injected at a flow rate of 4 mL/min. The sandpack was then shut in for a time period that was at least twice the bulk gel time to allow the gelant to mature before the injection of oil.

After the shut-in period, oil was injected (Run 9) at a constant pressure drop of 20 psi, which is equivalent to a average pressure gradient of 20 psi/ft, to create channels through the gelled sandpack. Effluent samples of brine and oil were collected in fractions. Brine in the samples was analyzed for polymer and Cr(III) concentrations and oil in the samples was analyzed for stilbene. The stilbene tracer allowed for the calculation of the amount of pretreatment residual oil that was displaced from the pack. Connections between the ports on the sandpack and the pressure transducers were closed during the relatively long process to develop channels through the pack. This was done to eliminate brine from displacing oil in the transducer tubings so that material balances performed on the sandpacks would be more accurate.

The channel development process was terminated when the brine production rate was less than 1mL/day for weak gels and 0.5 mL/day for strong gels, except in Sandpacks TN007 and TN010. The brine production rate was 2 mL/day for TN007 and 4 mL/day for TN010 when oil injection was terminated. The exit screens in Sandpack TN004 became partially blocked on the second day of oil injection and most of the applied pressure drop was observed across Section 6, leaving a reduced pressure gradient across the remainder of the pack length. TN004 was then brine flooded at the reduced pressure gradient. The exit screens were replaced after the brineflood and a second channel development process was conducted by an oilflood at an average pressure gradient of 20 psi/ft (the average pressure gradient across the internal sections was 22.9 psi/ft).

Table 7.2 – Sequence of experiments in each sandpack**.**

Run	Experiment	Pressure Gradient (psi/ft	Comments
0	Pack preparation		Packed sand and saturated porosity with water. Porosity ranged from 33.1 to 34.1%.
1	Base permeability		Water was injected stepwise at 10 different rates. Permeability ranged from 4.1 to 4.5 Darcy.
2	Tracer test		Verification of pore volume.
3	Brine saturation		Water was displaced by 1.0% KCl brine.
4	Oilflood		Oil was injected until negligible amount of brine was displaced. S_{wr} ranged from 13 to 15%. k_o at S_{wr} ranged from 3.49 to 3.74 Darcy.
5	Brineflood		Brine was injected until negligible amount of oil was displaced. k_w at S_{or} ranged from 2.31 to 2.98 Darcy.
6	Tracer test		Verification of S_{or}. S_{or} ranged from 13 to 17%.
7	Gelant injection		Gelant was injected into the sandpack.
8	Shut-in period		Sandpack was shut in to allow for gelation.
9	Oilflood	20	Oil was injected to develop channels. Run terminated when a negligible amount of brine was produced.
10	Brineflood	20	Brine was injected until oil displacement was negligible.
11	Rate test	1–23	Brine was injected at various flow rates in a range such that pressure gradients did not exceed 20 psi/ft.
12	Oilflood	20	Oil was injected until brine displacement was negligible.
13	Rate test	1 – 23	Oil was injected at various flow rates in a range such that pressure gradients did not exceed 20 psi/ft.
14	Oilflood	50	Oil was injected to further develop channels. Run terminated when a negligible amount of brine was produced.
15	Brineflood	50	Brine was injected until oil displacement was negligible.
16	Rate test	3–57	Brine was injected at various flow rates in a range such that pressure gradients did not exceed 50 psi/ft.
17	Oilflood	50	Oil was injected until brine displacement was negligible.
18	Rate test	2–53	Oil was injected at various flow rates in a range such that pressure gradients did not exceed 50 psi/ft.
19	Tracer test		Oil tracer was injected to verify mobile oil volume (based on material balance).

After oil injection at 20 psi/ft, brine was injected at a constant pressure of 20 psi (Run 10), which is equivalent to an average pressure gradient of 20 psi/ft, until oil displacement was negligible. Effluent fractions containing oil and brine were collected and analyzed as was done in Run 9. Rate tests (Run 11) were then conducted by injecting brine at various flow rates over a range such that the overall pressure gradient did not exceed a pressure gradient of 20 psi/ft. This was done to determine whether permeability and residual resistance factor to water were a function of pressure gradient and to determine the reproducibility of the results.

Oil was then injected at an overall pressure gradient of 20 psi/ft (Run 12) until brine displacement was negligible. Effluent brine and oil samples were collected and analyzed. Rate tests were then conducted during oil injection (Run 13) at pressure gradients not exceeding 20 psi/ft and endpoint permeabilities to oil at various pressure gradients were determined.

Injections of oil and brine at pressure gradients of 50 psi/ft were conducted in sandpacks containing strong gels that were prepared with polymer concentrations of 3,000 ppm or higher. Oil was injected in Run 14 to determine the effect of the higher pressure gradient on the development of flow channels through the sandpacks. The procedure for Run 14 was the same as for Run 9, except the pressure gradient was 50 psi/ft. This was followed by a brineflood at 50 psi/ft (Run 15). Brine was then injected at different rates (Run 16) to determine the effect of pressure gradient on permeability measurements. An oilflood at 50 psi/ft (Run 17) was conducted followed by oil-rate tests (Run 18). The rate tests were conducted at pressure gradient values of 50 psi/ft or less.

A tracer test during the injection of oil (Run 19) was conducted to determine the volume of displaceable oil contained in the channels or "new" pore volume. Oil containing 10 ppm stilbene was injected and the effluent concentration of stilbene was determined as a function of the volume of oil injected. Integration of these data determined the displaceable oil in the "new" pore space. This tracer test was conducted after Run 13 for the sandpacks where the weaker gels containing less than 3000 ppm polymer were placed.

Analytical Measurements. Effluent samples collected during oil- and brinefloods (Runs 9 to 17) were analyzed for stilbene concentration in the oil and for polymer and Cr(III) concentrations in the brine. Stilbene was analyzed with a UV/Vis spectrometer at a wavelength of 296 nm. The KNO_3 tracer in brine or water phases was determined by absorbance at a wavelength of 302 nm. Polymer concentration in the brine samples was determined by measuring total organic carbon (TOC) using a Shimadzu TOC 5000 A. The TOC data were converted to polymer concentrations, assuming the samples did not contain carbon from the acetate ions. Carbon from the acetate ions corresponded to 7% of the carbon from the polymer in the gelant formulations. Cr(III) in the brine samples was converted to Cr(VI) using 1% H_2O_2 and 1 N KOH, and the chromium concentration was then determined by measuring absorbance at a wavelength of 373 nm (UV/Vis Lambda 20 Spectrometer). Detailed procedures are given by Nguyen [2003].

Bottle tests were conducted at 30°C to determine bulk gel times and to monitor syneresis of the gels. Small samples were withdrawn at different times for viscosity measurement in a cone-and-plate geometry at two different shear rates. When the viscosity was less than 103 cp, a shear rate of 22.5 s^{-1} was used, and when the viscosity of gelant was greater than 103 cp, the samples were

sheared at a rate of 2.25 s^{-1}. Gel time was defined as the time when the viscosity of gelant reached 1000 cp. However, for the gelant with polymer concentration of 2,100 ppm, the gel time was taken as 27 days when the viscosity of the gelant reached 300 cp. The viscosity of this weak gelant was still approximately 300 cp after 7 months.

Results and Discussion

Bulk Gel Time and Gel Syneresis. Bottle tests were used to determine bulk gel times and to monitor the gels for syneresis. Gel times decreased significantly with polymer concentration as shown in Figure 7.2. Gels containing 4,000-, 3,000-, and 2,500-ppm polymer and a polymer-to-Cr(III) mass ratio of 40:1 underwent slight syneresis after 3.5 months at 30 °C. The syneresis volume was less than 1.2% of the gel volume after 4 months. Effluent samples of gel collected during gelant injection for the flow experiments were also monitored. No syneresis was observed during the 3-month time period required for the post-treatment oil- and brinefloods.

Channel Development. Volume balances on the oil and brine contained in the packs and chemical analyses on the oil and brine effluents from the packs were interpreted to conceptualize the fluid flow behavior that occurred before, during, and after the gel treatments. It was assumed after gelant injection and the following shut-in time period that the pack was fully saturated with gel and residual oil that was encapsulated by the gel. The volume of gel removed was equated to the aqueous volume produced during the initial oilflood.

Flow channels developed slowly through the gelled sandpacks when oil at 20 psig was applied to the inlet. Brine production at the outlet started between 8 and 150 minutes after contact by the pressurized oil. Longer elapsed times before brine production correlated with higher concentrated gels as listed in Table 7.3 along with other results related to the channel.

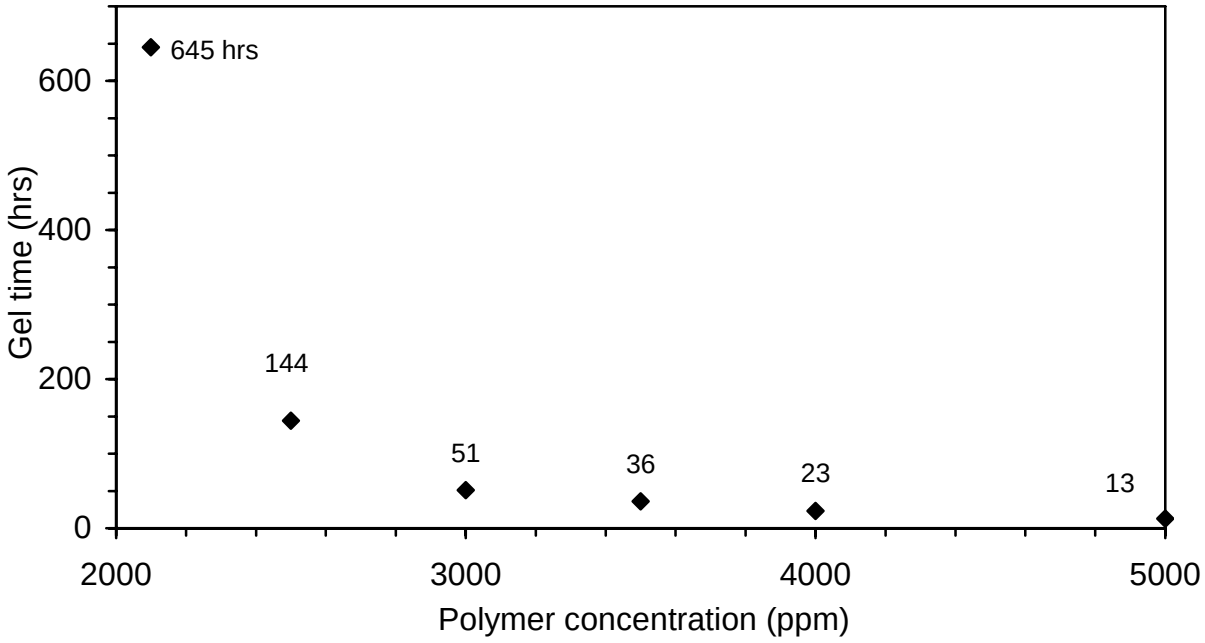

Figure 7.2 - Bulk gel times as a function of polymer concentration.

Table 7.3 – Development of flow channels during oil injection at 20 psi/ft.

Sandpack No.	Polymer Conc. of Injected Gelant (ppm)	Elapsed Time Between Start of Oil Injection and Production of Aqueous Phase (minutes)	Total Time of Oil Injection (hours)	Volume Fraction of Gel Converted to Flow Channels (%)	Fraction of Polymer Recovered (%)	Avg. Polymer Conc. of Gel Remaining in Sandpack (ppm)	[Displacement] Vol. Fraction of Gel Removed at Initial Conc. (%)	[Dehydration] Vol. Fraction of Gel Removed as Brine (%)	Total Channel Volume (% of pore space)
TN010*	2100	8	33	67	43	3500	65	35	-
TN004	2500	10	170	67	29	5300	44	56	76
TN009	2500	13	210	66	28	5300	43	57	71
TN007*	3000	10	210	57	23	5400	40	60	64
TN006	3500	30	672	66	24	7800	36	64	-
TN011	3500	75	991	65	13	8900	20	80	72
TN003	4000	150	941	68	45	6900	66	34	73

*Oilflood terminated early.

development process. After brine was produced for a few minutes, oil breakthrough occurred and a mixture of brine and oil was displaced from the sandpacks. The aqueous phase was fluid with no visible gel fragments. The time required to develop channels also increased with gelant concentration as listed in Table 7.3 and shown in Figure 7.3 where the volume fraction of gel removed (aqueous phase produced) is plotted as a function of time from start of oil injection. The volume fraction of gel that was converted to flow channels ranged from 65 to 68% and was not a strong function of polymer concentration. Volume fractions for Sandpacks TN004 and TN007 were possibly lower than for the other sandpacks because oil injection was terminated prematurely as described in the experimental section.

Polymer concentrations in the aqueous effluent during the initial oilflood at 20 psi/ft were normalized to polymer concentrations in the injected gelant, and are shown in Figure 7.4 as a function of the aqueous volume produced in the effluent. Polymer concentrations in the effluent were always less than in the injected gelant and generally decreased with volume produced. With the exception of TN003, the profile of the normalized polymer concentrations were lower with increased concentrations of the injected gelant. The fraction of polymer recovered during oil injection was less than the fraction of gel converted to flow channels, and is indicative that dehydration of the gel occurred. The channel development process increased the average polymer concentration of the gel remaining in the pack as shown in Table 7.3.

A simple model describing the aqueous production is that a portion of the production represents the displacement of gelant at the polymer concentration of the injected gelant and the remaining portion represents dehydration of the gelant resulting in brine production without polymer present. It is noted that the aqueous effluent samples were visually homogeneous, not composed of gel fragments and brine. Percentages of these two mechanisms for channel development through the gelled sandpacks are given in Columns 8 and 9 of Table 7.3. The fraction of the channel that was developed by dehydration increased with polymer concentration in the gelant with the exception of TN003. We suspect but cannot confirm a problem with the polymer analysis of effluent in TN003, as indicated by the erratic values of polymer concentration shown in Figure 7.4. The portions of channel development attributed to gel dehydration are conservative estimates in that the percentage of polymer recovered from the pack is quite likely overstated for several reasons. First, values of the polymer recovered in Table 7.3 are probably higher than the actual values, because the effluent samples likely contained acetate and the measured TOC values were attributed solely to polymer content in the calibration for the analysis. (see the experimental section). Second, average polymer concentrations of the gel initially in the sandpack are likely at higher levels than the injected concentration because of retention of polymer during the gelant injection process. Third, it is possible that polymer molecules or aggregates that are not attached to the gel network are squeezed out of the gel by the dehydration process rather than by gel displacement.

Our conceptual model is that channel development occurs by gel displacement and gel dehydration as well from the reconnection of residual oil ganglia during oil injection. Tracer in the residual oil phase allowed for the determination of the volume of residual oil that was reconnected and produced from the packs. Total channel volume by the three mechanisms as percent of the pore space is listed in the last column in Table 7.3. Tracer analysis of the oil

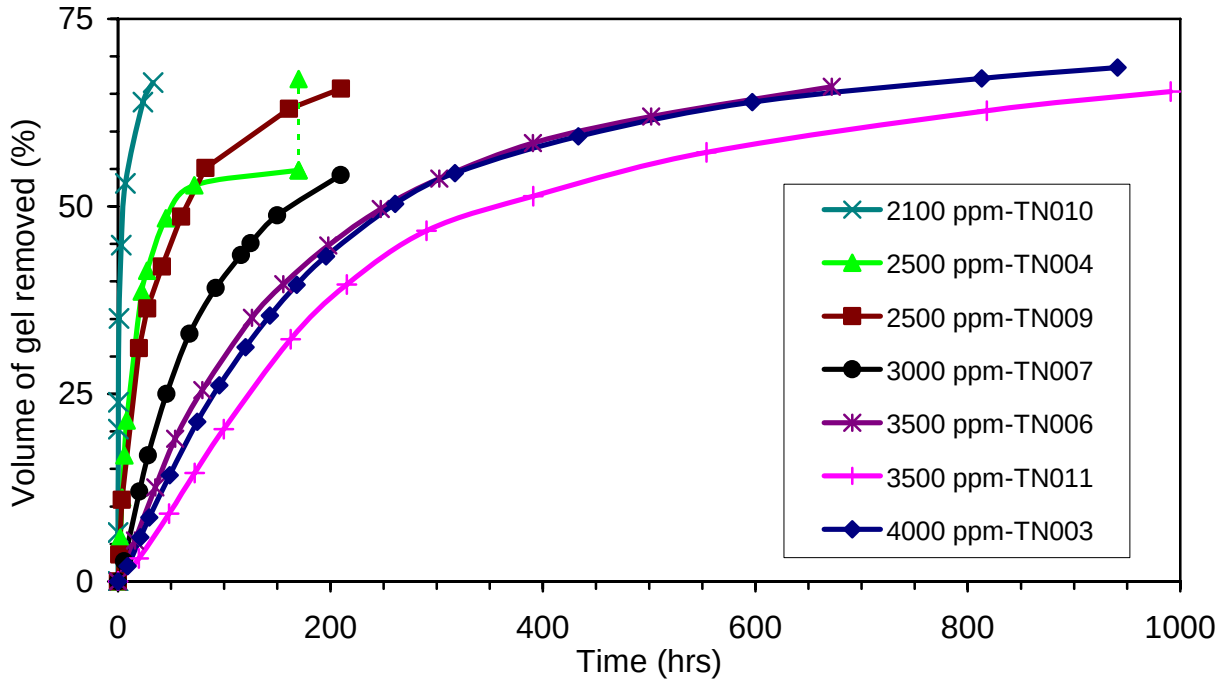

Figure 7.3 - Volume of gel removed as a function of time during oilflood at pressure gradient of 20 psi/ft.

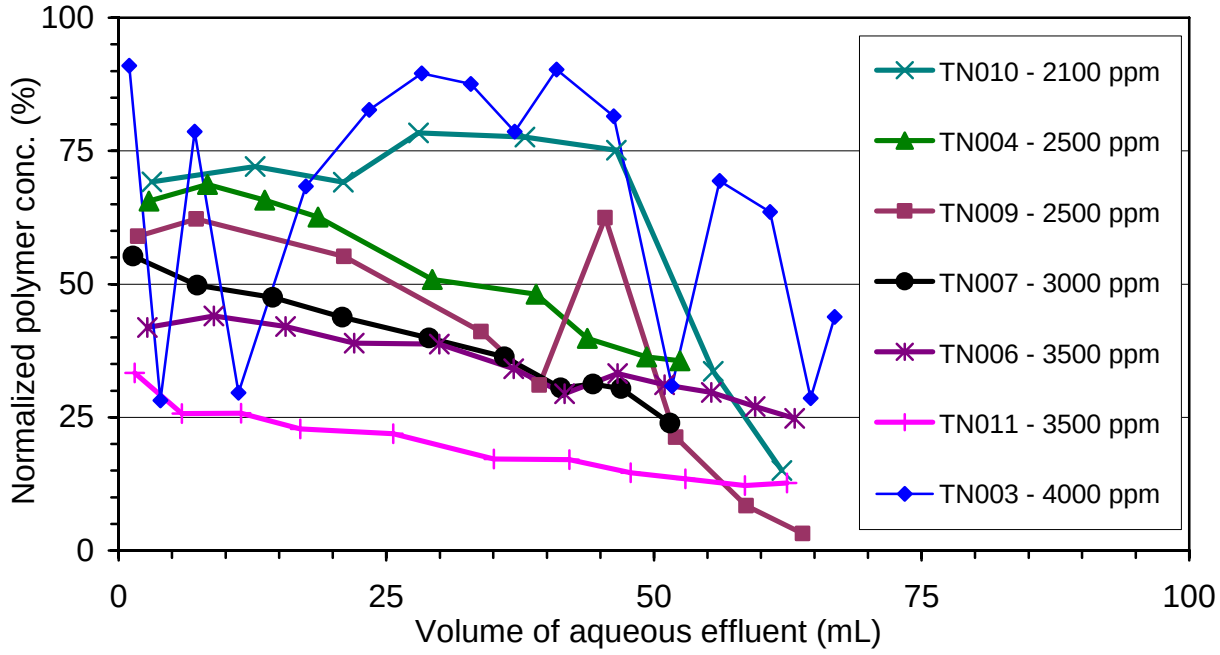

Figure 7.4 - Polymer production in aqueous phase during oilflood at pressure gradient of 20 psi/ft.

production was not conducted for Sandpacks TN0110 and TN006. Early termination of the oilflood resulted in lower channel volumes for TN004 and TN007.

Krishnan et al. [2000] showed that the amount of dehydration of bulk gels by pressurized oil was a function of the applied pressure. Sandpacks containing gel with polymer concentrations of 3,000 ppm and greater were subjected to an additional oilflood at the higher pressure gradient of 50 psi/ft. An additional 2 to 5% of the original gel volume was removed, indicating that the channel development process was a weak function of pressure gradient. Values of the fraction of gel removed, the fraction of polymer recovered, and the average polymer concentration of the gel remaining in the sandpacks after all the oil and brine displacements were conducted are listed in Table 7.4. Comparison of Tables 7.3 and 7.4 show small increases in the fraction of the gel removed and relatively larger increases in the fraction of polymer recovered. Polymer in the pack was solubilized in the brine and removed during brinefloods that were conducted after the initial oilflood at a pressure gradient of 20 psi/ft. It was assumed that the polymer was insoluble in the oil phase.

Table 7.4 – Channel development after all displacement runs.

Sandpack	Polymer Conc. in Gel (ppm)	Additional Oilflood at 50 psi/ft ?	Fraction of Gel Removed (%)	Fraction of Polymer Recovered (%)	Avg. Polymer Conc. of Gel Remaining in Sandpack (ppm)
TN010	2100	no	67	59	2600
TN004	2500	no	67	52	3600
TN009	2500	no	66	33	4500
TN007	3000	yes	59	34	4700
TN006	3500	yes	71	48	6200
TN011	3500	yes	67	54	4800
TN003	4000	yes	73	64	5400

Effluent brine samples in the post-treatment runs were also analyzed for chromium concentration. Chromium concentrations in the first aqueous sample during the initial oilflood at 20 psi/ft ranged between 54 and 67% of the chromium concentration in the injected gelant (the concentration value was likely related to sample size) and decreased with successive samples. The amount of chromium recovered and the average chromium concentration in the gel remaining in the packs after the initial oilflood at 20 psi/ft and after all oil and water displacements are given in Table 7.5. Generally, more polymer than chromium was recovered from the sandpacks, leaving a polymer-to-chromium mass ratio in the packs less than the original value of 40:1.

Permeability Reduction. Permeabilities to oil and water (brine) were determined after the gel treatment and channel development processes. Endpoint permeabilities at fractional flows of 100% were determined by the injection oil and brine at pressure drops of up to 20 psi over the 1-foot-long packs. Susequent runs at pressure drops of up to 50 psi were conducted in sandpacks

Table 7.5 - Material balances on chromium.

Sandpack	Chromium Conc. in Gel (ppm)	After Initial Oilflood at 20 psi/f		After All Oil and Water Displacements	
		Chromium Recovered (%)	Avg. Chromium Conc. of Gel Remaining in Sandpack (ppm)	Chromium Recovered (%)	Avg. Chromium Conc. of Gel Remaining in Sandpack (ppm)
TN010	52.5	35	102	43	89
TN004	62.5	29	98	37	119
TN009	62.5	28	132	33	122
TN007	75.0	26	130	36	116
TN006	87.5	21	204	27	220
TN011	87.5	21	200	30	185
TN003	100	21	250	28	267

containing gelants with polymer concentrations of 3,000 ppm or higher. Permeability data were determined over the 8-in.-long internal section (Sections 2 through 5) of the sandpacks to eliminate the influence of the coarse sand and other entrance/exit effects in Sections 1 and 6. Because the permeabilities of Sections 1 and 6 were greater than those of the internal sections, the pressure gradient over the internal sections was somewhat greater than the average pressure gradient over the entire core length. The endpoint permeability data are presented in two forms: (a) residual resistance factors for oil and for water (F_{rro}, F_{rrw}), and (b) selectivity, or the ratio of F_{rrw} to F_{rro}. Endpoint permeability to water in the channels or "new" pore space was determined by Darcy's law at various pressure gradients, and residual resistance factors for water, F_{rrw}, were determined by

$$F_{rrw} = \frac{k_{wb}}{k_{wa}}, \qquad \text{Eq. 7.1}$$

where $k_{wb}$is the permeability to water at S_{or} before the gel treatment, and k_{wa} is the permeability to water at S_{or}* after the gel treatment.

Permeability to oil was determined using Darcy's law, and the residual resistance factor for oil (F_{rro}) was determined by

$$F_{rro} = \frac{k_{ob}}{k_{oa}}, \qquad \text{Eq. 7.2}$$

where k_{ob} is the permeability to oil at S_{wr} before the gel treatment, and k_{oa} is the permeability to oil at S_{wr}* after the gel treatment.

Residual Resistance Factors. Endpoint permeabilities for both oil and water after the channel development process at 20 psi/ft were strong functions of polymer concentration, as shown in Figure 7.5, where the data are expressed as residual resistance factors defined by Equations 7.1

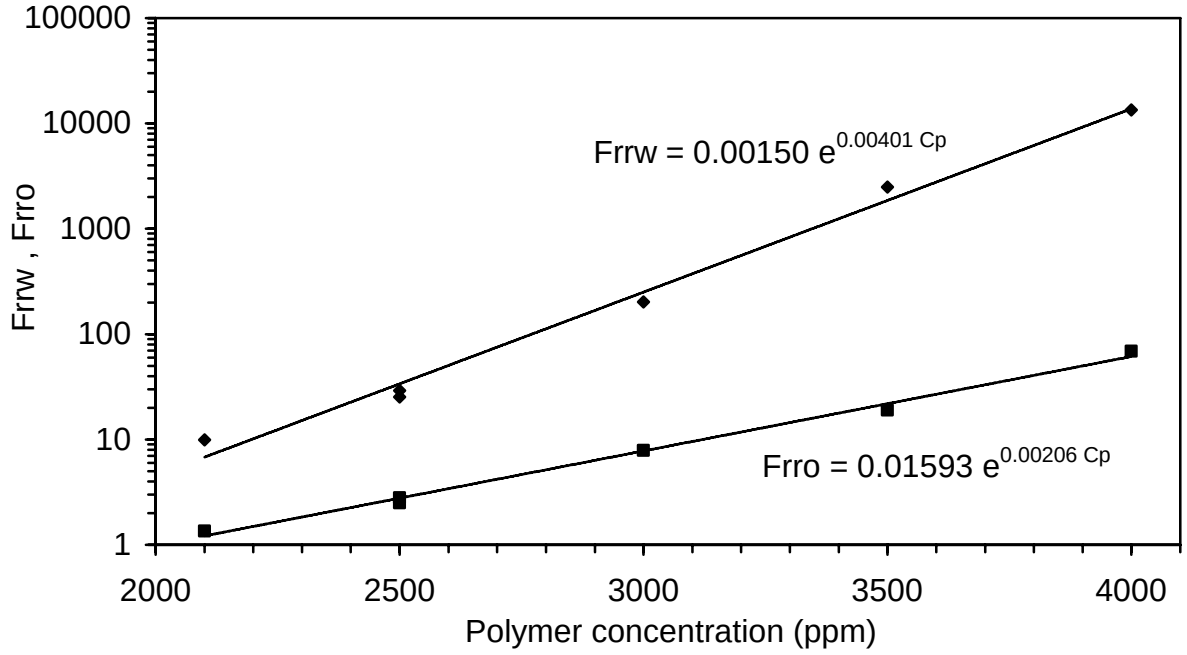

Figure 7.5 - Residual resistance factors for water and oil as a function of polymer concentration after the channel development process at a pressure gradient of 20 psi/ft.

and 7.2. Residual resistance factors decreased sharply with decreased gelant concentrations, as shown on the semilog plot and correlated by exponential functions. Residual resistance factors were much greater for water than for oil. Permeability decreased by factors from 69 to 1.3 for oil and by factors from 17,000 to 7.1 for water as polymer concentration decreased from 4,000 to 2,100 ppm.

Rate tests were conducted to determine whether endpoint permeabilities, or residual resistance factors, were a function of applied pressure gradient (or flow rate). Flow rates were varied from high to low, and some flow rates were replicated in a random order to determine whether the results were reproducible. Residual resistance factors based on endpoint permeability to oil at various pressure gradients for both strong and weak gels are shown in Figures 7.6 and 7.7, respectively. Oil permeability, and consequently F_{rro}, were not functions of the pressure gradient. Water permeability and F_{rrw} were functions of pressure gradients. As pressure gradient increased, F_{rrw} decreased (k_w increased) for strong gels, but F_{rrw} increased (k_w decreased) for weak gels as shown in Figures 7.8 and 7.9, respectively. k_o and k_w measurements were reproducible and were not a function of how the flow rate was varied. The numbers next to data points in Figures 7.6 through 7.9 indicate the order that the flow rates were varied after the initial series of flow rates (pressure gradients) which were run from high to low values.

The sandpacks containing gel with polymer concentrations of 3,000 ppm and higher were also subjected to an oilflood at a pressure gradient of 50 psi/ft. After additional channel development at 50 psi/ft, rate tests were conducted to determine the effect of pressure gradient on permeability and residual resistance factors. The residual resistance factors for oil and for water as a function of the applied pressure gradient are shown in Figures 7.10 and 7.11, respectively. F_{rro} remained relatively constant with pressure gradient while F_{rrw} decreased with increased pressure gradient.

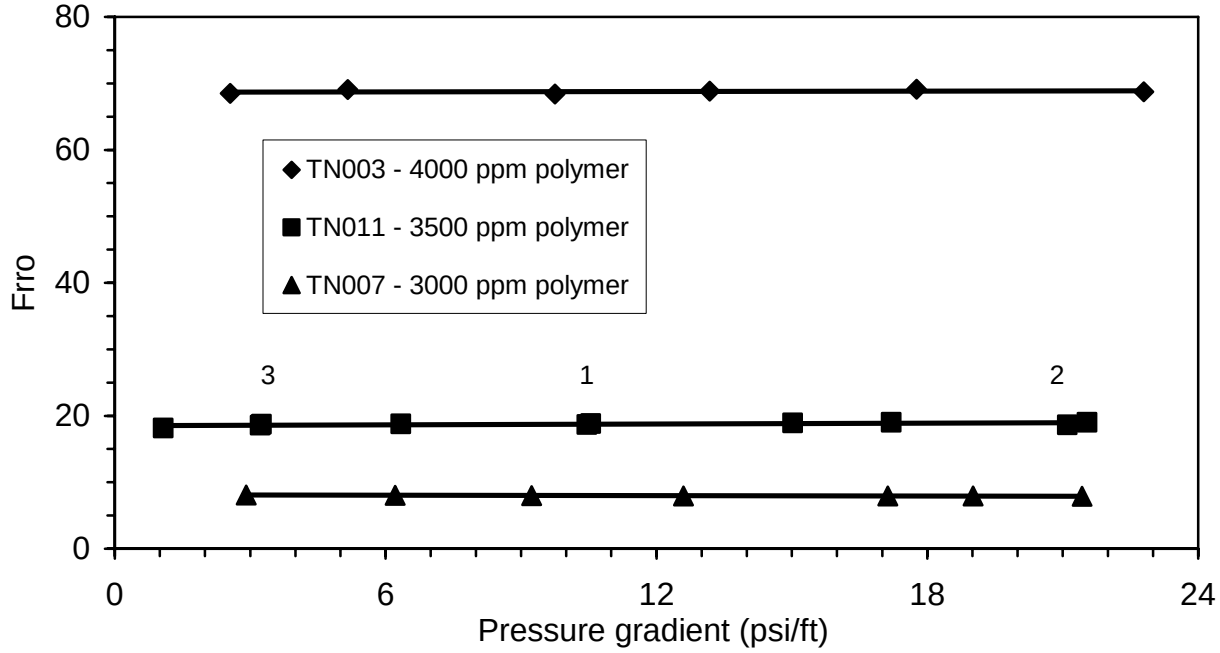

Figure 7.6 - Residual resistance factors for oil as a function of applied pressure gradient for strong gels (polymer concentrations of 3,000 ppm and higher) after the channel development process at a pressure gradient of 20 psi/ft.

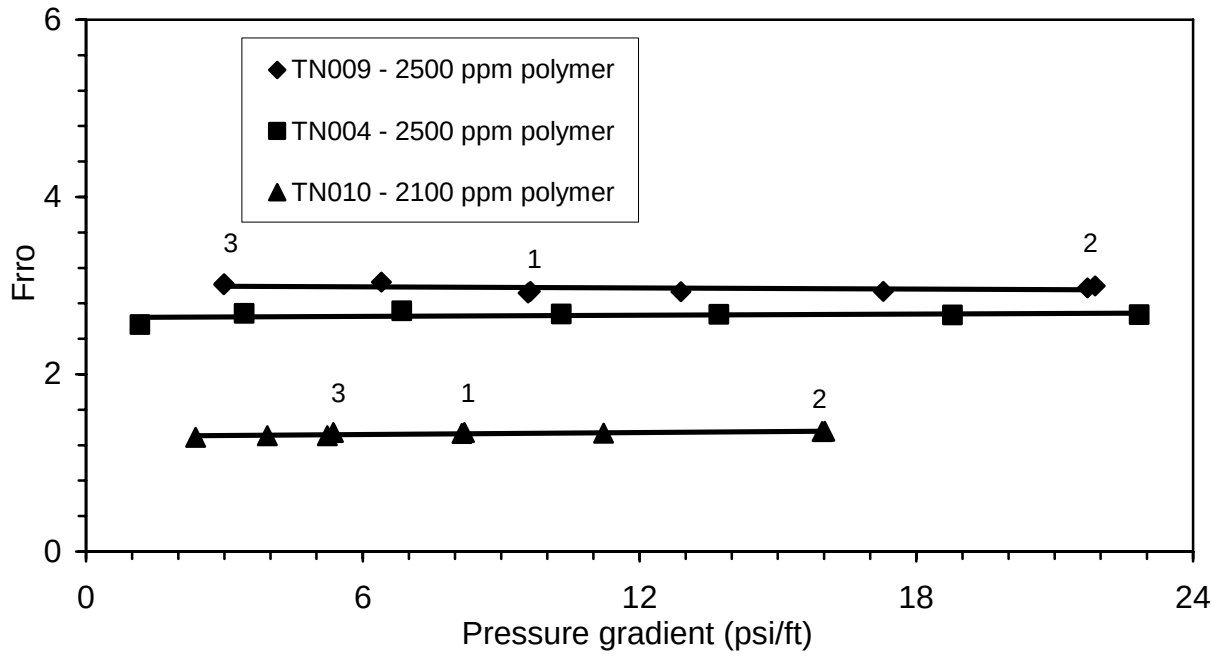

Figure 7.7 - Residual resistance factors for oil as a function of applied pressure gradient for weak gels (polymer concentrations of 2,500 ppm and 2,100 ppm) after the channel development process at a pressure gradient of 20 psi/ft.

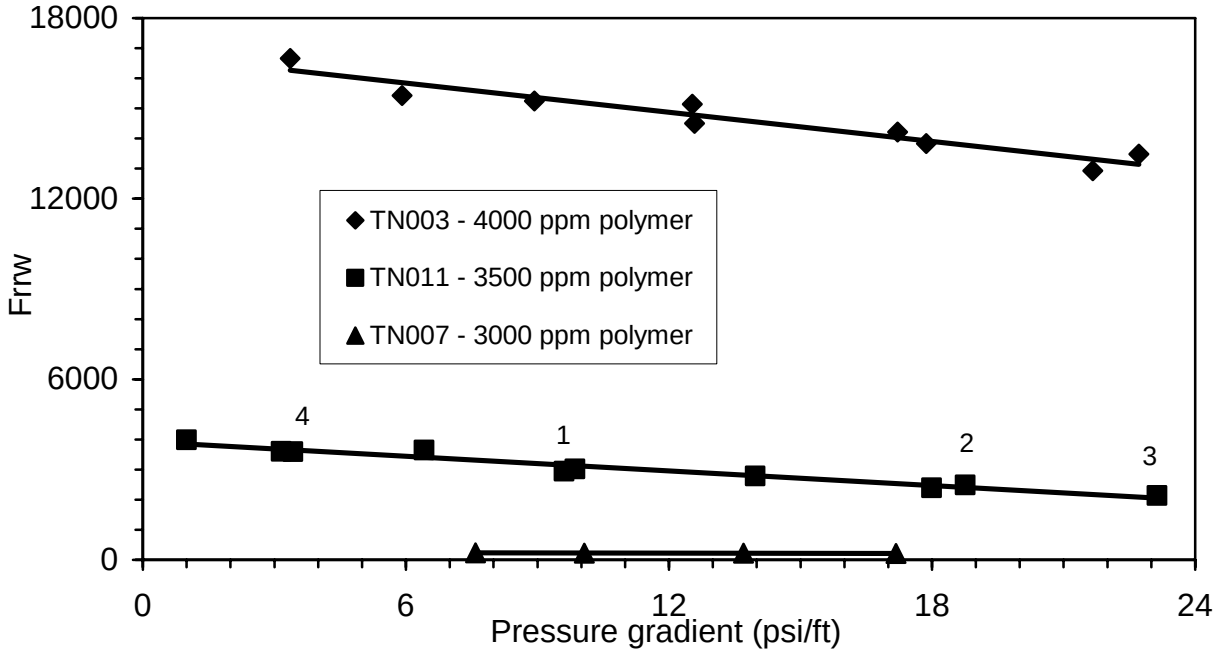

Figure 7.8 - Residual resistance factors for water as a function of applied pressure gradient for strong gels (polymer concentrations of 3,000 ppm and higher) after the channel development process at a pressure gradient of 20 psi/ft.

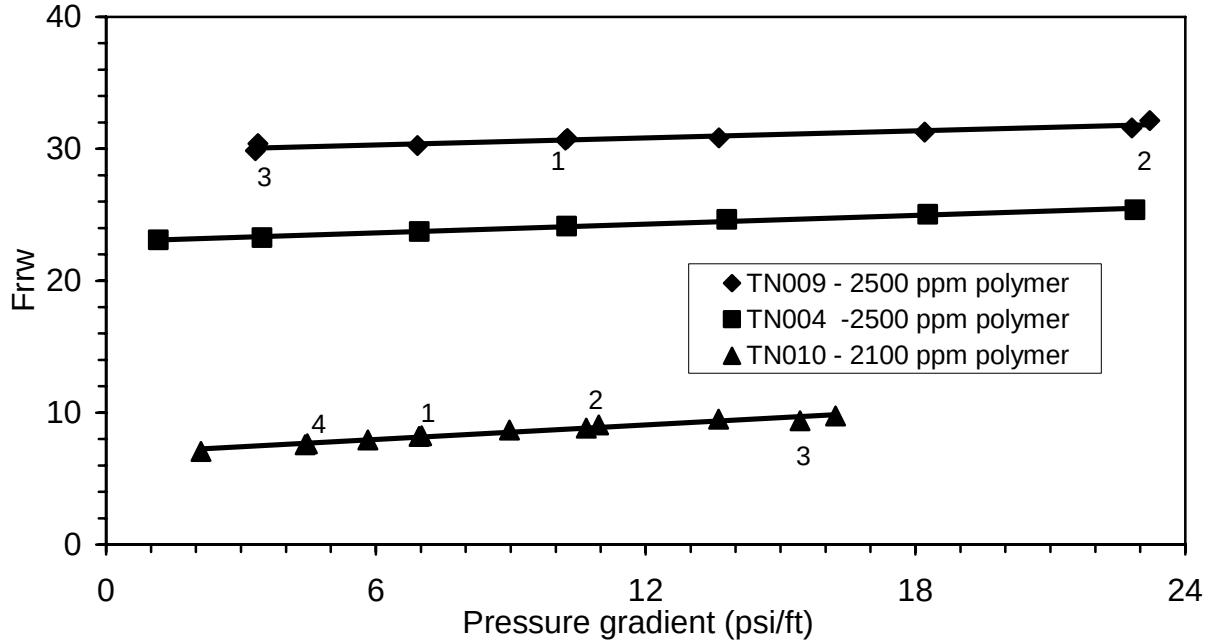

Figure 7.9 - Residual resistance factors for water as a function of applied pressure gradient for weak gels (polymer concentrations of 2,500 ppm and 2,100 ppm) after the channel development process at a pressure gradient of 20 psi/ft.

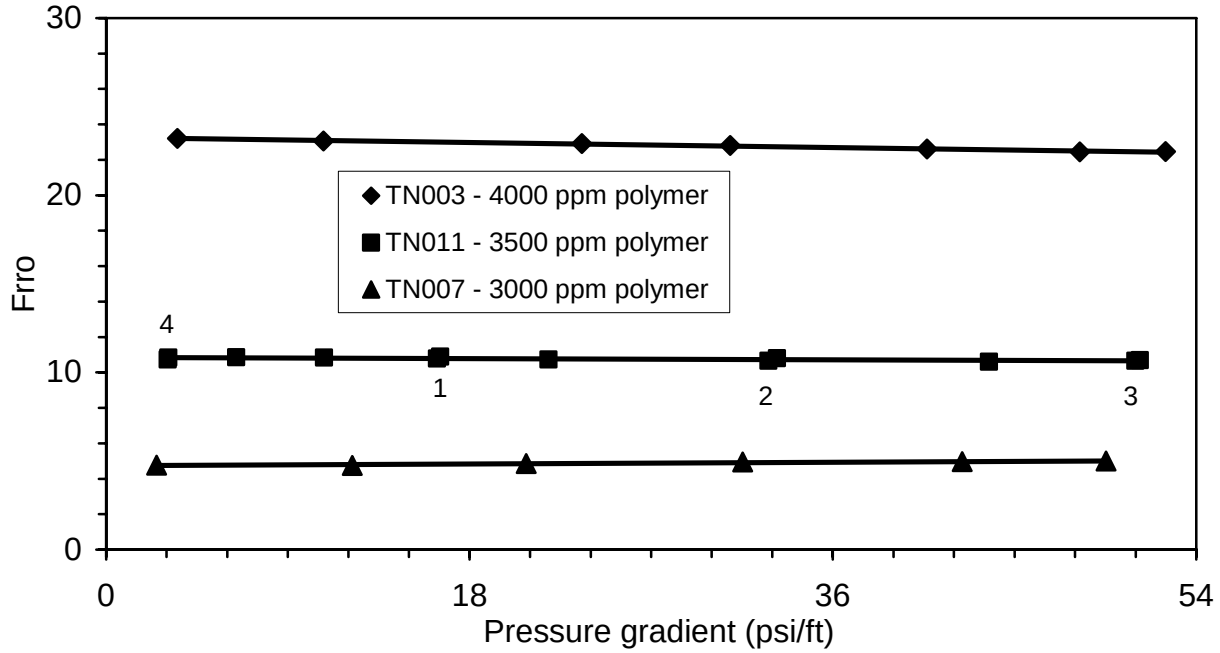

Figure 7.10 - Residual resistance factors for oil as a function of applied pressure gradient for strong gels (polymer concentrations of 3,000 ppm and higher) after the channel development process at a pressure gradient of 50 psi/ft.

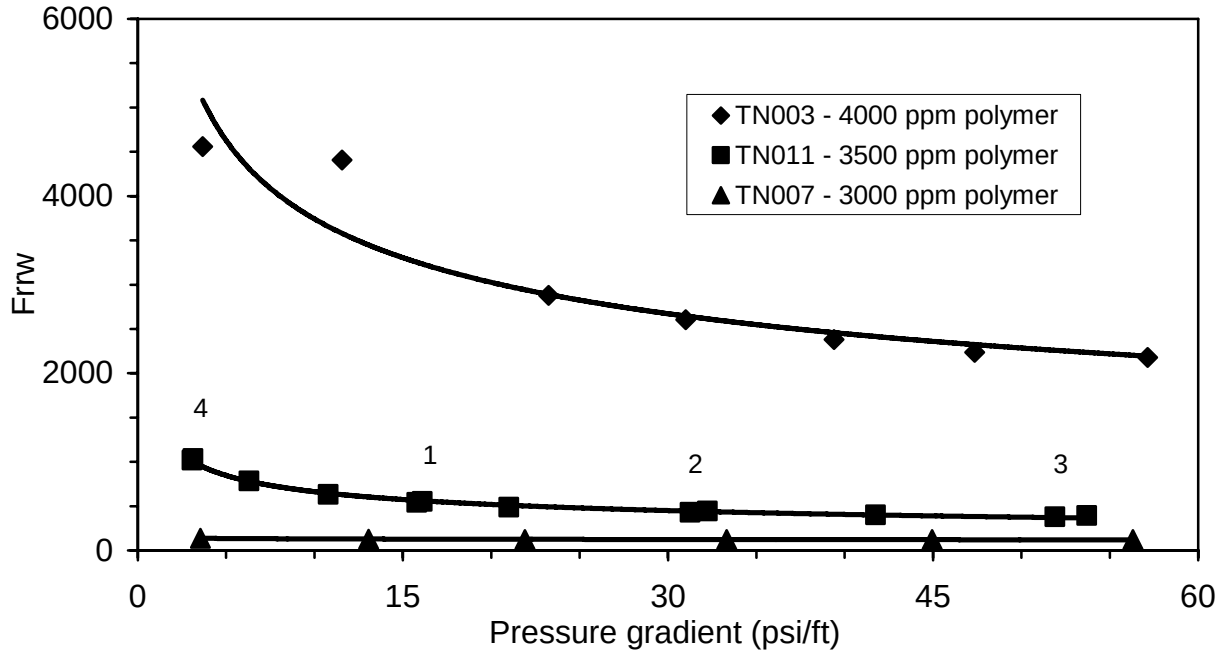

Figure 7.11 - Residual resistance factors for water as a function of applied pressure gradient for strong gels (polymer concentrations of 3,000 ppm and higher) after the channel development process at a pressure gradient of 50 psi/ft.

Comparison of the values of F_{rro} and F_{rrw} at pressure gradients less than approximately 20 psi/ft in Figures 7.10 and 7.11 with values in Figures 7.6 and 7.8 (channel development at a pressure gradient of 20 psi/ft) shows that the higher pressure gradient caused both residual resistance factors to decrease significantly. F_{rrw} decreased to a greater extent than F_{rro}. The additional removal of 2 to 5% of the gel volume resulting from the higher pressure gradient of 50 psi/ft significantly affected both F_{rro} and F_{rrw}. The numbers next to data points for Run TN011 in Figures 7.10 and 7.11 indicate the order that the flow rates were varied after the initial series of flow rate changes which were from high to low values. The data were not a function of how the flow rate was varied.

Liang et al. [1995] showed that F_{rrw} decreased and that F_{rro} was relatively constant with a decrease in superficial velocity in an experiment with a very strong gel (13,900-ppm polyacrylamide) placed in a strongly water-wet Berea core. Results from flow experiments on a sandstone slab with a strong gel (5,000-ppm polyacrylamide) showed a similar effect of decreased F_{rrw} with increasing pressure gradient [Ganguly et al. 2003]. In this study, in which the sandpacks were treated with various Cr(III)-acetate-HPAM gel compositions, F_{rro} was not a function of pressure gradient or superficial velocity for all gelant compositions. This agrees with the results reported by Liang et al. [1995] and Ganguly et al. [2003]. However, in this study, F_{rrw} decreased moderately for the stronger gels (Figure 7.8) and increased for the weaker gels (Figure 7.9) with increases in pressure gradient.

In summary, both F_{rro} and F_{rrw} values increased substantially with increased polymer concentration. F_{rrw} was a moderate function of imposed pressure gradient, but F_{rro} was not. As pressure gradient increased, F_{rrw} decreased for strong gels but increased for weak gels. Additional channel development at the higher pressure gradient of 50 psi/ft strongly reduced both F_{rro} and F_{rrw} from the values determined at a pressure gradient of 20 psi/ft. F_{rrw} was reduced by a greater factor than F_{rro} by application of the higher pressure gradient.

Selectivity. The magnitude of favorable DPR was termed "selectivity" and was defined as the ratio of F_{rrw} to F_{rro}. Higher selectivity values above unity represent more favorable DPR.

Selectivity of the internal section of the sandpack after the channel development process at 20 psi/ft is shown in Figure 7.12 as an exponential function of the polymer concentration in the gel. The values in Figure 7.10 were determined from floods conducted at 20 psi/ft. Selectivity decreased dramatically with decreased polymer concentration of the gel. Selectivity was always greater than 1, illustrating that the permeability reduction for water was much greater than for oil for all of the gel compositions studied.

Selectivities for the stronger gels after channel development at pressure gradients of 20 and 50 psi/ft are shown in Figure 7.13 as a function of pressure gradient. Weaker gels were only subjected to the pressure gradient of 20 psi/ft, and their selectivities as a function of the applied pressure gradient are shown in Figure 7.14. Selectivities generally decreased for the strong gels and increased slightly for the weak gels with increased pressure gradient. The higher pressure gradient of 50 psi/ft significantly reduced selectivity of the stronger gels as compared to the 20 psi/ft flood as shown in Figure 7.13. This occurred even though only a small additional amount of gel volume (2 to 5%) was converted to flow channels at the higher pressure gradient.

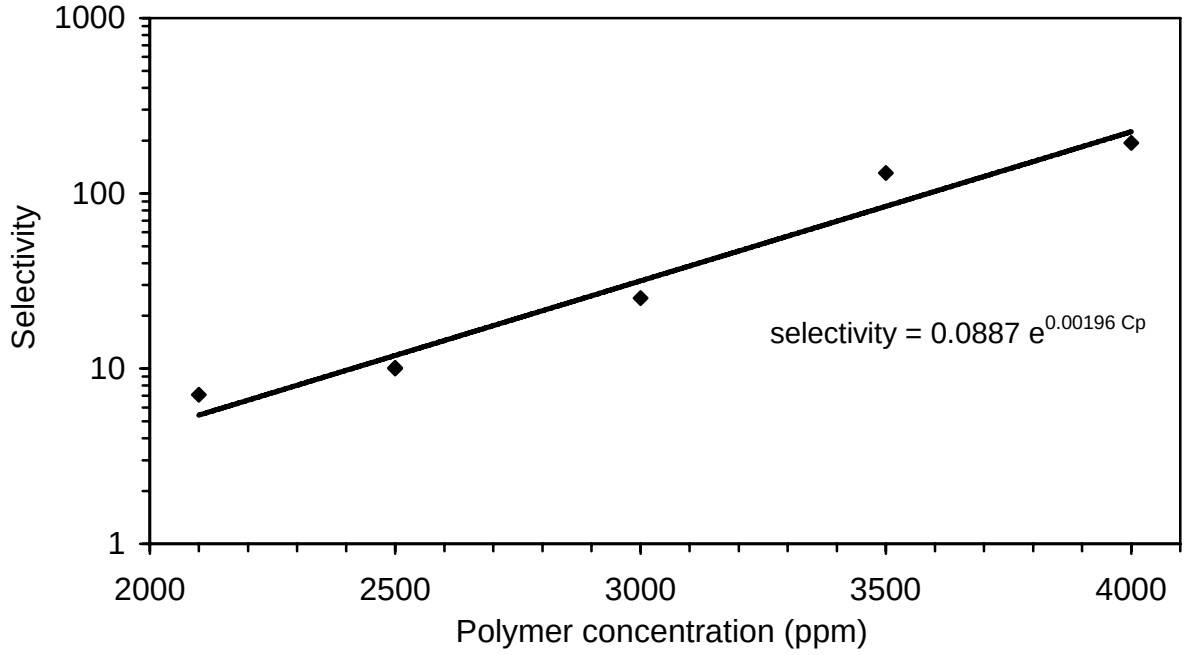

Figure 7.12 - Selectivity as a function of polymer concentration after the channel development process at a pressure gradient of 20 psi/ft.

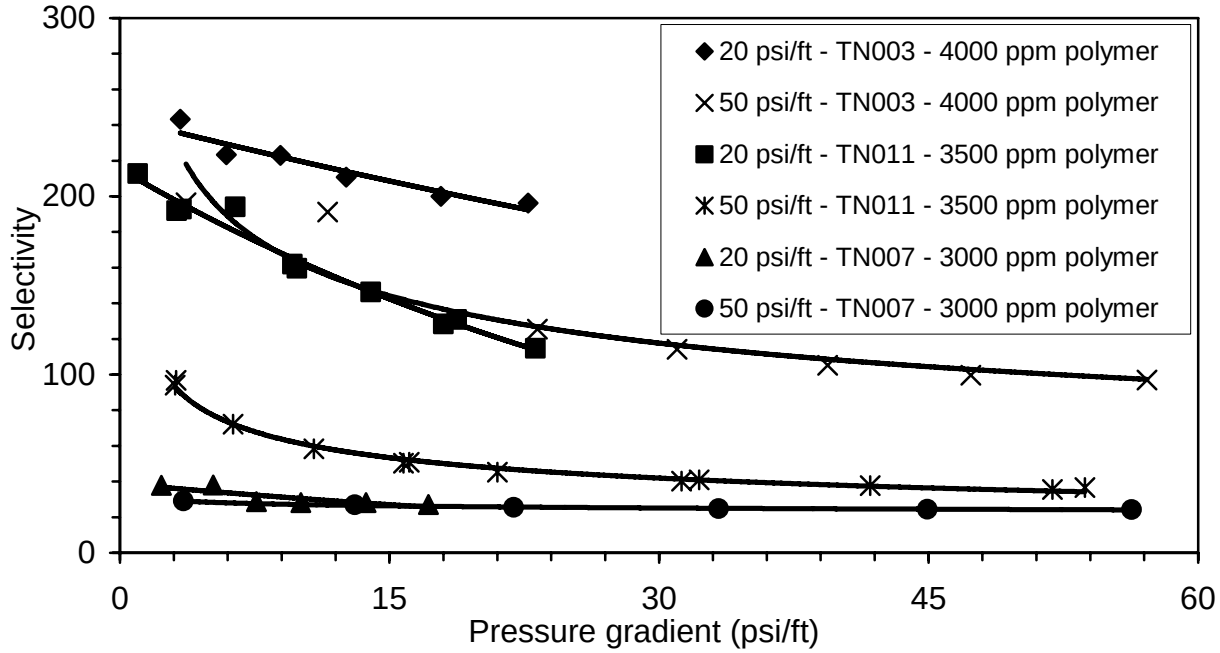

Figure 7.13 - Selectivity as a function of applied pressure gradient for strong gels (polymer concentrations of 3,000 ppm and higher) after the channel development process at a pressure gradients of 20 and 50 psi/ft.

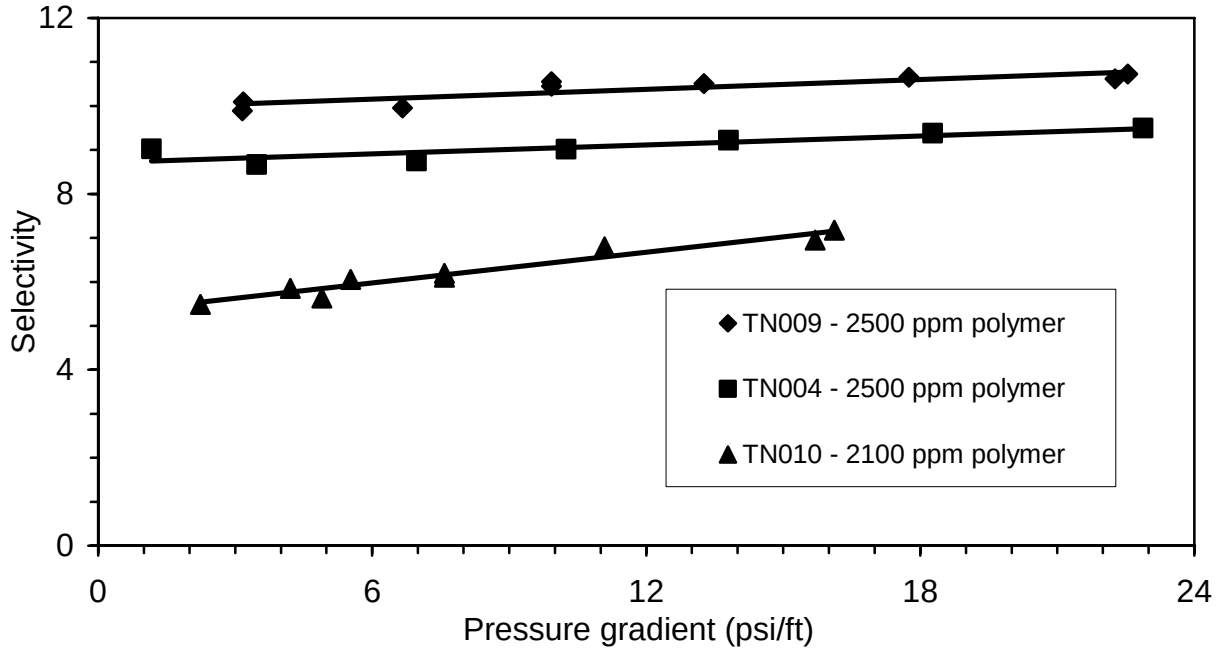

Figure 7.14 - Selectivity as a function of applied pressure gradient for weak gels (polymer concentrations of 2,500 ppm and2,100 ppm) after the channel development process at a pressure gradient of 20 psi/ft.

In summary, favorable DPR was observed in all sandpacks that were treated with the different gel compositions. Selectivity increased sharply with increased polymer concentration and decreased with the volume of gel converted to flow channels and/or the applied pressure gradient during the channel development process. Selectivity decreased with pressure gradient for the stronger gels, but increased with pressure gradient for the weaker gels.

Mechanisms of Disproportionate Permeability Reduction. The volumes of oil, brine, and gel contained in the sandpacks at the end of each flow experiment were determined by material balances. A few assumptions were used to perform the volume balances. It was assumed that all of the resident brine was displaced from the pack during the injection of gelant and that, after a shut-in period, the pore space was completely full of gel except for the residual oil. The residual oil was referred to as "encapsulated" oil; that is, encapsulated by the gel. The encapsulated oil contained stilbene tracer and the amount of the encapsulated oil displaced from the sandpack during oil- and brinefloods was determined by stilbene analysis of the effluent oil samples. It was also assumed that all of the brine that was dehydrated and all of the gel particles that were ripped from the structure by oil were displaced from the sandpack during the channel development process. In other words, the water saturation was assumed to be negligible in the channels or "new" pore space after each channel development process.

Results of the material balances are given in Tables 7.6 and 7.7 for Sandpacks TN003 and TN009, respectively. Data for other sandpacks are given by Nguyen [2003]. Saturations of water (S_w), gel (S_{gel}), and oil (S_o) and saturations of oil that was encapsulated (S_{oen}) and not encapsulated (S_{on}) by the gel were determined based on the initial pore volume. The channel volume, or new pore space, for oil and brine flow after the gel treatment is described by the

Table 7.6 – Saturation values and permeability data after each flow experiment in TN003; Gel contained 4000 ppm polyacrylamide.

Experiment	S_w (%)	S_o (%)	S_{gel} (%)	S_{oen} (%)	S_{on} (%)	ϕ^* (%)	S_w^* (%)	S_o^* (%)	k_w (md)	F_{rrw}	k_o (md)	F_{rro}
Brine saturation	100	0							4480			
Oilflood	14.3	85.7									3730	
Brineflood	87.6	12.4							2980			
Tracer S_{or}	87.1	12.9										
Gel placement	0	12.9	87.1	12.9								
Oilflood at 20psi/ft	~ 0	72.6	27.4	9.7	62.9	23.1	~ 0	100			52.6	70.9
Brineflood at 20 psi/ft	32.1	40.5	27.4	2.2	38.3	23.5	45.5	54.5	0.2	1350 0		
Oilflood at 20 psi/ft	10.7	61.8	27.4	1.8	60.0	23.6	15.1	84.9			54.3	68.7
Oilflood at 50 psi/ft	~ 0	76.6	23.4	0.9	75.8	25.3	~ 0	100			147	25.3
Brineflood at 50 psi/ft	33.8	42.8	23.4	0.4	42.4	25.4	44.4	55.6	1.4	2180		
Oilflood at 50 psi/ft	5.1	71.5	23.4	0	71.5	25.5	6.7	93.3			166	22.5
Tracer S_o^*					70.5		8.0	92				

effective porosity (ϕ^*). The new pore space was the sum of the space that was occupied by the gel that was dehydrated and displaced and the space occupied by the encapsulated (residual) oil that was reconnected. S_w^* and S_o^* are the water and oil saturations in the "new" porosity, the new flow channels. The last four columns are the average permeabilities and residual resistance factors of the internal sections (Sections 2 to 5) of the packs.

Inspection of the results of the material balance provides insight into the flow behavior of oil and water through a gel-treated porous medium. Porosity of the sandpacks decreased from initial values of 33 and 34% to values that ranged from 22 to 26% after all the post-treatment floods. Lower porosity in the same rock translates into a lower absolute permeability and, presumably, lower relative permeabilities to oil and to brine. The amount of encapsulated oil that was reconnected during the initial oilflood at 20 psi/ft generally decreased with the strength (polymer concentration) of the gelant. Most of the encapsulated oil was reconnected after all of the post-treatment brine- and oilfloods for all polymer concentrations.

Table 7.7 – Saturation values and permeability data after each flow experiment in TN009; Gel contained 2500 ppm polyacrylamide.

Experiment	S_w (%)	S_o (%)	S_{gel} (%)	S_{oen} (%)	S_{on} (%)	ϕ^* (%)	S_w^* (%)	S_o^* (%)	k_w (md)	F_{rrw}	k_o (md)	F_{rro}
Brine saturation	100	0.0							4220			
Oilflood	14.1	85.9							0		3490	
Brineflood	84.3	15.7							2620			
Tracer S_{or}	84.2	15.8										
Gel placement		15.8	84.2	15.8								
Oilflood at 20 psi/ft	~ 0	71.1	28.9	0.7	70.4	23.7	~ 0	100			1220	2.9
Brineflood at 20 psi/ft	54.8	16.3	28.9	0.4	15.9	23.8	77.5	22.5	83.0	31.6		
Oilflood at 20 psi/ft	3.2	67.9	28.9	0.0	67.9	23.9	4.5	95.5			1170	3.0
Tracer oil phase					68.0		4.3	95.7				

Residual saturations of water and oil (S_{wr}* and S_{or}*) in the "new" pore space were key to our interpretation of how DPR occurs. The values of S_{wr}* and S_{or}* after the oil- and brinefloods at 20 psi/ft are shown as a function of polymer concentration in Figure 7.15. Water saturations in the new flow channels at a 100% fractional flow of oil (S_{wr}*) were lower than the pretreatment values at the same condition (13 to 15%), except for the gelant at the highest polymer concentration of 4,000 ppm, where the value was comparable. Conversely, the residual saturations of oil at 100% fractional flow of water (S_{or}*) were much higher than S_{wr}* and significantly higher than the pretreatment values that ranged from 12 to 17%. The high residual oil saturations increased the flow resistance to water significantly, while oil flow was not as restricted because of the low residual water saturations, resulting in favorable DPR.

The increase with polymer concentration of the residual saturations of oil and water in the new pore space (Figure 7.15) correlated with increased residual resistance factors with polymer concentration as shown in Figure 7.5. It is noted that the residual oil saturations increased faster with polymer concentration (higher slope) than did the residual water saturations with polymer concentration, and this correlated with the increased selectivity with polymer concentration as shown in Figure 7.12.

Conclusions

The following conclusions are applicable to the studied gel systems and experimental conditions.

1. Gel treatments applied to sandpacks initially reduced the permeability to negligible values. A portion of the permeability was restored during a channel development process

that occurs when oil is injected into a sandpack that is saturated with gel and residual oil. The channels occupied a significant portion of the original porosity by dehydration and displacement of the gel and reconnection of residual oil ganglia. Most of the initial residual oil volume was converted to channel volume. Channels developed at slower rates for the more concentrated, or stronger, gels. The gelant volume removed during the channel development process was not a strong function of gel composition or the pressure gradient imposed during the channel development process.

2. Permeabilities to oil and water in the developed channels were disproportionately reduced compared to permeabilities determined prior to the gel treatment. The trapping of significant saturations of residual oil in the developed flow channels restricted brine flow to a greater extent than low saturations of residual water restricted oil flow. This mechanism plays an important role in the favorable disproportionate permeability reduction (increased selectivity) that was observed in the flow experiments.
3. Residual resistance factors to both oil and water increased significantly with increased composition, or strength, of the gel.
4. The selectivity of the treatments increased significantly with the strength of the gel.
5. A higher pressure gradient during channel development (50 vs. 20 psi/ft) increased the permeabilities to oil and water and decreased the selectivity.
6. The applied pressure gradient during oil flow in the channels did not affect the permeability. Permeability to water decreased moderately with applied pressure gradient for strong gels and increased moderately for weaker gels.

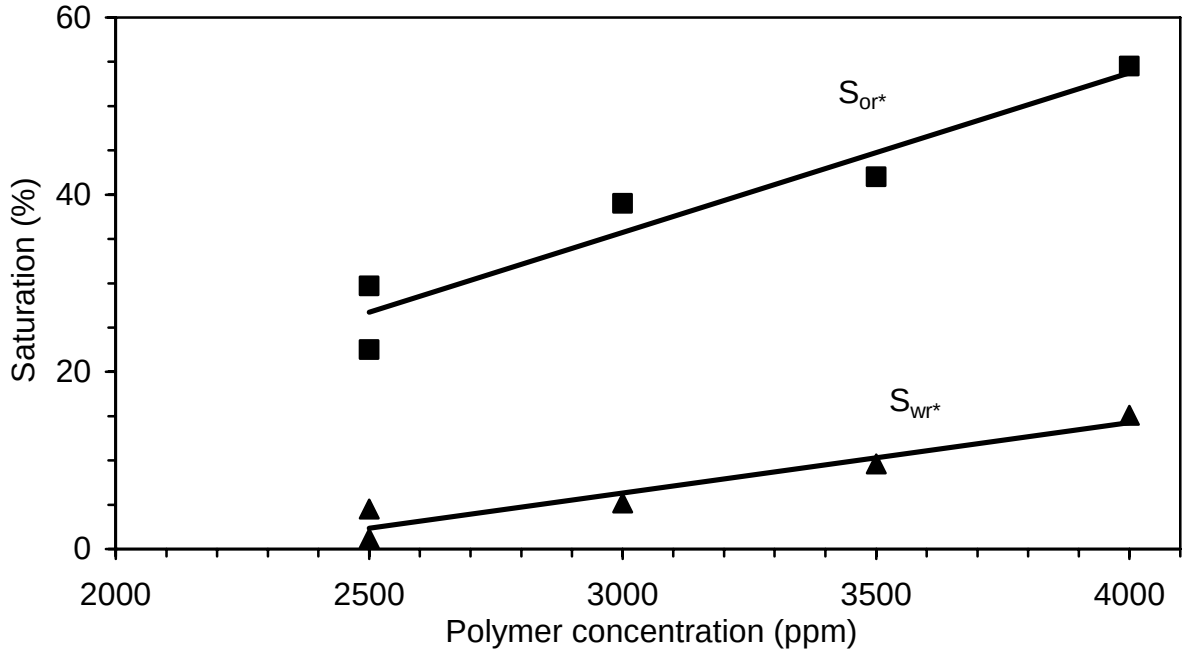

Figure 7.15 - Residual oil and water saturations in the new pore space as a function of polymer concentration and after floods at pressure gradients of 20 psi/ft.

Nomenclature

C_p = *polymer concentration (ppm)*
F_{rro} = *residual resistance factor to oil*
F_{rrw} = *residual resistance factor to water*
k = *absolute permeability (md)*
k_o = *permeability to oil (md)*
k_{oa} = *permeability to oil after gel placement (md)*
k_{ob} = *permeability to oil before gel placement (md)*
k_w = *permeability to water (md)*
k_{wa} = *permeability to water after gel placement (md)*
k_{wb} = *permeability to water before gel placement (md)*
S_{gel} = *gel saturation based on initial PV*
S_o = *oil saturation based on initial PV*
S_o* = *oil saturation in the "new" pore space based on effective PV*
S_{oen} = *saturation of oil encapsulated by gel and based initial PV*
S_{on} = *oil saturation not encapsulated by gel and based on initial PV*
S_{or} = *residual oil saturation based on initial PV*
S_{or}* = *residual oil saturation in the "new" pore space based on effective PV*
S_w = *water saturation in the sandpack based on initial PV*
S_w* = *water saturation in the "new" pore space based on effective PV*
S_{wr} = *residual water saturation in the sandpack based on the initial PV*
S_{wr}* = *residual water saturation in the "new" pore space and based on effective PV*
ϕ* = *effective porosity based on "new" pore space*

References

Al-Sharji, H.H., Grattoni, C.A., Dawe, R.A., Zimmerman, R.W.: "Pore-Scale Study of the Flow of Oil and Water Through Polymer Gels," paper SPE 56738 presented at the SPE Annual Technical Conference and Exhibition, Houston (3–6 October 1999).

Dawe, R.A. and Zhang, Y.: "Mechanistic Study of the Selective Action of Oil and Water Penetrating Into a Gel Emplaced in a Porous Medium," *Journal of Petroleum Science & Engineering,* **12** (1994) 113–125.

Gales, J.R., Young, T.S., Willhite, G.P., and Green, D.W.: "Equilibrium Swelling and Syneresis Properties of Xanthan Gum-Cr(III) Gels," *SPE Technology Series*, **2** No. 2 (1994) 190–212.

Ganguly, S., Willhite, G.P., Green, D.W., and McCool, C.S.: "Effect of Flow Rate on Disproportionate Permeability Reduction," paper SPE 80205 presented at the SPE International Symposium on Oilfield Chemistry, Houston, TX (5–7 February 2003).

Green, D.W., Willhite, G.P., McCool, C.S., Heppert, J.A., Vossoughi, and Michnick, M.J.: "In-Situ Permeability Modification Using Gelled Polymer Systems," Chapter 5, Final Report for the period June 10, 1996 to July 31, 1998, U.S. DOE Contract No. DE-AC22-94PC91008, Subcontract No. G4S60031, U. of Kansas (1998).

Krishnan, P., Asghari, K., Willhite, G.P., McCool, C.S., Green, D.W., and Vossoughi, S.:

"Dehydration and Permeability of Gels Used in In-Situ Permeability Modification Treatments," Paper SPE/DOE 59347 presented at the SPE/DOE Improved Oil Recovery Symposium, Tulsa, OK (3–5 April 2000).

Liang, J. and Seright, R.S.: "Further Investigations of Why Gels Reduce Water Permeability More Than Oil Permeability," *SPEPF,* **12** No. 4 (1997) 225–230.

Liang, J. and Seright, R.S.: "Wall-Effect/Gel-Droplet Model of Disproportionate Permeability Reduction," *SPEJ* **6,** No. 3 (2001) 268–272.

Liang, L., Sun, H., and Seright, R.S.: "Why Do Gels Reduce Water Permeability More Than Oil Permeability?" *SPERE,* **10**, No. 4 (1995) 282-286.

Nguyen, T.Q.: "Effect of Compostion of a Polyacrylamide-Chromium(III)-Acetate Gel on the Magnitude of Gel Dehydration and Disproportionate Permeability Reduction," MS thesis, U. of Kansas (2003).

Nilson, S., Stavland, A., and Jonsbraten, H.C.: "Mechanistic Study of Disproportionate Permeability Reduction," paper SPE 39635 presented at the SPE/DOE Improved Oil Recovery Symposium, Tulsa, OK (19–22 April 1998).

Sparlin, D.D. and Hagen, R.W.: "Controlling Water in Producing Operations—Part 5," *World Oil,* **7** (1984) 137–142.

White, J.L., Goddard, J.E., and Phillips, H.M.: "Use of Polymers to Control Water Production in Oil Wells" *JPT,* **25**, No. 2 (1973) 143–150.

Willhite, G.P., Zhu, H., Natarajan, D., McCool, C.S., Green, D.W.: "Mechanisms Causing Disproportionate Permeability Reduction in Porous Media Treated With Chromium Acetate/HPAM Gels" *SPEJ,* **7**, No. 1 (2002) 100–108.

Zaitoun, A., and Kohler, N.: "Two-Phase Flow Through Porous Media: Effect of an Adsorbed Polymer Layer," paper SPE 18085 presented at the SPE Annual Technical Conference and Exhibition, Houston, TX (2–5 October 1988).

Zaitoun, A., Bertin, H., and Lasseux, D.: "Two-Phase Flow Property Modifications by Polymer Adsorption. paper SPE 39631 presented at the SPE/DOE Improved Oil Recovery Symposium, Tulsa, OK (19–22 April 1998).

Chapter 8

Gel Dehydration and Disproportionate Permeability Reduction in Berea Sandstone Cores after Treatment with a Polyacrylamide-Chromium Acetate Gel System

Graduate Research Assistant: Tuan Q. Nguyen

Introduction

High water production is a major concern in mature hydrocarbon reservoirs. Costs of handling and disposing of water produced from oil reservoirs often shortens the life of a production well. Disposal of the water is also an environmental concern. In order to reduce water production, polymer gels have been used to modify the mobility of water and oil in petroleum reservoirs.

When some gels are placed in a petroleum reservoir, permeability reduction occurs to a much greater extent for water than for oil. This phenomenon is known as favorable disproportionate permeability reduction (DPR). Reduced permeability to water leads to decreased production of water, and sometimes increased oil production, thereby prolonging the useful life of the reservoir.

This chapter presents the results of a study on the effects of gel composition, i.e. partially hydrolyzed polyacrylamide (HPAM) and Cr(III) concentrations, and applied pressure gradients on the magnitude of gel dehydration, and on the magnitude of residual resistance factors and DPR during flow through gel-treated Berea sandstone cores. A similar study using sandpacks was reported in Chapter 7.

Experimental Materials, Procedures and Equipment

Gelants were prepared from partially hydrolyzed polyacrylamide and chromium acetate. The polymer was Alcoflood 935, Lot No. A2247 BOV. The weight-average molecular weight of the polymer was about 6 million. Cr(III) stock solution was prepared from a Cr(III) acetate solution that contained 12.4% Cr(III) and 42.2% acetate by weight (McGean Rohco, Lot No. 40086816). The acetate-to-Cr(III) mole ratio was 3:1. Polymer to Cr(III) mass ratio was maintained at 40:1. All gelants contained 1.0% KCl and 10 ppm sodium azide (bactericide). Oil and brine floods were conducted with n-dodecane and an aqueous 1% KCl solution, respectively.

Berea sandstone cores were prepared by attaching acrylic endplates to each end and then coating the core with epoxy. Two pressure ports were installed 5 cm from each end of the core, which divided the cores into three sections. The ports were made by drilling holes through the epoxy and into the rock and attaching tubing in the holes with epoxy. Properties of the cores are given in Table 8.1.

A series of runs was conducted in Cores 2 and 3. Core 2 was treated with a gelant containing 4000 ppm polymer and 100 ppm chromium that had a bulk gel time of 23 hours. Gelant injected into Core 3 contained 2500 ppm polymer and 62.5 ppm chromium with a bulk gel time of 6 days. Gelants also contained 1.0% KCl and 10 ppm of sodium azid (bactericide).

Table 8.1 - Properties of Berea sandstone cores.

	Diameter (cm)	Length (cm)	Length of section (cm)			Pore volume (mL)	Porosity (%)
			Section 1	Section 2	Section 3		
Core 2	3.15	15.2	5.0	5.2	5.0	24.5	21.1
Core 3	3.15	30.4	5.0	20.4	5.0	48.8	20.6

Table 8.2 summarizes the sequence of runs conducted with Core 2. Runs in Core 3 were the same except that the series was terminated after Run 12. The cores were saturated with brine and the pore volume and permeability were determined. The cores were flooded with oil containing a 102 ppm stilbene tracer to interstitial water saturation (S_{iw}). The end-point permeability to oil (at S_{iw}) was then measured. The stilbene tracer was used to determine the amount of residual oil that was displaced from the core during oil and brine floods conducted after the gel treatment. Brine was then injected to displace oil to residual saturation (S_{or}). The end-point permeability to water at S_{or} was measured. S_{or} was verified using a tracer (nitrate) during brine injection. Material balances were conducted on fluids injected and displaced from the cores in order to determine the saturations of the oil and aqueous phases. Saturations and permeabilities of the cores prior to gelant injection are given in Table 8.3.

Table 8.2 - Sequence of experiments.

Run	Description	Run	Description
1	Brine saturation	10	Flow tests
2	Tracer tests to verify pore volume	11	Oil flood at 20 psi/ft
3	Oil flood	12	Flow tests
4	Brine flood	13	Dehydration process at 50 psi/ft
5	Tracer tests to verify Sor	14	Brine flood at 20 psi/ft
6	Buffer injection	15	Flow tests
7	Gelant injection and shut-in	16	Oil flood at 20 psi/ft
8	Oil flood at 20 psi/ft	17	Flow tests
9	Brine flood at 20 psi/ft	18	Tracer tests to determine mobile oil volume

Table 8.3 – Saturations and end-point permeabilities prior to gelant injection.

	S_{iw} (%)	S_{or} (%)		k_o	k_{ro}	k_w	k_{rw}
	Material balance	Material balance	Tracer	(mD)		(mD)	
Core 2	22.4	37.6	37.9	495	1.03	38.1	0.08
Core 3	25.0	37.5	38.3	522	1.04	37.8	0.10

Several pore volumes of buffer solution (0.23% acetic acid, 0.86% sodium acetate, 1% sodium chloride, and 0.1% calcium chloride, pH = 5.0) were injected into the core just prior to gelant injection. This was done to moderate the fluid-rock interactions (carbonate dissolution) that increase the pH of the injected gelant. Gelant was prepared in bulk and injected into the core as quickly as possible within pressure constraints of the flow system. About 3 aqueous pore volumes [$(1-S_{or})\times$ pore volume] of gelant were injected into Core 2 and about 2 aqueous pore volumes were injected into Core 3 The core was then shut in to allow for gelation. The bulk gel time for the gelant injected into Core 2 was 23 hours and the core was shut in for six days. The

bulk gel time for the gelant injected into Core 3 was six days and the core was shut in for 43 days.

Oil was then injected at a constant pressure gradient of 20 psi/ft until aqueous production rate of less than 0.1 mL/day was achieved. The effluent was collected in fractions for analyses of stilbene in the oil phase and for polymer and chromium concentrations in the aqueous phase. Analyses on the aqueous phase fractions have not been conducted yet due to analytical problems. Brine was then flooded at 20 psi/ft until no oil was displaced. Flow tests (Run 10) were then conducted by changing flow rates in a pressure range that did not exceed the pressure gradient (20 psi/ft) during the dehydration run. After Run 10, oil was flooded at 20 psi/ft until no brine was displaced. Flow tests were conducted in the same manner as mentioned for Run 10. The procedures of Runs 13-17 in Core 2 were similar to Runs 8-12, except a higher pressure gradient of 50 psi/ft was used.

A tracer test during the injection of oil (Run 18) was conducted in Core 2 to determine the volume of displaceable oil. Oil containing 10 ppm stilbene was injected and the effluent concentration of stilbene as a function of the volume of oil injected was determined. Integration of these data determined the amount of displaceable oil.

A schematic of the experimental setup for flow experiments is shown in Figure 8.1. Pumps were used to inject fluids into the sandpack. The effluent was collected in fractions. Pressure drops across the entire sandpack and each of the sections were monitored and recorded by pressure transducers and a data acquisition system. The experimental system was maintained at 30°C.

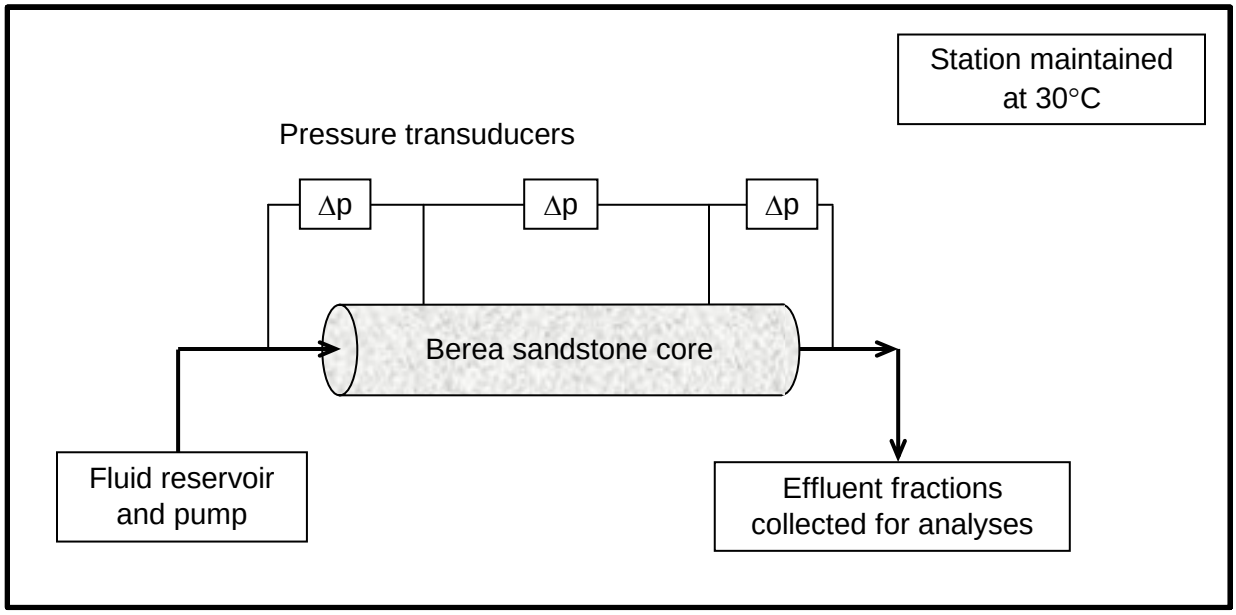

Figure 8. 1 – Schematic of equipment for flow experiments.

Results and Discussion

Gelant injection. Buffer was injected through Core 2 prior to gelant injection. About three aqueous pore volumes of gelant containing 4000 ppm polymer and 100 ppm Cr(III) were then injected. Effluent from the core was collected in fractions and the pH was measured and the color of the solution noted. Additionally, the viscosity of effluent samples that contained gelant was measured as a function of time to determine the gel time.

Figure 8.2 shows the pressure drop across the core as a function of injection time. During gelant injection, the flow rate was decreased in increments from 1.0 to 0.15 mL/min to keep the overall pressure drop across the core below 100 psi. One aqueous pore volume of gelant was injected at about 35 minutes. The pressure drop increased significantly with time at each flow rate such as 0.20 mL/min and 0.15 mL/min indicating increasing flow resistance. It took longer to inject three pore volumes of gelant than expected due to the increased flow resistance. Pressure drops across the individual sections were not measured during gelant injection in Core 2.

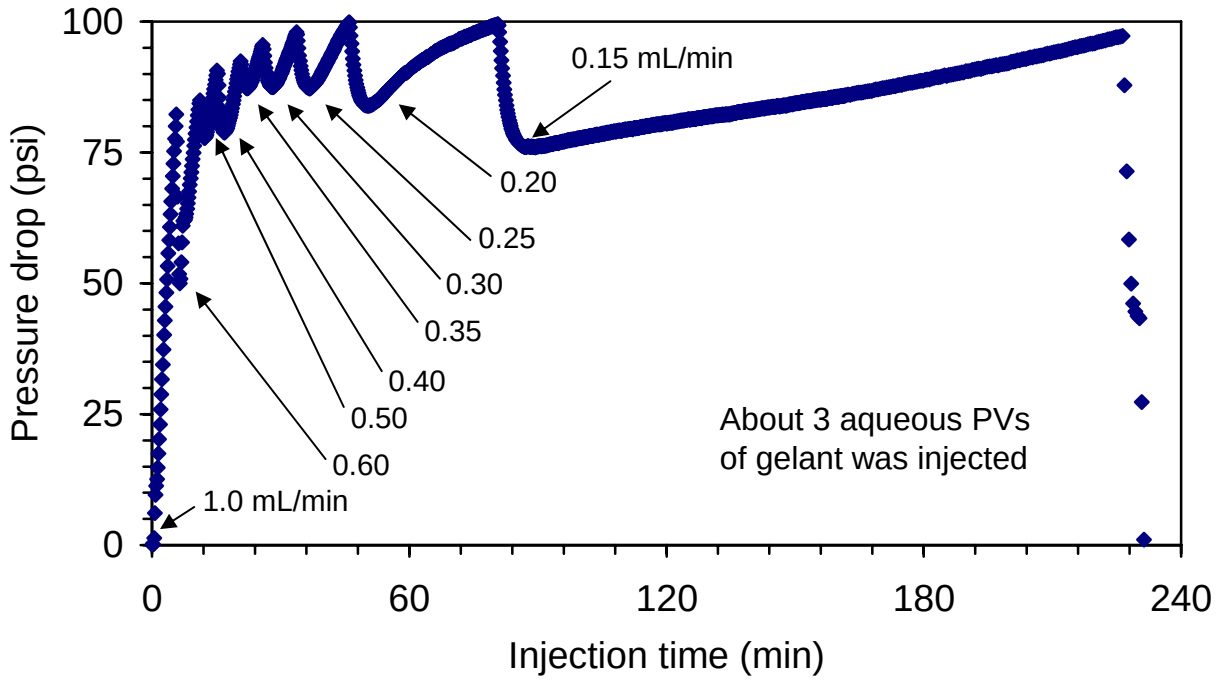

Figure 8.2 - Overall pressure drop as a function of flow rate and injection time during gelant injection, Core 2.

Table 8.4 summarizes the volume, pH, and color observations for each effluent sample. Gel times of the effluent samples were much longer than the gel time of injected gelant (23 hours) The pH of gelant samples in the effluent was higher than the injected gelant (4.76). Gelant that flowed through the core took longer to form gel than the injected gelant because pH was higher and polymer concentration was lower as evidenced by the increased flow resistance which indicated polymer retention in the core. The color of the effluent from Core 2 was orange when buffer was displaced from the core at low injection rates and indicated the presence of iron ions.

Table 8.4 - Volume, pH, and observation of effluent samples.

Sample	Process	Volume (mL)	pH	Color	Gel time
1	Brine displaced by buffer	15	7.46	Clear	
2	Buffer collected at 8.5 mL/min	20	5.32	Clear	
3	Buffer collected at 8.5 mL/min	20	5.14	Clear	
4	Buffer collected at 1.0 mL/min	40	5.24	Light orange	
5	Buffer collected at 8.5 mL/min	50	5.13	Clear	
6	Buffer displaced by gelant	10.5	5.27	Light orange	
7	Buffer and some gelant collected	8	5.46	Light orange	
8	Gelant collected	7	6.13	Light orange	no gel
9	Gelant collected	9	6.52	Light blue	> 60 hrs
10	Gelant collected	10.5	6.50	Light blue	52 hrs
11	Gelant collected	4	6.72	Light blue	52 hrs

Table 8.5 summarizes measurements and observation of effluent samples collected from Core 3 during the injection of buffer solution and gelant. This core has an aqueous pore volume that is two times larger than that of Core 2. About 2 aqueous pore volumes of gelant were injected through Core 3. Similar behavior was observed in Core 3 as in Core 2 except the orange color was darker, possibly due to the longer residence time in the core (longer core and lower flow rate). The effect of iron, or whatever caused the orange color, is not known. Similar pH behavior was observed in the effluent from Core 3 as that observed in Core 2.

Table 8.5 - Volume and pH of several effluent samples.

Sample	Process	Volume (mL)	pH	Color
	Injected buffer solution		4.98	Clear
	Injected gelant		4.67	Greenish
B1	Brine displaced by buffer solution		7.69	Clear
B2	First buffer solution collected @ 3.5 mL/min		7.04	Clear
B3	Second buffer solution collected @ 3.5 mL/min		5.54	Clear
B4	Buffer solution left in the core over night		6.35	Clear
B5	Re-injected buffer solution @ 0.1 mL/min		5.43	Light orange
B6	Re-injected buffer solution @ 3.5 mL/min		5.72	Light orange
1	Buffer solution displaced by gelant	11	5.24	Light orange
2	Buffer solution displaced by gelant	10	5.37	Dark orange
3	Buffer solution displaced by gelant	11	5.55	Dark orange
4	Buffer and gelant collected	10.5	6.12	Light orange
5	Gelant collected	9	6.50	Light orange
6	Gelant collected	8	6.52	Light orange

The effluent from Core 3 started to feel slippery to touch which indicated the presence of polymer at collection times after 180 minutes of injection when about 37 mL of the effluent was collected. The delay of the breakthrough of polymer at about 1.2 aqueous PV was also indicated by the pressure drop measured in Section 3 where an increase in pressure drop occurred at about 180 minutes (refer to Figure 8.3).

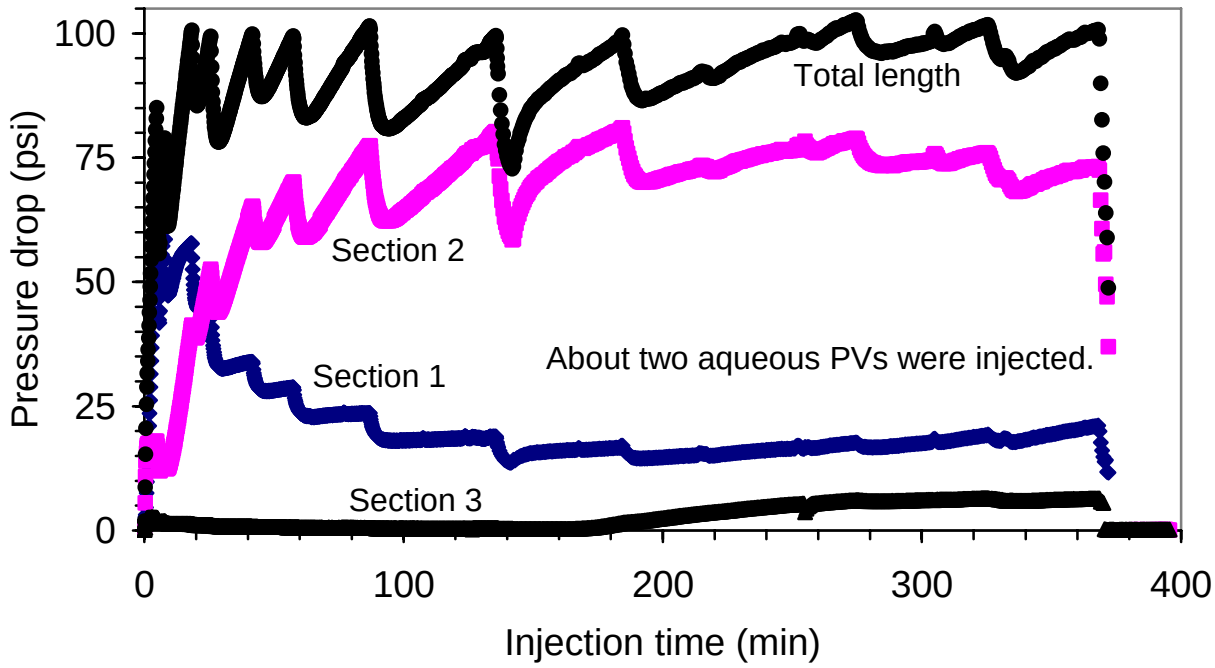

Figure 8.3 - Pressure drops as a function of flow rate and injection time during gelant injection into Core 3, 2500 ppm polymer and 62.5 ppm Cr(III) gelant.

Pressure drops measured across the sections of Core 3 as a function of time during gelant injection are shown in Figure 8.3. The flow rate was initially 1.0 mL/min and was decreased in increments to 0.08 mL/min due to a significant increase in flow resistance. Flow rates were much lower than expected due to increased flow resistance, indicating polymer retention in the core.

Figure 8.4 shows the pressure gradients across the sections of Core 3 as a function of time. High flow resistance initially occurred in Section 1. After 100 minutes, the pressure gradients in Sections 1 and 2 were about 100 psi/ft while the pressure gradient in Section 3 was much less. This indicated the difficulty of polymer propagation through the core.

Oil and brine floods after gel treatment in Core 2. After gelant injection and a shut in time period of six days to allow for gelation in situ, oil was injected into Core 2 to develop flow channels. Aqueous fluid was produced 20 minutes after the start of oil injection. Oil broke through in the effluent after 0.2 mL of the aqueous phase was collected. The aqueous effluent felt slippery to touch indicating polymer in the sample. Since the effluent was collected in small samples (0.7-1.7 mL), only the third sample was measured for viscosity. The viscosity of this sample was 20.7 cp (25°C, shear rate of 22.5/s) similar to the viscosity of the injected gelant. This behavior was not observed in sandpacks [Chapter 7] where aqueous samples collected during the post-treatment oil flood in sandpacks did not feel slippery to touch and the viscosities of the samples were about the same as brine, 1 cp at 25 ^{o}C. Viscosity measurements and the finger test (slippery to the touch) were the only indications of polymer content since polymer analyses were yet to be completed.

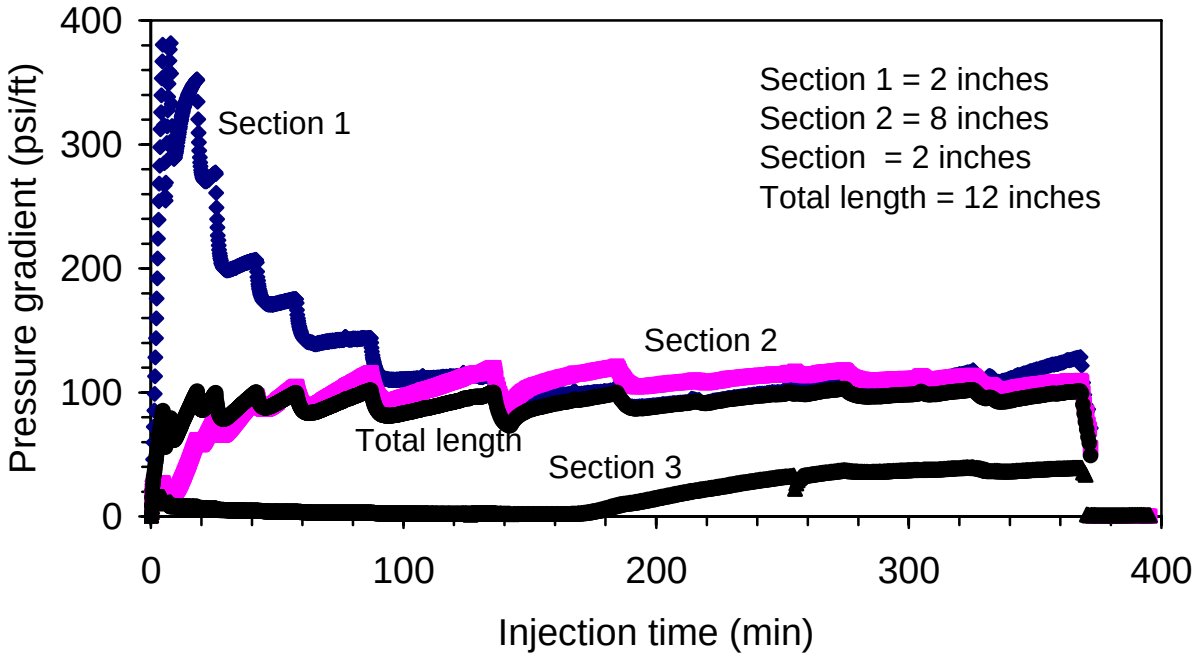

Figure 8.4 - Pressure gradients as a function of flow rate and injection time during gelant injection into Core 3, 2500 ppm polymer and 62.5 ppm Cr(III) gelant.

Figure 8.5 shows volume fraction of aqueous phase collected during the initial oil flood as a function of time. Total aqueous phase collected was 45.4% of gel placed in the core. The total volume fraction of collected aqueous phase was lower in the Berea sandstone than in sandpacks (68.8%) where the same gelant composition was tested [Chapter 7].

After the oil flood at 20 psi/ft, brine was flooded at 20 psi/ft. Brine was detected in the effluent after 6.7 mL of oil was displaced. After brine breakthrough, only an additional 0.1 mL of oil was collected. At the time of brine breakthrough, the aqueous phase felt slippery to touch. The first three aqueous fractions contained 0.5, 2.0, and 1.3 mL of fluid. Viscosities of the second and third samples were 11 and 7 cp (25°C, shear rate of 22.5/), respectively, indicating that a residual aqueous phase was trapped by the previous oil flood and that the trapped aqueous phase was liquid and contained a significant amount of polymer.

Permeabilities were measured at the end of floods when the fractional flow was 100%. The permeability data are presented in terms of the residual resistance factors. The residual resistance factor for oil (F_{rro}) was determined using Eq. 4.1.

$$F_{rro} = \frac{k_{ob}}{k_{oa}} \qquad \text{Eq. 8.1}$$

where

k_{ob} is the permeability to oil at S_{wi} before gel placement.

k_{oa} is the permeability to oil after the gel treatment at S_{wi}*.

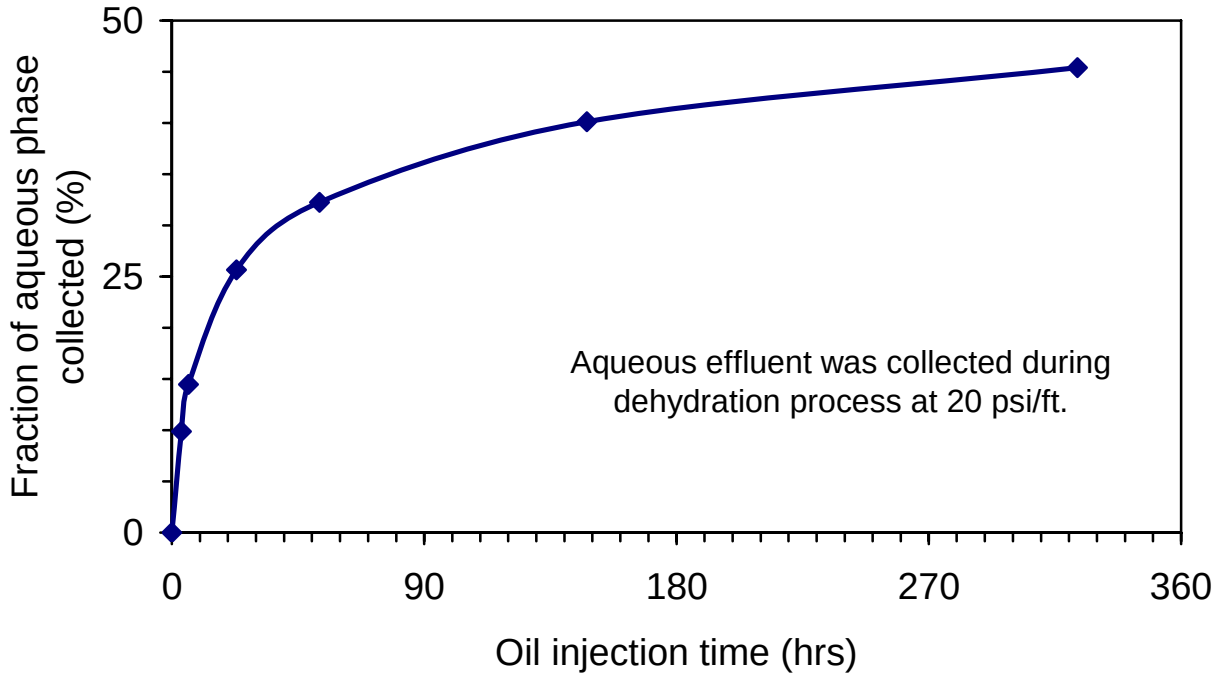

Figure 8.5 - Volume fraction of aqueous phase collected during dehydration process in Core 2.

The residual resistance factor for water (F_{rrw}) was determined using Eq. 4.2.

$$F_{rrw} = \frac{k_{wb}}{k_{wa}} \qquad \text{Eq. 8.2}$$

where

k_{wb} is the permeability to water at S_{or} before gel placement.

k_{wa} is the permeability to water at S_{or}* after the gel treatment.

An additional quantity, termed selectivity, was calculated to evaluate disproportionate permeability reduction (DPR). Selectivity was defined as the ratio of the residual resistance factor for water, F_{rrw}, to the residual resistance factor to oil, F_{rro}. Favorable DPR is expressed by increased values of selectivity above one, keeping in mind that the residual resistance factor to oil, F_{rro}, should be minimized.

The permeability to water was reduced by a factor between 30 and 90 by the gel treatment as shown in Figure 8.6 where the residual resistance factors to water (F_{rrw}) are plotted as a function of pressure gradient. The numbers next to data points for the total core length (average) indicate the order in which the flow rates were changed. The flow behavior after gel treatment in the Berea core was different than that observed in sandpacks. F_{rrw} was not a strong function of pressure gradient as was seen in a sandpack where the same gel composition was placed and the magnitude of F_{rrw} was much lower in the core than in the sandpack where F_{rrw} was on the order of 17,000.

An oil flood was performed on Berea Core 2 at a pressure gradient of 20 psi/ft to a fractional flow of oil of 1.0. This was followed by flow tests to determine the permeability to oil at pressure gradients at and below 20 psi/ft. Residual resistance factors for oil flow (F_{rro}) shown in Figure

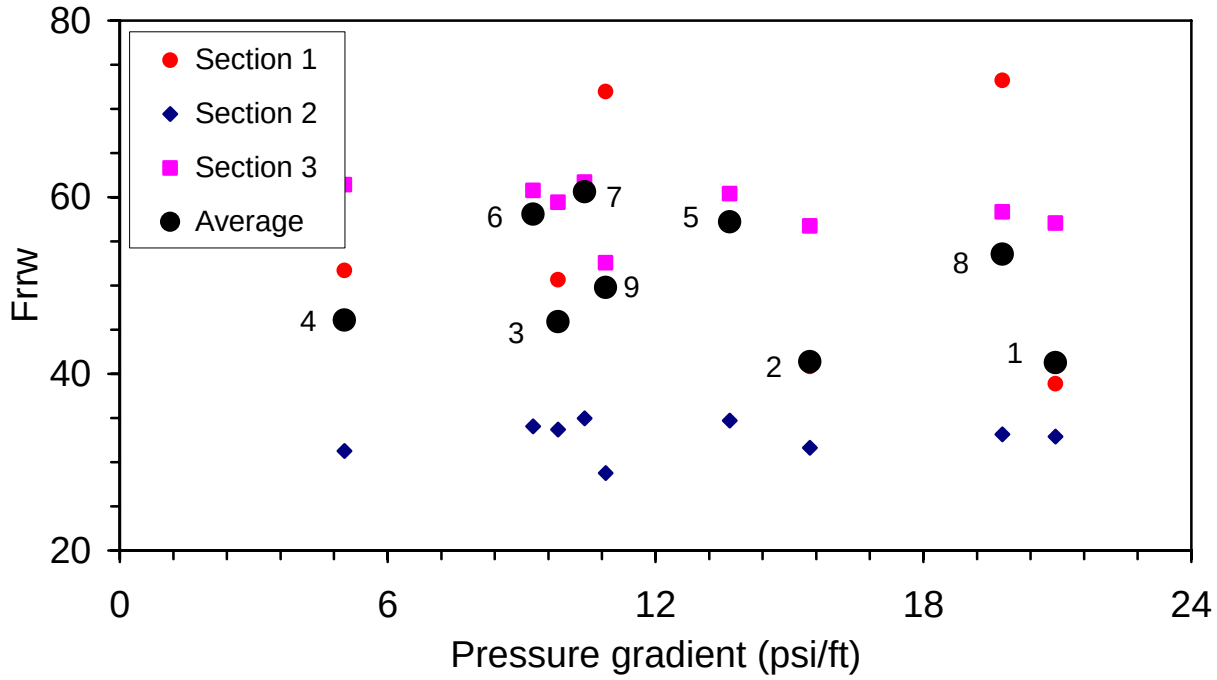

Figure 8.6 - F_{rrw} as a function of pressure gradient after dehydration process at 20 psi/ft in Core 2.

8.7 reveal low factors of permeability reduction and that F_{rro} was not a strong function of pressure gradient. Permeability reduction was the largest in Section 1 indicating higher polymer retention in Section 1.

The ratio of F_{rrw} to F_{rro}, termed selectivity, is shown in Figure 8.8 as a function of pressure gradient. Favorable disproportionate permeability reduction (DPR) occurred in Berea Core 2, but the magnitude of selectivity was much less than in a sandpack where the same gel composition was placed [Chapter 7]. Unlike the gel treatment in the sandpack, selectivity in the gel treated core was not a strong function of pressure gradient for this gel composition.

After the floods at 20 psi/ft, oil and brine floods at a pressure gradient of 50 psi/ft were conducted to determine how the permeability of the core was affected by pressure gradient of the floods. Oil was injected at 50 psi/ft following the oil flood at 20 psi/ft. An additional 0.5 mL of aqueous phase was collected during oil flood at the higher pressure gradient. Oil permeabilities were measured at selected pressure gradients at and below 50 psi/ft. The core was then flooded with brine at 50 pis/ft followed by the measurement of water permeabilites at and below 50 pis/ft. Figure 8.9 shows the residual resistance factors for oil and water, F_{rro} and F_{rrw}, at various pressure gradients. The residual resistance factor to water was much less than that after the flood at 20 psi/ft. A small decrease in the residual resistance factor to oil was observed at the higher pressure gradient. Figure 8.10 shows the ratio of F_{rrw} to F_{rro} or the selectivity. The selectivity was just greater than one, which indicates that DPR was not pronounced after the floods at the higher pressure gradient of 50 psi/ft.

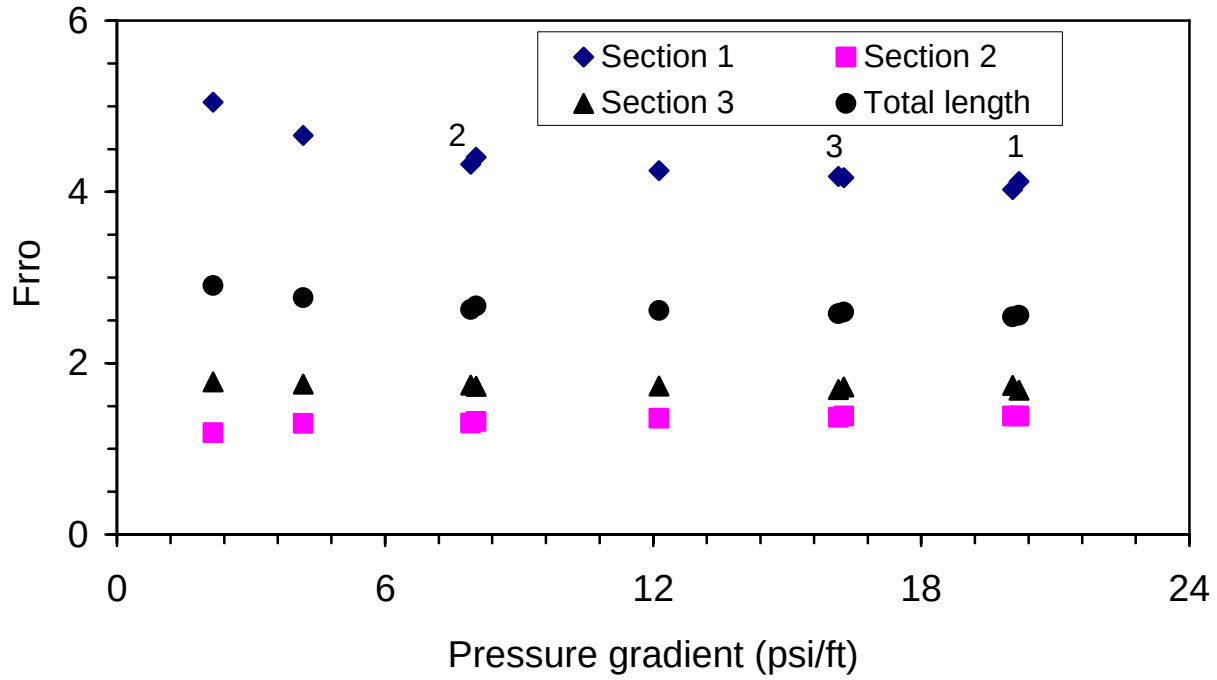

Figure 8.7 - F_{rro} at various pressure gradients after dehydration process at 20 psi/ft in Core 2.

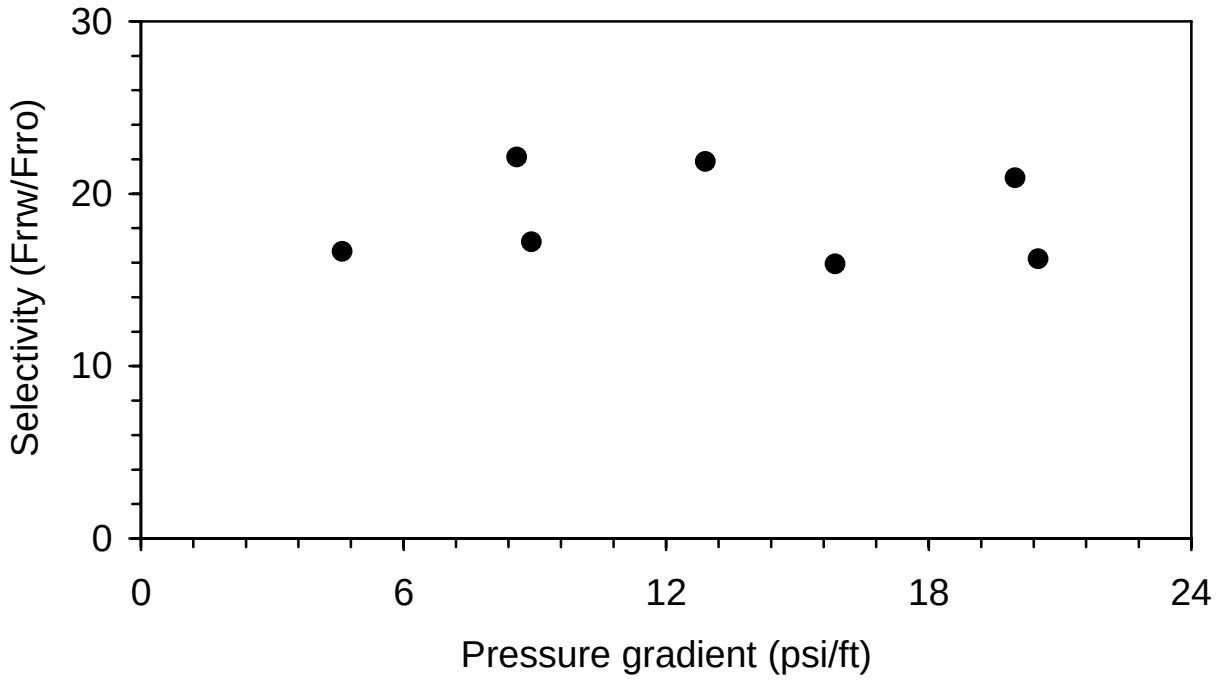

Figure 8.8 - Selectivity at various pressure gradients after dehydration process at 20 psi/ft in Core 2.

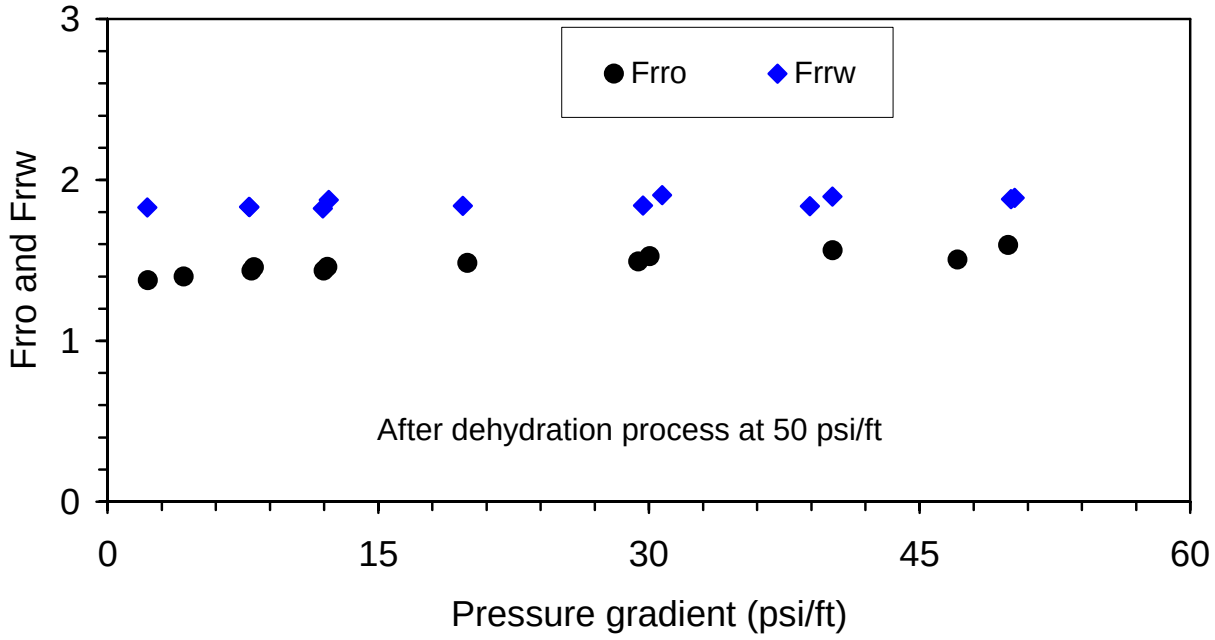

Figure 8.9 - F_{rro} and F_{rrw} at various pressure gradients after dehydration process at 50 psi/ft in Core 2.

The volumes of oil, brine, and gel contained in Core 2 at the end of each of the flow experiment were determined by material balances. A few assumptions were used to perform the volume balances. It was assumed that all of the resident brine was displaced from the core during the injection of gelant and that, after a shut-in period, the pore space was completely full of gel except for the residual oil. The residual oil was referred to as "encapsulated" oil, that is, encapsulated by the gel. The encapsulated oil contained stilbene tracer and the amount of the encapsulated oil displaced from the core during oil and brine floods was determined by stilbene analysis of the effluent oil samples. During the first oil flood after gel treatment, it was assumed that the oil develops channels through the gel with a portion of the channel volume coming from reconnection of the encapsulated oil. The channels through the gel are thought to be caused by dehydration of the gel and/or destruction of the gel. It was also assumed that all of the brine that was dehydrated from the gel and the destroyed gel was displaced from the core during the oil flood. In other words, the interstitial water saturation was assumed to be negligible in the channels or "new" pore space after the initial oil flood.

Results of the material balances are given in Table 8.6 for the flow experiments in Core 2. The assumptions for the material balance calculations were developed for similar experiments in sandpacks. The material balances, residual resistance factors and observations of the effluent during the injection of gelant and during the post-treatment floods indicate that an effective gel treatment did not occur in Berea Core 2. The assumptions for the material balance calculations are probably not justified for this treatment in a Berea sandstone core.

The gel treatment in Berea Core 2 reduced the permeability to brine but not to the extent that was expected if a firm gel had saturated the entire aqueous volume of the core. It is suspected that only a portion of the injected gelant formed gel as indicated by the viscosity of the aqueous

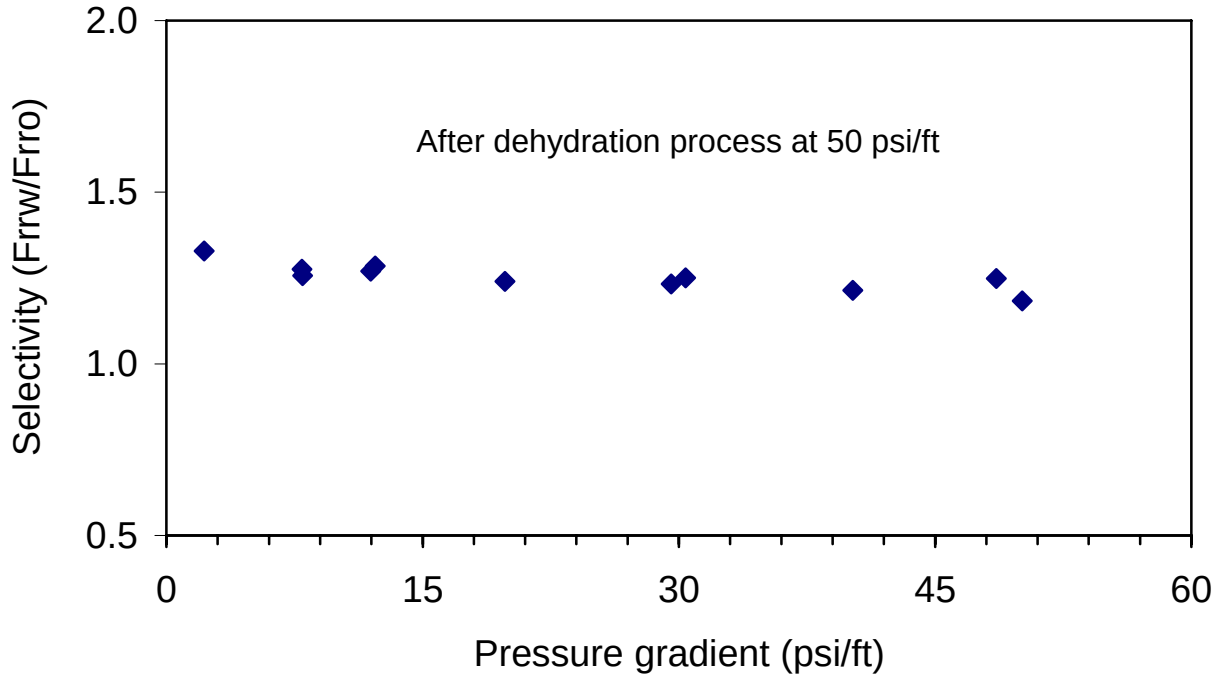

Figure 8.10 - Selectivity at various pressure gradients after dehydration process at 50 psi/ft in Core 2.

phase during the first post-treatment oil flood. Incomplete gelation was probably caused by fluid-rock interactions during the injection and shut-in time period. Properties of the gelant (pH, color, gel time) in the effluent during the injection process were significantly changed which probably inhibited gelation of the chemical system. Our conceptual model of the oil flood developing channels through the gelled porous medium does not appear to be applicable in Berea Core 2. Although some permeability reduction was observed, it is suspected that the post-treatment oil flood also displaced fluid gelant due to the incomplete maturation of the gel. With a fluid aqueous phase in the core, the oil displacement would likely trap a residual aqueous phase. The tracer run to determine the mobile oil phase (Run 19) showed 19.1 mL of mobile oil, a much larger volume of 13.1 mL of mobile oil as determined from volume balances. The 19.1 mL of mobile oil was close to the amount of mobile oil during the oil flood before the gel treatment (Run 2). This comparison does not include the 2.1 mL of "encapsulated" oil. Evidently, the treatment did affect the oil and brine saturations in the core but the volume balances after the treatment are not correct due to failure of the assumptions involved.

Oil and brine floods after gel treatment in Core 3. A less concentrated gelant was injected into Core 3 (2500 ppm polymer and 62.5 ppm chromium). After gelant injection and a shut-in time period to allow for gelation in situ, oil was injected into Core 2 at a pressure of 20 psi (nominal gradient of 20 psi/ft) to develop flow channels. Aqueous production was seen after five minutes of oil injection. Oil broke through after 1.6 mL of aqueous phase was collected. The aqueous phase in the effluent felt slippery to touch and relatively viscous. The viscosity of aqueous effluent was measured to be from 5.5 to 8.9 cp at a shear rate of 22.5/s, compared to the viscosity of the injected gelant of 8.0 cp at the same shear rate. It appeared that gel was not

Table 8.6 – Material balances, permeabilities and residual resistance factors for Core 2.

Experiment	Brine pro-duced (mL)	Oil pro-duced (mL)	Encap. oil (mL)	Encap. oil con-nected (mL)	Brine in SP (mL)	Total oil in SP (mL)	Gel in SP (mL)	S_w (%)	S_{gel} (%)	S_{ot} (encap. oil) (%)	S_{on} (not encap. oil) (%)	S_w* (%)	S_o* (%)	Mobile fluid (mL)	Eff. pore vol. (mL)	Effec-tive poro-sity (%)	k_w (md)	F_{rrw}	k_o (md)	F_{rro}
Brine saturation			0		24.5	0	0	100	0		0			24.5	24.5	21.0	482			
Oil flood	19		0		5.5	19.0	0	22	0		78			**19.0**	24.5	21.0			495	
Brine flood		9.8			15.3	9.2	0	62	0		38			15.3	24.5	21.0	38.1			
Tracer Sor					15.2	9.3	0	62	0		38			15.2	24.5	21.0				
Gel placement			9.3			9.3	15.2	0	62	38				94.8	24.5	21.0				
Shut-in			9.3			9.3	15.2	0	62	38					0.0	0.0				
Oil flood @ 20psi/ft	6.9		3.0	6.3	~ 0	16.2	8.3	0	34	12	54	0	100	13.2	13.2	11.4			384	1.3
Brine flood @ 20 psi/ft		6.8	2.9	0.1	6.8	9.4	8.3	28	34	12	27	51	49	6.8	13.3	11.4	0.92	41.3		
Oil flood @ 20 psi/ft	6.4		2.7	0.2	0.4	15.8	8.3	1.6	34	11	54	3	97	13.1	13.5	11.6			195	2.5
Oil flood @ 50psi/ft	0.5		2.2	0.5	~ 0	16.3	8.2	0	33	9	58	0	100	14.1	14.1	12.1			310	1.6
Brine flood @ 50 psi/ft		10	2.2	0.0	10	6.3	8.2	41	33	9	17	71	29	10.0	14.1	12.1	20.2	1.9		
Oil flood @ 50 psi/ft[1]	8.9		2.1	0.1	1.1	15.2	8.2	4	33	9	54	8	92	13.1	14.2	12.2			177	2.8
Tracer So*														**19.1**		16.4				

dehydrated by oil and that gelant was slowly displaced (broken/destroyed) by oil. The fraction of the aqueous phase displaced from the core as a function of time is shown in Figure 8.11. Total aqueous phase collected was 51% of initial gel in the core.

No permeability reduction to oil was observed as shown in Figure 8.12 where the residual resistance factor to oil (F_{rro}) is plotted as a function of pressure gradient. Core 3 was then flooded with brine and the permeability measured as a function of pressure gradient. The residual resistance factors to water (F_{rrw}) and the selectivity are shown in Figure 8.13 as a function of pressure gradient. The data show the gel treatment did not appreciably change the permeabilities to oil and brine. Further experiments and analyses on Core 3 were terminated.

Summary

The gel treatments applied to the Berea cores were compromised due to poor maturation of the gel system. Incomplete gelation during the shut-in period was thought to be caused by fluid-rock interactions that increased the pH of the gel system, significant polymer/gel retention during the injection process and possibly by the introduction of contaminants such as iron ions. High pH values can cause precipitation of chromium. The treatments reduced the brine permeability to a greater extent than oil permeability was reduced. Permeabilities were reduce by a much smaller factor than similar gel treatments that were applied to sandpacks [Chapter 7] that had much higher initial permeabilites and much less capacity for interfering fluid-rock interactions.

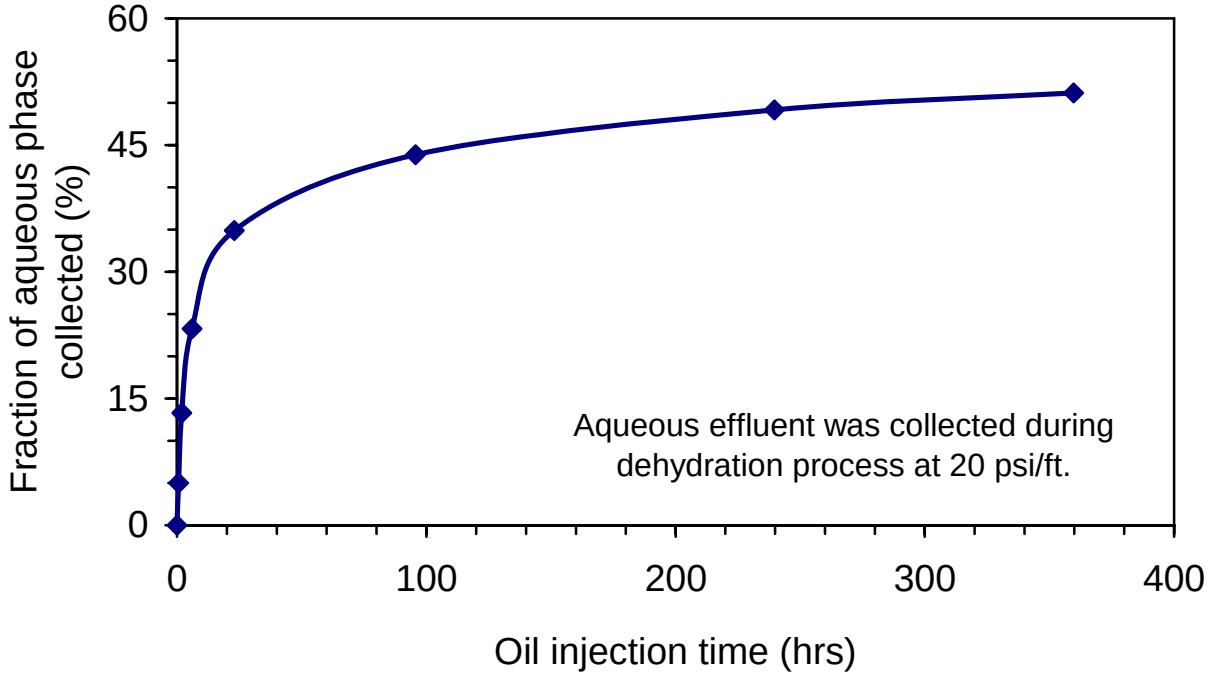

Figure 8.11 - Volume fraction of aqueous phase collected during dehydration process in Core 3.

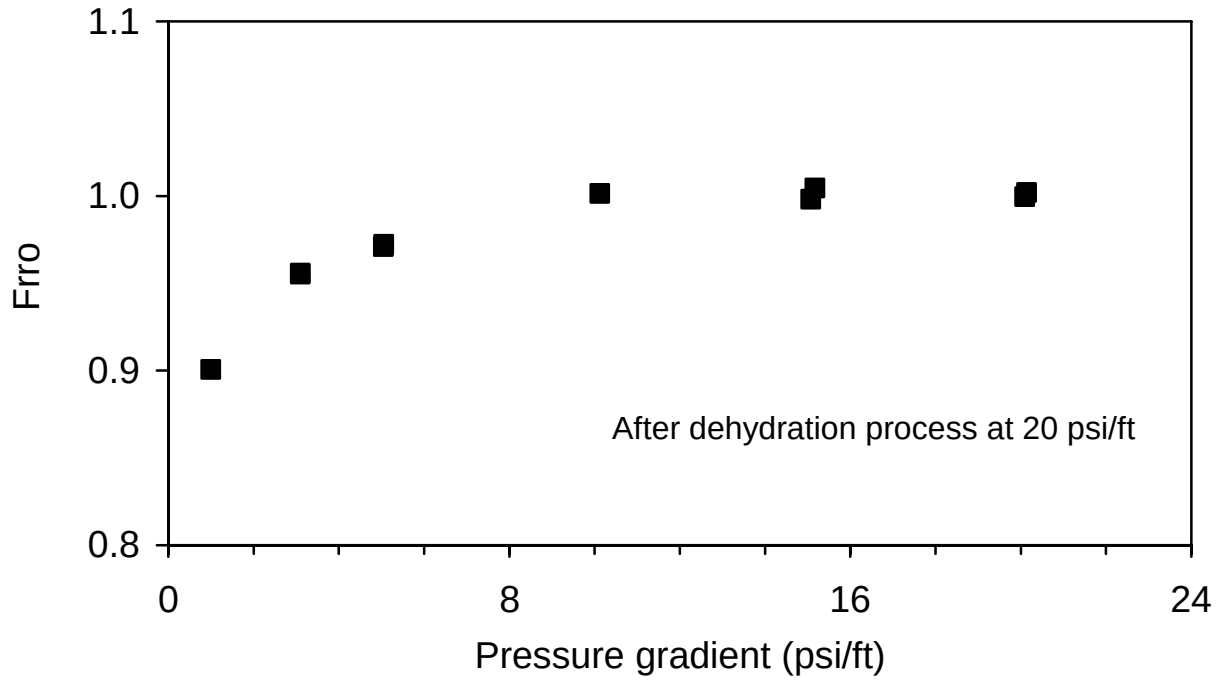

Figure 8.12 - F_{rro} at various pressure gradients after dehydration process at 20 psi/ft in Core 3.

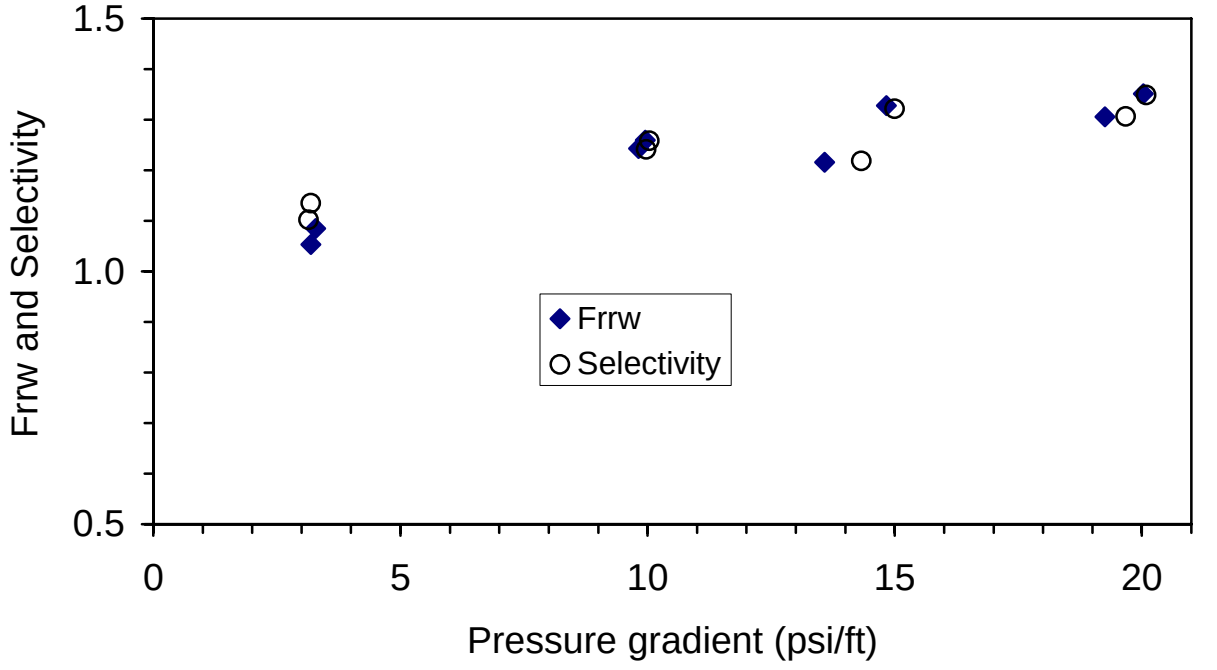

Figure 8.13 – Residual resistance factors to water and selectivity for Core 3.

Nomenclature

- F_{rro} - Residual resistance factor to oil.
- F_{rrw} - Residual resistance factor to water.
- k_b - Base permeability in md.
- k_o - Permeability to oil in md.
- k_{ob} - Permeability to oil before gel placement in md.
- k_{oa} - Permeability to oil after gel placement in md.
- k_w - Permeability to water in md.
- k_{wb} - Permeability to water before gel placement in md.
- k_{wa} - Permeability to water after gel placement in md.
- S_{gel} - Gel saturation in the sandpack determined based on the initial PV.
- S_{on} - Oil saturation that is not encapsulated by the gel based on the initial PV.
- S_{or} - Residual oil saturation.
- S_{or}* - Residual oil saturation in the "new" pore space determined based on effective PV.
- S_{oen} - Saturation of oil that was encapsulated by the gel and determined based on stilbene recovery and the initial PV.
- S_o* - Oil saturation in the "new" pore space determined based on effective PV.
- S_w - Water saturation in the sandpack determined based on the initial PV.
- S_w* - Water saturation in the "new" pore space determined based on effective PV.
- S_{wi} - Interstitial water saturation in the sandpack determined based on the initial PV.
- S_{wi}* - Interstitial water saturation in the "new" pore space and based on effective PV.

Chapter 9

Experimental Study of Filtration Mechanisms of Pre-Gel Aggregates during Flow of a Polyacrylamide-Chromium(III) Gel System in Sandpacks

Graduate Research Assistant: Behruz Shaker Shiran

Introduction

Partially hydrolyzed polyacrylamide polymer (HPAM)-chromium(III) gel systems are widely used in treatments of oil reservoirs to reduce the permeability of or block high permeability zones. These systems react to produce crosslinks between the polymers molecules to form pre-gel aggregates. In bulk form, the aggregates continue to crosslink to form a 3D network or gel.

Typically, field treatments consist of mixing solutions of polymer and crosslinker in line and injecting the gelant through the reservoir for time periods that are much longer the bulk gel times. Laboratory flow studies that simulate that scenario show a significant increase in the flow resistance at positions in the porous media behind the leading edge of the injected gelant. The developed flow resistance occurs at times less than the bulk gel time and limits the depth into the reservoir that the gelant can be placed [McCool et al., 1991. The development of flow resistance was interpreted to be caused by filtration of pre-gel aggregates. Filtration of aggregates is hypothesized to occur by straining and interception mechanisms. Straining occurs when the aggregates become trapped because their size is too large to penetrate a pore throat. Interception occurs when the aggregates encounter the pore walls and are retained by adsorption and reaction with previously retained polymer or aggregates. The relative significance of these filtration mechanisms is not known.

Previous investigators have determined the amount of adsorptive retention relative to non-adsorptive retention in polymer flow through porous media by the comparison of flow retention with static adsorption for a given adsorbent medium [Szabo, 1973] or by the comparison of flow retention data from hydrophilic and hydrophobic porous media [Dominquez and Willhite, 1976; Cohen and Christ, 1986]. Cohen and Christ [1986] modified chemically the silica surface using a silane-treating procedure that rendered silica sand a hydrophobic substrate that inhibited adsorption. Their experimental method allowed them to directly determine the adsorptive and non-adsorptive polymer retention from flow experiments.

The original objective of this work was to determine the relative significance of adsorptive and non-adsorptive mechanisms during flow of gelant through sandpacks. Flow experiments were conducted with silanized and non-silanized sandpacks similar to the procedure developed by Cohen and Christ. It was discovered during the course of this work that the silanization procedure did not reduce but increased adsorption of the selected polymer on the sand grains. This fact precluded the original objective but experiments did provide information on the absorptive mechanism that occurs during gelant flow in sandpacks.

A second attempt to differentiate filtration mechanisms was by the injection of aged gel solutions into sandpacks. This was accomplished by a delay component that the in-line mixed gelant

flowed through before injection into the sandpack. The delay allowed for injection of larger aggregates into the sandpacks due the longer reaction time.

Experimental materials, equipment and procedures

Gel solution and chemicals. Polymer stock solutions were prepared at a concentration of 10,000 ppm of partially hydrolyzed polyacrylamide (Alcoflood 935, Lot# A2247BOV, ≈ 10% hydrolyzed) in a brine solution containing 2% KCl and 10 ppm sodium azide (bactericide). The solution was stirred for about 48 hours to ensure complete solubility and hydration of polymer. The polymer solution was filtered through a 1-micron fiberglass filter using air pressure of 15 psig. Chromic acetate solutions were prepared at a concentration of 200 ppm chromium from a 50% chromium acetates solution (McGeane and Rohco, Lot# 40086816) The 200 ppm chromium solution was kept at 30 °C and allowed to age for 14 days before use. Gel times decreased with age of the chromium solution up to 14 days and remained approximately constant thereafter.

Stock polymer and chromium acetate solutions were mixed at a weight ratio of 1:1 to prepare gel solutions. The mixing was done manually for bulk samples and with pumps and an in-loine mixer for flow experiments. Compositions of gel solutions were 5,000 ppm of Alcoflood 935 partially hydrolyzed polyacrylamide (HPAM), 2.0% potassium chloride, 5 ppm sodium azide and 100 ppm chromium from chromium acetate. Bulk mixed samples were mixed for several minutes to ensure a homogeneous solution and the pH was measured. The pH for all gel samples in bulk gel experiments was 4.73±0.01. Samples were placed in a temperature box maintained at constant temperature of 30 °C.

Static adsorption tests. Experiments were conducted to quantify the amount of polymer adsorption on silica sand and on silane-treated sand. The static adsorption experiments with 5,000 ppm hydrolyzed polyacrylamide polymer (Alcoflood 935, Lot# A2247BOV, 10% hydrolysis) in 1% KCl were performed at 30±0.5 °C with both non-silanized and silanized silica sand. Known amounts (20 g) of dry sand were weighed into glass vials and a known amount (15 g) of polymer solution of 5000 ppm concentration was poured into the vials. Controls in which water without polymer was added to the sand were also prepared to determine the amount of carbon from the sand, particularly for the silanized sand. The vials were gently shaken by hand every 6 hours and after sufficient time of equilibration (48 hours) liquid samples were taken to polymer concentration determination. The polymer concentration was determined by Total Organic Carbon (TOC) analysis. The mass balance between polymer concentrations -before and after contact with sand- was used to calculate the polymer adsorption level.

Flow experiments -equipment and procedures. A schematic diagram of the experimental set up used for flow experiments are shown in Figure 9.1. Polymer and chromium(III) solutions were injected each at a constant rate of 0.33 mL/min (Darcy velocity = 1.37 ft/d) by two liquid chromatography pumps into an in-line static mixer. The in-line mixed gel solution was flowed at a constant rate of 0.66 ml/min (Darcy velocity = 2.74 ft/d) into the sandpack. In some experiments, a delay line was placed between the in-line mixer and the sandpack. The delay line was a large diameter in-line mixer with sufficient volume corresponding to selected delay times. In-line mixers were used to minimize the radial velocity distribution during flow through a tube.

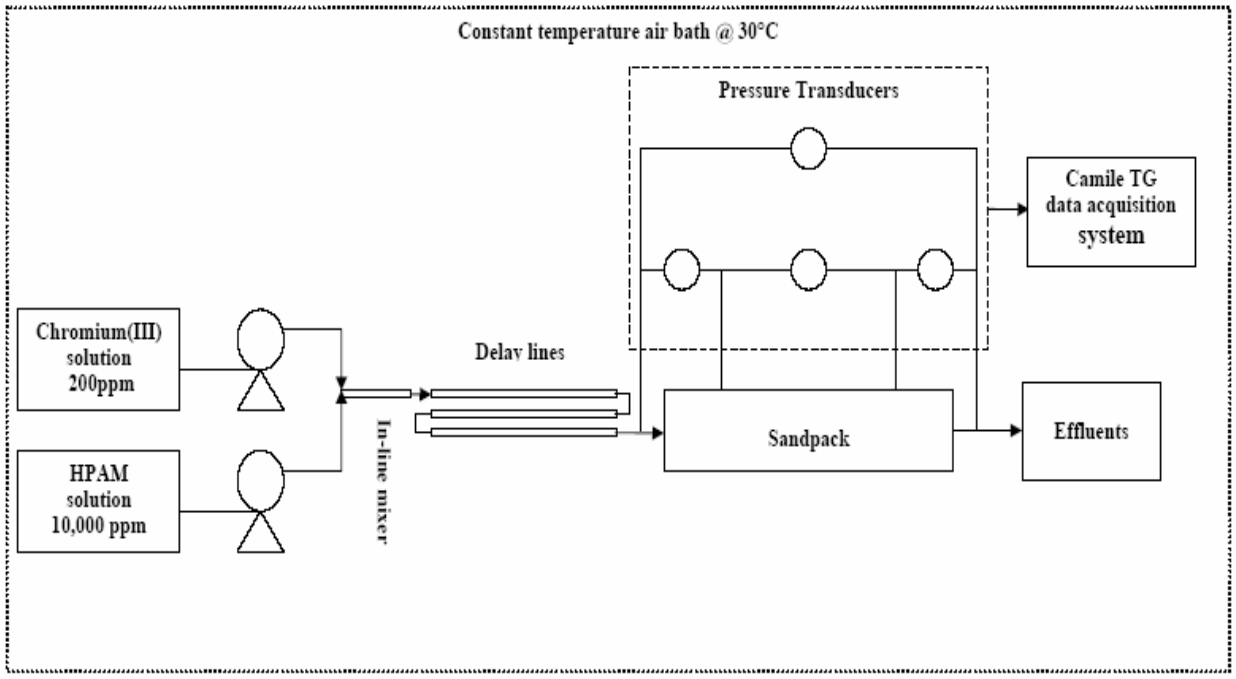

Figure 9.1 - Schematic diagram of the experimental set up for in-situ gelation experiments.

Preliminary experiments showed that the delay lines did not affect gel times that were measured from the time the gelant exits the initial in-line mixer. Effluent samples were collected manually every 30 minutes at the outlet of the sandpack. Flowrate, pH, initial viscosity, gel time and polymer and chromium concentrations of the effluent samples were measured.

Pressure ports were installed along the length of the sandpack to measure differential pressures of each section and the whole sandpack. Differential pressures were sensed by a Validyne transducer / demodulator system. Three 10 psi diaphragms were used to measure differential pressures of individual sections and a 200 psi diaphragm was used to measure differential pressure of the whole sandpack. The transducers were calibrated before each permeability measurement and displacement experiment. Differential pressures were recorded using Camile TG data acqusition system. The experimental system was maintained in an air bath at a constant temperature of 30 °C.

For each run, several gelant samples were prepared or collected and their gel times were determined to ensure consistency of the injected gelant and proper operation of the injection system. A bulk gel sample was hand-mixed and a sample was collected from the outlet of the in-line mixer (pre-run in-line mixed sample) before injection into the sandpack was initiated. In the experiments using delay lines, an additional sample was collected from the outlet of the delay line (pre-run sample from delay lines) before injection into the sandpack. Samples from the in-line mixer and the delay lines were also collected after termination of flow into the sandpack. Viscosities of the samples were monitored with Brookfield viscometer and gel times were determined.

The flow experiment was initiated by injection of the gel solution from the in-line mixer (or from the delay lines) into the sandpack. Pressure data were collected using the transducer set up and

data acquisition system. Effluents were collected manually from the outlet of the sandpack at 30 minutes interval. The effluents first were weighed to check the flowrate, and then analyzed for pH and viscosity soon after they were collected. The viscosity measurement for effluents was continued to determine gel times. The chromium and polymer concentrations of the effluents were analyzed at the end of displacement experiments. The displacement experiments were terminated when the differential pressure over Section 2 of the sandpack rose to more than 10 psi (the upper bond of transducer).

Sandpacks. Sand holders were constructed from acrylic plastic stock with an ID of 1.5 inch and a length of 3.75 inch. They were fitted with end plates and sealed with an O-ring. Grooves were cut in the inner face of the end plates to allow uniform distribution of the injected fluids in inlet and outlet of the sandpack. To stabilize the sand in the holder and prevent sand particles from entering the transducer tubing, 360-mesh screens (70 microns) were inserted in the pressure ports.To prevent sand movement and washout from the sandpack, one coarse screen was placed at the inlet and one fine screen and one coarse screen was place at the outlet of the sandpack. The fine screen (273 mesh) was placed at the sand side of the outlet.

Ottawa F-110 silica sand (50 mesh) was used to make an unconsolidated sandpack. The sand was sieved to remove all +50 mesh grains and then the sand was washed by soaking in concentrated hydrochloric acid for a few days. The sand was washed with distilled water many times until the wash liquid attained a neutral pH. The washed sand was then dried in an oven at 40 °C for 48 hours.

A schematic of the sandpacks is shown in Figure 9.2. Pressure ports divided the pack into three sections. The main section which was filled with fine sand had a length of 2 inches. The other two sections had a length of 0.875 inch and were composed of two parts: one part filled with fine sand and had a length of 0.5 inch and the other part filled with coarse sand and had a length of 0.375 inch.

The holders were packed with sand using a vibrator. Sandpacks were checked for possible leakage and then they were saturated with water. Porosity and permeabilities of the 3 sections of the pack were determined and the values are listed in Table 9.1.

Analytical measurements and procedures. Gel times were determined using a Brookfield Microviscometer (Model LVDVI+CP). Samples of gel solution (0.5 ml) were periodically

Table 9.1 – Sandpack properties.

Run No.	1-1	1-2	2-2	2-3	3	4	4-4	5
Pore volume, mL	36.9	37.0	36.5	37.3	36.7	35.9	37.4	37.5
Porosity	33.9	34.1	35.0	34.4	33.8	33.1	34.4	34.5
Permeability, D								
Total length	5.1	5.4	5.6	5.1	5.1	5.1	4.9	5.3
Section 1	5.3	7.4	6.2	6.6	6.0	5.9	5.4	6.6
Section 2	4.7	4.5	5.0	4.8	4.9	4.7	4.6	4.7
Section 3	5.5	7.1	6.2	5.0	5.5	5.3	5.4	6.0

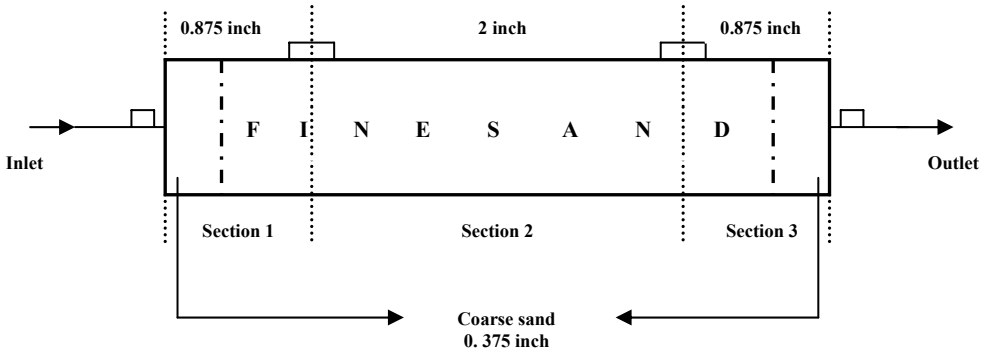

Figure 9.2 - Schematic of the sandpack used for in-situ gelation experiments (Length= 3.75 inch, ID= 1.5 inch).

measured with a cone-and-plate geometery. Initial measurements were conducted at a shear rate of 22.5 s^{-1} upto viscosity limit of 102.8 cP. A shear rate of 2.25 s^{-1} was used thereafter. The time when the viscosity of gel solution increase sharply to a value of about 500 cp was defined as the gel time.

Polymer concentrations in effluent samples were determined by Total Organic Carbon (TOC) analysis. The gel was broken by an oxidation process. About 1 gram of gel sample was placed in glass vials with 1 mL of hydrogen peroxide and 1 mL potassium hydroxide. The vials were placed without the cap in an aluminum heater block at 85°C and heated for two hours. The samples were then diluted with water and analyzed by TOC method. The polymer concentration of the effluent samples was determined using calibration curve from TOC, dilution factors, and polymer concentration in diluted samples.

Concentrations of chromium in effluent samples were determined using a spectrophotometer after the oxidation process described above for polymer analysis. The oxidation process broke the gel and converted the chromium to chromium (VI) which was measured at a wave length of 375 nm. The samples were diluted to be in the linear range between 0 and 20 ppm chromium.

Results and Discussion

Static adsorption experiments. Experiments were performed to determine the adsorption level of 5000 ppm partially hydrolyzed polyacrylamide (10% hydrolysis) on untreated silica sand and silanized silica sand. The average static adsorption of polymer on untreated silica sand was 77.4 µg polymer per gram of sand. Adsorption of polymer on silanized silica sand was 106.8 µg polymer per gram of sand.

The results showed that the silanization technique did not reduce the adsorption level of polymer, but increased the adsorption by 38%. These results are in contrast to the results of Cohen and Christ [1986], which showed that silane surface treatment effectively eliminated HPAM

adsorption on silica sand. Cohen and Christ [1986] used a polyacrylamide with 25% hydrolyzed groups.

In a different study by Broseta et al. [1995] the silanization technique increased the adsorption of neutral polymer (~0% hydrolysis) and reduced the adsorption of hydrolyzed polyacrylamides (27% and 45% hydrolysis) on silanized sand. The adsorption behavior of 10% hydrolyzed polyacrylamide used in this work on silanized silica sand was similar to the behavior of neutral polyacrylamides.

In-situ gelation experiments Eight flow experiments were conducted under comparable conditions except for the silanization treatment of the sand and the age of the gel entering the sandpack (see Table 9.2). Runs conducted with injection of un-aged gleant were conducted twice to test reproducibility. Runs 1-1 and 1-2 provide the base case for comparison to the varied parameters. Results from Run 1-2 are presented in detail followed by comparisons of key results with other runs. Details of all runs are given by Shiran [2006].

Table 9.2 – Parameters for flow experiments.

Run No.	1-1	1-2	2-2	2-3	3	4-4	5
Silanized sand, ?	no	no	yes	yes	no	no	no
Injected gelant age, min	0	0	0	0	26	42	59
Residence time, min	56	56	55	57	56	57	57
Bulk gel time, min	175	188	174	180	187	179	178
Injected pore volumes	3.2	2.75	2.44	2.47	1.72	1.45	1.23

A bulk-mixed gelant sample and in-line mixed gelant samples collected before and after the displacement experiment from the in-line mixer and from the delay lines were monitored to determine gel times for verifying proper gelant performance. Viscosity as a function of time for these samples is shown in Figure 9.3. Gel times for the bulk samples were consistent in the range from 170 to 190 minutes.

Run 1-2: Non-silanized porous media, non-aged gel solution. Runs 1-1 and 1-2 were base cases where the sand was not salinized and there was no delay after the in-line mixer prior to injection into the sandpack. Pressures drops across each section and across the sandpack length during gelant injection are shown in Figure 9.4 as a function of time and injected pore volumes. Gel injection was injected terminated after about 2.75 pore volumes. Differential pressures and initial permeabilities were used to calculate apparent viscosities in each section and across the sandpack and these results are shown in Figure 9.5 versus time and injected pore volumes. The apparent viscosity profiles show that the most of the buildup of flow resistance occurred in Section 2, the test section. Timing of the increased flow resistance was comparable to the bulk gelation time.

Effluent samples were collected every 30 minutes to determine the flow rate, viscosity, pH, and concentrations of chromium(III) and polymer. Flow rate measurements showed the injection

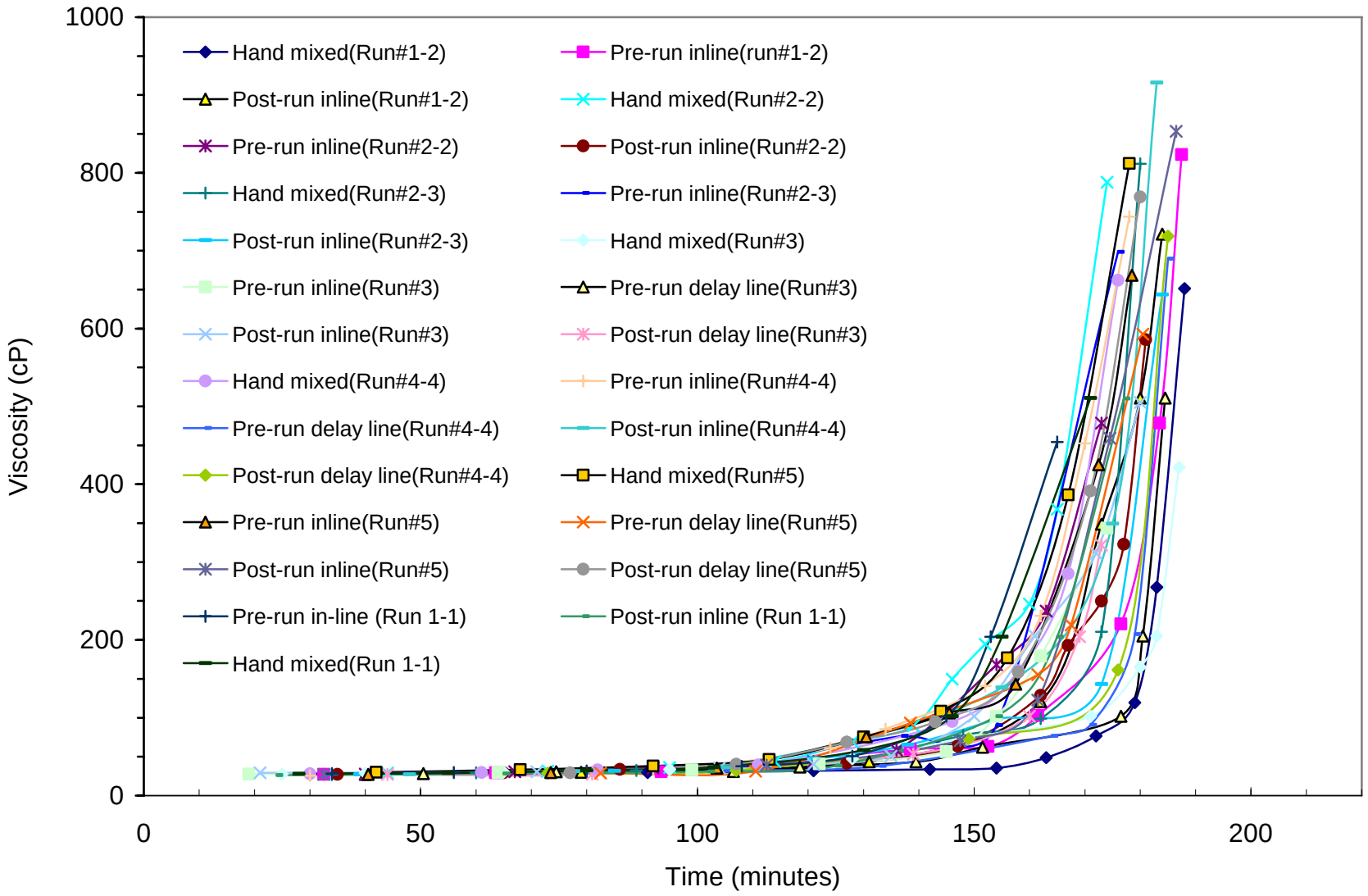

Figure 9.3 – Gel time determination for bulk samples to assess proper performance of the flow experiments.

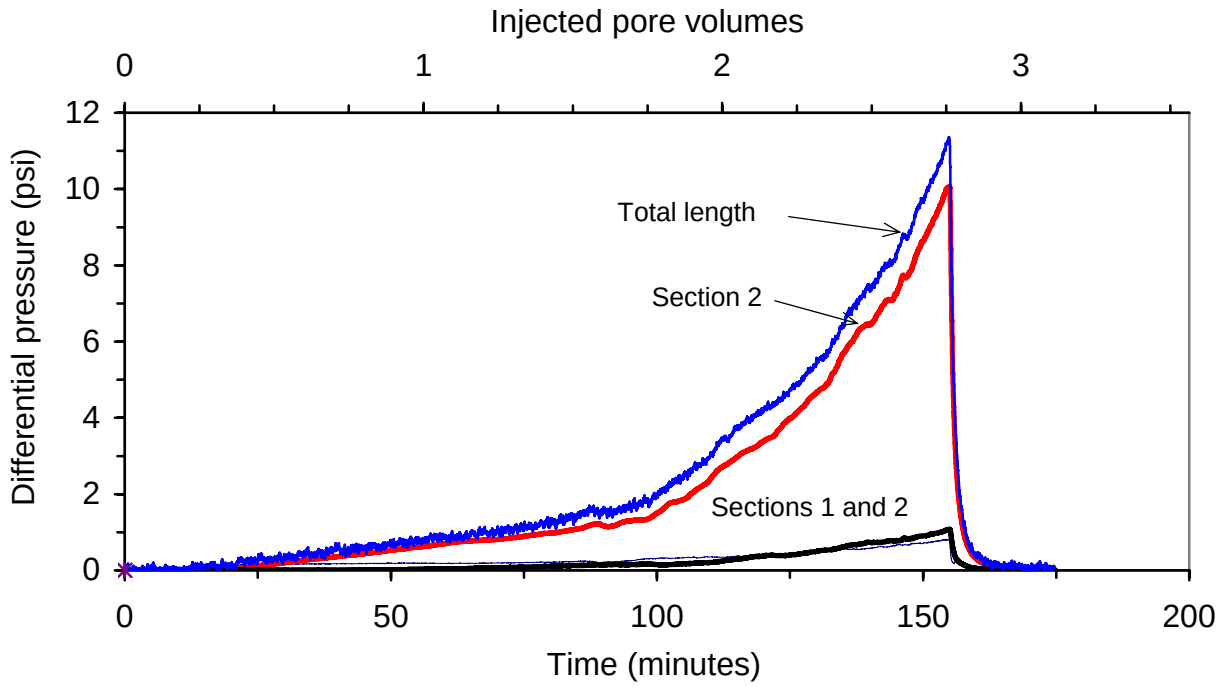

Figure 9.4 - Pressure drops across the sandpack and the three sections during gelant injection in Run#1-2.

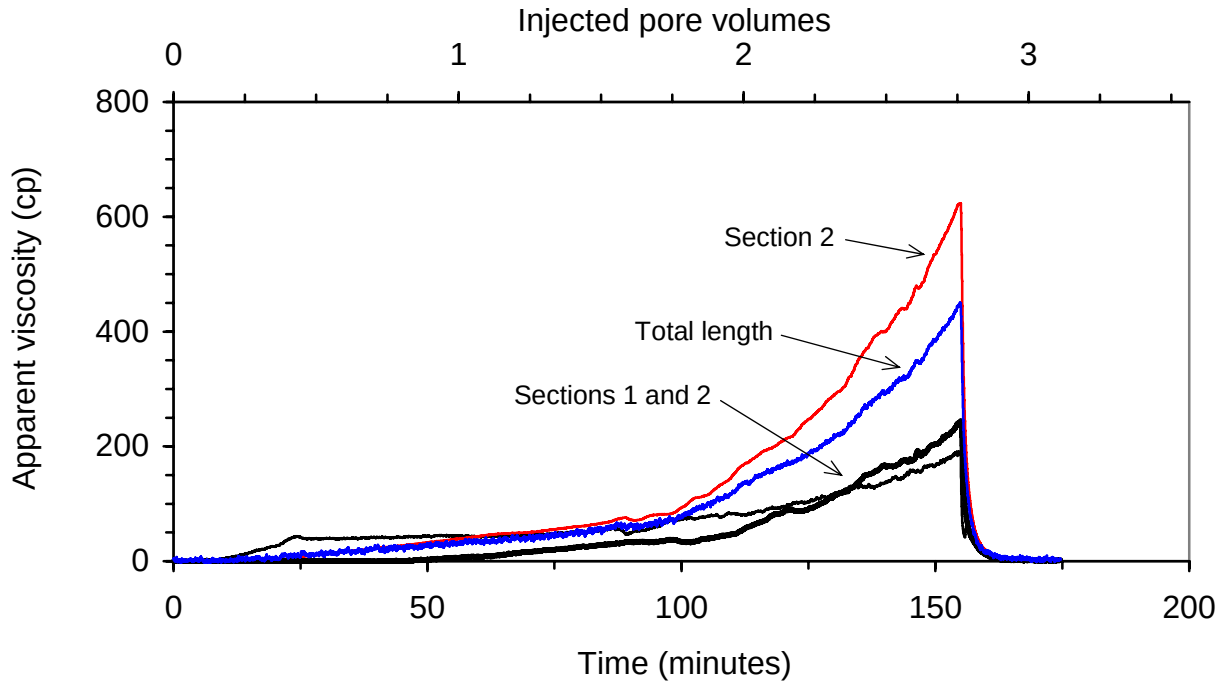

Figure 9.5 - Apparent viscosity in the sandpack and the threee sections during gel injection in Run#1-2.

system worked properly. Chromium concentration and pH of the fractions are shown in Figure 9.6 and the initial viscosity and polymer concentration are shown in Figure 9.7. These data are plotted at the mid point of the time interval over which the sample was collected. Effluent fractions #1 and #2 were essentially the displaced resident brine. Fractions #3, #4 and #5 represented gelant that had traversed the sandpack. Chromium concentrations after 1 PVI were somewhat greater than the measured injected concentration of 108 ppm and show little retention of chromium in the sandpack. The effluent pH values were comparable to the value of the injected gelant. Significant amounts of polymer were retained as shown by the effluent polymer concentrations below the injected value of 5000 ppm and the viscosity lower than the injected value of 27 cp.

Viscosity of effluent fractions collected after 1 PVI were monitored to assess their gelation behavior. Viscosities are presented in Figure 9.8 as function of the time from mixing at the inline mixer and assuming plug flow through the sandpack. Effluent samples took longer to gel than the bulk mixed gelant. Gel times were shorter with successive fractions which correlated with higher polymer concentration in successive fractions.

Comparisons between silanized and natural sand. Four runs were conducted with no delay between the in-line mixer and the sandpack. Runs 1-1 and 1-2 were conducted with untreated sand and Runs 2-2 and 2-3 were conducted with silanized sand. Apparent viscosities of the fluid flowing through the test section, Section 2, for the four runs are presented in Figure 9.9. The data are comparable for the runs with silanized sand. Earlier development of flow resistance in Run 1-2 as compared to Run 1-1 might have been due the lower permeability of Section 2 in Run1-2 (4.5 D) as compared to the other runs (4.7 to 5.0 D). Flow resistance increased faster in the runs with silanized sand.

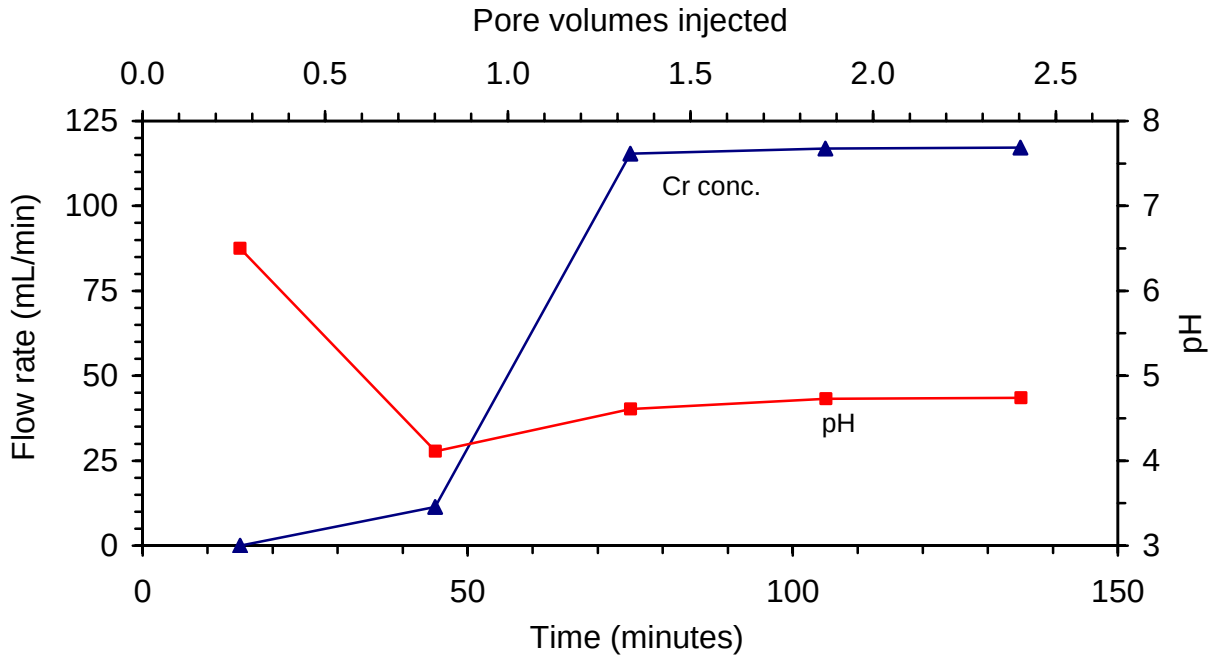

Figure 9.6 – Chromium concentration and pH of effluent fractions in Run 1-2.

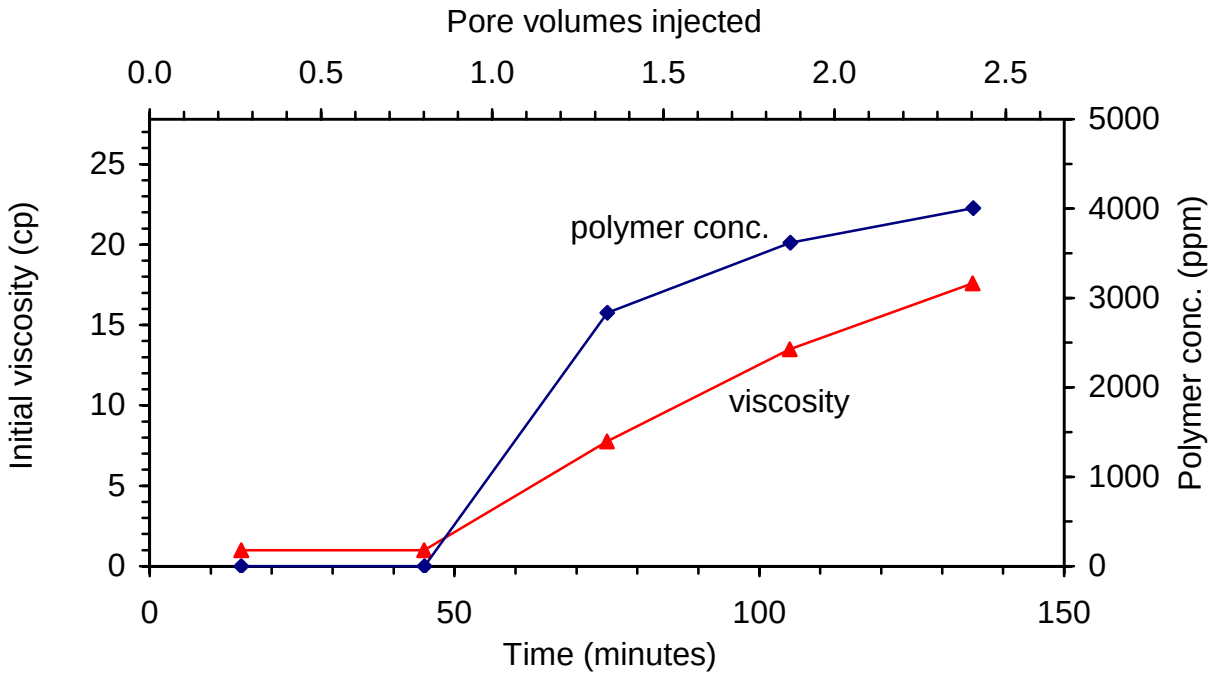

Figure 9.7 – Polymer concentration and initial viscosity of effluent fractions in Run 1-2.

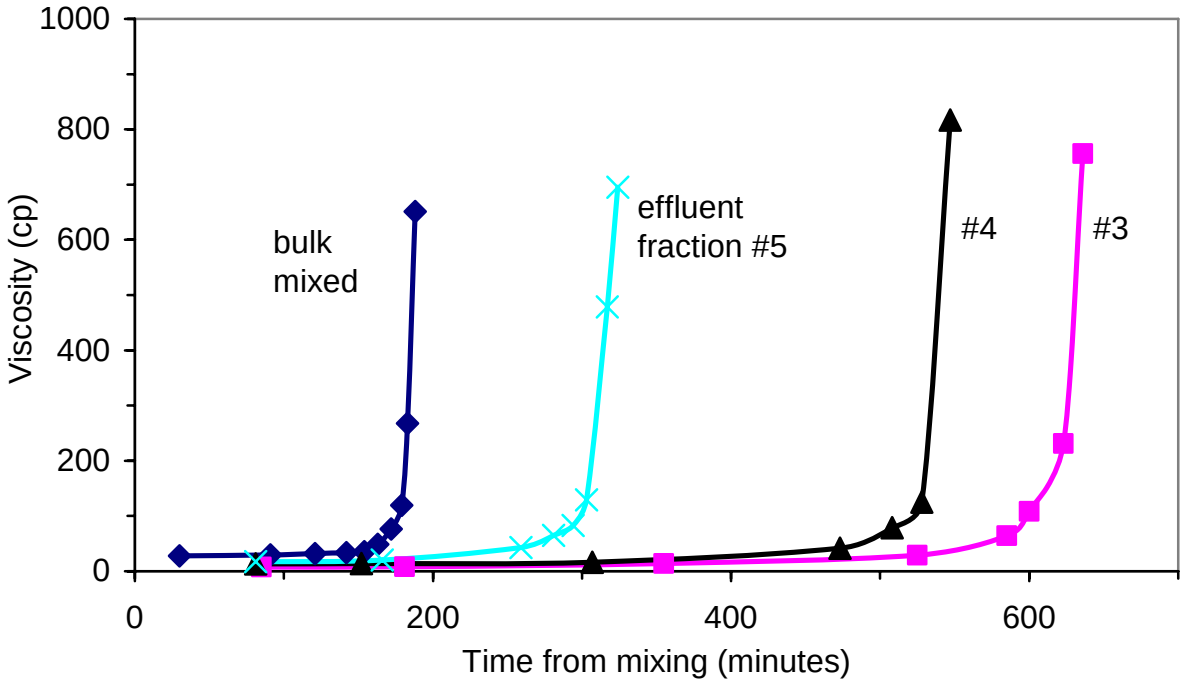

Figure 9.8 – Viscosity of effluent fractions as function of time from mixing for Run 1-2.

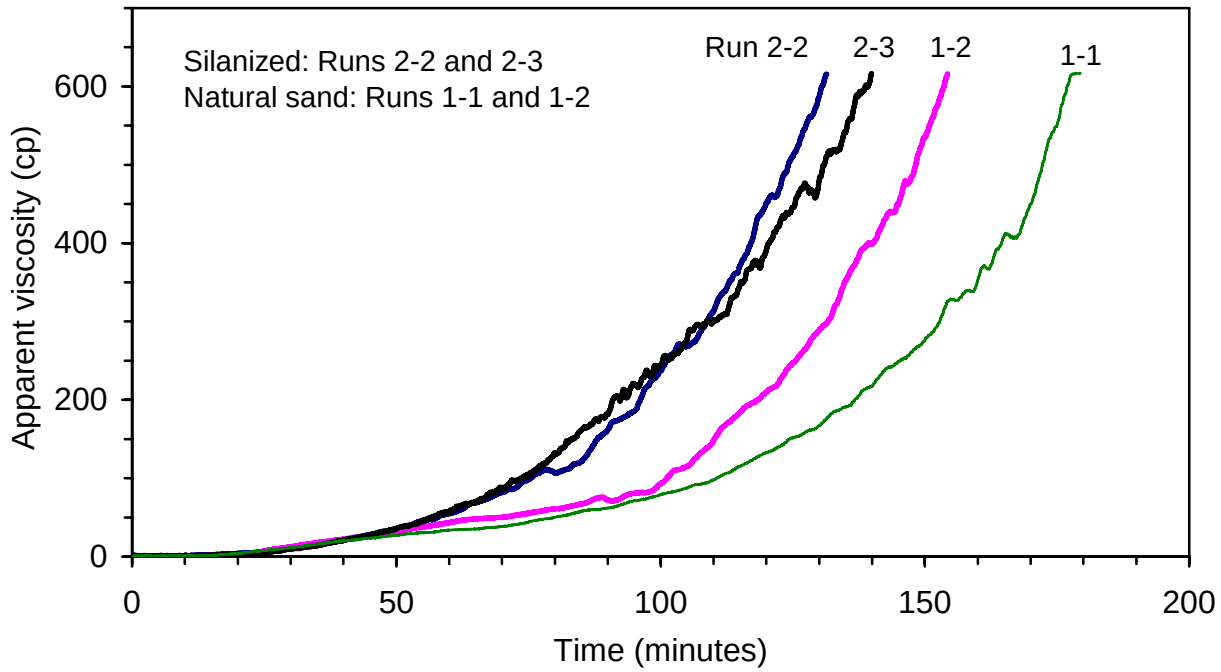

Figure 9.9 – Development of flow resistance in runs with natural and silanized sand.

Polymer concentrations in the effluent are presented as a function of pore volumes injected in Figure 9.10. These data are plotted at the end of the collection interval for each sample collected. More polymer was retained at the gelant front for Run 2-3 in the silanized sand. Polymer concentrations were not measured for Run 2.2. Effluent viscosities measured shortly after collection are plotted against pore volumes injected in Figure 9.11. The effluent viscosities show a similar trend as the polymer concentrations. Higher polymer retention on the silanized sand due to adsorption and reaction with previously retained was responsible for the faster development of flow resistance.

Effect of gelant age on development of flow resistance. Runs were conducted to determine the effect of age of the injected gelant on the development of flow resistance. Change in the gelant age that was injected into the sandpack was accomplished by inserting different lengths of delay lines between the in-line mixer and the sandpacks. Flow resistances during these runs and for the two runs using un-aged gelant are shown in Figure 9.12 where time was measured from when the gelant was injected into the sandpack. All of these runs were conducted in natural sand. Flow resistance developed faster with age of gelant. Growth of gel aggregates in aged gel solutions and filtration of the larger aggregates caused the flow resistance to increase sooner and at a faster rate. This is also shown in Figure 9.13 where the amount of gelant that passed through the midpoint of Section 2 is plotted against the age of the solution at that same position. In addition to lessening the amount of throughput, less polymer retention occurred with increased age of the gelant as shown in Figure 9.14. These data are plotted at the end of the collection interval for each sample collected. With increased gelant age, there was less retention and less throughput of gelant at the time of high flow resistance. This is indicative of the retention of a few large aggregates and supports the idea that the straining mechanism increases with gelant age.

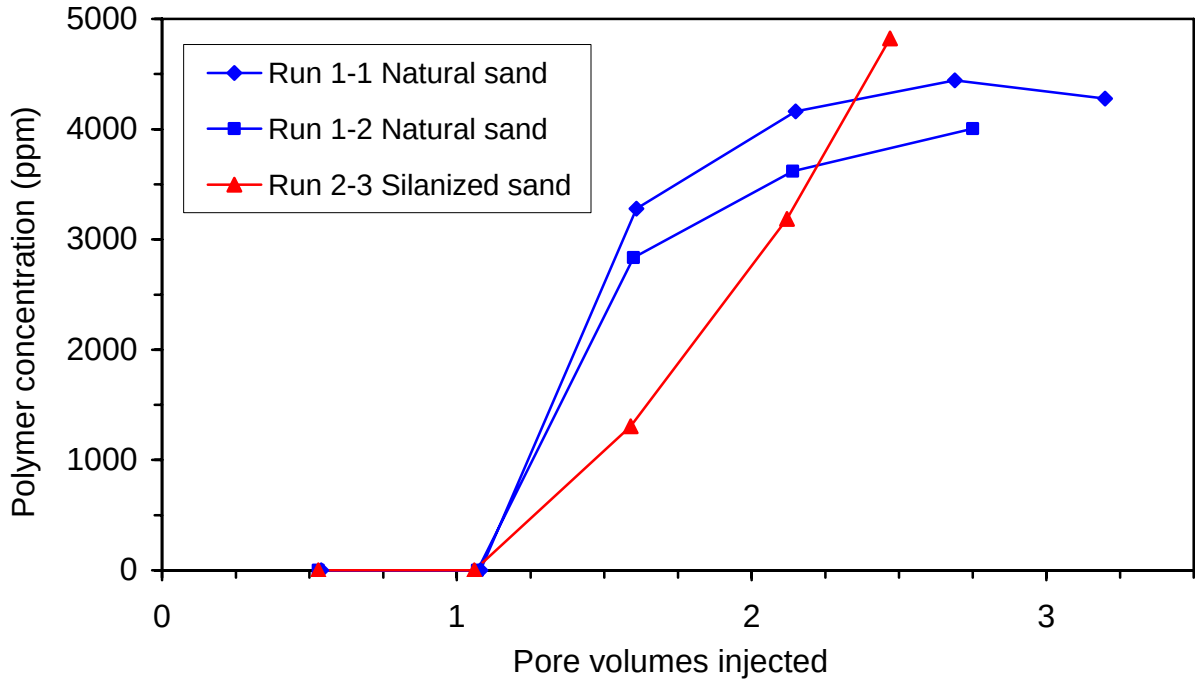

Figure 9.10 – Comparison of effluent polymer concentrations in runs conducted in natural and silanized sand.

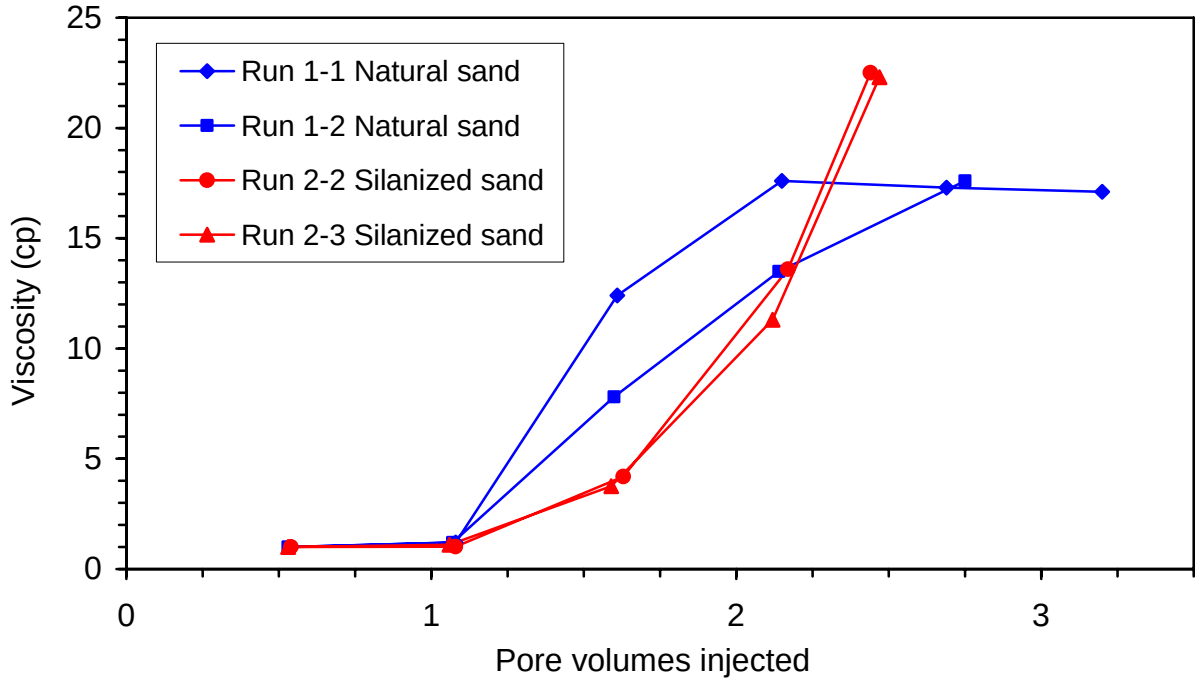

Figure 9.11 – Comparison of effluent viscosities measured shortly after collection in runs conducted in natural and silanized sand.

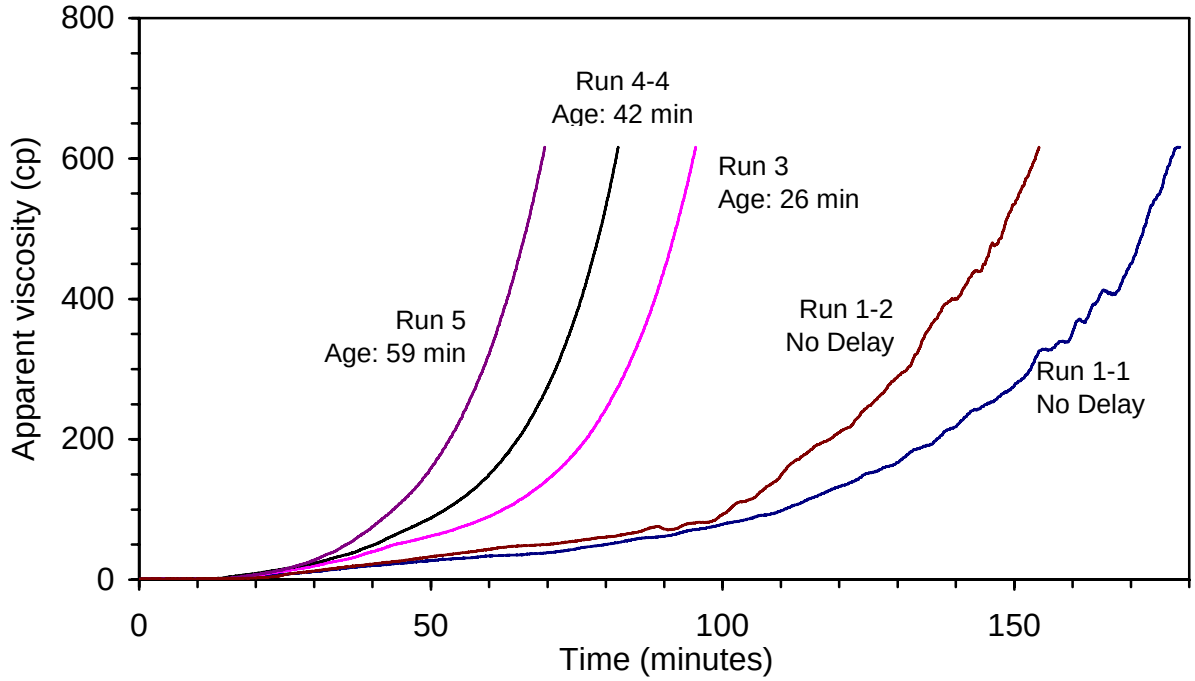

Figure 9.12 – Flow resistance in Section 2 for runs with different injection-delay times. Time 0 is the time when the gel solution is injected into the sandpack.

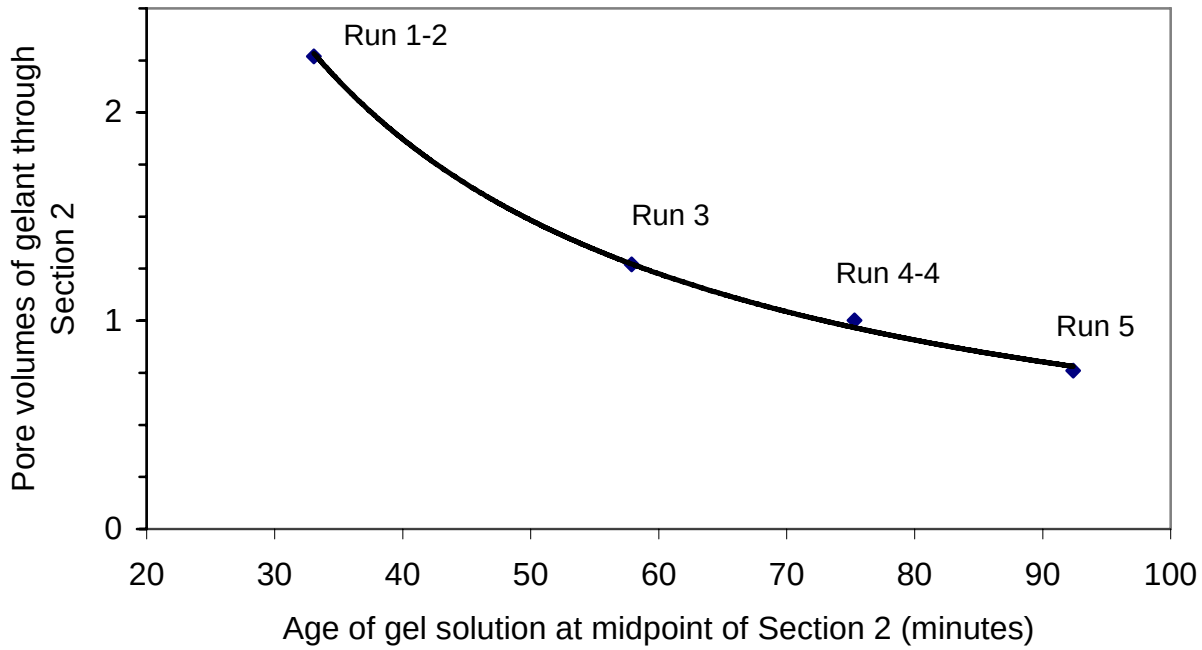

Figure 9.13 - Relationship between the age of gel solution at the middle of Section 2 and the pore volumes of gelant that passed through the midpoint when the injection was terminated.

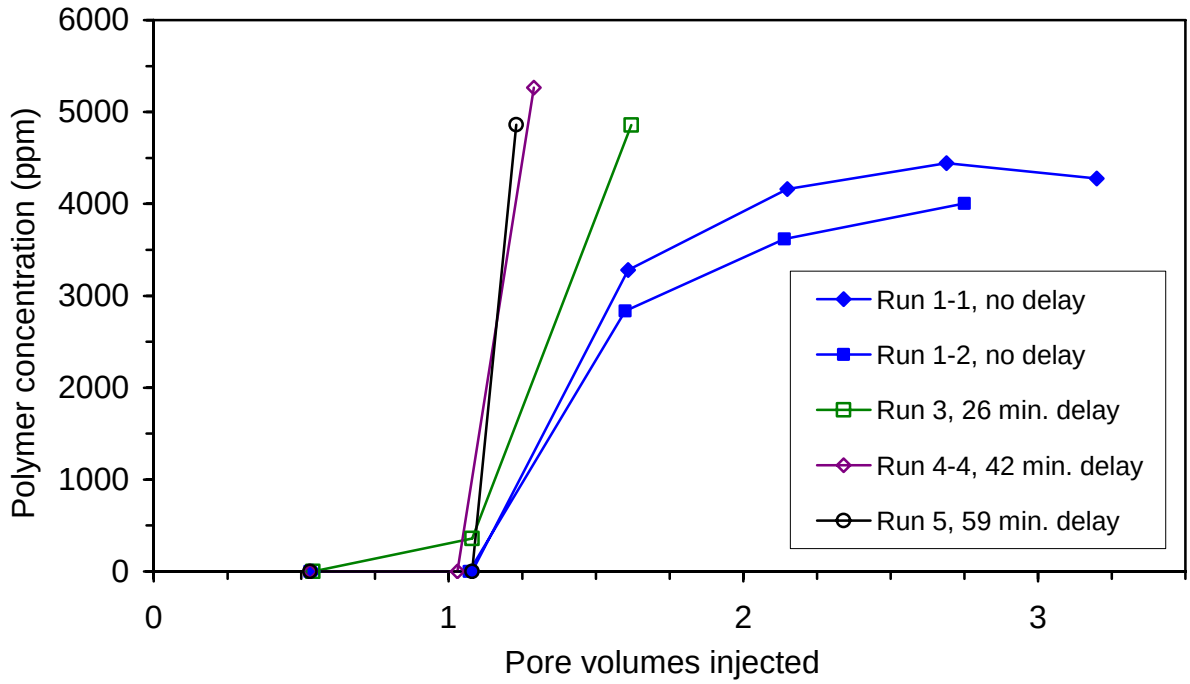

Figure 9.14 – Comparison of effluent polymer concentrations in runs conducted at different delay times and in natural sand.

Conclusions

The following conclusion based on and limited to the particular polymer (Alcoflood 935), gelant system (Alcoflood-chromium acetate) and porous medium (Ottawa F-110 silica sand) that were studied.

1. Silanization of the Ottawa F-110 silica sand increased the adsorption of Alcoflood 935 polyacrylamide as compared to the untreated sand in static tests. Adsorption was 77 μg of polymer per gram of untreated sand and 107 μg of polymer per gram of silanized sand.
2. Adsorption of polymer and crosslinked polymer aggregates plays a significant role in the buildup of flow resistance during flow of an Alcoflood 935-chromium acetate gelant through silica sandpacks. Increase adsorption of polymer and aggregates caused earlier buildup of flow resistance in sandpacks made from silanized sand than in sandpacks prepared with untreated sand.
3. Adsorption of polymer decreased and retention due to the straining mechanism increased with the age of the gelant. Polymer analyses showed higher retention in runs with non-aged gleant than in runs where aged gelants were injected.

References

Cohen, Y., and Christ, F. R.: "Polymer Retention and Adsorption in the Flow of Polymer Solutions Through Porous Media," *SPE Reservoir Engineering*, **1,** No. 2 (March 1986).

Broseta, D., Medjahed, F., Lecourtier, J., and Robin, M.: "Polymer Adsorption/Retention in Porous Media: Effects of Core Wettability on Residual Oil," *SPE Advanced Technology Series*, **3** No. 1 (March 1995) 103-112.

Dominguez, J. G., and Willhite, G. P.: "Retention and Flow Characteristics of Polymer Solutions in Porous Media," paper SPE 5835, SPE-AIME Fourth Symposiumon Improved Oil Recovery, Tulsa, OK (22-24 March 1976).

McCool, C.S., D.W. Green and G.P. Willhite: "Permeability Reduction Mechanisms Involved in In Situ Gelation of a Polyacrylamide/Chromium(VI)/Thiourea System in Porous Media," *SPE Reservoir Engineering,* **6,** No. 1 (February 1991) 77.

Szabo, M. T.: "Some Aspects of Polymer Retention in Porous Media Using a C^{14}-Tagged Hydrolyzed Polyacrylamide," paper SPE 4668, SPE–AIME 48th Annual Fall Meeting, Las Vegas, NV (September 30-October 3, 1973).

Chapter 10

Technology Transfer

Research conducted under Contract DE-FC26-02NT15363 was presented to the industry through oral presentations and technical papers and a listing of these works is given below. A few works were based on research conducted under a previous contract (DE-AC26-99BC15209).

Presentations

Willhite, G.P., "Disproportionate Permeability Reduction," Forum on Arbuckle Water Control, Petroleum Technology Transfer Council, Wichita, KS (4 February 2003).

Willhite, G.P., "Effect of Flow Rate on Disproportionate Permeability Reduction," S. Ganguly, G.P. Willhite, D.W. Green and C.S. McCool, SPE International Symposium on Oilfield Chemistry, Houston, TX (5-7 February 2003).

Willhite, G.P., "Overview of the Tertiary Oil Recovery Project's Gelled Polymer Research and Field Applications," Workshop on Reducing Water Production Using Gelled Polymers, Petroleum Technology Transfer Council, Wichita, KS (31 July 2003).

Jain, R., "Reaction Kinetics of the Uptake of Chromium(III) Acetate by Polyacrylamide," R. Jain, C.S. McCool, D.W. Green, G.P. Willhite and M.J. Michnick, SPE Paper No. 89399, SPE/DOE Fourteenth Symposium on Improved Recovery, Tulsa, OK (17-21 April 2004).

McCool, C.S., "Effect of Composition of a Polyacrylamide-Chromium Acetate Gel on the Magnitude of Gel Dehydration and Disproportionate Permeability Reduction," T. Nguyen, D.W. Green, G.P. Willhite and C.S. McCool, SPE Paper No. 89404, SPE/DOE Fourteenth Symposium on Improved Recovery, Tulsa, OK (17-21 April 2004).

Cheng, M., "Modeling of Pre-Gel Aggregate Growth During the Gelation of a Polyacrylamide-Chromium(III) Acetate Gel System Using the Theory of Branching Processes," M. Cheng, C. Wang, C.S. McCool, D.W. Green and G.P. Willhite, SPE Paper No. 93354, 2005 SPE International Symposium on Oilfield Chemistry, Houston, TX (2-4 February 2005).

Chen, F., "Experimental and Modeling Study of the Transport of Chromium Acetate Solutions Through Carbonate Rocks," F. Chen, C.S. McCool, D.W. Green and G.P. Willhite, SPE Paper No. 100064, 2006 SPE/DOE Sympsoium on Improved Oil Recovery, Tulsa, OK (22-26 April 2006).

Willhite, G.P., " Formation and Propagation of Gel Aggregates Using Partially Hydrolyzed Polyacrylamide and Aluminum Citrate," A.A. Al-Assi, G.P. Willhite,D.W. Green and C.S. McCool, SPE Paper No. 100049, 2006 SPE/DOE Sympsoium on Improved Oil Recovery, Tulsa, OK (22-26 April 2006).

Technical Papers

"The Effect of Fluid Leakoff on Gel Placement and Stability in Fractures," S. Ganguly, G.P. Willhite, D.W. Green and C.S. McCool, *SPE Journal*, **7** (September 2002) 309-315.

"Effect of Flow Rate on Disproportionate Permeability Reduction," S. Ganguly, G.P. Willhite, D.W. Green and C.S. McCool paper No. SPE 80205, SPE International Symposium on Oilfield Chemistry, Houston, TX (5-7 February 2003).

"Propagaton of Chromium(III) Acetate Solutions Through Dolomite Rock," H. Jin, C.S. McCool, G.P. Willhite, D.W. Green and M.J. Michnick, *SPE Journal*, **8** (June 2003) 107-113.

"Modeling of Pre-Gel Aggregate Growth During the Gelation of a Polyacrylamide-Chromium(III) Acetate Gel System Using the Theory of Branching Processes," M. Cheng, C. Wang, C.S. McCool, D.W. Green and G.P. Willhite, SPE Paper No. 93354, 2005 SPE International Symposium on Oilfield Chemistry, Houston, TX (2-4 February 2005) under review.

Jain, R, C.S. McCool, D.W. Green, G.P. Willhite and M.J. Michnick, "Reaction Kinetics of the Uptake of Chromium(III) Acetate by Polyacrylamide," *SPE Journal* (September 2005) **10**, No.3.

Nguyen, T.Q., D.W. Green, G.P. Willhite and C.S. McCool "Effects of Gelant Composition and Pressure Gradients of Water and Oil on Disproportionate Permeability Reduction of Sandpacks Treated with Polyacrylamide-Chromium Acetate Gels," scheduled to be published *SPE Journal* (June 2006) **11**, No. 2.

"Experimental and Modeling Study of the Transport of Chromium Acetate Solutions Through Carbonate Rocks," F. Chen, C.S. McCool, D.W. Green and G.P. Willhite, SPE Paper No. 100064, 2006 SPE/DOE Sympsoium on Improved Oil Recovery, Tulsa, OK (22-26 April 2006) under review.

"Formation and Propagation of Gel Aggregates Using Partially Hydrolyzed Polyacrylamide and Aluminum Citrate," A.A. Al-Assi, G.P. Willhite, D.W. Green and C.S. McCool, SPE Paper No. 100049, 2006 SPE/DOE Sympsoium on Improved Oil Recovery, Tulsa, OK (22-26 April 2006) under review.